

**A Genome-Wide Screen on Modifiers of Tau-Induced
Neurodegeneration Using RNAi-Mediated Gene
Silencing in *Drosophila***

Doctoral Thesis

Malte Butzlaff

Göttingen, March 2011

Für Annette und
unseren kleinen Sprössling

**A Genome-Wide Screen on Modifiers of Tau-Induced
Neurodegeneration Using RNAi-Mediated Gene
Silencing in *Drosophila***

Doctoral Thesis

In partial fulfilment of the requirements for the degree “Doctor rerum
naturalium (Dr. rer. nat.)” in the Molecular Medicine Study Program at the
Georg-August University Göttingen

submitted by

Malte Butzlaff

born in

Celle, Germany

Göttingen, March 2011

Members of the Thesis Committee

Supervisor

Prof. Dr. Jörg B. Schulz
Head of Department Neurology
University Hospital of the RWTH Aachen
Pauwelsstraße 30
D-52074 Aachen

Second member of thesis committee

Prof. Dr. Gerhard Hunsmann
former Head of Dept. for Virology and Immunology
German Primate Centre
Leibniz-Institute for Primate Research
Kellnerweg 4
D-37077 Göttingen

Third member of thesis committee

Prof. Dr. Reinhard Schuh
Dept. of Molecular Developmental Biology
Max Planck Institute for Biophysical Chemistry
Am Fassberg 11
D-37077 Göttingen

Date of Disputation: 20.05.2011

Affidavit

I hereby declare that my doctoral thesis, entitled “A Genome-Wide Screen on Modifiers of Tau-Induced Neurodegeneration Using RNAi-Mediated Gene Silencing in *Drosophila*”, has been written independently with no other sources and aids than quoted.

Göttingen, March 2011

Malte Butzlaff

Parts of this work have been already published with authorisation of the thesis committee, represented by Prof. Dr. Jörg B. Schulz, head of Department Neurology, University Hospital of the RWTH Aachen.

Talk “A Genome-Wide Screen for Modifiers of Tau-Induced Neurodegeneration Using RNAi-Mediated Gene Silencing in *Drosophila*” at the *Drosophila* Regional Meeting in Munich. (10.08.2008)

Talk “A Genome-Wide Screen for Modifiers of Tau-Induced Neurodegeneration Using RNAi-Mediated Gene Silencing in *Drosophila*” at the PhD Meeting of Prof. Dr. Gerhard Hunsmann, at the German Primate Centre in Göttingen. (30.01.2009)

Poster “A Genome-Wide Screen for Modifiers of Tau-Induced Neurodegeneration Using RNAi-Mediated Gene Silencing in *Drosophila*” at the *Drosophila* Regional Meeting in Münster. (28.08.2009)

Acknowledgements

This work was conducted at the Department of Neurodegeneration and Restorative Research, UMG, Göttingen, Germany and the Department of Neurology, University Hospital of the RWTH Aachen, Germany (for both head of the department: Prof. Dr. Jörg B. Schulz). I would like to thank Prof. Dr. Jörg B. Schulz as my supervisor for intellectual support and giving me the opportunity to conduct this work. I thank Prof. Dr. Reinhard Schuh and Prof. Dr. Gerhard Hunsmann for intellectual support and their membership in my thesis committee. I am indebted to my advisor Dr. Aaron Voigt for his encouragement and intellectual and practical support.

My special thanks go to Dr. Peter Karsten for his endless goodwill and assistance. I thank Hannes Voßfeldt, Katja Prüßing, Anne Lankes, Sabine Hamm, Róisín-Ana Ní Chárthaigh and the rest of the fly laboratory at the Department of Neurology, Aachen, for their assistance and backup.

I would like to thank Petra Füger, Shabab Hannan and Dr. Tobias Rasse (Research Group Synaptic Plasticity, Herthie-Institute for Clinical Brain Research, Tübingen) for giving me the opportunity to work in their lab, helping me with the axonal transport experiments and conducting the *in vivo* time-lapse measurements. I owe thanks to Dipl.-Ing. Manfred Bovi (Institute for Pathology, University Hospital of the RWTH Aachen) for recording the scanning electron micrographs. I also have to thank the Vienna *Drosophila* RNAi Centre for the RNAi library and the Developmental Studies Hybridoma Bank, USA for their antibodies.

Last but not least I have to thank the Competence Network Degenerative Dementias for financing this project.

Table of Contents

List of Figures	XI
List of Tables	XII
List of Abbreviations	XIII
Abstract	1
1 Introduction	2
1.1 Frontotemporal dementia with Parkinsonism linked to chromosome 17.....	2
1.2 Alzheimer's disease	2
1.2.1 Amyloid plaques	4
1.2.2 Linking amyloid plaques and neurofibrillary tangles	4
1.3 Tau and its regulatory modifications	6
1.3.1 Phosphorylation of Tau	7
1.3.2 Tau proteolysis.....	8
1.3.3 Other post-translational modifications of Tau	8
1.3.4 Clearance of toxic Tau species	9
1.3.5 Mutations in the gene coding for Tau	9
1.4 Models of Tau pathology	10
1.4.1 Loss of function	10
1.4.2 Tau aggregation	10
1.4.3 Direct cytotoxicity.....	11
1.5 Microtubule-based transport and Tau	11
1.5.1 Axonal transport.....	11
1.5.2 Kinesins	12
1.5.3 The Dynein/Dynactin complex.....	12
1.5.4 Axonal transport and neurodegeneration.....	15
1.5.5 Effects of Tau on axonal transport.....	16
1.5.6 Distribution of Tau.....	16
1.6 The role of the lysosome in Tau toxicity.....	17
1.7 <i>Drosophila melanogaster</i> as a model organism	18
1.7.1 The UAS/Gal4 expression system	18
1.7.2 High-throughput approaches.....	19
1.7.3 Inhibition of gene expression by RNA interference	19

1.8	<i>Drosophila</i> models for neurodegenerative diseases	20
1.8.1	The rough eye phenotype	21
1.8.2	<i>Drosophila</i> models for Tau-induced neurodegeneration	21
1.9	The conducted screen	23
2	Material and Methods	24
2.1	Chemicals, buffers and equipments	24
2.2	Transgenic animals and fly keeping conditions	28
2.3	Site-directed integrations	29
2.4	Breeding procedures	30
2.5	Phenotypic analysis	30
2.6	Documentation of compound eye phenotypes	31
2.7	Cell death events in eye imaginal discs	31
2.8	Longevity analysis	32
2.9	Quantification of mRNA levels using qPCR	32
2.10	Immunochemical evaluation of protein levels	34
2.11	Immunohistochemical staining of paraffin sections	35
2.12	Immunohistochemical stainings in <i>Drosophila</i> larval motorneurons	36
2.13	Quantification of CSP accumulations in segmental nerves	37
2.14	<i>In vivo</i> time-lapse quantifications of axonal transport	37
3	Results	39
3.1	Characterisation of the used <i>Drosophila</i> transgenes	39
3.1.1	Rough eye phenotypes of the models	39
3.1.2	Developmental effects of Tau expression	40
3.1.3	Comparison of Tau expression levels	42
3.1.4	Longevity of the disease models	43
3.2	Database for a high-throughput screen	43
3.3	The Screen	44
3.3.1	Exclusion of RNAi lines inducing phenotypic changes in the absence of Tau	44
3.3.2	Primary screen	45
3.3.3	Specificity of RNAi effects for Tau-induced REP	45
3.3.4	Verification of the RNAi effects	48
3.3.5	Quantification of the RNAi effects	49
3.4	Candidates modifying cellular Tau protein levels	50
3.5	Comparing Tau variants using site-directed integration transgenes	51
3.5.1	Specificity of the candidates for Tau[R406W]-induced pathology	54
3.5.2	Candidate effects in phospho-specific Tau models	55

3.6 Evaluation of Tau phosphorylation due to candidate effects	57
3.7 Modification of Tau-induced toxicity by knockdown of the Dynein/Dynactin transport complex	58
3.7.1 Microtubule network in the motorneuron axon of larvae.....	59
3.7.2 Axonal Tau levels.....	59
3.7.3 The morphology of neuromuscular junctions	60
3.7.4 Axonal accumulations of transported vesicles	61
3.7.5 Detailed analysis of the axonal transport using <i>in vivo</i> time-lapse imaging.....	63
3.7.6 Effects of Tau[R406W] expression on transcription levels of transport proteins.....	64
3.7.7 The role of the Dynein/Dynactin-based transport in the lysosomal pathway	64
4 Discussion	67
4.1 Characterisation of the transgenes in <i>Drosophila</i>	67
4.2 Modifiers of Tau-induced REP in the compound eye of <i>Drosophila</i>	69
4.3 Specificity of selected candidates for the R406W mutation of Tau	71
4.4 Alteration of intracellular Tau protein levels as a mechanism for modulation of toxicity	72
4.5 SP and TP phosphorylation sites in Tau-induced toxicity	73
4.6 The Dynein/Dynactin complex in Tau-induced neurodegeneration	74
4.6.1 The axon as the putative site of Dynein/Dynactin and Tau interconnection.....	75
4.6.2 Lysosomal involvement in Tau-induced pathology	77
4.7 Summary and conclusions	78
5 References	80
Curriculum Vitae	100
Private Danksagungen	102
Appendix	103

List of Figures

PATHOLOGICAL HALLMARKS OF AD.....	3
SCHEMATIC VIEW OF THE SIX TAU ISOFORMS FOUND IN HUMAN CNS.....	6
REPORTED PHOSPHORYLATION SITES OF 4R0N TAU.....	7
THE DYNEIN/DYNACTIN COMPLEX.....	15
AN OVERVIEW OF THE UAS/GAL4 EXPRESSION SYSTEM.....	18
PATHWAY OF RNA INTERFERENCE BY TRANSGENIC SHRNA.....	20
THE ROUGH EYE PHENOTYPE (REP) AS A HIGH-THROUGHPUT READOUT.....	21
MUTATED PHOSPHORYLATION SITES OF PHOSPHO-SPECIFIC TAU MODELS AND USED PHOSPHO-SPECIFIC ANTIBODIES.....	22
PHENOTYPES INDUCED BY GMR-MEDIATED EXPRESSION OF THE DIFFERENT TRANSGENES.....	40
DEVELOPMENTAL EFFECTS OF TAU[R406W] EXPRESSION IN THE EYE IMAGINAL DISC OF <i>DROSOPHILA</i>	41
TAU mRNA LEVELS IN THE USED TAU[R406W] MODEL.....	42
LONGEVITY OF THE DISEASE MODELS.....	43
SUMMARY OF THE SCREEN RESULTS AND THE OBTAINED CANDIDATES.....	45
QUANTIFICATION OF RNAi EFFECTS BY CANDIDATE SHRNAs.....	49
ALTERATIONS IN TAU PROTEIN LEVELS INDUCED BY KNOCKDOWN OF CANDIDATE GENES.....	50
ROUGH EYE PHENOTYPES INDUCED BY EXPRESSION OF THE SITE-DIRECTED INTEGRATION TRANSGENES WITH DIFFERENT TAU VARIANTS.....	52
GMR-MEDIATED TAU EXPRESSION BY ATTB ₂ TAU VARIANTS.....	52
LONGEVITY OF SITE-DIRECTED INTEGRATION TAU TRANSGENES.....	53
SECONDARY SCREEN ON CANDIDATE SPECIFICITY FOR R406W MUTATION OF TAU.....	54
SCREEN ON MODIFIERS OF REP INDUCED BY EXPRESSION OF PHOSPHO-MIMICKING TAU VARIANTS.....	56
EVALUATION OF SELECTED CANDIDATE SHRNAs FOR THEIR IMPACT ON TAU PHOSPHORYLATION.....	57
THE DYNEIN/DYNACTIN COMPLEX AS A MODIFIER OF TAU-INDUCED NEURODEGENERATION.....	58
TUBULIN NETWORK IN AXONS OF LARVAL MOTORNEURONS.....	59
TAU STAINING INTENSITY IN MOTORNEURON AXONS AFTER KNOCKDOWN OF MEMBERS FROM THE DYNEIN/DYNACTIN COMPLEX.....	60
NMJ MORPHOLOGY OF <i>DROSOPHILA</i> LARVAL MOTORNEURONS.....	61
CSP ACCUMULATIONS IN MOTORNEURONS OF <i>DROSOPHILA</i> LARVAL SEGMENTAL NERVES.....	62
<i>IN VIVO</i> TIME-LAPSE ANALYSIS OF ANTEROGRADE AND RETROGRADE AXONAL TRANSPORT.....	63
CHANGES IN TRANSCRIPT LEVELS OF TRANSPORT CANDIDATES DUE TO TAU[R406W] EXPRESSION.....	64
SCHEMATIC VIEW OF A LATERAL PART OF A FRONTAL SECTION THROUGH AN ADULT FLY HEAD.....	65
ADULT <i>DROSOPHILA</i> BRAIN STAINED FOR hTAU (5A6), LAMP1 AND TAU ⁴²¹ (TAUC3).....	66
OVERLAPS BETWEEN THE THREE SCREENS FOR MODIFIERS OF TAU-INDUCED PATHOLOGY.....	70
MODEL OF TAU CLEARANCE FROM THE AXON BY RETROGRADE AXONAL TRANSPORT.....	75
INCREASED TAU TOXICITY BY LYSOSOMAL MALFUNCTION AND CASPASE-3 ACTIVATION.....	77

List of Tables

LIST OF DYNEIN HEAVY CHAINS IN <i>HOMO SAPIENS</i> AND <i>DROSOPHILA MELANOGASTER</i> HOMOLOGUES.....	13
DYNACTIN SUBUNITS AND HOMOLOGUES IN <i>DROSOPHILA MELANOGASTER</i>	14
CHEMICALS AND BUFFERS	24
EQUIPMENT	26
SOFTWARE AND ONLINE TOOLS.....	26
OBTAINED TRANSGENIC <i>DROSOPHILA MELANOGASTER</i> FLY STRAINS USED IN THIS STUDY	28
STRATEGIES FOR SUB-CLONING INTO PUAS-ATTB.....	29
STOCKS USED FOR THE SCREENING PROCEDURE.....	30
PRIMERS USED FOR QUANTIFICATION OF TRANSCRIPT LEVELS USING QPCR	33
ANTIBODIES USED FOR IMMUNOBLOTTING	35
ANTIBODIES USED FOR IMMUNOHISTOCHEMICAL STAININGS.....	36
ANTIBODIES USED IN STAININGS OF LARVAL MOTORNEURONS	37
LIST OF CANDIDATES MODIFYING TAU-INDUCED REP IN <i>DROSOPHILA MELANOGASTER</i>	46
SHRNAs SHOWING A SIGNIFICANT DECREASE OF TARGET mRNA AFTER PAN-NEURAL EXPRESSION.	49

List of Abbreviations

Abbreviation	Explanation
AD	Alzheimer's disease
ALS	Amyotrophic lateral sclerosis
AO	Acridine orange
AP	Tau variant non-phosphorylatable at 14 SP or TP sites
APOE	Apolipoprotein E
APP	Amyloid precursor protein
<i>app</i>	Gene coding for the Amyloid precursor protein
Arp	Actin-related protein
A β	Amyloid beta peptide
BACE	β site APP cleaving enzyme
CMT	Charcot-Marie-Tooth disease
CNS	Central nervous system
CSP	Cysteine string protein
DNHC	Dynein heavy chain
dTau	Endogenous <i>Drosophila</i> Tau
E14	Tau variant pseudo-phosphorylated (glutamate) at 14 SP or TP sites
EO-FAD	Early onset familial Alzheimer's Disease
FTDP-17	Frontotemporal dementia and Parkinsonism linked to chromosome 17
HRP	Horseradish peroxidase
HSP	Hereditary spastic paraplegia
hTau	Transgenic Tau of <i>Homo sapiens</i>
MAP	Microtubule-associated protein
<i>mapt</i>	Gene coding for microtubule-associated protein Tau
MBD	Microtubule-binding domain
MF	Morphogenic Furrow
mRNA	Messenger RNA
MT	Microtubule
MTOC	Microtubule organisation centre
NFL	Neurofibrillary lesion
NFT	Neurofibrillar tangles
NMJ	Neuromuscular junction

Abbreviation	Explanation
PD	Parkinson's disease
PHF	Paired helical filament
Q ₇₈	C-terminal fragment of Ataxin-3 containing a repeat of 78 glutamines
qPCR	Quantitative polymerase chain reaction
REP	Rough eye phenotype
RISC	RNA-induced silencing complex
RLC	RISC loading complex
RNAi	RNA interference
SEM	Scanning electron microscopy
SF	Straight filament
shRNA	Short hairpin RNA
siRNA	Short interfering RNA
SP	Proline-guided serine phosphorylation site
TP	Proline-guided threonine phosphorylation site
UAS	Upstream activating sequence
VDRC	Vienna Drosophila RNAi Centre
WT	Wildtype

Abstract

Intraneuronal inclusions of Tau protein are a common feature of the so-called Tauopathies. Frontotemporal dementia with Parkinsonism linked to chromosome 17 (**FTDP-17**) is one of the Tauopathies and is caused by different mutations of the gene coding for Tau. In FTDP-17 intraneuronal inclusions of Tau called neurofibrillary tangles (**NFT**) compose the pathology. The most common Tauopathy is Alzheimer's disease (**AD**). The two neuropathological hallmarks of AD are extracellular amyloid plaques and intraneuronal NFTs.

In order to elucidate molecular mechanisms contributing to Tau-induced neurodegeneration a genome-wide modifier screen on a well-established *Drosophila* model was conducted: a transgenic fly expressing a mutant variant of the microtubule-associated protein Tau (Tau[R406W]) associated with FTDP-17 in humans. Upon expression of Tau[R406W] in the compound eye, a distinct pathological manifestation, the rough eye phenotype (**REP**), is seen. This can be used to evaluate modifications of Tau-induced pathology. The screen was conducted using RNAi-mediated knockdown of all *Drosophila* genes known to have a human homologue. Out of 7881 screened RNAi lines about one percent were identified to modify Tau-induced REP. To shed a light on the role of these candidates in disease, they were first grouped according to their known molecular function or mechanistic relevance. Interestingly, several candidates were found, which are involved in transport mechanisms such as the Dynein/Dynactin complex responsible for retrograde microtubule-based transport. Experiments to elucidate the functional interaction of retrograde transport and Tau-induced toxicity indicated an involvement of lysosomal dysfunction in modification of Tau pathology by knockdown of the Dynein/Dynactin complex. Additional experiments could identify candidates specific for the R406W mutation of Tau and candidates, where modifications depend on the phosphorylation status of Tau.

Taken together, the conducted screen produced a list of formerly unknown modifiers of Tau-induced pathology and several results elucidating putative modes of modification. This work not only stands for itself, but also creates a variety of approaches to investigate Tau pathology. This can be used for future research, which eventually might lead to the development of novel therapeutic strategies.

1 Introduction

Common findings in neurodegenerative diseases are pathological aggregates of proteins in the brain. Filamentous deposits of microtubule-associated protein Tau, the so-called neurofibrillary tangles (**NFT**), are found in several neurodegenerative diseases known as Tauopathies. The two most common Tauopathies are Alzheimer's disease (**AD**) and frontotemporal dementia with Parkinsonism linked to chromosome 17 (**FTDP-17**), which can be associated to mutations in the gene coding for Tau (microtubule associated protein tau *mapt*).

1.1 Frontotemporal dementia with Parkinsonism linked to chromosome 17

Frontotemporal dementia (**FTD**) is a very heterogeneous disease which was already described in 1892 by Arnold Pick [1]. Subtypes of FTD can be differentiated based on the pattern of protein deposits in the brain. Not all FTD cases show Tau-positive inclusions, but of the hereditary FTD cases, 10-40 percent can be associated to numerous mutations in *mapt*. These were categorised as FTDP-17 [2]. To date over 25 exonic or intronic mutations are known to cause the disease (see chapter 1.3.5). FTDP-17 is characterised by atrophy of the brain, accompanied by neuronal loss within the frontotemporal neocortex [2]. The disease was initially described to cause behavioural and motor disturbances, which are later accompanied by a cognitive impairment [3]. In FTDP-17 the pathological hallmark is the presence of intraneuronal NFTs [4]. NFTs are inclusions, which are composed of Tau and are common in most Tauopathies (like AD, see chapter 1.2). Physiological Tau is associated to and stabilises microtubules (**MT**). MTs are essential for the overall integrity of the cell as they are responsible for cell structure and intracellular transport of metabolites, neurotransmitters and organelles [4]. Phosphorylation of Tau decreases the affinity of the protein to the MT, therefore hyperphosphorylation of Tau causes destabilisation of microtubules [4]. Conditions that lead to hyperphosphorylation might thus result in Tau aggregation, impaired cell function and eventually cell death [4, 5].

1.2 Alzheimer's disease

AD is the most common cause of dementia in the elderly, with an estimated global prevalence of 24.3 million and an incidence of about 4.6 million new cases being diagnosed per year [6, 7]. Knowledge of mechanisms and possible treatments of known

dementias such as AD are of even higher importance in developing countries, in which life expectancy increases. The disease is diagnosed if two of the following symptoms are present: loss of episodic memory, aphasia (impairment of speech), apraxia (disorder of motor planning) and agnosia (loss of ability to recognize persons, objects, sounds or smells although senses are not affected) [8]. The progressing symptoms of the disease invariably lead to an individual's inability to perform everyday tasks [9]. The average age of onset of AD is 65, but the range is wide and influenced by certain genetic factors. Early-onset familial Alzheimer's disease (**EO-FAD**) is caused by mutations in one of three genes that are inherited in an autosomal dominant fashion. In 20-70 % of EO-FAD cases mutations in *presenilin-1* occur, in 10-15 % of the cases mutations in the *amyloid precursor protein (APP)* gene occur and rare cases are linked to mutations in *presenilin-2* [10]. Alleles of the gene coding for Apolipoprotein E (**APOE**) are associated with late-onset AD [11, 12].

The neuropathological hallmarks of AD are two distinct forms of aggregates (Figure 1): amyloid-based neuritic plaques, which are extracellular aggregates of Amyloid- β (**A β**) peptides and intracellular NFTs. Although AD has been a topic of intensive research over several decades, the cellular pathways leading to the disease remain elusive and still no cure has been developed.

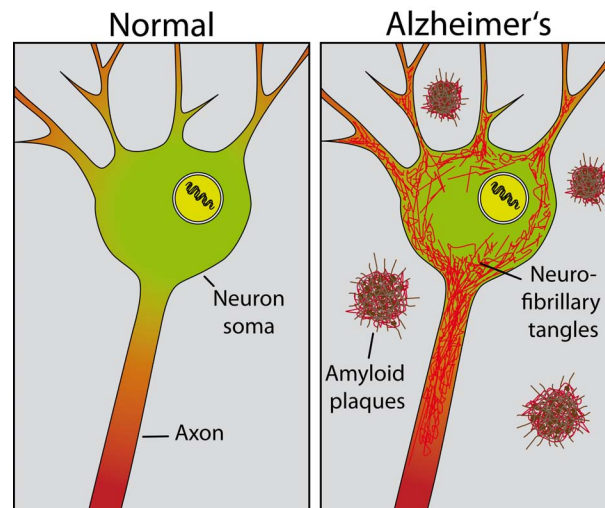


Figure 1: Pathological hallmarks of AD.

The pathological state classically shows two types of aggregates: the intracellular neurofibrillary tangles (NFTs) and the extracellular amyloid plaques.

1.2.1 Amyloid plaques

The plaque is formed by an aggregation of a 42 amino acid-long fragment of APP. APP is a membrane-bound surface protein involved in neurite growth, cell adhesion, synaptic functions and the induction of apoptosis [13]. APP has a short intracellular domain and a longer extracellular domain, which is physiologically cleaved through three secretase enzymes, the α , β and γ secretases [14, 15]. Normally, a physiological fragment is formed after cleavage with the α and γ secretases resulting in a 40 amino acid-long β peptide [13, 16]. In the Alzheimer's brain, the β secretase (β site APP cleaving enzyme **BACE**) produces, in combination with the γ secretase, the $A\beta_{42}$ fragment [15]. This $A\beta_{42}$ fragment is able to form oligomers. These oligomers eventually fibrillate and mature into insoluble neuritic plaques [13, 16, 17].

1.2.2 Linking amyloid plaques and neurofibrillary tangles

Linking the two pathological hallmarks, amyloid plaques and NFTs, has been an important research field in the past decade. Mutations in the genes coding for APP (*app*) and *mapt* are known to induce severe neurodegenerative diseases in humans, but pathology differs. Mutations in *mapt* can cause hereditary FTDP-17, characterized by intracellular Tau deposits like NFTs in the absence of amyloid plaques (see chapter 1.3.5). Nevertheless, mutations in *app* leading to amyloid plaques, as well as direct intracranial injection of $A\beta$ peptides, increase NFT formation in a murine Tau model, implying a directed mechanistic influence of amyloid effects on Tau pathology [18, 19]. In addition, a knockout of Tau could rescue from pathological effects induced by expression of human APP in mice [20]. The cascade from APP to Tau is poorly understood, but several hypotheses are raised:

The first hypothesis to describe the link between amyloid plaques and NFTs was formulated in 1992 by Hardy and Higgins as the amyloid cascade hypothesis [21]. It is first of all based on the assumption that a toxic species of $A\beta$ peptides is the cause of AD. Through mutations in *app* or *presenilin*, or environmental factors, the accumulation of a toxic species is responsible for disease onset and progression. Formation of NFTs by modified Tau was explained as a downstream event of $A\beta$ toxicity, which contributes to neurodegeneration [22]. Limiting this straight hypothesis is the finding that amyloid plaques and NFTs appear in independently distributed patterns [23, 24] and the severity of AD is rather correlated to accumulating NFTs [25, 26].

A second approach is a unifying view published recently as the revitalised Tau hypothesis [27]. Activated microglia produce proinflammatory cytokines that trigger signal cascades in neuronal cells [28]. Kinases and phosphatases are deregulated, leading to abnormally phosphorylated Tau protein and in consequence to fibrillary degeneration. The toxic species of Tau is released by degenerating neurons, contributing to microglia activation and leading into a deleterious cycle of progressive degeneration [29]. Induction of microglia is suggested to be additionally initialised by A β peptides, free radicals, iron overloads and other environmental factors [27]. This goes in line with recent publications showing induction of neurodegenerative-related processes by extracellular application of either A β peptides [30] or Tau protein [31].

A third approach is a newly discovered dendritic function of Tau [32]. Tau guides the Src kinase Fyn to the postsynaptic compartment, where it transduces the excitotoxic triggers of amyloid- β via the NMDA receptor. In Tau-deficient mice Fyn could not be located to dendrites and toxic effects of A β were prevented.

Another possible mechanistic link is the activation of caspases. It has been shown in cell culture that extracellular amyloid deposits activate caspase-2 and 3 [33]. Caspase-3 is able to truncate Tau protein at the C-terminus creating Tau¹⁻⁴²¹ [34-36]. This truncated version is found in NFTs of AD and related Tauopathies [37-39] and has an increased aptitude to fibrillate, as the 20 truncated amino acids inhibit filament assembly *in vitro* [40]. Still, pathways leading to caspase activation via extracellular amyloid remain elusive.

1.3 Tau and its regulatory modifications

The gene coding for Tau, *mapt*, is located on chromosome 17. It consists of 16 exons, although only 11 are constitutive for the isoforms found in the central nervous system (CNS) [41, 42]. Alternative splicing of exons 2, 3 and 10 results in six different isoforms present in the human brain, differing in size between 352 and 441 amino acids (Figure 2). Interaction of the protein Tau with microtubules is mediated by three (3R) or four (4R) C-terminal microtubule-binding domains (MBD) [42-44]. Differential splicing of the exons 2 and 3 is responsible for three different N-terminal variants of Tau: without exon 2 and 3 (0N), with exon 2 (1N) and with both (2N) (Figure 2). In the adult human brain, the 3R and 4R variants are found in same amounts, while 1N, 0N and 2N are found in the ratio 54%, 37% and 9 % of total Tau [45]. Tau was originally discovered as a microtubule-associated protein (MAP) expressed in the CNS [46], where it is predominantly found in axons [47]. As a MAP, Tau is able to promote microtubule nucleation, growth and bundling [44, 48] and is responsible for MT stabilisation [49]. In line with its MAP function in neurons, Tau is mainly found in the axonal and synaptic compartments (for details see chapter 1.5.6 Distribution of Tau). An additional but related function of Tau is its involvement in neurite outgrowth and stabilisation. In insect cells, overexpression of Tau was able to induce sprouting of long processes with axonal shape [50]. However, Tau

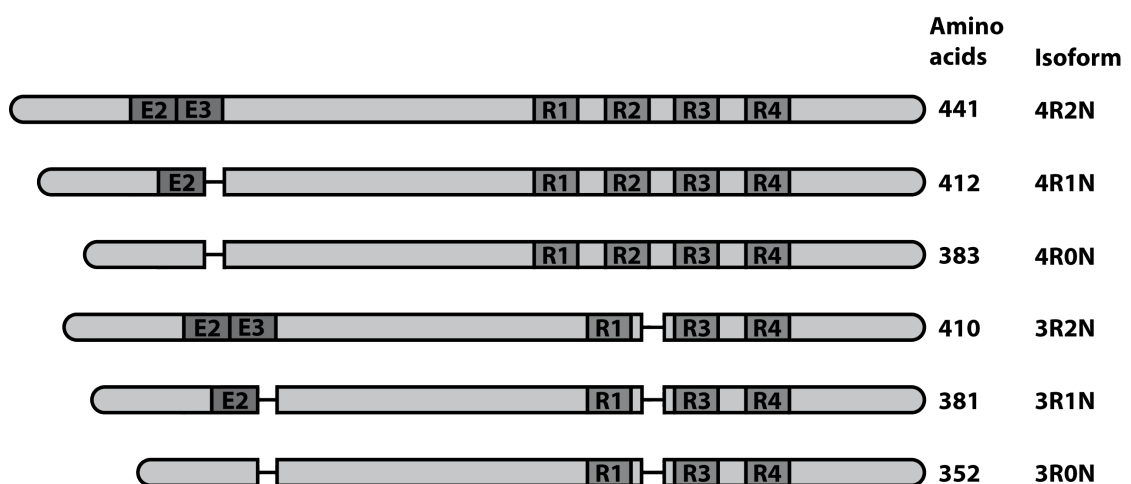


Figure 2: Schematic view of the six Tau isoforms found in human CNS.

The six isoforms found in human CNS differ in three exons: two N-terminal exons with unknown function, exon 2 (E2) and exon 3 (E3), and exon 10 which resembles the MBD repeat 2 (R2). Nomenclature for the isoforms is depicted on the right. First, the number of C-terminal MBD repeats (R) is listed, followed by the number of included N-terminal exons (N).

is not essential for axonal formation as knockout mice did not display overall phenotypic changes [51], except for a delay in axonal sprouting of primary hippocampal cultures. This effect could be rescued by expression of human Tau [52]. In addition to its interaction with microtubules, Tau is assumed to also interact with cytoskeletal proteins like Actin [53] and Spectrin [54]. Recent findings also show an involvement of Tau in Src family tyrosine kinase signalling pathway (interaction with Fyn [55]) and phospholipase C- γ signalling pathway [56]. Taken together, Tau is suggested to play a role in regulating the functional organisation of the neuron by establishing the axonal morphology, growth and polarity in different ways.

1.3.1 Phosphorylation of Tau

All Tauopathies share a pathological state, which is the occurrence of hyperphosphorylated and abnormally phosphorylated Tau protein. The two components of neurofibrillary lesions (NFL) in AD, paired helical filaments (PHF) and straight filaments (SF) predominantly consist of abnormally phosphorylated Tau protein [42, 58-61]. Pathological Tau from human FTDP-17 brain is also known to be hyperphosphorylated [62, 63]. Tau isolated from PHFs shows an approximate 3.5 times higher phosphorylation level compared to a control brain (stoichiometric difference) [64]. Of all known mutations in Tau leading to a disease, no mutation is known to create

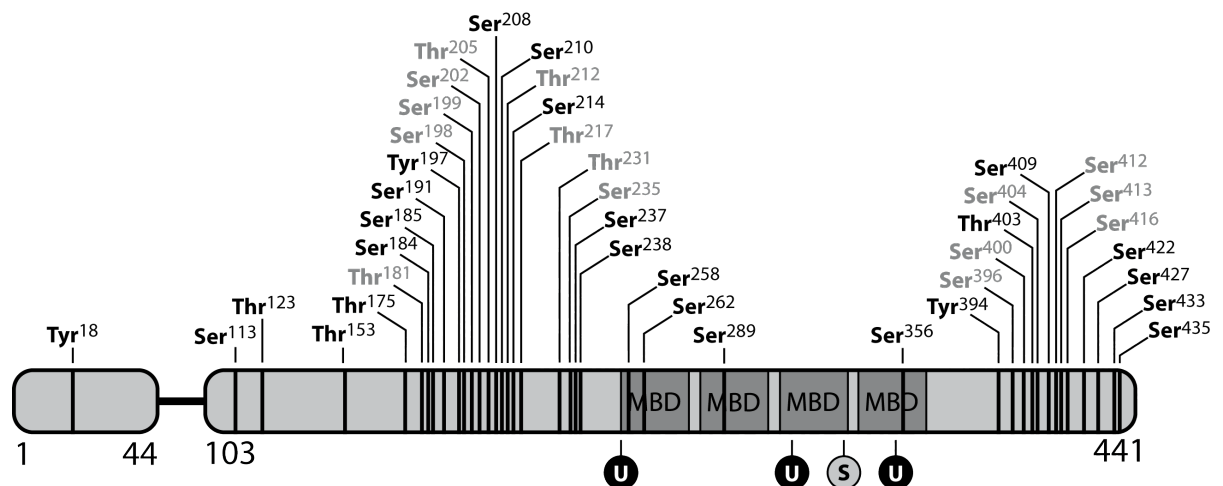


Figure 3: Reported phosphorylation sites of 4R0N Tau.

Of all serine (Ser), threonine (Thr) and tyrosine (Tyr) phosphorylation sites, 25 are mainly found to be phosphorylated in AD brains (black), while others also appear phosphorylated in normal brain (grey). Most phosphorylation sites are clustered at a proline-rich region and the C-terminal region flanking the microtubule-binding domains (MBD). Also depicted are the three known ubiquitination sites (U) and the single known site of sumoylation (S). The numbering of amino acids as used in literature is derived from the 4R2N Tau variant (isoform 2). The Tau variant used in this work is the 4R0N variant (isoform 3).

additional phosphorylation sites. Nevertheless, all Tau mutations are associated with formation of filaments composed of hyperphosphorylated Tau protein [65]. Therefore, Tau hyperphosphorylation must be an event downstream of the primary effects. There are many sites of phosphorylation known in Tau and many kinases are known to phosphorylate Tau [66] (Figure 3). Accordingly, different effects of abnormal Tau phosphorylation are reported: conformational changes of Tau [67], decreased microtubule binding and assembly promotion [68-70] and increased instability of microtubules [44, 49].

1.3.2 Tau proteolysis

Recent publications suggest that truncated versions of Tau protein might be prone to assemble filaments. Specific truncations occur after hyperphosphorylation [71, 72], but as an upstream event to filament assembly [73]. Associated with a higher aptitude in forming filaments are two distinct truncations of the Tau protein. First a truncated variant cleaved at amino acid 391 was shown to be an important component of the PHF core [74-77]. Second a truncated Tau, cleaved at position 421 was reported to be a product of cleavage via caspases in the pathology of AD and related Tauopathies [37-39]. Tau¹⁻⁴²¹ lacks a 20 amino acid long C-terminal peptide, which seems to inhibit formation of polymeric filaments [40]. Especially caspase-3 is responsible for Tau truncation at position 421 [34-36], which might resemble a link between amyloid plaques and Tau pathology (see chapter 1.2.2).

1.3.3 Other post-translational modifications of Tau

In addition to phosphorylation, truncation and ubiquitination of Tau protein (see also chapter 1.3.4), several other Tau modifications are known to be altered in AD. This includes abnormal glycosylation, glycation, prolyl-isomerisation, nitration, polyamination, sumoylation and oxidation [78-85]. While glycation, nitration, polyamination, sumoylation and oxidation seem to promote Tau aggregation and PHF stabilisation [84-88], glycosylation and prolyl-isomerisation by Pin1 might contribute to dephosphorylation of Tau and restore its function [81, 89]. In combination with phosphorylation, truncation and clearance this draws a complex picture of influences on Tau pathology. Diverse impacts obviously act on inhibition and promotion of the pathological pathway.

1.3.4 Clearance of toxic Tau species

If Tau is responsible for the above-mentioned pathomechanisms, the active clearance of the toxic species might be a path to avoid or postpone disease onset. Ubiquitination is a physiological mechanism to mark proteins for degradation by the proteasome. Tau is known to be ubiquitinated in pathological but not under normal conditions. Ubiquitin is found in SDS-insoluble PHFs [90] and in filamentous species of Tau causing neurodegenerative diseases other than AD [91]. However, ubiquitination of PHF occurs after NFT formation, suggesting it to be a late event [92, 93]. Additionally, the predominantly found monoubiquitinations [93] might not be sufficient for ubiquitin-mediated degradation [94, 95]. Nevertheless, the proteasome seems to play an important role in Tau degradation as pharmacological inhibition of the proteasome increases Tau accumulation in rat brain [96].

A second mechanism of Tau degradation might be autophagy and subsequent degradation by lysosomes. Lysosomes are the cellular compartment for autophagy and proteolysis of cellular and endocytotic proteins [97]. The putative involvement of the lysosomal system in Tau pathology is explained in detail in chapter 1.6.

1.3.5 Mutations in the gene coding for Tau

Several mutations of *mapt*, the gene coding for Tau, are known to be associated with human FTDP-17. In 1998, first exonic and intronic mutations were found [63, 98, 99]. To date there are over 25 known alterations of *mapt* known to be associated with the disease [100]. Most of them are exonic missense mutations, several intronic alterations could be associated to causative splicing variation and there is one exonic silent mutation known to inhibit splicing of exon 10 [101]. The majority of known mutations alter the splicing of exon 10 in different ways shifting the ratio of Tau isoforms [100] (isoforms see chapter 1.3). However, most of the alterations lead to one species of Tau filaments. The only two mutations, which do not alter isoform ratios and result in PHFs and SFs, are V337M in exon 12 [99] and R406W in exon 13 [98, 102]. Both lead to a decreased affinity to bind microtubules and an increased formation of filaments. PHFs and SFs found include all six isoforms and are comparable to those observed in Tau NFLs of AD brains [103-105].

1.4 Models of Tau pathology

Ricardo Maccioni recently stated that “*Alzheimer’s disease is one of the human disorders that has triggered the largest number of hypotheses to explain its pathogenesis*” [27]. Although he is also referring to Amyloid-mediated mechanisms, several hypotheses have been raised to explain Tau-mediated neurodegeneration. Three main concepts of toxic triggers by Tau are presented in this chapter.

1.4.1 Loss of function

Tau was discovered as a MAP being responsible for microtubule network maintenance [46]. After the discovery that Tau is the main constituent of NFTs found in AD brains [106, 107], the loss of function hypothesis was the first to be raised. To date, a variety of publications using cell-free assays, cell culture models and animal models contributed to this hypothesis. Pathological triggers prevent Tau from fulfilling its function. It loses the ability to bind, stabilise and regulate microtubule structure and microtubule-based transport (for an overview of publications see [100]). This loss of function and the resulting disturbances by an impaired microtubule network are suggested to be the cause for Tau-induced toxicity.

1.4.2 Tau aggregation

Different experimental approaches were used to elucidate the role of aggregates *per se* in Tau-induced pathology. Tau in its soluble physiological form is suggested to have no significant secondary structure, although published data varies [108-110]. In contrast to its native form, aggregated Tau shows either a cross- β [111, 112] or an α -helical [113] conformational structure. Among the previously mentioned post-translational modifications of Tau protein (chapter 1.3), hyperphosphorylation is particularly able to change secondary structure [114-116]. The altered conformation is suggested to promote Tau aggregation and thereby evoke toxic effects. In AD brain the sites of neurodegeneration correlate quite well with the distribution of NFTs [117]. Moreover, death of NFT-affected neurons has been shown in several Tau expressing mouse models [118-120]. Despite these facts, it is very difficult to identify the direct cause of neuron loss, as different Tau modifications and cellular dysfunctions always accompany or even head NFT manifestation. It has been suggested that aggregation of a toxic protein might even be a general protective cell response [121]. There are several animal models with Tau-induced neurodegeneration lacking NFTs or inclusions (see chapter 1.4.3).

1.4.3 Direct cytotoxicity

Cytotoxicity and degeneration might be triggered by a toxic Tau species itself. This hypothesis is derived from several publications of cell culture and animal models where neurodegenerative phenotypes could be observed in the absence of Tau aggregates. Direct induction of apoptosis without accumulations of Tau could be observed in several neural and neuronal cell lines [122, 123]. This was confirmed *in vivo* as toxicity was observed in *Caenorhabditis elegans* and *Drosophila melanogaster* models of Tauopathy, without displaying obvious accumulations [124, 125].

1.5 Microtubule–based transport and Tau

The physiological role of Tau and its importance for microtubule integrity has already been mentioned. In neurons, all long distance transport mechanisms are based on motor complexes, which allow transport of vesicles, organelles or protein complexes along microtubules [126-129]. Microtubules are polymers of globular Tubulin subunits arranged in a tube-shaped structure. Each Tubulin subunit is a heterodimer composed of two monomers, namely α - and β -Tubulin. Due to its biochemical nature, the microtubule structure has a distinct polarity, allowing directed transport using different motor proteins. In a physiological situation the orientation of microtubules is based on the microtubule-organizing centres (**MTOCs**) where assembly of microtubules is initiated. There are exceptions as for dendrites where mixed polarities are found [130].

Few motor proteins are known to be responsible for distinct cargos and directions. Most of the motor protein complexes are only active during mitosis and will not be named here. Different motor proteins, the Kinesins and cytosolic Dynein, are responsible for MT-based transport. The Kinesins are transporting cargo in an anterograde direction (away from the MTOC, towards the cell periphery). Dynein is the motor complex for the retrograde transport (towards the MTOC/cell body) [131].

1.5.1 Axonal transport

As with all active transport mechanisms, axonal transport occurs along structures of the cytoskeleton. Next to microtubule-based transport there are three major structural components in the axon that are devoted to transport mechanisms – microtubules, Actin filaments and intermediate filaments. Intermediate filaments are composed of the Neurofilament polypeptides NF-L, NF-M and NF-H. These filaments do not have a polarity and thus do not allow directed long distance transport. Actin filaments show a polarity

and are utilised for short distance, dispersive movements. Long distance movement is primarily driven by microtubule-based motor proteins. In mature neurons the highly dynamic microtubules gain stability by interacting with stabilizing microtubule-associated proteins such as Tau. Along the axon microtubules are organized in the expected polarity – resulting in the two distinct transport directions: anterograde axonal transport towards the synapse and retrograde axonal transport towards the cell body.

1.5.2 Kinesins

As mentioned before, Kinesins are responsible for the anterograde transport. This also holds true for axonal transport. The proteins of the Kinesin superfamily all share a conserved motor domain, but differ in the cargo interaction domains. Therefore, Kinesins themselves show specificity for their cargo. In addition to direct cargo binding, cargo attachments can be indirect and mediated by scaffolding or adaptor proteins. Thus redundant Kinesins can restore many anterograde transport functions. Nevertheless a few mutations in Kinesins are known to cause neurodegenerative diseases (e.g. a mutation in KIF1B β , a member of the kinesin-3 family, leads to Charcot-Marie-Tooth (**CMT**) disease Type 2A [132]).

1.5.3 The Dynein/Dynactin complex

Compared to the Kinesin motors (see chapter 1.5.2), the retrograde transport based on cytoplasmic Dynein is far more complex. The Dynein protein itself is formed by a dimer of the Dynein heavy chain (**DNHC**), including the domains of force production and microtubule binding [133] (Figure 4). Associated to the DNHCs are several intermediate and light chains, which are thought to stabilise the complex and regulate binding of accessory and cargo proteins [134-140]. In total, *Homo sapiens* genome encodes 15 different known DNHCs, which can be divided into two functional groups: axonemal and cytoplasmic (Table 1). Although the cytoplasmic members are supposed to be more important for microtubule-based transport, the number of the axonemal proteins is much higher and the function is in most cases only predicted by sequence similarities. The two cytoplasmic and 13 axonemal DNHCs in *Drosophila* and their human homologues are listed in Table 1.

Table 1: List of Dynein heavy chains in *Homo sapiens* and *Drosophila melanogaster* homologues.

Type	Human protein (Gene) ¹	<i>Drosophila</i> homologue ²
Cytoplasmic DNHC	cytoplasmic dynein 1 heavy chain 1 (DYNC1H1)	Dhc64C
	cytoplasmic dynein 2 heavy chain 1 (DYNC2H1)	btv (Dhc36D)
Axonemal DNHC	axonemal dynein heavy chain 1 (DNAH1)	CG14651
	axonemal dynein heavy chain 2 (DNAH2)	kl-2, CG9068
	axonemal dynein heavy chain 3 (DNAH3)	CG17150
	axonemal dynein heavy chain 5 (DNAH5)	CG9492
	axonemal dynein heavy chain 6 (DNAH6)	Dhc16F
	axonemal dynein heavy chain 7 (DNAH7)	Dhc36C
	axonemal dynein heavy chain 8 (DNAH8)	kl-3
	axonemal dynein heavy chain 9 (DNAH9)	CG3339
	axonemal dynein heavy chain 10 (DNAH10)	Dhc98D
	axonemal dynein heavy chain 11 (DNAH11)	kl-5 (DhcYh3)
	axonemal dynein heavy chain 12 (DNAH12)	Dhc62B
	axonemal dynein heavy chain 14 (DNAH14)	-
	axonemal dynein heavy chain 17 (DNAH17)	Dhc93AB

¹ All Dynein heavy chains as listed by Ensembl [141].

² Corresponding homologues as found in the Homologene Database [142] or by primary structure comparison [143].

Although Dynein itself is sufficient to generate a driving force along a microtubule, a complex of Dynein and Dynactin fulfils most transport processes. Dynactin is a complex molecule composed of several subunits (Figure 4). The base is formed by an Actin-like octameric polymer of the Actin-related protein 1 (**Arp**) [144, 145]. Arp1 can directly bind to β III spectrin, which might be a general mechanism for Dynactin to bind a variety of subcellular structures [146]. The plus end of this Arp1 rod terminates with the conventional actin-capping protein CapZ [144, 147]. The opposite end of the rod bears a second Actin-related protein, Arp11 [148], and the Dynactin p62 subunit [144]. Arp11 seems to serve as a cap for the Arp1 filament minus end. It does not allow any further subunit addition. p62 seems to support protein-protein interactions via a zinc-binding motif [148-150] and might be responsible for binding Arp1, Arp11, other Dynactin subunits or sub-cellular cargo structures. However, loss of p62 does not impact stability of Dynactin [151]. The two smallest Dynactin subunits, p25 and p27, associate with p62 and Arp11 and are predicted to represent a novel form of protein interaction domain [152]. Unlike the other subunits they are also available in a free soluble pool and thus might

provide functions independent of the Dynactin complex as adapter proteins targeting Dynactin to its cargo [145]. Extending from the Arp1 rod is a flexible structure which contains three additional subunits: p150^{Glued}, Dynamitin and p24/p22. Each Dynactin molecule contains four copies of Dynamitin and two copies of p150^{Glued} and p22/24, respectively. Dynactin p150^{Glued} is the largest subunit and binds to microtubules with its N-terminus [153, 154]. The microtubule-binding ability seems to be necessary to increase motility of the Dynein motor function [155]. The microtubule-binding ability is crucial especially for neuronal function. A mutant form of p150^{Glued} lacking the microtubule-binding activity results in motor neuron disease [156]. The middle portion of p150^{Glued} is essential for binding of Dynactin to the motor Dynein at different sites [153, 157-159]. The C-terminal end directly binds to the Arp1 filament [154]. In addition, an interaction of the C-terminus of p150^{Glued} and the p25 subunit was detected [160]. The subunit Dynamitin interacts with p150^{Glued}, p22/24 and the Arp1 rod and therefore plays an important role in Dynactin structure maintenance [161]. Furthermore, Dynamitin seems to be a regulator of Dynein/Dynactin-mediated movements as it is able to inhibit dynein-based movements when overexpressed [162, 163]. p22/24 stabilizes the complex of p150^{Glued} and Dynamitin, as it is known to bind both [148, 164], allowing formation of a stable complex of all three proteins [148, 164].

Table 2: Dynactin subunits and homologues in *Drosophila melanogaster*.

Human protein (Gene) ¹	<i>Drosophila</i> homologue ²	Function
Arp1 (ACTR1A)	Arp87C	Octameric polymer for cargo binding
Arp11 (ACTR10)	Arp11	Stabilisation of Arp1 rod
CapZ α/β	capping protein a/b (cpa/cpb)	Stabilisation of Arp1 rod
p62 (DCTN4)	CG12042	Stabilisation of Arp1 and Arp11
p25 (DCTN5)	Dynactin p25	Adaptor protein
p27 (DCTN6)	l(2)37Ce	Adaptor protein
Dynamitin (DCTN2)	Dynamitin	Stability of Dynactin structure
p22/24 (DCTN3)	-	Stabilisation of Dynamitin and p150
p150 (DCTN1)	Glued (Dynactin p150)	Dynein and microtubule binding

¹ All Dynein heavy chains as reviewed [145].

² Corresponding homologues as found in the Homologene Database [142] or by primary structure comparison [143].

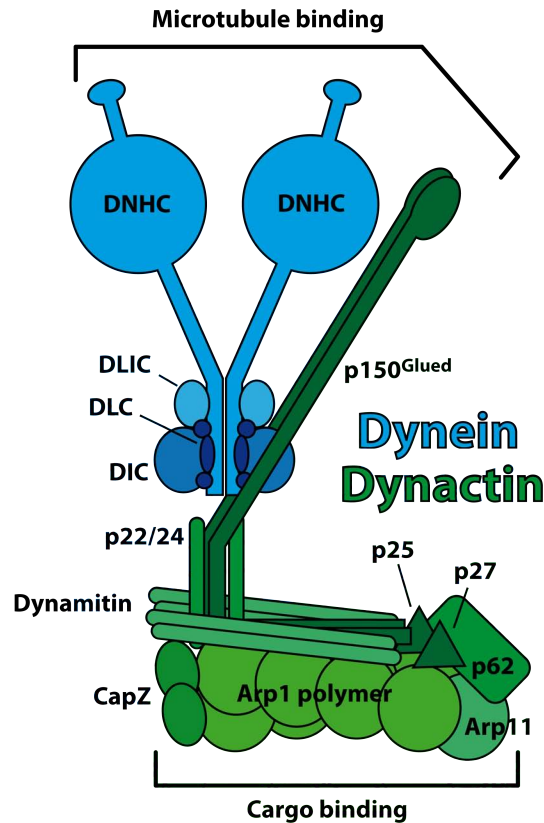


Figure 4: The Dynein/Dynactin complex.

The proteins of Dynein (**in blue**) and Dynactin (**in green**) form a macromolecule for microtubule-based movements. Whereas especially the Dynein heavy chains (**DNHC**) are responsible for microtubule binding, the members of the Dynactin complex are responsible for stabilisation of the complex and the cargo binding. **DLIC**: Dynein light intermediate chain, **DLC**: Dynein light chain, **DIC**: Dynein intermediate chain, **Arp1/Arp11**: Actin-related protein 1/ 11.

1.5.4 Axonal transport and neurodegeneration

Axonal transport is an important issue, since neurons are highly polarised cells, and intracellular distances in human axons can exceed one meter (e.g. in motorneurons). An intact axonal transport is crucial for neuronal function. As the transport mechanisms are complex and in parts not redundant (see chapters 1.5.2 and 1.5.3), there are a variety of possible pathomechanisms leading to transport deficits. Disturbances of axonal transport are described in many major neurodegenerative diseases like amyotrophic lateral sclerosis (**ALS**) [165], spinal muscular atrophy [166], hereditary spastic paraplegia (**HSP**) [167], AD [168-170], polyglutamine diseases [171-173], Parkinson's disease (**PD**) [174] and CMT [132, 175, 176]. In some of these diseases, transport deficits have even been shown to be the cause or early pathogenic events, suggesting a causative or at least promoting role (ALS [177], HSP [167], AD [170] and CMT [132]).

1.5.5 Effects of Tau on axonal transport

Tau as a MAP has a high impact on the axonal transport mechanisms. Its classical role is the stabilisation of the axon's microtubule network (see chapter 0), the base for main transport processes. Therefore pathological changes of the Tau protein have an impact on the transport processes. It has been shown that hyperphosphorylated Tau decreases efficiency of axonal transport *in vivo* [178]. In line with these findings, different kinases have been reported to regulate transport via Tau phosphorylation [179, 180]. Disturbances of the transport machinery by Tau directly lead to "traffic jams" caused by disorganised microtubules in sea hares (*Aplysia*) [181]. In mammalian cells, inhibition of axonal transport is also non-specifically induced by accumulations of Tau in the axon, followed by degeneration of synapses [182]. That the interactions of Tau and motor proteins are not only non-specific (by microtubule destabilisation or traffic jams) has been first shown for the Dynactin complex. The N-terminal part of Tau is able to bind the C-terminus of p150^{Glued}, enhancing its microtubule binding activity and thereby reducing transport velocity [183]. Recently it has been reported that the effects of Tau on Kinesin- and Dynein-based transport are indeed diverse. Whereas Kinesin detaches or pauses as an effect of Tau interaction, Dynein/Dynactin shows neither detachment, nor a rest, but rather an reverse transport direction (anterograde) [184]. Moreover, recent data has provided evidence that Tau modification and pathology can also be induced by transport impairments [185, 186].

1.5.6 Distribution of Tau

The distribution of Tau in neurons seems to contribute to Tau function and malfunction. Under physiological conditions Tau is found in a gradient along the axon, with highest levels at the synapse, and the lowest levels in the somato-dendritic compartment [53, 187-189]. However, to date the mechanisms of Tau distribution have not been fully understood. Tau has been reported to be transported at rates comparable to slow axonal transport [190]. In contrast, small accumulations of Tau seem to be transported by fast axonal transport mechanisms [191]. Opposing diffusion/reaction based models (suggesting that the gradient is formed by diffusion and axonal trapping [192]), models of active transport have been raised. Tau is suggested to travel as a passenger on anterogradely transported MT fragments [193]. MT fragments are known to be transported by stationary motor complexes like the Dynein/Dynactin complex bound to the cytoskeleton [194, 195]. In addition, Kinesin1 is able to transport Tau by direct

interaction, which is reduced when Tau is hyperphosphorylated [196]. In the disease case Tau gets redistributed to the somato-dendritic compartment [197, 198] contributing to several pathomechanisms. The axonal microtubule network becomes destabilised (see chapter 1.4.1) and the increased Tau levels in the soma might inhibit initiation of Kinesin-guided anterograde transport. This may lead to starvation of the synapse and axonal degeneration [184]. Moreover, the increase of Tau levels in the dendritic compartment might increase A β induced toxicity (see chapter 1.2.2).

1.6 The role of the lysosome in Tau toxicity

Recent studies have shown that the integrity of the lysosomal compartment and its function contribute to the mechanisms of Tau-induced neurotoxicity. In an AD mouse model expressing mutant Tau, affected brain regions showed an increased number and structurally abnormalities of lysosomes [199]. Similar observations were published for human AD brains [200, 201]. Although there are several hypotheses for the link between Tau and lysosomal function, the mechanistic role remains elusive. One hypothesis explains the promotion of neurodegeneration by decreased lysosomal stability: Lysosomes releasing their content occur downstream of cytotoxic stressors and induce caspase-dependent apoptosis [202]. In contrast it has also been suggested that lysosomal expansion might be a response of the cell to AD pathomechanisms, increasing degradation of toxic proteins via autophagy [203]. *Vice versa* a defective lysosomal system could lead to an accumulation or abnormal processing of the disease protein [201]. In both cases, functional lysosomes and its proteases could be responsible for Tau degradation and clearance, which has been shown *in vitro* and *in vivo* culture [204, 205].

One major component of the lysosome, the protease Cathepsin D, seems to play a key role in the lysosomal contribution to neurotoxicity. Both mRNA and protein levels of Cathepsin D are upregulated in degenerating neurons of AD patients [206, 207]. Mutations in the Cathepsin-encoding gene are also associated with sporadic AD [208, 209]. Although Cathepsin D has been reported as a pro-apoptotic protein [210], recent publications suggest a cytoprotective role as well. Removal of Cathepsin D specifically enhances Tau-induced neurodegeneration, although it does not alter Tau levels nor its phosphorylation state in a fly model [211]. Nevertheless, in flies as well as in mammalian models, the loss of Cathepsin D led to markedly increased levels of an C-terminally truncated version of Tau, most likely by activation of caspase-3 [211]. This truncated Tau¹⁻⁴²¹ is found in neurofibrillary tangles of AD and related Tauopathies [37-39]. In a

direct comparison in *Drosophila*, Tau¹⁻⁴²¹ was substantially more toxic than wildtype (WT) Tau and in contrast to the wildtype, Tau¹⁻⁴²¹ toxicity could not be elevated by removal of Cathepsin D [211].

1.7 *Drosophila melanogaster* as a model organism

The use of the fruit fly *Drosophila melanogaster* (from now on shortly termed *Drosophila*) has a long history in research. The fruit fly has several advantages in comparison to other animals in research. The genome was one of the first to be completely sequenced and *Drosophila* genetics are well established. It is a fast reproducing organism which can be easily handled in high numbers and short time periods. These advantages make *Drosophila* an ideal model for high-throughput approaches. It is possible to model human hereditary diseases in *Drosophila*, by creating transgenic animals expressing disease-correlated toxic gene products.

1.7.1 The UAS/Gal4 expression system

A tool frequently used as an expression system in *Drosophila* is the so-called UAS/Gal4 system [212-214] (Figure 5). It is based on the yeast transcriptional activator Gal4 and its binding site, the Upstream Activation Sequence (UAS). Gal4 binds to the UAS and activates transcription of downstream target genes. A silent transgenic line containing a UAS-flanked target gene can be crossbred to Gal4-expressing transgenic lines leading to expression of the gene of interest in the offspring. So-called Gal4 driver lines expressing Gal4 in many different spatiotemporal manners (e.g. by endogenous

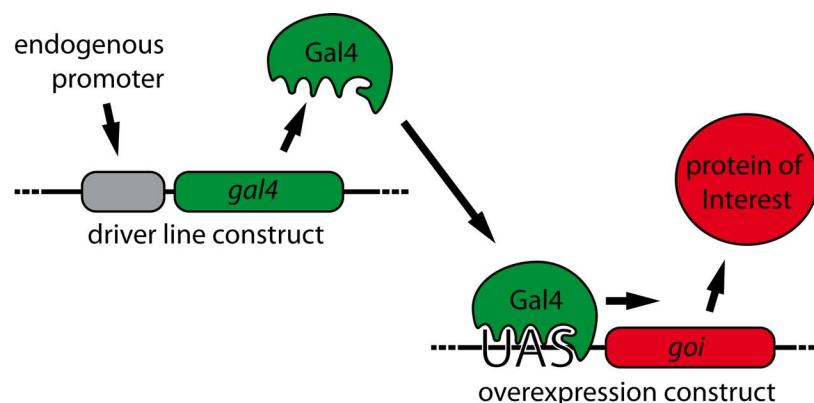


Figure 5: An overview of the UAS/Gal4 expression system.

The usage of two different constructs allows changing time point and/or tissue where the protein of interest is expressed. A driver line leads to expression of the yeast protein Gal4 (green) in a specific spatiotemporal manner by endogenous triggers (a variety of different driver lines are commercially available). The overexpression transgene bears an upstream activation sequence (UAS) where Gal4 binds and expression of the transgene is initialised (red).

promoters) are available. Thus target gene expression can be easily achieved in different spatiotemporal manners using one transgenic UAS line.

1.7.2 High-throughput approaches

Among the high-throughput approaches for genetic screens is misexpression of endogenous genes [215]. However, misexpression creates artificial expression states and one is only able to cover small portions of the *Drosophila* genome. A new approach for high-throughput genetic screens in *Drosophila* is the use of RNAi-mediated gene silencing. This mimics classical knockout experiments, silencing gene transcripts via small interfering RNAs [216] (see chapter 1.7.3). In 2007 an RNAi library was generated utilising the conditional expression system UAS/Gal4 [217]. The RNAi fly lines contain short hairpin RNAs (**shRNA**) under control of a UAS sequence and are therefore silent unless they are crossbred to a Gal4 driver line leading to expression in the pattern of interest.

1.7.3 Inhibition of gene expression by RNA interference

The effect of RNA interference (**RNAi**) was first reported in *Caenorhabditis elegans* in 1998 [218]. It was discovered that regulation of transgene translation via RNAi is a conserved mechanism in plants and animals, e.g. in *Drosophila* [219-221]. There are different species of short interfering RNAs (**siRNAs**) responsible for RNAi effects. They can be classified according to their origin, biogenesis, mode of interference and size. In this work knockdown of single genes was achieved by introduction of a transgene coding for an shRNA. These shRNAs consist of an inverted repeat of 100 – 400 base pairs separated by a spacer allowing to form a stem-loop structure (Figure 6). This shRNA is then processed to short double-stranded siRNAs [221-223]. In *Drosophila*, this maturation is mediated by Dicer-2 cleaving the loop and the appending ends of the RNA [224]. The siRNA is bound and guided to the RNA induced silencing complex (**RISC**) by the protein R2D2, a component of the RISC loading complex (**RLC**) [225]. R2D2 is also a sensor to distinguish between the guide strand (responsible for target recognition) and passenger strand (which will be processed) [226]. The RLC recruits Argonaute2, to which it transfers the siRNA duplex. Ago2 then cleaves the passenger in the same way as it will process the target messenger RNA (**mRNA**) [227]. The RISC complex is formed by release of the passenger siRNA strand. Afterwards the complex can recognise, bind and process the target mRNA using the guide strand of the siRNA for target recognition [219]. RNAi is

a powerful tool to knockdown expression of a gene in a targeted manner. Experiments can be done without creating time-consuming knockouts.

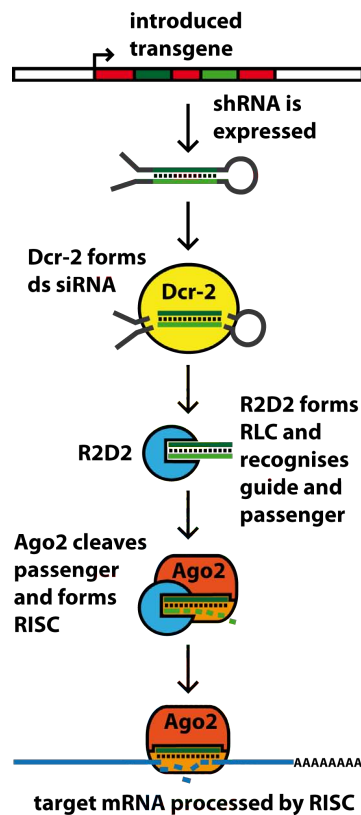


Figure 6: Pathway of RNA interference by transgenic shRNA.

The transgene expresses an RNA, which forms a stem-loop structure due to an inverted repeat. This shRNA is processed by Dicer-2 (**Dcr-2**) to a double stranded (**ds**) siRNA. This is recognized by R2D2 leading it to Argonaute2 (**Ago2**). Ago2 removes passenger strand and forms the RNA induced silencing complex (**RISC**) with the guide strand of the siRNA. The RISC is then able to recognise and cleave the target mRNA.

1.8 *Drosophila* models for neurodegenerative diseases

Many biochemical and signalling pathways are conserved in flies and humans [228]. Consequently, processes impaired in neurodegenerative diseases in humans can be modelled in *Drosophila*. Thereby, the use of *Drosophila* models for human neurodegenerative disorders provides a tool for elucidation of such disease mechanisms.

Human neurodegenerative disorders like Tau-induced FTDP-17 can be modelled in *Drosophila*. Models have already been described and share key features of the human disease such as reduced lifespan and progressive neurodegeneration [125]. Using disease models in combination with high-throughput screens might identify modifiers of toxicity,

thereby revealing pathomechanisms of Tau and might elucidate targets for therapeutic research.

1.8.1 The rough eye phenotype

The compound eye is a highly organised structure consisting of ommatidia (unit eyes) and sensory bristles. Loss of retinal neurons is usually reflected by changes in the regularity of the compound eye structure leading to a rough eye phenotype (**REP**) and the degree of neuron loss correlates to REP severity. Therefore, the REP provides an ideal readout for neurodegenerative diseases, since changes in the regularity of the compound eye texture and size can be easily examined using a normal dissecting microscope [229]. Thus as a readout for a high-throughput modifier-screen on neurodegeneration the REP is frequently chosen [230-232].

For our screening approach, we targeted expression of Tau, in combination with UAS-shRNA transgenes, to the eye. Using the driver *GMR-Gal4*, expression of the two transgenes is limited to post-mitotic cells of the compound eye including photoreceptor neurons [233]. For a screen model a moderate REP is recommended in order to detect phenotypic changes of both directions, enhancement and suppression of the REP (Figure 7).

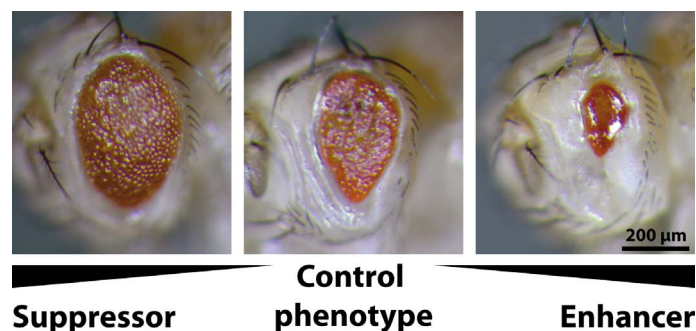


Figure 7: The rough eye phenotype (REP) as a high-throughput readout.

A *Drosophila* model showing an REP used for modifier screens, revealing an easy readout for interactions with modifiers suppressing (**Suppressor**) or enhancing (**Enhancer**) the model phenotype.

1.8.2 *Drosophila* models for Tau-induced neurodegeneration

Expression of Tau[WT] and two mutated variants in Tau-linked human FTDP-17 were previously described as neurodegenerative models in *Drosophila* [125]. Pan-neural expression (*elav¹⁵⁵-Gal4* [234]) of Tau[WT] and the two mutated variants Tau[R406W]

and Tau[V337M] caused key features of neurodegenerative disorders, similar to those seen in human: reduced lifespan, progressive neurodegeneration, enhanced toxicity of mutant Tau versus Tau[WT] and accumulation of abnormally phosphorylated Tau. However, no neurofibrillary tangles were observed in either of the models [125]. The Tau[V337M]-induced REP has been successfully used in an misexpression-based modifier screen for Tau-induced neurodegeneration [232].

Steinhilb et al. published models mimicking two different phosphorylation states of Tau [235, 236]. They introduced 14 missense mutations disrupting all 14 serine-proline (SP) or threonine-proline (TP) phosphorylation sites (see Figure 8). In the non-phosphorylatable Tau[AP] model, the 14 sites are changed to alanine-proline (AP). Mutations of the 14 sites resulting in glutamate were used to mimic a phosphorylated state (E14). The non-phosphorylatable Tau[AP] was reported to show a decreased neurodegeneration compared to Tau[WT] [236, 237]. In contrast, the Tau[E14] mimicking a state of hyperphosphorylation led to an increased toxicity [237]. This is in line with the suggested mechanisms of toxicity and emphasises a causative role of phosphorylation for Tau toxicity.

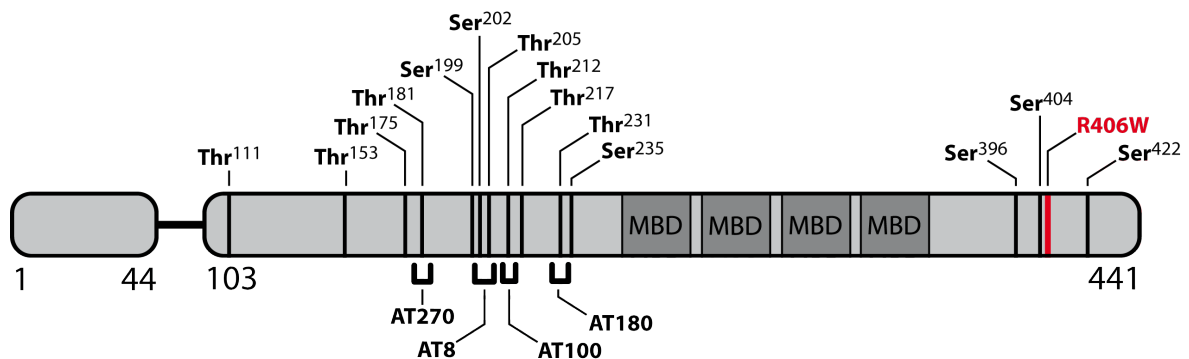


Figure 8: Mutated phosphorylation sites of phospho-specific Tau models and used phospho-specific antibodies.

The Tau[R406W] variant bears a missense mutation at amino acid number 406 (in red). The 14 either threonine or serine phosphorylation sites depicted above the protein are those mutated in the two phospho-specific Tau variants Tau[AP] and Tau[E14]. AT8, AT100, AT180 and AT270 are phospho-specific monoclonal antibodies used to determine the phosphorylation states of the depicted sites. The numbering of amino acids as used in literature is derived from the 4R2N Tau variant (isoform 2). The Tau variant used in this work is the 4R0N variant (isoform 3).

1.9 The conducted screen

The goal of this study was to perform a high-throughput genome-wide screen to find modifiers of Tau-induced neurodegeneration in *Drosophila* in order to elucidate pathological mechanisms and potential therapeutical approaches for Tauopathies. For that an easily detectable neuronal readout is required. As mentioned before, *GMR-Gal4*-driven expression of Tau results in a REP (see chapter 1.8.1), which can be utilised to screen for modifications as previously described [230, 232, 238]. A published screen on Tau[V337M] was based on misexpression approaches [232]. In contrast, the screen conducted in this study was based on a gene silencing approach, mimicking classical knockouts and it aims to target all *Drosophila* genes known to have a human homologue (Sub-library of the Vienna Drosophila RNAi Centre (VDRC) library [217]). UAS-shRNA fly lines were used, containing shRNA transgenes each directed against a distinct gene. These shRNAs were co-expressed with the toxic Tau[R406W] protein in the compound eye. The resulting phenotype was examined with respect to changes in the REP. A modification of the REP due to a knockdown by the RNAi effect might indicate a function of the silenced gene in the pathological pathway of Tau.

2 Material and Methods

In this work, genes, proteins, transgenes and flies are notated according to following rules. *Drosophila* genes and mRNA are written in italics and small letters. If referring to the human homologue, genes are written as the official short form according to Gene database [239] in capital letters. Candidate genes are always referred to as the human homologue genes. Transgenes, fly stocks and fly genotypes are written in italics according to Flybase nomenclature [240].

All materials and methods that were used in this study are listed below. Recipes for solutions are found in Table 3 and will only appear with their name in methods description.

2.1 Chemicals, buffers and equipments

Table 3: Chemicals and buffers

Name	Recipe or origin
Acridine Orange	3,6-bis[Dimethylamino]acridine (A-6014), Sigma, USA
Acrylamid	Acrylamid 2K (30 %), AppliChem, Germany
APS	Ammoniumperoxidisulfate \geq 98 % p.a. (9592.2), Roth, Germany
Bromophenol Blue	(A512.1), Roth, Germany
CaCl ₂ x 2H ₂ O	\geq 99 % p.a. (5239.2), Fluka, Germany
Chloroform	Trichlormethane/Chloroform \geq 99 % (3313.1), Roth, Germany
Citrate buffer	1.8 mM citric acid and 8.2 mM sodium citrate, pH 6.0
Citric acid	(1.00244.1000), Merck, Germany
DEPC	Diethylpyrocarbonat (K028.1), Roth, Germany (to treat H ₂ O: stir 0.1 % DEPC in bidest H ₂ O over night and autoclave)
Desflurane	Suprane, Baxter, Germany
DNase kit	RQ1 RNase-free DNase (M6101), Promega, USA
Drosophila's Ringer	182 mM KCl, 46 mM NaCl, 3 mM CaCl ₂ x 2 H ₂ O, 10 mM Tris, pH 7.2, autoclaved
DTT	1,4-Dithiothreit (6908.1), Roth, Germany
Ethanol	\geq 99,8 % p.a. (9065.4), Roth, Germany
FastDigest® BamHI	(FD0054), Invitrogen, Germany
FastDigest® BglII	(FD0083), Invitrogen, Germany
FastDigest® KpnI	(FD0524), Invitrogen, Germany
FastDigest® NotI	(FD0594), Invitrogen, Germany
FastDigest® XhoI	(FD0694), Invitrogen, Germany

Fluoromount	Fluoromount-G (0100-01), SouthernBiotech, USA
Glycerol	99 % (G5516-1L), Sigma, USA
Glycine	≥ 99 % p.a. (3908.2), Roth, Germany
HEPES	≥ 99.5 % p.a. (9105.4), Roth, Germany
HL3 buffer	70 mM NaCl, 5 mM KCl, 20 mM MgCl, 10 mM NaHCO ₃ , 5 mM Trehalose, 115 mM Sucrose, 5 mM HEPES, pH 7.2
Immun-Star™	Immun-Star™ WesternC™ Kit (170-5070), Bio-Rad, USA
iQ™ SYBR® Green Supermix	(170-8882), Bio-Rad, USA
iScript™ cDNA Synthesis Kit	(170-8890), Bio-Rad, USA
Isopropanol	2-Propanol (T910.1), Roth, Germany
KCl	≥ 95.5 % p.a. (6781.1), Roth, Germany
KH ₂ PO ₄	≥ 99 % p.a. (3904.1) Roth, Germany
Laemmli lysis buffer (2X)	0.004 % Bromophenol Blue, 400 mM DTT, 20 % Glycerol, 4 % SDS, 125 mM Tris, pH 6.8
Methanol	(717.1), Roth Germany
Methylbenzoat	(8.22330.1000), Merck, Germany
MgCl	≥ 98.5 % p.a (KK36.1), Roth, Germany
Na ₂ HPO ₄ x H ₂ O	≥ 99.5 % p.a. (1.06580.1000), Merck, Germany
NaCl	≥ 95.5 %, p.a., Roth, Germany
NaH ₂ HPO ₄ x H ₂ O	≥ 99 % p.a. (1.06342.1000), Merck, Germany
NaHCO ₃	≥ 99 % pure (8551.1), Roth, Germany
NGS	(S-2007), Sigma, USA
Nitrocellulose membrane	Protran® BA 83 (10 402 396), Whatman®, Germany
Paraffin	32.3 % Paraffin 42-44 (107150), 32.3 % Paraffin 51-53 (107157), 32.3 % Paraffin 57-60 (107158), all Merck, Darmstadt, Germany and 3.2 % bees wax (5825.2), Roth, Karlsruhe, Germany
PBS	8 mM Na ₂ HPO ₄ x 2 H ₂ O, 1.8 mM NaH ₂ HPO ₄ x H ₂ O and 0.1 M NaCl
PBT	0.14 M NaCl, 6 mM Na ₂ HPO ₄ , 2.7 mM KCl, 1.5 mM KH ₂ PO ₄ , 0.05 % Triton
PFA (4 %)	4 % paraformaldehyde (0335.2 , Roth, Germany) in PBS
Qiagen RNeasy Mini Kit	(74106) Qiagen, Germany
Resolving gel buffer	0.4 % SDS, 1.5 M Tris, pH 8.8
RNase Inhibitor	RiboLock™ RNase Inhibitor 40 u/μl (EO0381), Fermentas, Germany
Running buffer	0.1 M Tris, 1 M Glycine and 0.5 % SDS
SDS	AccuGene 10 % SDS (51213), Cambrex, USA
SDS gel (10 %)	Resolving gel: 1.25 ml resolving gel buffer, 2.08 ml bidest H ₂ O, 1.67 ml acrylamid, 25 μl TEMED, 25 μl 10 % APS Stacking gel: 625 μl stacking gel buffer, 1.25 ml bidest H ₂ O, 625 μl acrylamid, 12.5 μl TEMED, 12.5 μl 10 % APS
Skim milk	Milk Powder (T145.2), Roth, Germany
Sodium acetate	Sodium acetate (1.06268.0250, Merck, Germany) 3 M in H ₂ O, pH 5.4
Sodium citrate	(1.06448.0500), Merck, Germany
Stacking gel buffer	4 % SDS, 0.25 M Tris, pH 6.8

Sucrose	D(+)-Saccharose \geq 99.5 % p.a. (4621.1), Roth, Germany
TBS	25 mM Tris and 140 mM NaCl, pH 7.5
TBS-T	25 mM Tris and 140 mM NaCl, pH 7.5, 0.05 % Tween
TEMED	N,N,N',N'-Tetramethylethylenediamide, AppliChem, Germany
TOPO TA kit	TOPO TA Cloning® Kit Dual Promoter pCR®II-TOPO® vector (45-0640) Invitrogen, Germany
Transfer buffer	25 mM Tris, 192 mM glycine and 20 % methanol
Trehalose	D(+)-Trehalose Dihydrat (5151.1), Roth, Germany
Tris	\geq 99.3 % (AE15.2), Roth, Germany
Triton	Triton X100, Sigma, USA
Trizol®	TRIzol® Reagent (15596-026), Invitrogen, Germany
Tween	Tween® 20 (9127.1), Roth, Germany
Vectashield	Vectashield mounting medium, Vector, USA
Xylol	Otto Fischar, Germany

Table 4: Equipment

Name	Trade name and origin
Leica inverse	DMI 6000B with camera DFC 420, Leica, Germany
Microtome	Thermo Scientific microtome HM 360
Olympus binocular	SZX10 with ring light S80-55 RL and camera SC30, Olympus, Germany
Olympus BX51	BX51 with light source X-Cite® 120 Q and camera DP72, Olympus, Germany
Speedmill	Speedmill P12, Analytik Jena AG, Germany
Real-time cycler	MyiQ2 two colour realtime cycler, Bio-Rad, Germany
Western blot documentation	Alliance LD4.77.WL.Auto, Biometra, Germany
Zeiss Axiovert	Zeiss Axiovert with LSM710 scan head and Plan-Apochromatix X63 oil 0.55 NA objective, Carl Zeiss, Germany
Scanning electron microscope	ESEM XL 30 FEG, FEI, Eindhoven, Netherlands

Table 5: Software and online tools

Name	Purpose
Adobe Illustrator CS4	Compilation of illustrations and figures
Adobe Photoshop CS4	Rotation and clipping of phenotypic images / Clipping of western blot images
http://blast.ncbi.nlm.nih.gov	Alignments for detailed determination of gene homologues between <i>Drosophila melanogaster</i> and <i>Homo sapiens</i> .

GraphPad Prism	Illustration of quantitative data (qPCR, time-lapse etc.) and according statistics
Olympus Cell A	Documentation of rough eye phenotypes
Olympus Cell F	Documentation of immunohistochemical micrographs
Sequencher 4.10.1	Handling sequence files, designing cloning strategies and primers
http://www.ncbi.nlm.nih.gov/tools/primer-blast/	Generating primers in high numbers for qPCR analysis
Leica Application Suite®	Documentation of acridine orange stainings of eye imaginal discs
ImageJ 1.42	Analysis for CSP accumulations and transport rates and speeds
Zen 2009	Carl Zeiss software for confocal microscope systems
iQ5	Handling of MyiQ2 real-time cycler and documentation of qPCR
Alliance UVItec 15.11	Software for documentation of Western blots
Axiovision 4.8.1	Carl Zeiss Software for light microscope systems
BioDoc Analyse 2.1	Software for quantification of Western blots

2.2 Transgenic animals and fly keeping conditions

Flies were kept at a temperature of 18 °C (± 1 °C) and a relative humidity of at least 50 % on standard food. Unless otherwise specified, experiments with embryos, larvae and adult *Drosophila melanogaster* were conducted at a temperature of 25 °C (± 1 °C) and a relative humidity of at least 50 %.

Table 6: Obtained transgenic *Drosophila melanogaster* fly strains used in this study

Transgenic line	Genotype ¹	Origin
<i>Tau[R406W]</i>	<i>w[*];;P{w[+mC]=UAS-hTau[R406W]}</i>	Wittmann <i>et al.</i> [125]
<i>Tau[WT]</i>	<i>w[*];;P{w[+mC]=UAS-hTau[WT]}</i>	Wittmann <i>et al.</i> [125]
<i>GFP</i>	<i>w[*];P{w[+mC]=UAS-eGFP}/CyO</i>	Dr. Aaron Voigt
<i>Oregon R</i>	<i>wildtype</i>	Bloomington #5
<i>GMR-Gal4</i>	<i>w[*];P{w[+mC]=Gal4-ninaE.GMR}12/CyO</i>	Bloomington #1104
<i>elav^{C155}-Gal4</i>	<i>P{w[+mW.hs]=GawB}elav[C155]</i>	Bloomington #458
<i>Aβ₄₂</i>	<i>w[*];P{w[+mC]=UAS-Aβ₄₂}</i>	Finelli <i>et al.</i> [241]
<i>Q78bl</i>	<i>w[*];P{w[+mC]=UAS-MJD.tr-Q78}c211.2</i>	Bloomington #8150
<i>Tau[AP]</i>	<i>w[*];P{w[+mC]=UAS-hTau[AP]}</i>	Steinhilb <i>et al.</i> [235, 236]
<i>Tau[E14]</i>	<i>w[*];P{w[+mC]=UAS-hTau[E14]}</i>	Steinhilb <i>et al.</i> [235, 236]
<i>CxD/TM3</i>	<i>y[1],w[*];CxD/TM3,Sb[1],Ser[1]</i>	Bloomington #6309
<i>D42-Gal4</i>	<i>w[*];;P{w[+mW.hs]=GawB}D42/TM3,Sb[1],Ser[1]</i>	Bloomington #8816
<i>mitoGFP</i>	<i>w[1118];P{w[+mC]=UAS-mitoGFP.AP}3</i>	Bloomington #8443

¹ genotype is written in the format suggested by Flybase [240]

RNAi fly lines were obtained from the library of the Vienna *Drosophila* RNAi Centre (VDRC) [217] and were generated by random integrations of transgenes transcribing shRNAs under control of the UAS-Gal4 system into the *Drosophila* genome (*UAS-shRNA*). The RNAi lines used in this study are a subset of 7881 RNAi lines silencing all *Drosophila* genes with known or predicted human homologues selected by the VDRC (complete list in the appendix). Fly lines that were used to verify candidate shRNA effects induced by GMR-mediated expression in the screening model are listed in the appendix. These include misexpression lines, deficiencies and amorphic alleles obtained from Bloomington Stock Centre, Indiana, USA and additional RNAi lines obtained from either Bloomington Stock Centre or from NIG-Fly (Genetic Strain Research Centre, National Institute of Genetics, Mishima, Shizuoka, Japan).

2.3 Site-directed integrations

The plasmids for site-directed integration of transgenes *attB_Tau[WT]*, *attB_Tau[R406W]*, *attB_Tau[AP]* and *attB_Tau[E14]* were generated utilizing existing Tau transgenic animals (Table 6). The DNA fragments coding for Tau[WT] and Tau[R406W] were amplified from genomic DNA of *Tau[WT]* and *Tau[R406W]* flies obtained from Wittmann *et al.* [125], the fragments coding for Tau[AP] and Tau[E14] from *Tau[AP]* and *Tau[E14]* flies from Steinhilb *et al.* [235, 236] by using the primers TauATG (ATGGCTGAGCCCCGCCAG) and TauSTOP (CACAAACCCTGCTTGGCCAGG). The fragments were cloned into *pCR®-II* Topo TA vector (using the dual promotor *pCR®-II* kit) and subcloned into *pUAS-attB* vector used to create site-directed integrations into the *Drosophila* genome using the ϕ C31 integrase [242]. Sub-cloning strategies using FastDigest® enzymes are shown in Table 7.

Table 7: Strategies for sub-cloning into pUAS-attB

Tau variant	Direction in pCR®-II	Enzymes for digestion of donor	Enzymes for digestion of pUAS-attB (acceptor)
Tau[WT]	sense	<i>NotI</i> , <i>KpnI</i>	<i>NotI</i> , <i>KpnI</i>
Tau[R406W]	antisense	<i>BamHI</i> , <i>XhoI</i>	<i>BglII</i> , <i>XhoI</i>
Tau[AP]	antisense	<i>BamHI</i> , <i>XhoI</i>	<i>BglII</i> , <i>XhoI</i>
Tau[E14]	antisense	<i>BamHI</i> , <i>XhoI</i>	<i>BglII</i> , <i>XhoI</i>

Transgenic fly lines were generated by BestGene, USA. The plasmids were injected into flies with the attP integration site at the estimated genomic location 76A2 (3rd chromosome) (*y[1],w[1118];;PBac{y+-attP-9A}VK00013*). Flies obtained from BestGene were balanced using balancer stock *CxD/TM3* (Table 6). In this work four generated transgenic fly lines are referred to as *attB_Tau[WT]* (*PBac{attB[+mC]=UAS-hTau[WT]}VK00013*), *attB_Tau[R406W]* (*PBac{attB[+mC]=UAS-hTau[R406W]}VK00013*), *attB_Tau[AP]* (*PBac{attB[+mC]=UAS-hTau[AP]}VK00013*) and *attB_Tau[E14]* (*PBac{attB[+mC]=UAS-hTau[E14]}VK00013*). To differentiate between Tau protein being expressed by random and by site-directed integration transgenes, Tau protein expressed by site-directed integration transgenes from now on is notated as attB-Tau (*attB_Tau[WT]*, *attB_Tau[R406W]*, *attB_Tau[AP]* and *attB_Tau[E14]*).

2.4 Breeding procedures

For the primary (see chapter 3.3.2) as well as for the secondary screens (see chapter 3.5) breeding procedure are identical. *GMR-Gal4* and Tau expressing flies (*Tau[R406W]*, *attB_Tau[WT]*, *attB_Tau[R406W]*, *attB_Tau[AP]* and *attB_Tau[E14]*) (Table 6 and chapter 2.3) were used to create five screening stocks: *GMR_Tau[R406W]*, *GMR_attB_Tau[WT]*, *GMR_attB_Tau[R406W]*, *GMR_attB_Tau[AP]* and *GMR_attB_Tau[E14]* (Table 8). For the screens these stocks were crossbred with the *UAS-shRNA* fly lines from VDRC. In addition, the *GMR-Gal4* fly itself was used as a control screening stock, showing effects by expression of the shRNA *per se*.

The random integrations of shRNA constructs in the VDRC lines affect chromosomes one, two and three. RNAi lines with integration on the first chromosome (gonosome X) were generated as lines with an additional artificial double X (dX) gonosome (male XY; female dXY; dXX is lethal). As integrations are found on the normal X gonosome, only male flies contain the shRNA transgene. Therefore, virgins of the screening stocks were crossbred to male flies of the RNAi lines and effects were analysed in female offspring.

Table 8: Stocks used for the screening procedure

Screening stock	Genotype
<i>GMR_Tau[R406W]</i>	<i>w[*];P{w[+mC]=Gal4-ninaE.GMR}12/CyO;P{w[+mC]=UAS-hTau[R406W]}/TM3,Sb[1]</i>
<i>GMR_attB_Tau[WT]</i>	<i>w[*];P{w[+mC]=Gal4-ninaE.GMR}12/CyO;PBac{attB[+mC]=UAS-hTau[WT]}VK00013</i>
<i>GMR_attB_Tau[R406W]</i>	<i>w[*];P{w[+mC]=Gal4-ninaE.GMR}12/CyO;PBac{attB[+mC]=UAS-hTau[R406W]}VK00013</i>
<i>GMR_attB_Tau[AP]</i>	<i>w[*];P{w[+mC]=Gal4-ninaE.GMR}12/CyO;PBac{attB[+mC]=UAS-hTau[AP]}VK00013</i>
<i>GMR_attB_Tau[E14]</i>	<i>w[*];P{w[+mC]=Gal4-ninaE.GMR}12/CyO;PBac{attB[+mC]=UAS-hTau[E14]}VK00013</i>

2.5 Phenotypic analysis

In order to evaluate REP of flies, at least ten flies including females were used to determine REP severity. Modifications of the screening phenotype induced by shRNA expression (*GMR_Tau[R406W]* X *UAS-shRNA*) were categorized as follows: “wild type like phenotype”, “obvious suppression”, “subtle suppression”, “no change”, “subtle enhancement”, “obvious enhancement” and “lethal”. Modifications of the eye phenotype

induced by shRNA alone (*GMR-Gal4 X UAS-shRNA*) were characterised as “no change”, “subtle enhancement” or “obvious enhancement”. shRNAs leading to any change of the control phenotype were excluded from the screen, as the shRNA effect then is thought to be independent of Tau[R406W]-induced pathology. Expression of shRNAs that did not show any effects in the control but did show at least obvious changes in the Tau[R406W]-induced phenotype were included as suppressing/enhancing the Tau[R406W]-induced REP in detailed analysis.

2.6 Documentation of compound eye phenotypes

Pictures of *Drosophila* compound eyes were taken using the Olympus binocular (Table 4) and the Olympus Cell A software (Table 5). Selected REP were documented using scanning electron microscopy (**SEM**). Unfixated and uncoated flies were imaged using the ESEM scanning electron microscope (Table 4) in “low vacuum mode” (0.8-1.5 Torr) and an accelerating voltage of 10 kV. Adobe Photoshop CS4 was used to rotate and clip all images. Orientation of all compound eye phenotype images in this work is anterior-left and dorsal-up.

2.7 Cell death events in eye imaginal discs

Dissection and acridine orange stainings on eye imaginal discs of L3 larvae have been conducted according to Sullivan and Ashburner [243]. Eye imaginal discs were dissected in *Drosophila's* Ringer solution containing 1.6×10^{-6} M acridine orange dye. Preparation of GMR-mediated GFP expressing eye imaginal discs was done in *Drosophila's* Ringer only. Dissected eye imaginal discs were placed into a drop of the Ringer medium on a glass slide and covered with cover slides. Pictures of the eye imaginal discs were directly acquired with the Leica fluorescence microscope using 20x and 40x objectives and Leica application Suite® software.

2.8 Longevity analysis

To evaluate life span, male flies with the genotype of interest raised at 25 °C were selected, grouped into vials containing 20 individuals and kept at 29 °C for the longevity experiment. Events (dead flies or exclusions) were counted at least every second day and flies were flipped to fresh food every two to three days. For Kaplan-Meyer plotting and statistical analysis GraphPad Prism was utilised. Log-Rank test was conducted for comparison of two longevity curves and P-values were corrected using the Bonferroni correction for multiple testing.

$$p_{corr} = p * K \quad \text{with} \quad K = \text{number of testings conducted}$$

2.9 Quantification of mRNA levels using qPCR

For RNA preparation from fly heads 30 heads were lysed in 100 µl Trizol using the speedmill (Table 4) and prepared for next step via chloroform extraction (using 50 µl of chloroform). The aqueous phase was mixed with 100 µl 70 % ethanol and RNA was purified from this solution using the Qiagen RNeasy kit as described in the supplier's instructions. 2.5 µg of RNA from column eluate were treated with DNase (DNase kit, Table 3) as recommended by supplier with additional 0.5 µl RNase inhibitor. Afterwards, the DNase-treated RNA was precipitated using 2 volumes H₂O (DEPC-treated, see Table 3, 67 µl), 0.3 volumes sodium acetate (3 M, 10 µl) and 2.1 volumes isopropanol (70 µl).

1 µg of sample RNA was reverse transcribed using the Iscript cDNA synthesis kit following manufacturer's instructions. The cDNA samples were diluted tenfold with DEPC treated H₂O (quantification of Tau mRNA was done from non-diluted samples, chapter 3.1.3).

Quantitative polymerase chain reaction (**qPCR**) from cDNA samples was conducted using the iQ™ SYBR® Green Supermix and the MyiQ2 real-time cycler with iQ5 software. Measurements were done in film-covered microtiter plates. Reaction was composed as recommended by the iQ™ SYBR® Green Supermix supplier with a total volume of 15 µl (1 µl cDNA and 5 pmol of each primer, see Table 9 for primer list). The general protocol used for real-time analysis was as follows.

30 seconds at 95 °C
 2 x 3 minutes at 95 °C for acquisition of internal well factor
 3 minutes at 95 °C
 40 repeats of:
 10 seconds at 95 °C
 30 seconds at 55 °C
 30 seconds at 72 °C with data acquisition
 10 seconds at 95 °C
 30 seconds at 55 °C
 41 repeats of 30 seconds starting at 55 °C, increasing 1 °C with each step for melt curve acquisition

Table 9: Primers used for quantification of transcript levels using qPCR

Target	Primers used¹
General	
<i>actin5C</i>	CCAGTCATTCTTTCAAACC, GCAACTTCTTCGTCACACATT
<i>elav</i>	TGACAACAGCCATTGGCCGG, TCCCACACTCTCTTCGGTTGTCC
<i>mapt</i> (hTau)	AAGAGGGTGACACGGACGCT, CATGCGAGCTTGGGTCACGT
<i>rp49</i>	TCGGATCGATATGCTAAGCTGTCGCAC, AGGCGACCGTTGGGGTTGGTGAG
<i>tau</i> (dTau)	GCCACGCCCTCGAACAAGTC, GGTGAAGGCGCATGTCCGAC
Targeting candidate genes	
ADHFE1	CTCCAACCGCCTCCCAAACG, TGCGAAGATCGGCTCCCCT
BM11	CCCATCCGCGGTTTCCAGTG, CATTGCGTTCGCGACAGCC
C17orf90	CAACGACGGGCACTGACACTC, TGTGCGTAGTCCAGCCAAACG
C18orf32	GCGGAAAACACAACGCACACAA, TTGCCGCTCTTCAAGGGCCA
C4orf31	CCCAGCAACGATGACGAGGC, TGCAATGGTGGCTCTGCTGC
CDC20	TCTAAGACGCCAGGAGGCGG, TTGCTGTTGCTCGAGGTGGC
DAB1	ATCCGGGACGCTTTTTTCGGC, CGCCCGGATGGCCATTTTTGA
DCTN1	AGCGACACGGCCATTGCAAA, ACGTGCTGATCGCTTGGCAG
DDX42	TCCATCTGCAACCAGGTGCG, TGGCCTCGTTCAGGTCTCCC
DSTN	GCAACATCGCTACGCGGTCT, TTGGATCCGGCACGTTGCAG
FLOT2	GATCGCGAGCTCACTGGCAC, GGGCACCCCTCGATGGTCTGA
HIPK2	AAGGAGTCGCCGGCTCATCA, CGGCGAGCTTTCCTTACCC
HM13	CCTCCTGGTGGCCCTCATCC, TGACGCCCTCGTCTTCTCC

IGF2R	AACGGAATCGCACCTTCGCC, CGAACGTAGCACGGGCTGTC
IGFALS	CCTGTCCGGAGCTCAGTCCC, ATCGCCGTGGAAGACAACGC
LAMTOR31	GCACCGAAGATCCAGGTGCG, GCTGAGGCCATCGGAGTTGC
LAP3	TGTCAGTGCTACGTCCGAACTGA, TCTTCGATTTTCTGTGCCGCTTCA
LMO7	GTA CTGGCACATGCCGCTGAT, CGCTCTCTGCCCGATCGACT
MAD1L1	TTCAACCGGCTTTCCGCCTC, AGCCATGGAATCGTTGGCGG
MED14	AGTCCATTGCCAAGCTGCC, ACGGAAACGCAACTCCAGGC
MORF4L1	GCTTCCACGGACCGCTCATC, TGAGGACTCGGTTCTCGGGC
NEDD8	TCAAGGAGCGCGTGGAGGAA, TGCAC TTTGTAGTCCGCCGC
PARD6G	TGATCGGGCGGATCGGAGAA, CGCTTGAAGCTCCACCTCCG
PTRH2	CGGACCAGGATCCCGTGAA, ACTTGCCGAAGGCCAAAACCG
RAB30	AGCCGTTGGCCAGCTAGTGA, TCCTCCATTGGGGATGTTGCCA
RDBP	CGGCAACAAGGTCACCGAGG, CGACTCGGGTTTGGCGAAGG
RPS10	AGGCGCTCCAAAACCGATG, CGTAGCGAGAAGCACGACCG
SCAMP1	TCGCCCGCTCCTATGTCTG, CCACCGCTGCACAATCGAG
SMG5	CCAGCGAGTGCCCATAGAC, CCAGTTGCTTGGAGGCGGTG
TEX261	CTGGGATGGGTTTCGCTGGC, GATGCACTTCCTAGCCGCCG
TMEM135	TGCAGTTGGGATTGGCGCTG, GCCGGAATGGCGAAGAGAGC
TRAPPC9	ACGGGGACGGACATTCAGGG, GCTGCACGAGCGTGCTTGA
TRMT2A	GGTGGCGGAAGCTCTCTACG, TCGGCTGATCGAATTGCGGC
UCK2	TCGAGGAGTTCTGCTCGCCC, TGTGCGCTGTTGGTAGTGGC
ZBTB20	CTGGCGATGTGTCCGGTTCG, GCGGCTTGTAACACGGACGA
ZNF800	GCTGACCTTTCTGCAGGCCG, GCCCTTCGGCTGCACATCTC

¹ Primers were all generated by Invitrogen, Germany

The raw data generated by iQ5 software (Ct values) were analysed according to Vandesompele *et al.* [244] using either Δ Ct or $\Delta\Delta$ Ct analysis. For quantifications of Tau transcript levels (dTau and hTau, chapter 3.1.3), measurements were performed using mRNA levels of *actin5C* for normalisation. Significance was tested using t-test analysis in GraphPad Prism. Measurements of RNAi effects (chapter 3.3.5) were normalised with a normalisation factor combining transcript levels of *elav* and *rp49*. One-sample t-test was calculated using GraphPad Prism comparing results to a hypothetical mean of 1.0.

2.10 Immunochemical evaluation of protein levels

All protein blot analyses were done using the same protocol. Adult fly heads were lysed in 2 x Laemmli lysis buffer (10 μ l per head) in the speedmill. Lysates were incubated for 5 minutes at 95 °C and stored at -20 °C. Prior to electrophoresis, heat treatment was

repeated. Proteins were separated in 10 % SDS gels using running buffer (Table 3, 1.5 hours at 100 V) and transferred to nitrocellulose membrane in a semi-dry blotter using transfer buffer (Table 3, one hour at 225 mA per blot). Nitrocellulose membranes were blocked with skim milk (0.5 % in TBS) for one hour and incubated with primary antibodies over night at 4 °C (in TBS with 0.05 % skim milk, antibody concentrations as listed in Table 10). After washing steps (thrice 5 minutes in TBS-T), blots were incubated with horseradish peroxidase-coupled α mIgG secondary antibody in TBS containing 0.05 % skim milk for one hour at RT. After washing steps (thrice 5 minutes in TBS-T) blots were incubated with Immun-Star™ chemiluminescence reagent and analysed with Alliance LD4 documentation system and Alliance UVItc software. For quantification of band intensity BioDoc Analyse software was used.

Table 10: Antibodies used for immunoblotting

Antibody	Recognises	Used concentration	obtained from
primary antibodies			
AT8	Tau with phosphorylation of Ser ²⁰² and Thr ²⁰⁵	1:250	Abcam
AT180	Tau with phosphorylation of Thr ²³¹	1:250	Abcam
AT270	Tau with phosphorylation of Thr ¹⁸¹	1:250	Abcam
5A6	pan-hTau	1:100	DSHB
8C3	Syntaxin	1:5,000	DSHB
secondary antibody			
α mIgG	mouse Immunglobulin (HRP coupled antibody)	1:10,000	Pierce

2.11 Immunohistochemical staining of paraffin sections

Heads of adult female flies were fixated in 4 % PFA for 60 minutes before they were dehydrated (30 minutes in each: 70 %, 80 %, 90 %, twice in 100 % ethanol). After 60 minutes incubation in methylbenzoat fly heads were incubated for three times 30 minutes in 62 °C paraffin before they were embedded and paraffin was hardened over night at RT. Embedded fly heads were cut into 5 μ m thick frontal sections using a Thermo Scientific microtome. Sections were incubated twice for 20 minutes in Xylol, rehydrated (five minutes in each: twice in 100 %, 90 %, 80 %, 70 %) and then incubated for five minutes in PBS. A denaturing step was carried out in citrate buffer (Table 3) for 10 minutes at 1000 W in a microwave oven. Afterwards sections were again washed in PBS for five minutes,

blocked for 30 minutes in 3 % NGS and incubated over night at 4 °C with the primary antibody in PBS (concentration as listed in Table 11). After washing for five minutes in PBS, sections were incubated for 30 minutes with Alexa488-coupled secondary antibody in PBS (according to Table 11) followed by a last washing step in PBS for five minutes, and mounting using Fluoromount. Images shown in this work were taken with the Olympus BX51 and the Cell-F software.

Table 11: Antibodies used for immunohistochemical stainings

Antibody	Species	Recognises	Used concentration	Obtained from
primary antibodies				
TauC3	mouse	Tau truncated at amino acid 421	1:100	Abcam
Lamp1	rabbit	lysosomal protein Lamp1	1:1000	Abcam
5A6	mouse	pan-hTau	1:1000	DSHB
secondary antibodies				
α mIgG(488)	goat	mouse Immunglobulin (Alexa488)	1:500	Invitrogen
α rbIgG(488)	goat	rabbit Immunglobulin (Alexa488)	1:500	Invitrogen

2.12 Immunohistochemical stainings in *Drosophila* larval motorneurons

Filet preparations for stainings of *Drosophila* larval motorneurons were performed according to Sullivan and Ashburner [243]. L3 larvae were covered with HL3 buffer (Table 3). The bodywall was cut at a medial longitudinal line at the dorsal side, pinned down and inner organs were removed except from CNS and segmental nerves. Afterwards HL3 medium was replaced by 4 % PFA and filets were fixated for ten minutes. Fixative then was replaced by PBT. Filets were transferred into a reaction vial, blocked for 30 minutes in PBT containing 5 % NGS on a rotating wheel (applies to all incubation steps) and incubated with primary antibodies (see Table 12) in PBT containing 5 % NGS over night at 4 °C. Filets were washed three times for 20 minutes in PBT, incubated with secondary antibodies in PBT containing 5 % NGS (antibody concentrations see Table 12) for two hours at RT, washed thrice for 20 minutes in PBT and incubated for 30 minutes at 4 °C in Vectashield mounting medium. Finally, samples were placed on glass slides and mounted with Vectashield.

For evaluation of NMJ morphology z-stacks taken with the Zeiss Axiovert microscope, were combined to maximum projections and coloured with pseudo-colours using the ZEN 2009 software.

Table 12: Antibodies used in stainings of larval motorneurons

Antibody	Species	Recognises	Used concentration	obtained from
primary antibodies				
12G10	mouse	alpha-Tubulin	1:10	DSHB
6D6	mouse	CSP (synaptic vesicles)	1:50	DSHB
5A6	mouse	pan-hTau	1:500	DSHB
secondary antibodies				
α mIgG(488)	goat	mouse Immunglobulin (Alexa488)	1:500	Invitrogen
HRP-Cy3	rabbit	neuronal membranes	1:500	Jackson ImmunoResearch

2.13 Quantification of CSP accumulations in segmental nerves

For quantification of larval segmental nerves (dissection see 2.12) affected by CSP accumulations, pseudo z-stacks of a 20x visual field of all present segmental nerves proximal to the ventral ganglion were generated (5 images automatically shifted 3 μ m along the z-axis as a stack, Axiovision software). For every genotype five larvae were analysed. The image files were then analysed in a blinded manner. For every image stack all segmental nerves and segmental nerves affected by obvious CSP accumulations were counted using ImageJ software.

2.14 *In vivo* time-lapse quantifications of axonal transport

In vivo analysis of transport was performed as described previously [245]. In order to analyse axonal transport, mitoGFP (labels mitochondria with GFP [246]) was expressed in motorneurons together with Tau[R406W] and shRNAs under control of *D42-Gal4* [247]. Expressing of only mitoGFP were analysed as a control. Larvae were anaesthetised using desflurane and mounted on the imaging chamber. For imaging, a Zeiss Axiovert microscope with a LSM710 scan head and a Plan-Apochromatix X63 oil 0.55 NA objective was utilised. Imaging was performed at 19 °C. A small segment of a segmental nerve proximal to the larval ventral ganglion was bleached and movement of

GFP-labelled mitochondria was recorded in this bleached area. Movies were recorded using the ZEN 2009 software and analysed using the freeware ImageJ.

Measurements of speeds were performed using two imaginary lines crossing the nerve within the bleached area. In the movies taken, time is measured for GFP positive particles to travel from one line to another (t). The measured distance (d) of the two lines is used to calculate the speed (v) of transport. This is done for particles travelling in both directions, resembling anterograde and retrograde axonal transport, respectively.

$$v\left[\frac{\mu\text{m}}{\text{s}}\right] = \frac{d[\mu\text{m}]}{t[\text{s}]}$$

In order to quantify the rates of axonal transport particles are counted crossing an imaginary line in the bleached area. Moving particles for both directions were counted representing anterograde and retrograde axonal transport, respectively. Transport rates are calculated as number of particles (N) crossing this line per time frame (t). For increase in information value, the calculations are corrected for the diameter of the segmental nerve to have an estimation of rates passing the line in the whole cross section. The diameter of the recorded nerve (d_R) and the mean diameter of segmental nerves ($d_M=57 \mu\text{m}$) are included in the calculation.

$$\text{rate}\left[\frac{\text{particles}}{\text{s}}\right] = K * \frac{N}{t * \pi * \frac{d_R^2}{4}} \quad \text{with} \quad K = \pi * \frac{d_M^2}{4}$$

3 Results

As described in chapter 1.9 the aim of this work is to identify modifiers of Tau induced pathology. This was done in a genetic modifier screen using an RNAi-based approach and the REP induced by Tau as a readout (see chapter 1.8.1). Thus, characterisations of the used transgenes were performed according to their REP induction and life span.

3.1 Characterisation of the used *Drosophila* transgenes

Two transgenic lines modelling Tau-induced toxicity were kindly provided by Mel Feany [125]. The two transgenes *Tau[WT]* ($P\{w[+mC]=UAS-hTau[WT]\}$) and *Tau[R406W]* ($P\{w[+mC]=UAS-hTau[R406W]\}$) were used to model Tau-induced neurodegeneration (FTDP-17). Besides Tau, two other transgenes were evaluated for induction of a REP, when expressed in the compound eye: *A β ₄₂* ($P\{[+mC]=UAS-A\beta_{42}\}$) used to model amyloid-induced AD [241] and *Q₇₈* ($P\{[+mC]=UAS-MJD.tr-Q78\}$) used to model the poly-glutamine disease spinocerebellar ataxia type 3 [248]. These two Tau unrelated transgenes were utilised to analyse specificity of found modifiers for Tau pathology.

3.1.1 Rough eye phenotypes of the models

For the evaluation of transgene-induced toxicity in photoreceptors, the transgenes were expressed in post-mitotic cells of the compound eye (*GMR-Gal4* [233]). Several controls for eye appearance were used (Figure 9 A-D). In contrast to the wildtype eye phenotype (Figure 9 A), a very subtle REP was visible after GMR mediated Gal4 expression (Figure 9 B). Comparable phenotypes could be observed in GFP expression (transgene $P\{[+mC]=UAS-eGFP\}4$) and transcription of a control shRNA (shRNA directed against ZIC4) (Figure 9 C, D).

GMR-Gal4 mediated expression of *Tau[WT]* and *Tau[R406W]* showed a severe REP, with loss of texture and reduced size of the compound eye (Figure 9 E, F). In flies expressing *Tau[R406W]*, necrotic spots in the eye could be observed occasionally. Since the *Tau[R406W]*-induced phenotype was found to be more robust, with only minor inter-individual differences compared to *Tau[WT]*, GMR-mediated expression of the mutant variant *Tau[R406W]* was chosen for further analysis and the modifier screen.

The REP induced by expression of *A β ₄₂* (Figure 9 G) did not differ from the control phenotypes (Figure 9 B-D) (in contrast to published data [241]). Nevertheless,

enhancement of the phenotype induced by modifiers should be observable. Expression of Q_{78} (a C-terminal fragment of MJD containing a stretch of 78 glutamines) induced a severe REP. Although the eye size is not affected by Q_{78} expression, texture and ommatidial structure are impaired and dints as well as necrotic spots occur (Figure 9 H).

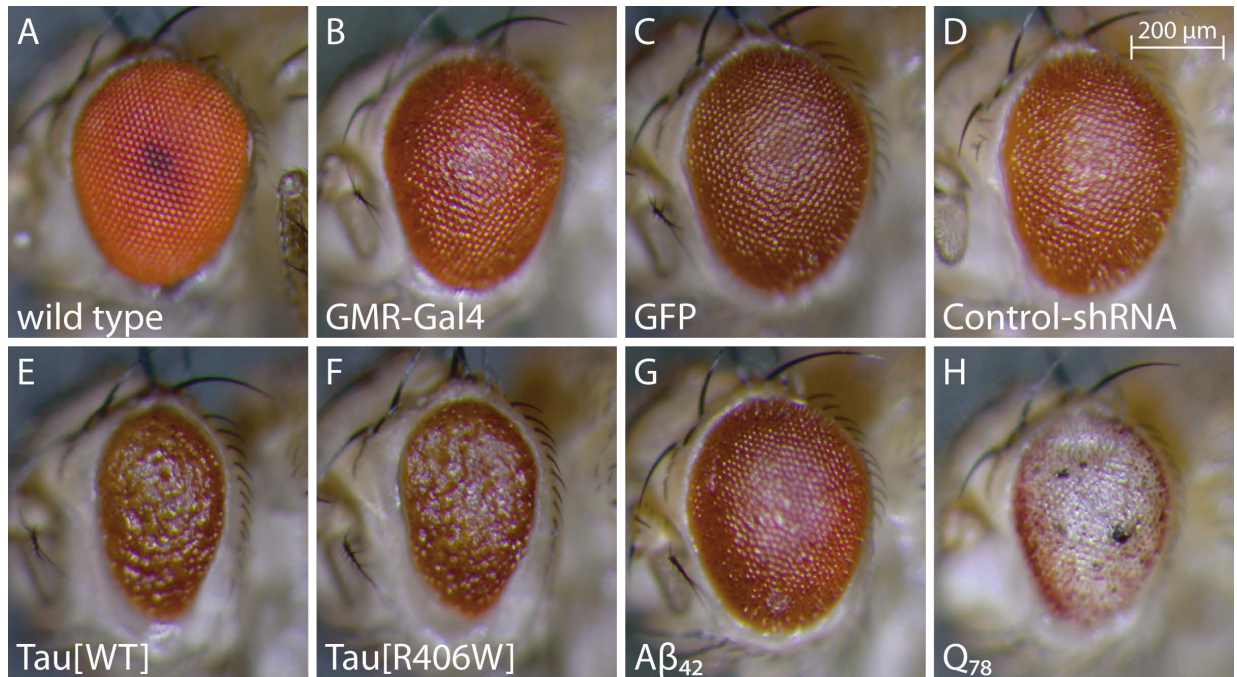


Figure 9: Phenotypes induced by GMR-mediated expression of the different transgenes.

Compound eye phenotypes of wildtype flies (A), control situations (B-D) and flies expressing transgenes modelling neurodegenerative diseases (E-H). Compared to wildtype flies (A), the *GMR-Gal4* driver alone induces a subtle REP (B), which is also present in *GMR-Gal4* mediated GFP expression (C) and control shRNA transcription (D). Expression of either Tau[WT] (E) or Tau[R406W] (F) induces a severe REP with disturbances of ommatidial structure and eye size. The REP induced by Gal4-mediated expression of $A\beta_{42}$ (G) is not distinguishable from the phenotypes of control situations. Severe changes of eye texture, accompanied by dints and necrotic spots are found in expression of the Q_{78} fragment (H). Orientation of the images is dorsal-up and cranial-left. The magnification is depicted in D (bar = 200 μ m).

3.1.2 Developmental effects of Tau expression

As the REP is a sign of neurodegeneration already present after hatching of the adult fly, larval eye progenitors were examined to determine the onset of neurodegenerative effects. The structure in *Drosophila* L3 larvae, which will form the compound eye, is called eye imaginal disc. The eye imaginal disc is a two-layered epithelial sack-like structure connected *posterior* to the optic lobes and *anterior* to the antenna imaginal disc (Figure 10 A). During development specification of neurons takes place in a spatiotemporal order starting *posterior*. The so called morphogenic furrow (MF) represents the border of neuron specification dividing post-mitotic neuronal precursor cells on the *posterior* and

yet unspecified cells on the *anterior* side is [249, 250]. The GMR-mediated expression of transgenes is specific for post-mitotic cells *posterior* of the MF (Figure 10 B). Loss of cells leading to the REP observed in adult flies might be already visible in the imaginal disc of the *Drosophila* compound eye [229, 251]. To examine cell death events induced by Tau expression, eye disc of *Drosophila* were stained with acridine orange (AO). AO labels dying cells *in situ*, due to their inability to exclude AO. In these cells AO intercalates into DNA resulting in green fluorescence signal [252].

Eye imaginal discs of *GMR-Gal4* flies, showed a small number of AO positive cells directly at the morphogenic furrow where supernumerary cells are eliminated (Figure 10 C). In eye imaginal discs with *GMR-Gal4*-induced Tau[R406W] expression an increased number of AO positive cells was detectable in the area *posterior* of the morphogenic furrow (Figure 10 D), suggesting that toxic effects of Tau[R406W] already induce cell death in the developing eye of *Drosophila* and are not exclusively mediated by long-term accumulation of a toxic protein species.

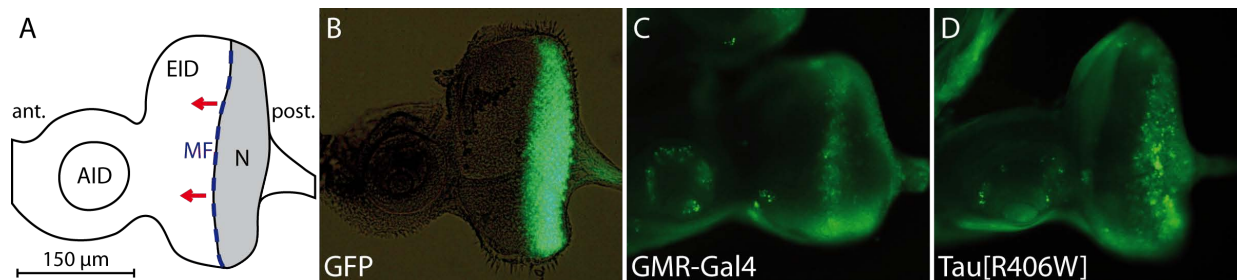


Figure 10: Developmental effects of Tau[R406W] expression in the eye imaginal disc of *Drosophila*.

Schematic view of the antenna imaginal disc (AID) and the eye imaginal disc (EID) (A). The morphogenic furrow (MF) is the border of cell differentiation starting *posterior* (post.). The differentiation results in post-mitotic neuronal precursor cells (N) posterior of the MF. These resemble the area of *GMR-Gal4*-mediated expression (grey), also visible in *GMR*-driven GFP expression (B). In *GMR-Gal4* flies AO-positive cells undergoing apoptosis are found directly at the MF (C). In eye imaginal discs with *GMR*-mediated expression of Tau[R406W] an increased number of AO-positive cells are found which are not restricted to the MF (D). Orientation of the images is anterior-left and dorsal-up. Magnification is depicted in A (bar = 150 μm). B is an overlay of brightfield and fluorescence microscopy.

3.1.3 Comparison of Tau expression levels

To evaluate the expression levels in the screening stock, quantitative PCR (qPCR) analysis was performed. Transcript levels of endogenous *Drosophila* Tau (**dTau**) as well exogenous transgene Tau[R406W] (human Tau **hTau**) were quantified in RNA extracts from heads of flies expressing Tau[R406W] under control of the pan-neural *elav^{C155}-Gal4* driver. As a control, the driver line was used without any transgene expression. $\Delta\Delta\text{Ct}$ analysis revealed no significant change of endogenous dTau mRNA levels in Tau[R406W] expressing flies, compared to control flies, normalised to ACTG1 (Actin 5C) (Figure 11 A). To evaluate Tau[R406W] transcript levels ΔCt analysis was performed comparing Tau[R406W] mRNA to dTau mRNA. Transcript levels of transgenic Tau[R406W] were significantly increased (1.8-fold, $p=0.0006$) compared to measured dTau mRNA levels (Figure 11 B).

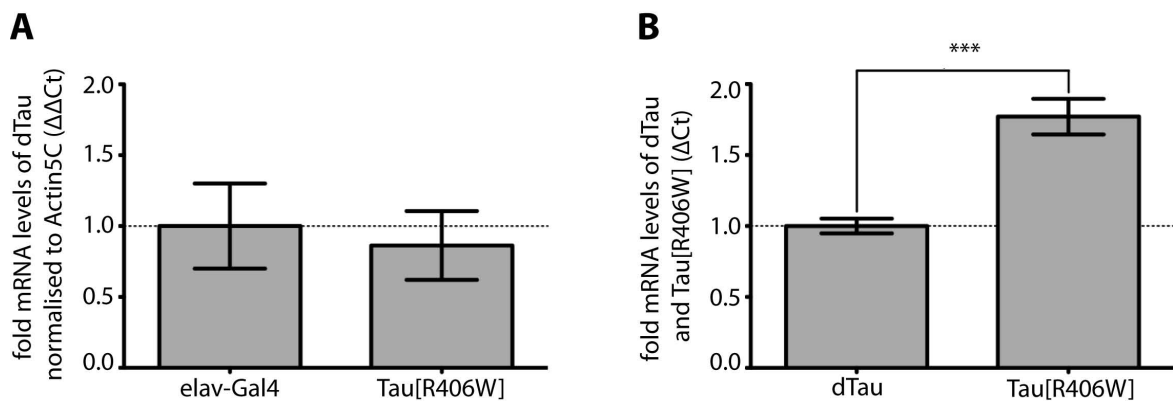


Figure 11: Tau mRNA levels in the used Tau[R406W] model.

(A) The effect of elav-driven Tau[R406W] expression on endogenous dTau mRNA levels in total RNA preparations from the head. No significant change is measurable. (B) Comparison of dTau and Tau[R406W] mRNA levels in total RNA preparations from head in flies with elav-driven Tau[R406W] expression. The Tau[R406W] transgene has 1.8 times higher transcription levels compared to endogenous dTau (standard t-test: *** $p<0.001$).

3.1.4 Longevity of the disease models

Human neurodegenerative diseases are progressive disorders with ongoing loss of neuronal function, leading to reduced life span. This can also be modelled in *Drosophila* [125, 241, 248]. Therefore, transgenes are expressed via pan-neural *elav^{C155}-Gal4* driver. Compared to GFP expression as a control, both Tau[R406W] and A β ₄₂ expression led to a significant decrease in life span (Figure 12 A). Pan-neural expression of Q₇₈ under control of *elav^{C155}-Gal4* was already lethal during pupal stage and therefore could not be used for longevity analysis.

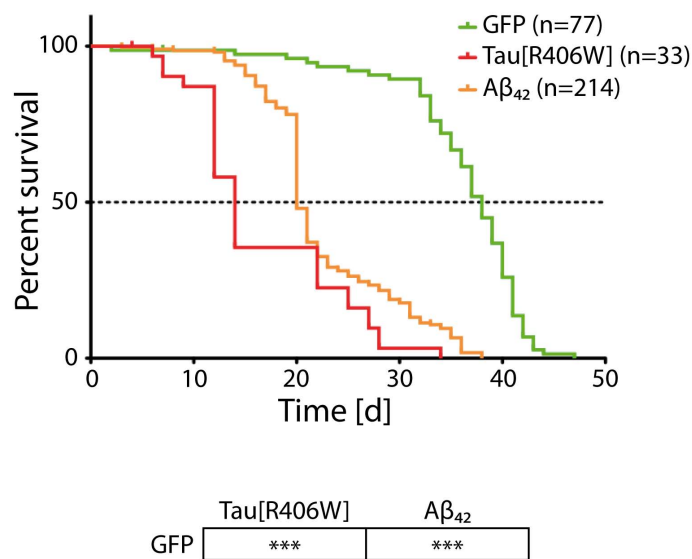


Figure 12: Longevity of the disease models.

Kaplan-Meier analysis of life expectancies. Pan-neural expression of GFP (green), A β ₄₂ (orange) and Tau[R406W] (red). In comparison to GFP expression A β ₄₂ and Tau[R406W] expression led to significant decreases of median survival (GFP 38 days, A β ₄₂ 20 days and Tau[R406W] 14 days). Significances depicted on the bottom are Log-Rank test results corrected for multiple testing using the Bonferroni method. (***) $p < 0.001$

3.2 Database for a high-throughput screen

As large amounts of data were obtained from the modifier screen, I created a web-based database for handling shRNA information and screening results. The database itself was programmed using the relational database management system MySQL. The browser-based user interface was programmed in php language. It facilitates data implementation of the VDRC-derived RNAi fly lines and documentation of all results by user-friendly forms. All fly lines were entered into the database and obtained an internal

number to create a blinded experiment situation. Besides data storage and stock-handling, the database could be used to collect information about single shRNA from VDRC and Flybase. Therefore information of the RNAi line like chromosomal integration site, viability and specificity are available, as well as detailed information about the target gene. This database provided the opportunity to collect results without the necessity of handling complicated paperless lists. In addition, results could be exported and even graphically visualised by the database. Thereby it minimised time for data handling and facilitated communication of results to colleagues and cooperation partners.

3.3 The Screen

As mentioned before the conducted modifier screen was based on an RNAi approach. Therefore a sub-library of the Vienna *Drosophila* RNAi centre (VDRC) was obtained with 7881 transgenic lines coding for shRNAs directed against all *Drosophila* genes known to have a human homologue (complete list in appendix). The conducted primary screen can be separated in several phases. First these 7881 lines were evaluated for induction of obvious phenotypic changes by the shRNAs themselves. The RNAi lines that did not induce Tau-unrelated effects were then evaluated according to modifications of the Tau[R406W]-induced REP. The RNAi lines that induced obvious modifications (from now on termed candidates) were additionally analysed for their ability to modify Tau-unrelated REPs induced by expression of A β ₄₂ and Q₇₈. To verify effects induced by knockdown of the candidate target genes, reproduction of the effects by additional systems was used where available (misexpression lines, deficiency lines, classical alleles and additional RNAi lines). In parallel I tried to quantify the RNAi effect of candidate shRNAs using qPCR.

3.3.1 Exclusion of RNAi lines inducing phenotypic changes in the absence of Tau

To screen for RNAi lines inducing unspecific effects, the RNAi lines (*UAS-shRNA*) were crossbred to *GMR-Gal4* driver line. The F1 generation with GMR-mediated expression of the shRNA was evaluated for obvious changes in eye phenotype. 7780 of the 7881 RNAi lines could be analysed. 857 RNAi lines did induce obvious changes in the eye phenotype and were excluded from the screen (Figure 13). The remaining 6923 RNAi lines did not induce obvious effects and were used for analysis in the modifier screen (see chapter 3.3.2).

3.3.2 Primary screen

To identify genes modifying Tau-induced toxicity, the RNAi lines were crossbred to flies expressing Tau[R406W] in the compound eye of *Drosophila* (*GMR_Tau[R406W]*). The offspring co-expressing Tau[R406W] and shRNAs mediated by *GMR-Gal4* was then analysed regarding modifications of the Tau[R406W]-induced REP. Of the 6923 analysed 34 could not be analysed, RNAi lines 6816 did not show any changes in the Tau[R406W]-induced REP, 15 did show an obvious suppression and 58 an obvious enhancement (including lethality) of the model phenotype (Figure 13 A, images in appendix). These results were confirmed by three independent experiments. In addition, 585 RNAi lines induced subtle effects (suppression: 140; enhancement: 445).

A rough categorisation of the 73 candidates by their annotated predicted function (GO process terms from [253]) revealed four major categories. 25 candidates can be associated to general mechanisms in protein anabolism and catabolism, ten candidates are involved in intracellular transport mechanisms and five have a kinase or phosphatase function. The other 33 candidates are listed as miscellaneous (Figure 13 B and Table 13).

3.3.3 Specificity of RNAi effects for Tau-induced REP

In addition, the 73 candidate target genes were silenced in flies expressing either A β ₄₂ or Q₇₈ in the compound eye to evaluate the specificity of candidates for Tau patho-

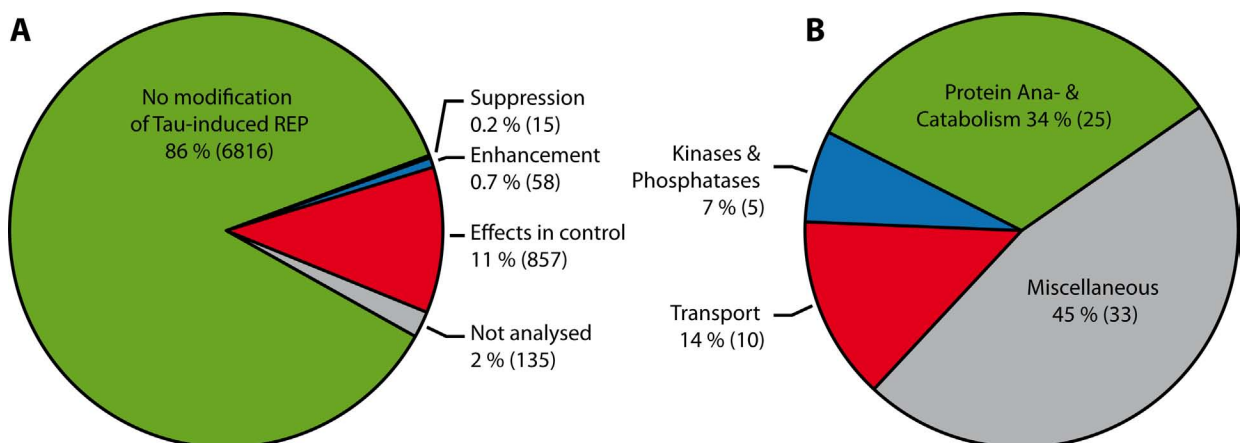


Figure 13: Summary of the screen results and the obtained candidates.

(A) Results of the primary screen. Of 7881 RNAi lines, 155 have not been analysed, 857 were excluded due to Tau-unrelated effects in the control and 6796 did not show a modification of the Tau-induced REP. Only 73 of the RNAi lines produced an obvious modification: 15 led to a suppression of the screening phenotype and 58 led to an obvious enhancement. (B) A rough characterisation by known function of the 73 candidate target genes. 25 candidates are directly involved in protein anabolism and catabolism, five are known to act as kinases or phosphatases and ten are directly involved in intracellular transport processes. The additional 33 candidates have unknown or diverse functions are depicted as miscellaneous.

mechanisms. Knockdown of 47 candidate genes did not induce phenotypic modifications in the two additional models, but either analogous or contrary results could be observed for single candidates in the two lines independently (Table 13). In GMR-mediated expression of A β ₄₂, four enhancers showed an analogous effect (two of transport group, one of protein anabolism and catabolism group, one miscellaneous). The phenotype of flies expressing Q₇₈ was modified by candidate knockdown in the same direction in 21 cases (one of transport group, 11 of protein anabolism and catabolism, one of kinases/phosphatases group and eight miscellaneous) and in the opposite direction in two cases (one of protein anabolism and catabolism and one miscellaneous) (Table 13).

Table 13: List of candidates modifying Tau-induced REP in *Drosophila melanogaster*.

Drosophila gene^a	Human homologue^b	Involved in Process^c	Tau^d	Confirmed by^e	A^f	Q^g
Transport						
Lerp	IGF2R	lysosomal transport	E		E	-
Gl	DCTN1	microtubule-based transport	E	Add. RNAi lines	-	-
Dmn	DCTN2	microtubule-based transport	E	NIG-Fly 8269R-3	-	-
Dhc93AB	DNAH17	microtubule-based transport	E	Df(3R)e-R1	-	-
alphaTub84B	TUBA1A	microtubule-based transport	E	Add. RNAi lines	-	-
alphaTub67C	TUBA1C	microtubule-based transport	E	Add. RNAi lines	-	-
Rab30	RAB30	protein transport	E		E	E
Scamp	SCAMP1	protein transport	E		-	-
CG14621	SLC35E1	transport	S		-	-
g	AP3D1	vesicle-mediated transport	E	g[1]	-	-
Protein anabolism and catabolism						
Aats-his	HARS	gene expression	E		-	E
MED14	MED14	gene expression	E	Df(3L)emc-E12	-	E
Prp8	PRPF8	gene expression	E	Df(2R)BSC40	-	E
Nelf-E	RDBP	gene expression	E		-	E
RpS10a	RPS10	gene expression	E		-	E
CG11985	SF3B5	gene expression	E		-	E
Elongin-B	TCEB2	gene expression	E		-	-
Spp	HM13	membrane protein proteolysis	E	Df(2L)ast2	-	-
snRNP-U1-C	SNRPC	nuclear mRNA splicing	E		-	-
Prosalph7	PSMA3	protein catabolism	E		-	-
Prosbeta2	PSMB7	protein catabolism	E	EP ^{EP3067}	-	E
Rpn9	PSMD13	protein catabolism	E	Df(3R)mbc-R1	-	E

Drosophila gene^a	Human homologue^b	Involved in Process^c	Tau^d	Confirmed by^e	A^f	Q^g
CG6418	DDX42	protein localisation	S		-	-
CG31534	LMO7	protein ubiquitination	S		-	-
CG32351	LAP3	proteolysis	S		-	-
Nedd8	NEDD8	proteolysis	E		E	-
bic	BTF3L4	regulation of transcription	E	Df(2R)CX1	-	E
MRG15	MORF4L1	regulation of transcription	S		-	S
Fer1	PTF1A	regulation of transcription	E		-	-
lola	ZBTB20	regulation of transcription	S	EP ^{EP2537}	-	-
CG10979	ZNF800	regulation of transcription	E		-	-
Cwc25	CWC25	RNA processing	E	Df(2L)C144	-	-
CG3808	TRMT2A	RNA processing	E		-	S
Hop	STIP1	stress response	S		-	S
CG17327	PTRH2	translation	E		-	-
Kinases/Phosphatases						
hipk	HIPK2	protein phosphorylation	E	Df(3L)emc-F12	-	-
hep	MAP2K7	protein phosphorylation	S		-	-
CG32666	STK17A	protein phosphorylation	E		-	-
CG6364	UCK2	protein phosphorylation	E	NIG-Fly 6364R-2	-	E
CG6330	UPP2	uridine metabolism	E		-	-
Miscellaneous						
CG5500	C17orf90	-	S		-	-
CG5986	C1orf55	-	E		-	-
CG31259	TMEM135	-	S		-	-
CG6873	DSTN	actin polymerisation	E		-	E
Su(z)2	BMI1	brain development	E	Df(2R)CX1	-	-
Nrx-IV	CNTNAP2	cell adhesion	E		-	E
Flo-2	FLOT2	cell adhesion	E		-	-
CG7896	IGFALS	cell adhesion	E		-	-
CycJ	CCNJ	cell cycle	E		-	E
fzy	CDC20	cell cycle	E	Df(2L)r10	-	-
Mad1	MAD1L1	cell cycle	S		-	-
CG8086	ODF3	cell differentiation	E		E	E
bru	TRAPPC9	cell differentiation	E		-	E
Shroom	SHROOM3	cell morphogenesis	S		-	-
CG8664	PCLO	cytoskeleton organisation	E		-	-
CG8108	CIZ1	DNA replication	E		-	E

Drosophila gene ^a	Human homologue ^b	Involved in Process ^c	Tau ^d	Confirmed by ^e	A ^f	Q ^g
Snp	ERI2	exonuclease activity	E		-	-
nord	C4orf31	extracellular matrix organisation	S		-	-
Apf	NUDT2	induction of apoptosis	E		-	-
Vha16	ATP6V0C	insulin receptor signaling	E		-	-
Vha36	ATP6V1D	insulin receptor signaling	E		-	-
CG32442	ARV1	lipid metabolism	E	Df(3L)ED4978	-	-
CG14184	LAMTOR1	lysosome organisation	E		-	-
krz	ARRB1	MAPK signaling pathway	E		-	-
Ard1	NAA10	metabolic process	E		-	E
Dab	DAB1	nervous system development	E		-	S
Smg5	SMG5	nonsense-mediated mRNA decay	E		-	E
T3dh	ADHFE1	oxidation-reduction process	E	Df(2R)X58-12	-	-
CG3500	TEX261	regulation of apoptosis	E	Df(2R)vir130, EPEY00630	-	-
CG42788	FRMPD4	regulation of synapse plasticity	S		-	-
CG18508	C18orf32	signal transduction	S		-	-
Gdi	GDI1	signal transduction	E		-	-
par-6	PARD6G	tight junction assembly	E		-	-

^a Drosophila gene according to the official symbol listed in the Gene database of NCBI [239].

^b Human homologue as listed in the HomoloGene database [142], or found by BLAST analysis [143]. Official symbol as listed in the Gene database of NCBI [239].

^c Selected GO terms (process) as listed in the Gene Ontology Annotation database [253].

^d Obvious modification of Tau[R406W]-induced Rough Eye Phenotype; Enhancement (E), Suppression (S).

^e Modification confirmed by an additional shRNA construct (VDRC, Bloomington or NIG), an amorphic allele, misexpression transgenes (EP) or deficiency lines (Df).

^f Obvious modification of A β ₄₂-induced Rough Eye Phenotype; Enhancement (E), Suppression (S).

^g Obvious modification of Q₇₈-induced Rough Eye Phenotype; Enhancement (E), Suppression (S).

3.3.4 Verification of the RNAi effects

For verification of the candidates from the primary screen effects on Tau[R406W]-induced REP were reproduced by additional approaches, where available. These were amorphic alleles, misexpression transgenes, deficiencies or other RNAi lines directed against the candidate target genes. Lines for verification were obtained for 38 of the 73 candidates (List of used lines in appendix). For 21 candidates the modification of the REP could be reproduced, in 12 cases by a deficiency line, in 3 cases by misexpression transgenes, in 5 cases by additional shRNA constructs (from VDRC, Bloomington or NIG) and in 1 case the effect could be reproduced by an amorphic allele (Table 13).

3.3.5 Quantification of the RNAi effects

To evaluate RNAi effects by candidate shRNAs from the primary screen, quantifications of target mRNA levels were performed using quantitative PCR (qPCR) analysis of reverse transcribed RNA. The RNA was isolated from fly heads with pan-neural expression of respective shRNAs. In nine cases, pan-neural expression of the candidate shRNA induced lethality. A random selection of 36 candidate shRNAs not inducing lethality in pan-neural expression was analysed. Significant reduction of target mRNA levels could only be measured in 31 % of analysed shRNAs (Figure 14 and Table 13).

Table 14: shRNAs showing a significant decrease of target mRNA after pan-neural expression.

shRNA against	Fold mRNA level ^a	P-value ^b
IGFALS	0.560	0,0246
DDX42	0.342	0,0042
SMG5	0.270	0,0418
PARD6G	0.263	0,0089
HM13	0.257	0,0043
FLOT2	0.207	0,0037
RDBP	0.203	0,0023
C17orf90	0.085	0,0005
TEX261	0.073	0,0002
SCAMP1	0.008	< 0.0001
PTRH2	0.005	< 0.0001

^a compared to expression of a control shRNA.

^b Results of a one sample t-test comparing results to a hypothetical mean of 1.0.

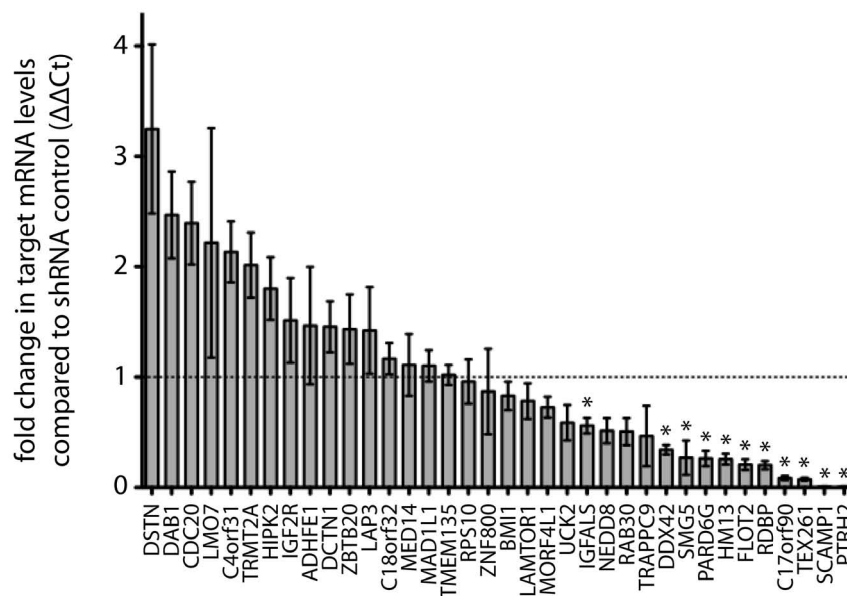


Figure 14: Quantification of RNAi effects by candidate shRNAs.

To evaluate the RNAi effect induced by candidate shRNAs qPCR analysis was conducted. Target gene mRNA levels were measured in head RNA preparations of flies pan-neurally expressing the shRNAs and compared to target gene mRNA levels in flies expressing a control shRNA (directed against LRP2). Levels were normalised to *elav* and *rp49* transcripts. To analyse significances one-sample t-tests were run comparing the fold change to a hypothetical mean of 1.0: * $p < 0.05$.

3.4 Candidates modifying cellular Tau protein levels

To characterise the ability of candidates to change cellular levels of Tau protein, western blot analysis was performed using the pan-Tau antibody 5A6. A random selection of 10 candidates from the protein anabolism and catabolism group and 3 candidates from the transport group was analysed. Candidate shRNA modifying the intracellular Tau protein levels in pan-neuronal expression of Tau[R406W] were identified by quantification of 5A6 band intensity. Quantifications were normalised to band intensity of Syntaxin, a protein found in neuronal membranes (antibody 8C3). Co-expression of the 13 candidate shRNAs with Tau[R406W] resulted in a notably increase of Tau protein in one case (knockdown of CDC20) and led to decreased Tau levels in two cases (knockdown of STIP1 and LAMTOR1) (Figure 15). Knockdown of CDC20 increasing Tau protein levels, was found to enhance Tau-induced REP in the primary screen. The shRNA directed against STIP1 decreasing Tau levels has been identified as suppressing the Tau[R406W]-induced REP. However, knockdown of LAMTOR1 resulted in a decrease of 5A6 band intensity, although it was identified to enhance Tau pathology in the compound eye.

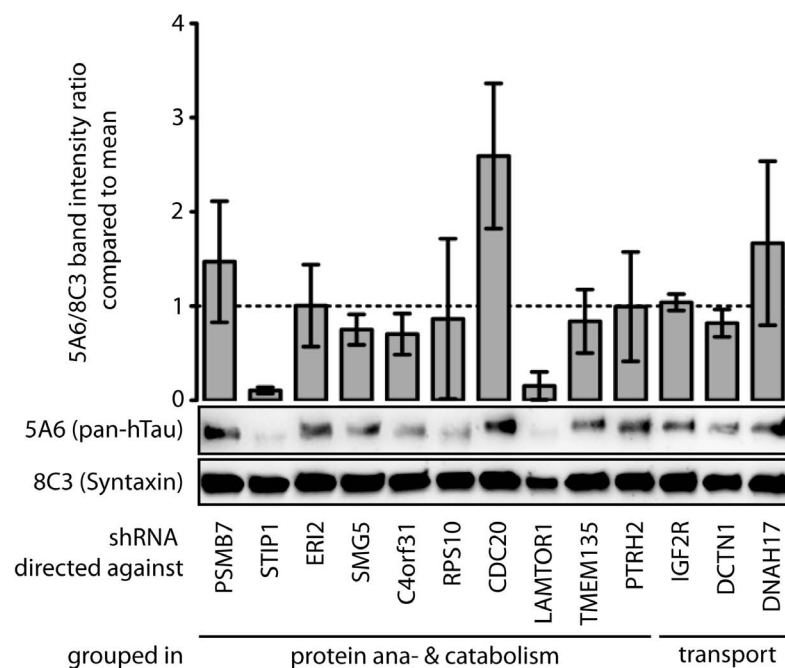


Figure 15: Alterations in Tau protein levels induced by knockdown of candidate genes.

Immunoblot and quantification of head lysates from flies pan-neurally expressing Tau[R406W] and candidate shRNAs, probed for pan-hTau (antibody 5A6) and Syntaxin (for normalisation, antibody 8C3). Results revealed changes in intracellular Tau protein levels due to candidate gene knockdown. Ten candidate shRNAs of protein anabolism and catabolism group and three of transport group were analysed. Plot shows notably increase of hTau protein levels after knockdown of CDC20 and a decrease after knockdown of STIP1 and LAMTOR1 compared to mean levels. Significance was not tested, as analysis was only reproduced once.

3.5 Comparing Tau variants using site-directed integration transgenes

For direct comparison of different Tau variants, additional transgenes were utilised. These were generated by site-directed integration of the transgenes using the ϕ C31 integrase. This technique is used to generate transgenes with comparable transcription levels [242]. To compare effects on Tau[WT] and Tau[R406W] induced REP two lines were generated with integration of transgenes *Tau[WT]* and *Tau[R406W]*: *attB_Tau[WT]* (*PBac{attB[+mC]=UAS-hTau[WT]}VK00013*), *attB_Tau[R406W]* (*PBac{attB[+mC]=UAS-hTau[R406W]}VK00013*). In addition two site-directed integrations of transgenes were generated with the two Tau variants Tau[AP] and Tau[E14] mimicking different Tau phosphorylation states (see chapter 1.8.2): *attB_Tau[AP]* (*PBac{attB[+mC]=UAS-hTau[AP]}VK00013*) and *attB_Tau[E14]* (*PBac{attB[+mC]=UAS-hTau[E14]}VK00013*). These four site-directed integration transgenes were first also analysed for their neurodegenerative characteristics.

GMR-mediated expression of the site-directed integration transgenes led to very subtle REPs (Figure 16). The REPs of the site-directed integration transgenes differ from the REP induced by the random integration of Tau[R406W] (Figure 9) as they show reduced Tau expression levels (data not shown). Although the transgenes produced comparable phenotypes, the wildtype variant seems to induce a slightly less (Figure 16 A), the R406W mutant a slightly enhanced REP (Figure 16 B), compared to the two expression of the two Tau variants mimicking different phosphorylation states: *attB_Tau[AP]*¹ and *attB_Tau[E14]* (Figure 16 C and D). qPCR analysis was also used to compare hTau transcript levels of the four transgenes *attB_Tau[WT]*, *attB_Tau[R406W]*, *attB_Tau[AP]* and *attB_Tau[E14]*. Pan-neural expression of *attB_Tau[AP]* resulted in lethality, therefore head RNA preparations were obtained from flies with *attB-Tau* expression mediated by *GMR-Gal4*. As the eye sizes of flies expressing the different Tau variants are comparable (chapter 3.1.1), head RNA samples should be comparable, although expression is restricted to the compound eye. However, transcript levels of hTau differed in GMR-mediated expression of the *attB_Tau* transgenes (Figure 17 A). Compared to the wildtype variant, expression of *attB_Tau[R406W]* and *attB_Tau[E14]* resulted in significantly decreased mRNA levels, while *attB_Tau[AP]* expression showed a notable, although not significant, increase of transcript levels.

¹ To differentiate between hTau protein expressed by random and by site directed integration transgenes, the latter are referred to as *attB_Tau*.

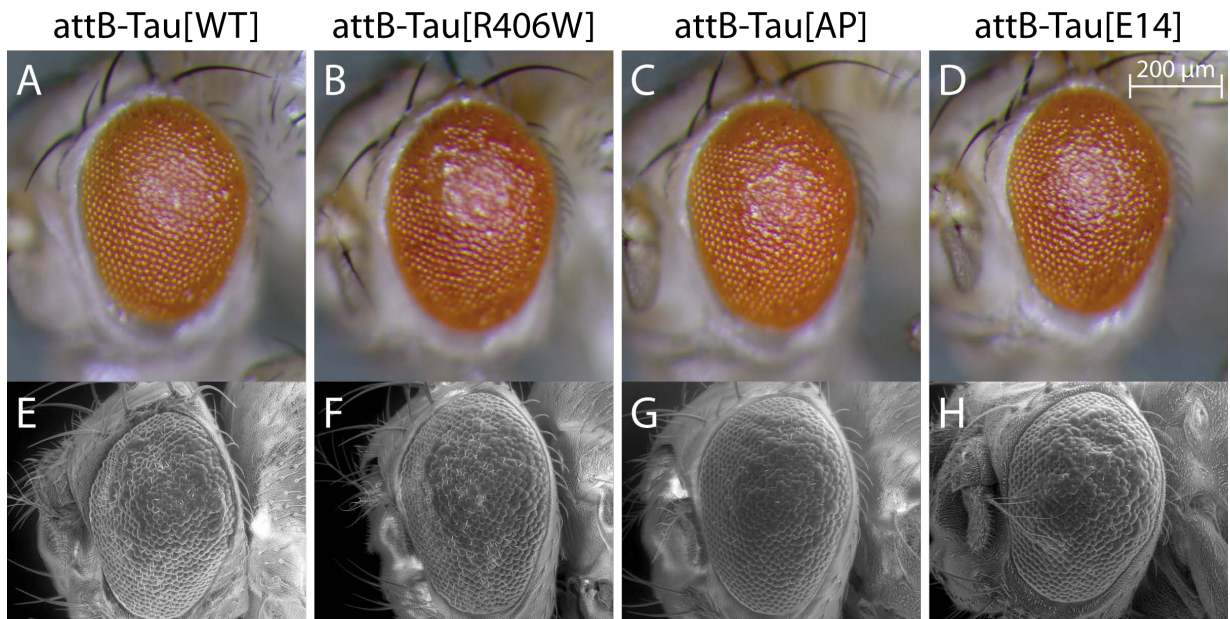


Figure 16: Rough eye phenotypes induced by expression of the site-directed integration transgenes with different Tau variants.

Compound eye phenotypes (imaged using light microscopy (A-D) and scanning electron microscopy (E-H)) after GMR-mediated expression of the site-directed integration transgenes *attB_Tau[WT]* (A, E), *attB_Tau[R406W]* (B, F), *attB_Tau[AP]* (non-phosphorylatable variant) (C, G) and *attB_Tau[E14]* (phosphomimick variant) (D, H). The different Tau transgenes induce a subtle rough eye phenotype. Although all four Tau transgenes lead to comparable phenotypes, the wildtype variant seems to produce a slightly less severe (A), the R406W variant a slightly increased REP (B) compared to the two transgenes mimicking different phosphorylation states of Tau (*attB_Tau[AP]* and *attB_Tau[E14]*) (C and D). Orientation of all images is dorsal-up and cranial-left. The magnification is depicted in D (bar = 200 μm).

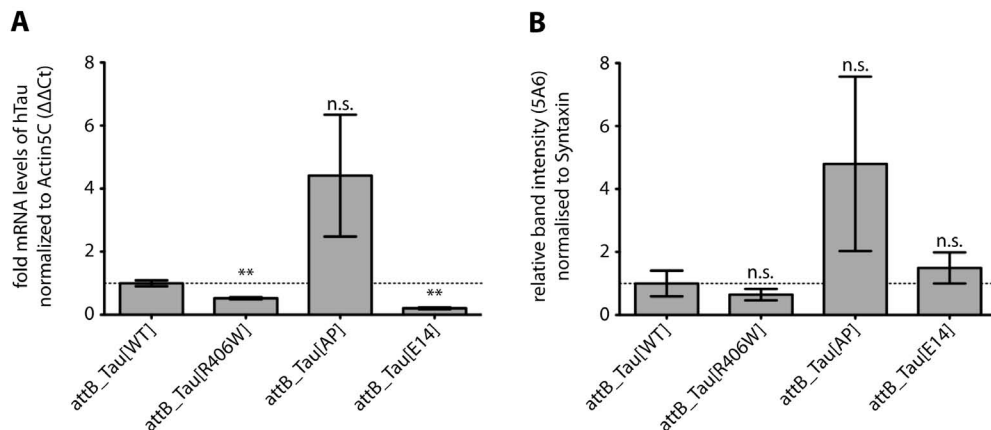


Figure 17: GMR-mediated Tau expression by *attB_Tau* variants.

(A) Transcript levels in head RNA preparations of flies with GMR-mediated expression of *attB_Tau[WT]*, *attB_Tau[R406W]*, *attB_Tau[AP]* and *attB_Tau[E14]*. Expression of *attB_Tau[R406W]* and *attB_Tau[E14]* show significantly less mRNA levels compared to wildtype variant and expression of *attB_Tau[AP]* results in increased transcript levels (not significant). (B) Quantification of 5A6 (total hTau) band intensity on an immunoblot of head protein lysates from flies with GMR-mediated expression of the transgenes *attB_Tau[WT]*, *attB_Tau[R406W]*, *attB_Tau[AP]* and *attB_Tau[E14]*. The differences found in protein levels after GMR-mediated expression reflect measured mRNA levels in *attB_Tau[WT]* and *attB_Tau[AP]*. However, 5A6 band intensity is slightly increased in GMR-Gal4-mediated expression of *attB_Tau[E14]*, although transcript levels are significantly decreased (difference between mRNA and protein level not significant). Statistics: standard t-test comparing column mean to *attB_Tau[WT]*; n.s. not significant, ** $p < 0.01$.

In addition protein levels of *GMR-Gal4*-driven expression of the four site-directed integration transgenes were analysed. Expression of attB_Tau[WT], attB_Tau[R406W] and attB_Tau[E14] did not result in significant differences of Tau protein levels, although the differences found resemble the measured mRNA levels (Figure 17 B).

For comparison of differential effects on the life-span of the different Tau variants, longevities of flies with pan-neural expression of the site directed integration transgenes were analysed (Figure 12 B). There is no difference in life span of attB_Tau[WT] and attB_Tau[R406W] expression, with median survival (time point, where 50 % of flies died) of about 38 days. The phospho-mimic variant Tau[E14] led to a reduction of the median survival to 20 days (Figure 12 B). Interestingly, pan-neural expression of attB_Tau[AP] was already lethal in a late pupal stage.

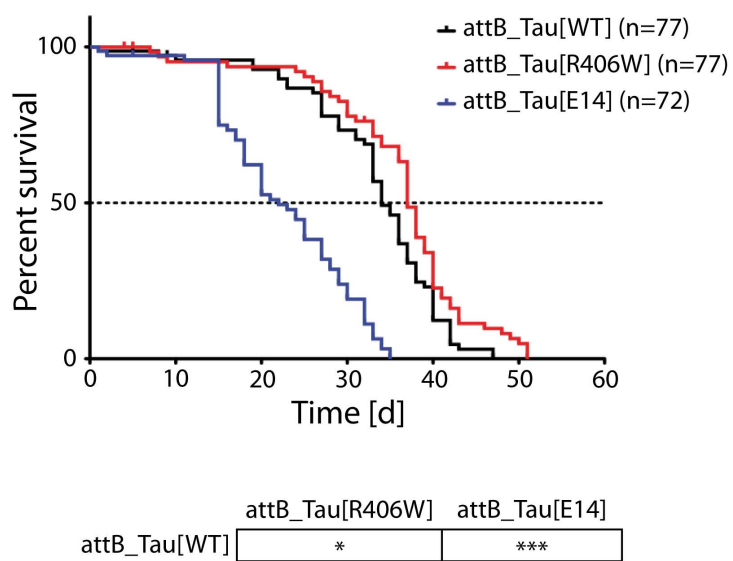


Figure 18: Longevity of site-directed integration Tau transgenes.

Kaplan-Meier analysis of life expectancies. Pan-neural expression of attB_Tau[WT] (black), attB_Tau[R406W] (red) and attB_Tau[E14] (blue). Although the difference is significant, expression of attB_Tau[WT] and attB_Tau[R406W] led to similar median survivals (attB_Tau[WT] 34 days and attB_Tau[R406W] 37 days). Expression of attB_Tau[E14] reduces median survival dramatically compared to wildtype variant (22 days). Notable pan-neural expression of the attB_Tau[AP] induced lethality during pupal stage. Significances depicted on the bottom are Log-Rank test results corrected for multiple testing using the Bonferroni method. (* $p < 0.05$, *** $p < 0.001$)

3.5.1 Specificity of the candidates for Tau[R406W]-induced pathology

As the primary screen was conducted using Tau[R406W] expression, effects of some candidates might be specific for the Tau[R406W] mutant variant. To evaluate putative specificity, candidates were analysed for their ability to modify attB_Tau[WT]- compared to attB_Tau[R406W]-induced REP. Of the 73 candidates identified in the primary screen, 69 were analysed. For only three candidates there was an obvious difference observed between modification of attB_Tau[WT]- and attB_Tau[R406W]-induced REP (Figure 19). These three candidate shRNAs induced an enhancement on the primary screen. While expression of the shRNAs against PSMB7 and CWC25 together with attB_Tau[R406W]

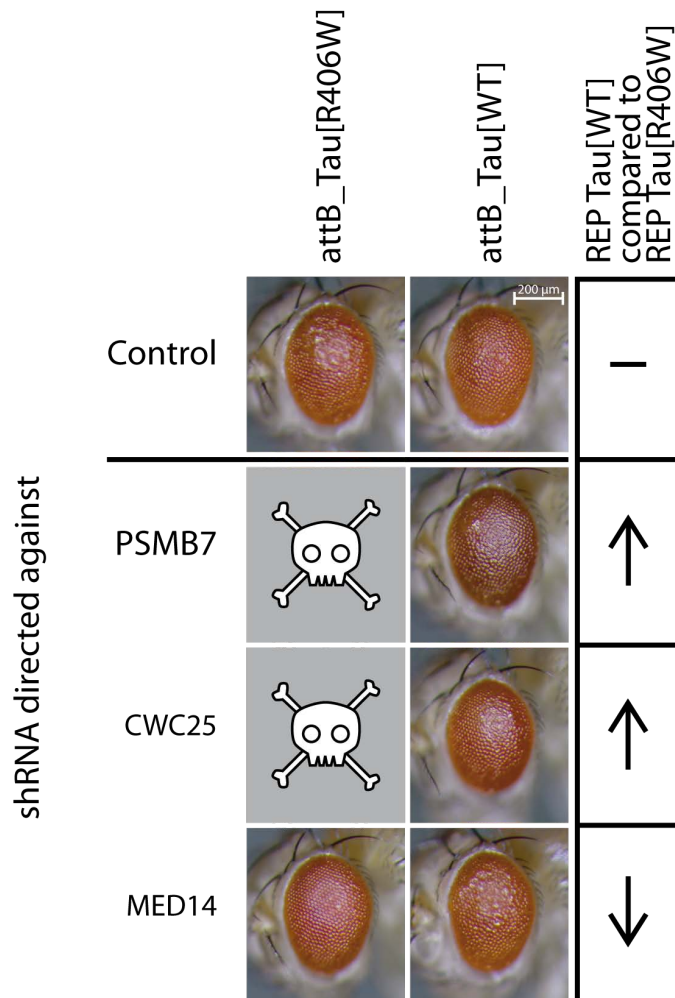


Figure 19: Secondary screen on candidate specificity for R406W mutation of Tau.

Differences in GMR-mediated REP modification between expression of attB_Tau[R406W] and attB_Tau[WT]. In the first column phenotypes of candidate shRNA and Tau[R406W] co-expression are depicted. In the second column phenotypes are shown induced by expression of shRNA and attB_Tau[WT]. A schematic view of phenotype modification in Tau[WT] compared to Tau[R406W] expressing flies are shown in the third column (↓ REP worse, ↑ REP improved, —=REP comparable). Orientation of the imaged compound eyes is anterior-left and dorsal-up. Magnification is depicted in the first row (bar=200 µm).

resulted in lethality, expression of these shRNAs did not enhance attB_Tau[WT]-induced REP. Compared to attB_Tau[R406W], knockdown of MED14 enhanced the REP when co-expressed with attB_Tau[WT].

3.5.2 Candidate effects in phospho-specific Tau models

To evaluate specificity of candidates for Tau phosphorylation status a screen was conducted comparing the candidate shRNA effects on attB_Tau[R406W]-induced REP to modification of attB_Tau[AP]- and attB_Tau[E14]-induced REP. Tau[AP] resembles a variant of Tau, that is not able to be phosphorylated at all 14 known AP/TP phosphorylation sites. Tau[E14] resembles a phospho-mimick variant, in which all 14 AP/TP phosphorylation sites are mutated to EP (see chapter 1.8.2).

The secondary screen on modifications of GMR-induced REP of the three different site-directed integration transgenes (*attB_Tau[R406W]*, *attB_Tau[AP]* and *attB_Tau[E14]*) was conducted using candidate shRNAs identified in the primary screen. Of the 73 candidates 69 were analysed. Eight showed differences in GMR-Gal4-induced eye phenotype comparing co-expression of candidate shRNA with attB_Tau[AP] or attB_Tau[E14] to co-expression with attB_Tau[R406W] (Figure 20). Candidate shRNAs inducing a different REP in flies expressing non-phosphorylatable attB_Tau[AP] compared to attB_Tau[R406W] were all identified as enhancers in the primary screen. The shRNAs directed against TUBA1A, TUBA1C, ERI2, SMG5, ODF3 and SNRPC resulted in a more pronounced REP when co-expressed with attB_Tau[AP] compared to attB_Tau[R406W] (SNRPC lethal). While shRNA directed against PSMB7 induced lethality in attB_Tau[R406W] expressing flies, co-expression with attB_Tau[AP] was viable.

There was only one candidate shRNA, which induced a REP in flies expressing attB_Tau[E14] (the phospho-mimic variant) compared to attB_Tau[R406W]. Knockdown of STIP1, suppressing the primary readout did enhance the REP induced by attB_Tau[E14] expression compared to attB_Tau[R406W].

	attB_Tau[R406W]	attB_Tau[AP]	attB_Tau[E14]	REP Tau[AP] compared to REP Tau[R406W]	REP Tau[E14] compared to REP Tau[R406W]
Control				—	—
TUBA1A				↓	—
TUBA1C				↓	—
PSMB7				↑	—
ERI2				↓	—
SMG5				↓	—
ODF3				↓	—
SNRPC				↓	—
STIP1				—	↓

Figure 20: Screen on modifiers of REP induced by expression of phospho-mimicking Tau variants.

Differences in candidate shRNA-mediated modification of REPs induced by attB_Tau[R406W], attB_Tau[AP] and attB_Tau[E14]. In the three first columns the resulting phenotypes are shown. In the last two columns a schematic overview is given if the REP of Tau[AP] or Tau[E14] is either enhanced or reduced in comparison to Tau[R406W] (↓ REP enhanced, ↑ REP reduced, —=REP comparable). Orientation of the imaged compound eyes is anterior-left and dorsal-up. Magnification is depicted in the first row (bar=200 μm).

3.6 Evaluation of Tau phosphorylation due to candidate effects

Of the eight candidates showing differential effects on the REP induced by expression attB_Tau[R406W], attB_Tau[AP] and attB_Tau[E14] (see chapter 3.5.2), four could be evaluated for their influences on Tau phosphorylation. Head lysates from flies with pan-neuronal co-expression of Tau[R406W] and candidate shRNAs were analysed by western blotting, using three phospho-specific Tau antibodies AT8, AT180 and AT270, each specific for Tau phosphorylated at one (or two) distinct SP or TP site. AT8 recognises Tau phosphorylated at serine 202 and threonine 205. AT180 is specific for Tau phosphorylated at threonine 231 and AT270 is able to detect Tau if the threonine at position 181 is phosphorylated (Figure 8). Antibody 5A6 (hTau) was used to display levels of Tau regardless to its phosphorylation state. If compared to 5A6 band intensity immunoblotting revealed no obvious differences in Tau phosphorylation between the four candidates. Differences rather reflect the difference in cellular Tau[R406W] protein levels shown by the pan-hTau antibody 5A6 (Figure 21). Immunoblotting was also performed using AT100 (specific for phosphorylation at Thr²¹²), but no significant antibody signal was detectable (data not shown).

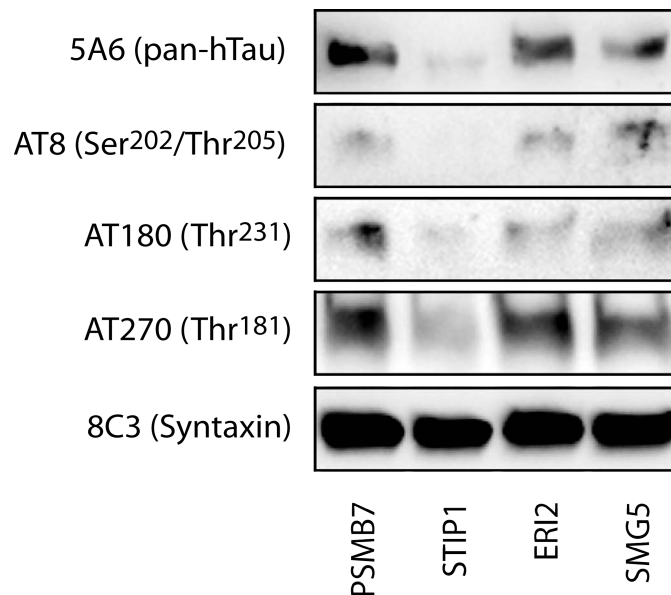


Figure 21: Evaluation of selected candidate shRNAs for their impact on Tau phosphorylation.

Using the phospho-specific antibodies AT8 (Ser²⁰²/Thr²⁰⁵), AT180 (Thr²³¹) and AT270 (Thr¹⁸¹) in immunoblotting after SDS-page gel electrophoresis shows phosphorylation of Tau protein. Syntaxin is used for normalisation and 5A6 (pan-hTau) to depict cellular Tau[R406W] level. Differences in phosphorylation of Tau in all three phospho-epitopes rather reflect overall Tau[R406W] levels.

3.7 Modification of Tau-induced toxicity by knockdown of the Dynein/Dynactin transport complex

In the primary screen, ten candidates were identified to modify Tau-induced REP, which are directly involved in intracellular transport processes. Of these, five candidates silence components of the Dynein/Dynactin complex, responsible for microtubule-based retrograde transport (see chapter 1.5.3). These silenced genes are TUBA1A, TUBA1C, DNAH17, DCTN1 and DCTN2 (Figure 22). Knockdown of three additional genes coding for subunits of Dynactin showed subtle effects in the primary screen (DCTN4, DCTN5 and ACTR10). In several experiments I attempted to elucidate the mechanistic correlations between the Dynein/Dynactin complex and Tau-induced toxicity.

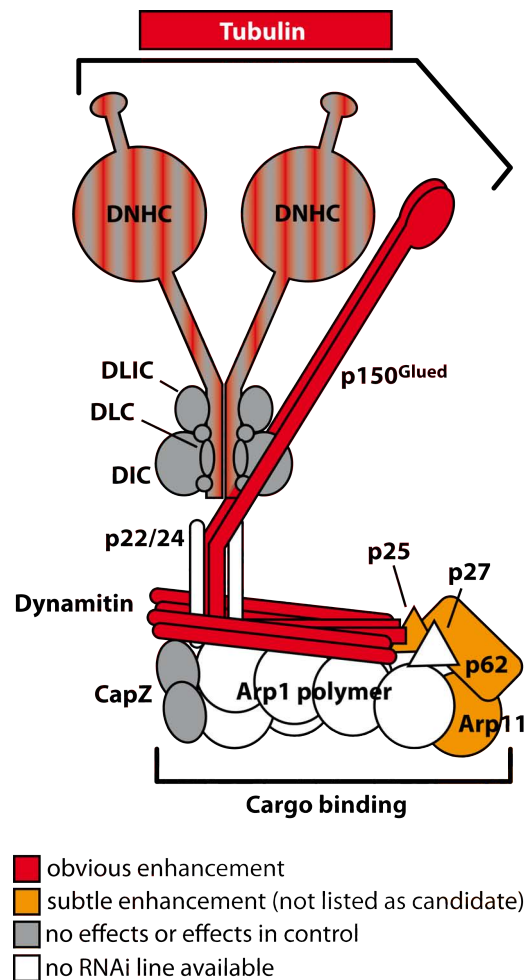


Figure 22: The Dynein/Dynactin complex as a modifier of Tau-induced neurodegeneration.

Schematic view of the five candidates identified as enhancing Tau[R406W]-induced REP, which silence genes coding for components of the Dynein/Dynactin complex: Tubulin α 1a (TUBA1A), Tubulin α 1c (TUBA1C), one of the numerous Dynein heavy chains (DNAH17), p150^{Glued} (DCTN1) and Dynamitin (DCTN2). In addition knockdown of three subunits was found to induce a subtle enhancement: Dynactin p25 (DCTN5), Dynactin p62 (DCTN4) and the capping protein Arp11 (ACTR10).

3.7.1 Microtubule network in the motorneuron axon of larvae

Experiments to evaluate axonal transport processes were conducted in motorneuron axons of L3 larvae. The long axons of motorneurons with distinct orientation provide the ability to address axonal transport processes easily. Using the driver line *D42-Gal4*, expression of Tau and shRNA was restricted to motorneurons. To first evaluate the base of axonal transport, the microtubule network was characterized. Expression of neither Tau[R406W], shRNA directed against components of the Dynein/Dynactin complex nor combined expression led to major changes in the microtubule network as shown by alpha-Tubulin staining (Figure 23).

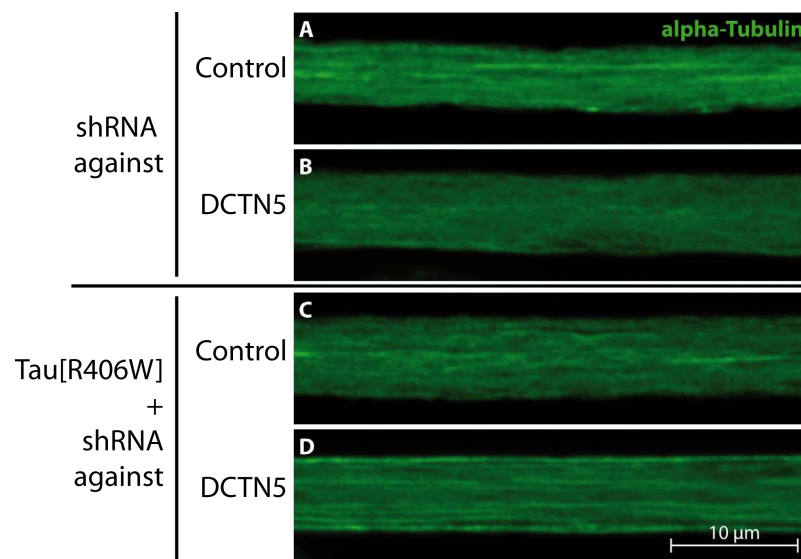


Figure 23: Tubulin network in axons of larval motorneurons.

To compare the microtubule network integrity, segmental nerves were analysed by alpha-Tubulin staining. (A) Segmental nerves of larvae expressing a control shRNA. Knockdown of DCTN5 found to be a subtle enhancer in the primary screen, coding for a member of the Dynein/Dynactin complex (B), expression of Tau[R406W] (C), nor the combination of Tau and shRNA (D) in motorneurons lead to obvious changes in microtubule network integrity. Magnification is depicted in D (bar=10 μ m)

3.7.2 Axonal Tau levels

Knockdown of subunits from the Dynein/Dynactin complex will reduce retrograde transport in the axon. This might lead to an increased accumulation of Tau in the axon. To evaluate axonal load of Tau[R406W] protein motorneuron of L3 larvae were stained for hTau using the 5A6 antibody. However, staining did not show any accumulations in the axon neither in flies expressing Tau[R406W] nor with combined knockdown of Dynein/Dynactin components. Notably, neither was there any significant Tau staining

present in the neuromuscular junctions (NMJs) of motorneurons, neither with nor without Dynein/Dynactin complex knockdown. Quantifications to estimate axonal hTau levels did not show an increase of the staining intensity (normalised to horseradish peroxidase **HRP** staining intensity – HRP antibody stains neuronal membranes [254]). Knockdown of the Dynein/Dynactin machinery even led to a slight reduction of 5A6 staining intensity (Figure 24).

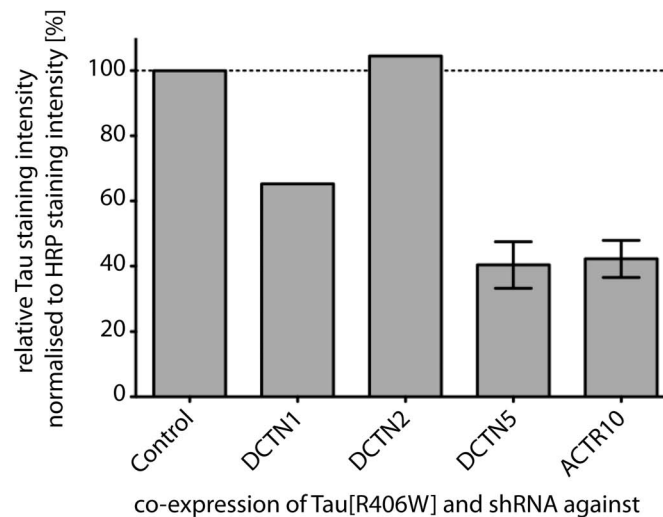


Figure 24: Tau staining intensity in motorneuron axons after knockdown of members from the Dynein/Dynactin complex.

To estimate Tau protein load in the axonal compartment of motorneurons, the Tau staining intensity was quantified and normalised to HRP staining intensity. Tau staining intensity in motorneurons expressing Tau[R406W] did not increase after knockdown of Dynein/Dynactin complex members. In fact intensity rather decreased, suggesting decreased axonal Tau levels under impaired retrograde transport conditions.

3.7.3 The morphology of neuromuscular junctions

The NMJs of examined motorneuron axons did not show an obvious staining for Tau protein. Nevertheless, Tau[R406W] expression resulted in robust changes in NMJ morphology. NMJs showed slight disturbances of the clear bouton-shaped structure compared to controls (Figure 25 A and B). In addition an antibody against HRP showed an increased staining intensity in NMJs if an shRNA directed against a component of the Dynein/Dynactin complex (DCTN5 – shRNA found to be a subtle enhancer of the primary screen REP) was expressed (Figure 25 C). Both, disturbed morphology and increased HRP staining intensity could be observed in co-expression of Tau[R406W] and DCTN5 shRNA (Figure 25 D). The increased HRP staining after knockdown of shRNA directed against DCTN5 indicates an increased vesicle load of the synapse induced by the reduced

retrograde transport. The disturbed morphology might be due to subtle changes in the microtubule-network due to Tau over-expression, which could not be observed in alpha-Tubulin stainings (see chapter 3.7.1).

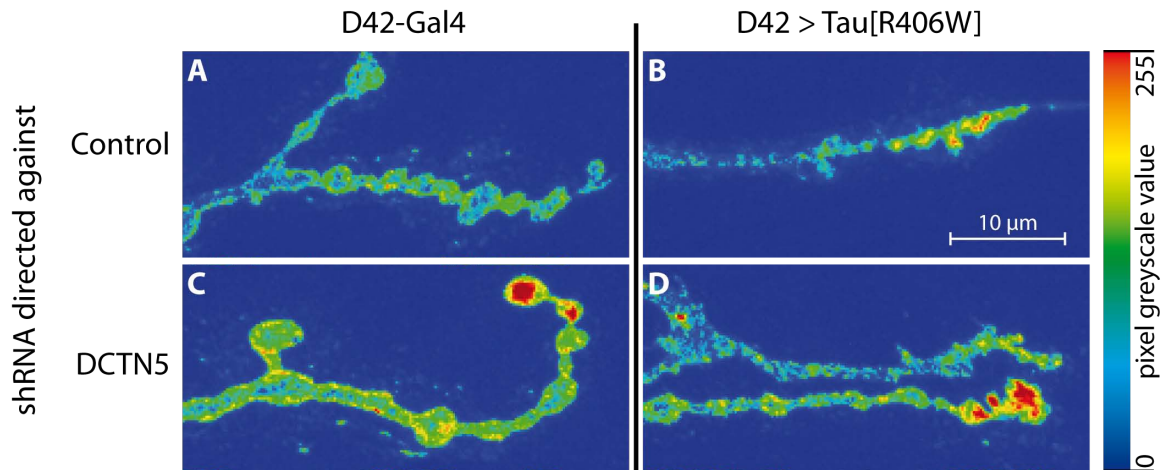


Figure 25: NMJ morphology of *Drosophila* larval motorneurons.

Pseudo-colour projections of Z-stack images, taken by confocal microscopy. The larval motorneurons were stained against HRP, labelling neuronal membranes. (A) Expression of a control shRNA reveals the homogenous staining of the clear button-shaped NMJ. (B) Expression of Tau[R406W] disturbs the clear NMJ morphology. (C) Expression of the shRNA directed against DCTN5 does not interfere with morphology, but increases staining intensity. (D) The combination of Tau[R406W] expression and DCTN5 knockdown leads to both, disturbances of the button-shaped morphology and increased HRP staining intensity. Colour-code for pseudo-colour display is depicted on the right. NMJs shown are from motorneurons innervating larval body wall muscle M4 in segment A3. Orientation of NMJs is anterior-right and distal-up. Magnification is depicted in B (bar=10 µm)

3.7.4 Axonal accumulations of transported vesicles

To visualise traffic jams in axonal transport, an antibody against cysteine string protein (CSP) served as a readout. CSP is a protein found in membranes of synaptic vesicles. If axonal transport is disturbed, transported vesicles accumulate and can be detected by staining with an antibody directed against CSP. *Drosophila* larvae were analysed expressing either Tau[R406W] or shRNAs directed against components of the Dynein/Dynactin complex or both, segmental nerves showing CSP accumulations were quantified. Expression of shRNAs against subunits of the Dynein/Dynactin complex led to an increase of CSP accumulations compared to expression of a control shRNA (ABCG4) (Figure 26 A). In larval motorneurons expressing Tau[R406W] a significant increase of CSP accumulation could only be observed in combination with knockdown of ACTR10 (Arp11 – found as a subtle enhancer in the primary screen) (Figure 26 B). Comparison of accumulations in motorneurons expressing solely shRNA and accumulations in cells co-

expressing shRNA and Tau[R406W] did not reveal significant differences (Figure 26 C). An exception was knockdown of DCTN1. Expression of DCTN1 shRNA in motorneurons led to a significant increase of CSP accumulation in segmental nerves compared to knockdown of the control shRNA (Figure 26 A). However co-expression of DCTN1 shRNA and Tau[R406W] led to significantly fewer CSP accumulations (Figure 26 C).

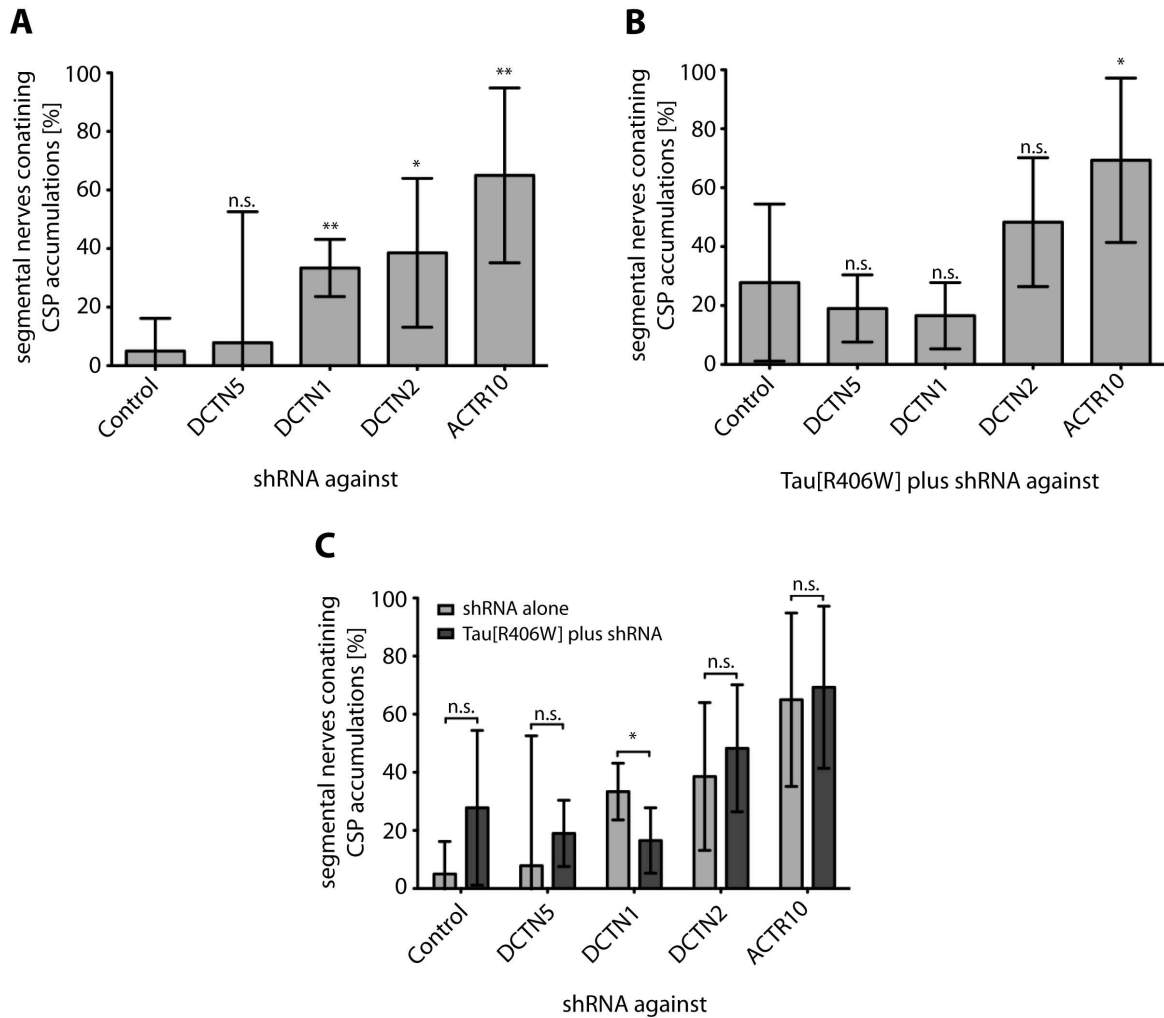


Figure 26: CSP accumulations in motorneurons of *Drosophila* larval segmental nerves.

Quantifications of larval segmental nerves with CSP accumulations. Segmental nerves of larvae with motorneuronal expression of shRNAs, Tau[R406W] or combination of both were analysed. (A) Quantification of CSP accumulations in larva expressing shRNA against members of the Dynein/Dynactin complex in motorneurons. (B) CSP accumulations found in segmental nerves of larvae with combined expression of Tau[R406W] and the shRNAs. (C) Combined plot of quantifications in larvae coding for the shRNAs without (light grey) and with Tau[R406W] expression (dark). The statistics depicted in A and B are t-tests comparing the means to white control. In C t-tests are comparing CSP accumulation with and without Tau expression respectively. (n.s. not significant, * $p < 0.05$, ** $p < 0.01$)

3.7.5 Detailed analysis of the axonal transport using *in vivo* time-lapse imaging

To evaluate axonal transport in Tau[R406W] expressing motorneurons and the effects of shRNAs directed against components of the Dynein/Dynactin complex on axonal transport, *in vivo* time-lapse analysis of transported mitochondria in motorneurons of *Drosophila* L3 larvae (labelled with mitoGFP [246]). This experimental setup allows to assay rates and speeds of both axonal transport directions, respectively. Quantifications in larval motorneurons expressing mitGFP and either Tau[R406W], shRNA directed against DCTN2 or combined expression were compared to transport speeds and rates in WT motorneurons (only expressing mitoGFP). Tau[R406W] expression led to a reduction of transport rates in anterograde direction (Figure 27 A). However, speed was reduced in both directions (Figure 27 B). Knockdown of DCTN2 did not alter the transport speed, but led to decreased rates in both transport directions (Figure 27 B). However, when Tau expression was combined with knockdown of DCTN2, the effects were diminished completely and rates and speeds were restored to WT levels.

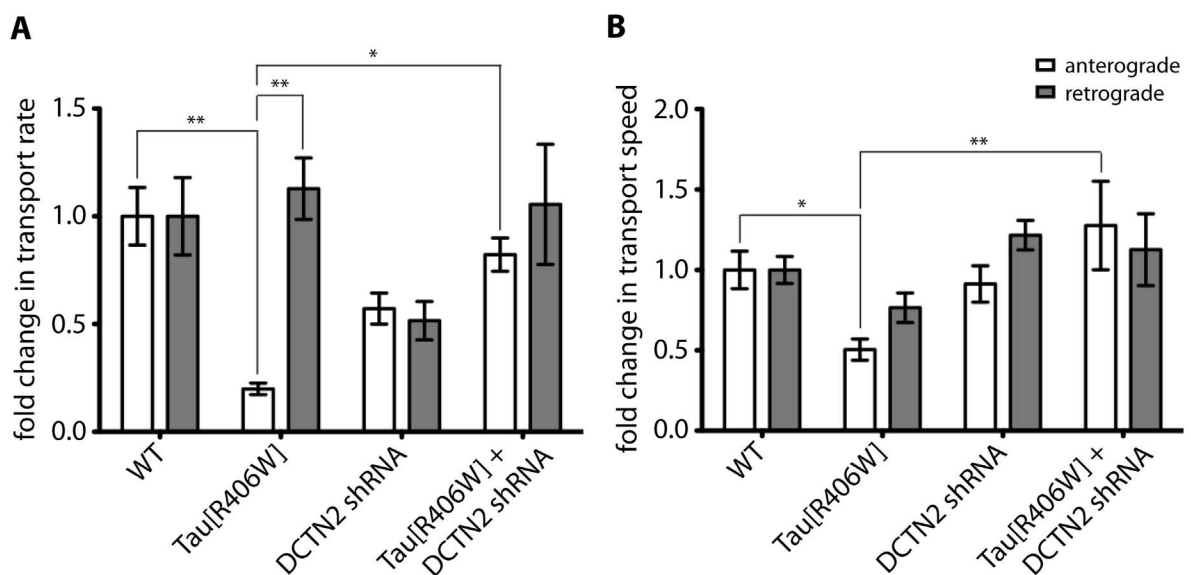


Figure 27: *in vivo* time-lapse analysis of anterograde and retrograde axonal transport.

Evaluation of rates (A) and speeds (B) of anterograde and retrograde transported mitochondria by *in vivo* time-lapse image analysis in *Drosophila* larval motorneurons. Expression of Tau[R406W] led to a significant reduction of anterograde transport rate and speed. The retrograde direction showed a decreased transport speed only (not significant). Knockdown of Dynamitin led to a significant decrease of transport rates in both directions, although transport speed was not altered. Interestingly the combination of Tau expression and knockdown restored WT transport rates and speeds. (*p < 0.05, **p < 0.005)

3.7.6 Effects of Tau[R406W] expression on transcription levels of transport proteins

I conducted a quantification of transcript levels of selected candidates in head RNA preparations of flies with pan-neural Tau[R406W] expression to test for Tau-mediated effects on transcription of members from the Dynein/Dynactin complex. The mRNA levels of TUBA1A, IGF2R (Lerp, a lysosomal transport candidate not correlated to the complex), DCTN1, DCTN2 and the axonemal DAHC17 were quantified. Analysis revealed severe changes in transcript levels (Figure 28 A). Levels of TUBA1A, IGF2R and DCTN1 mRNA were significantly increased, mRNA levels of DCTN2 and DAHC17 were dramatically increased (about 8-fold each). This was highly significant for DCTN2. The changes in DAHC17 transcript levels were not found to be significant. This might be due to very low mRNA levels in the head RNA preparations (10^{-5} fold compared to ACTG1) leading to high variances in qPCR analysis (Figure 28 B).

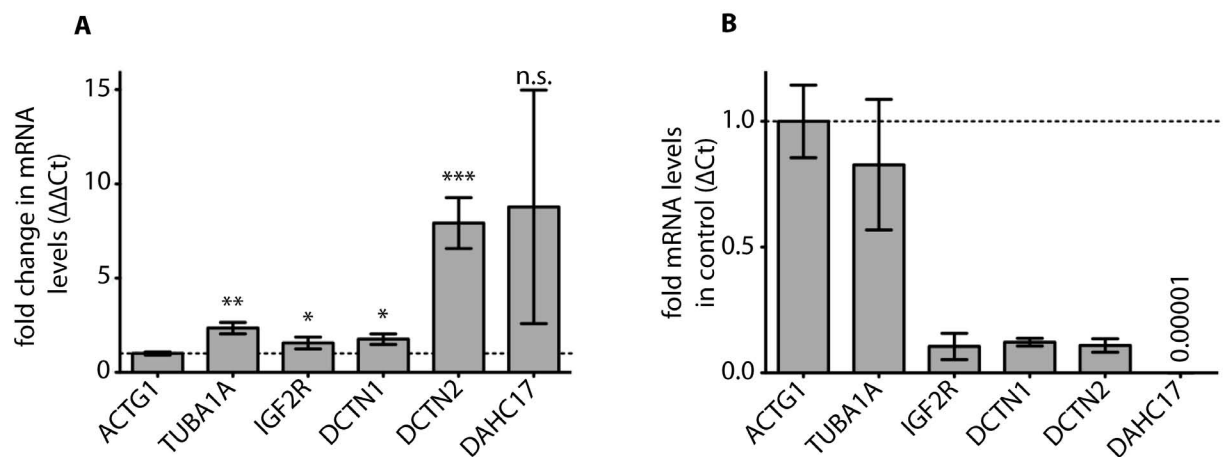


Figure 28: Changes in transcript levels of transport candidates due to Tau[R406W] expression.

(A) Quantification of changes of mRNA levels due to Tau[R406W] expression in head RNA extracts of adult flies expressing Tau[R406W] pan-neurally. Quantities were normalised to *actin5C* (ACTG1) and compared to levels in the *elav^{C155}-Gal4* driver line without expression of a transgene. Depicted statistics are t-tests comparing the means of target mRNA level differences to Actin 5C (ACTG1): n.s. not significant, * $p < 0.05$, ** $p < 0.005$, *** $p < 0.0005$. (B) ΔC_t analysis of mRNA levels in the head RNA extract of control flies. The data shows physiological transcript levels of the different candidate genes compared to ACTG1.

3.7.7 The role of the Dynein/Dynactin-based transport in the lysosomal pathway

As changes in structure and function of lysosomes are found in Tau pathology (see chapter 1.6), head paraffin sections of adult *Drosophila* were examined and

immunohistochemically stained for lysosome-associated membrane protein 1 (**Lamp1**), total hTau (antibody 5A6) and C-terminal truncated Tau⁴²¹ (antibody TauC3). Staining patterns of antibodies Lamp1, 5A6 and TauC3 were analysed in flies expressing Tau[R406W]. As the candidates of the transport group might contribute to lysosome function, expression of shRNA directed against DCTN1 (and combined expression of DCTN1 shRNA and Tau[R406W]) was also evaluated for modification in staining patterns of 5A6, Lamp1 and TauC3 antibodies. Staining patterns were only analysed for qualitative characteristics, and not quantified. In flies expressing DCTN1 shRNA, neither 5A6 nor specific staining of Lamp1 or TauC3 could be observed (Figure 30 A-C). Tau[R406W] expression led to 5A6-positive neurons in the brain, however Lamp1 and TauC3 staining appeared only in a few single cells (Figure 30 D-F). In brains from flies with expression of Tau[R406W] and DCTN1 shRNA, 5A6-positive neurons increased dramatically in number and staining intensity (Figure 30 G). The antibody against Lamp1 revealed a change in lysosome number and/or size (Figure 30 H). Lamp1-positive cells did not appear in the optic lobes. In addition the TauC3 antibody could detect eminent accumulations of truncated Tau in fibered structures within the optic lobe (Figure 30 I).

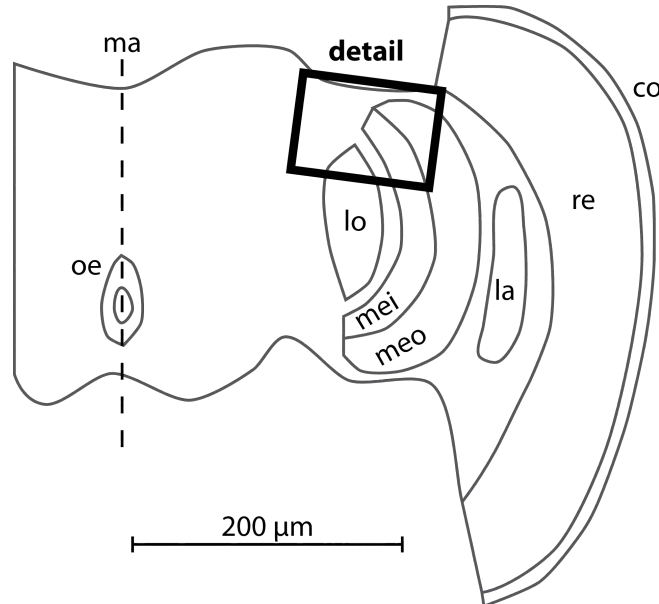


Figure 29: Schematic view of a lateral part of a frontal section through an adult fly head.

Schematic view of the adult fly optical lobe (frontal section) and the detail view used for Figure 30. For orientation, the oesophagus (**oe**) is found at the ventral part of the medial brain axis (**ma**). In the retina (**re**) covered by the cornea (**co**) the photoreceptors are found projecting into the lamina (**la**) and the outer part of the medulla (**meo**). Medial from the inner part of the medulla (**mei**) the lobula (**lo**) is found. The black box (**detail**) depicts the selection shown in Figure 30.

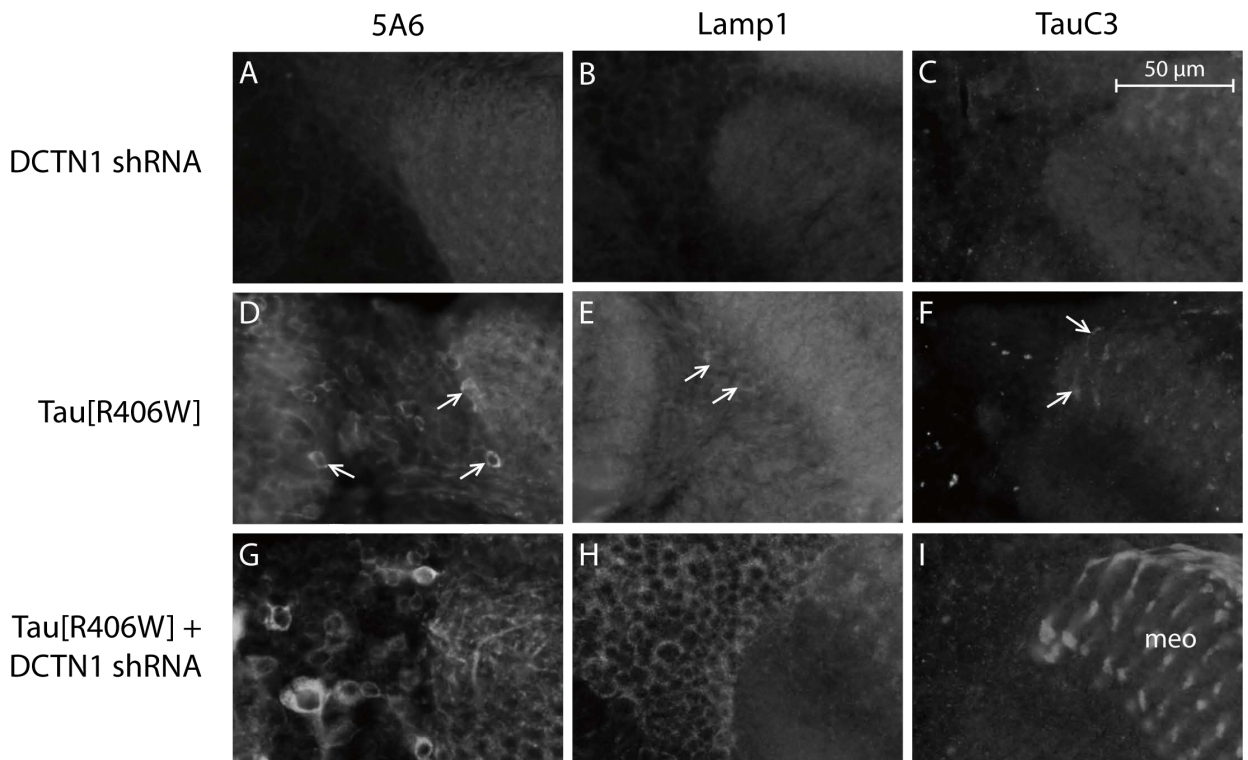


Figure 30: Adult *Drosophila* brain stained for hTau (5A6), Lamp1 and Tau⁴²¹ (TauC3).

To evaluate effects of Tau[R406W] and knockdown of DCTN1 on hTau protein, lysosomal load and Tau fragmentation, paraffin sections of adult *Drosophila* heads were stained for total hTau (antibody 5A6), lysosomal marker Lamp1 and the C-terminal truncated Tau⁴²¹ (antibody TauC3). Expression of shRNA directed against DCTN1 did not lead to immuno-reactivity of 5A6, Lamp1 and TauC3 antibodies (A - C). In flies expressing Tau[R406W], 5A6-positive neurons could be observed (D) and single cells appeared to be positive for Lamp1 (arrows) (E) and TauC3 antibody (arrows) (F). However, combination of Tau[R406W] expression and knockdown of DCTN1 dramatically increased number and size of 5A6-positive cells and filamentous Tau-positive structures could be observed (G). In addition, significant numbers of Lamp1-positive cells appeared surrounding the optic lobe (H). In the outer medulla (meo) of the optic lobe, fibered structures were found heavily stained for TauC3 antibody (I). Optic lobe structure and selection of shown area see Figure 29. Orientation of the images is lateral-right and dorsal-up. Magnification is depicted in C (bar=50 μm).

4 Discussion

This study was conducted as a genetic screen on modifiers of Tau-induced neurodegeneration in *Drosophila* in order to find new approaches for research in the field of Tauopathies. For this, models of Tau induced pathology were utilised, which have already been described (see chapter 1.8.2).

4.1 Characterisation of the transgenes in *Drosophila*

In line with the first publication by Wittmann et al. [125], expression of human Tau[WT] and Tau[R406W] in *Drosophila melanogaster* can serve as models of neurodegeneration without neurofibrillary tangles. Expressed in post-mitotic cells of the compound eye, severe REPs could be observed (Figure 9). The mutant Tau[R406W] variant induced the more stable phenotype, with a higher severity compared to Tau[WT]. As the GMR-mediated phenotype appeared to be more robust, Tau[R406W] expression was chosen to serve as a screening model for the modifier screen of Tau-induced neurodegeneration. As the two Tau transgenes were created by random genomic integration, direct comparison of effects induced by Tau[WT] and Tau[R406W] expression were not reasonable, because of presumptive different expression levels. In principle, these two transgenes also induced neurodegenerative effects such as reduced life span, as previously published [125] (Figure 12 A). Toxic effects of Tau[R406W] expression could also be observed during larval development (Figure 10).

Pan-neural expression of Tau[R406W] did not lead to decreased transcript levels of endogenous dTau. Comparison of transcript levels of dTau and hTau in head RNA of flies pan-neurally expressing Tau[R406W] revealed an approximate 1.8 fold higher mRNA level of the ectopic hTau (Figure 11). Thus, Tau[R406W] overexpression leads to significant intracellular levels of Tau, allowing to investigate mechanistic interactions.

In addition to the hTau transgenes, two additional transgenes were analysed in regards to their REP (induced by GMR-mediated expression) and life-span (in pan-neural expression): $A\beta_{42}$ (modelling amyloid-induced AD toxicity [241]) and Q_{78} (modelling the poly-glutamine disease spino-cerebellar ataxia type 3 [248]). These transgenes were used to evaluate Tau-specificity of the found modifiers. In both, the reported REP (Figure 9) and reduced life spans (Figure 12 A, pan-neural expression of Q_{78} appeared to be lethal)

could be observed, underlining their published ability to serve as neurodegenerative models [241, 248].

To directly compare the effects on different Tau variants, transgenes with site-directed genomic integrations were generated: *attB_Tau[WT]*, *attB_Tau[R406W]* and two variants mimicking different phosphorylation states *attB_Tau[AP]* (not phosphorylatable at all 14 SP and TP sites) and *attB_Tau[E14]* (phospho-mimicking glutamate at all 14 SP and TP sites). Flies pan-neurally expressing *attB_Tau[WT]*¹ and *attB_Tau[R406W]* showed similar life spans (Figure 12 B). In contrast flies expressing *attB_Tau[AP]* and *attB_Tau[E14]* had a significantly decreased life span (expression of *attB_Tau[AP]* was lethal). Tau[E14] variant was previously reported to be more toxic than Tau[WT] and Tau[R406W], but the non-phosphorylated Tau[AP] variant was reported to be the less toxic variant [235, 236]. However, we found that Tau[AP] seems to be even more toxic than Tau[E14] when expressed pan-neurally. Increased toxicity of a non-phosphorylatable Tau model in *Drosophila* has already been reported for a 2N4R Tau model with eleven mutated phosphorylation sites (TauS11A), eight of these shared with the Tau[AP] transgene. Chatterjee et al. observed more severe toxicity in their TauS11A model compared to Tau[WT], induced by increased microtubule binding activity [255]. In quantifications of hTau mRNA and protein levels in the head of flies with GMR-mediated expression of the four transgenes, an increase induced by the *attB_Tau[AP]* transgene could be observed (Figure 17). Assuming identical epigenetic conditions (created by the site-directed genomic integration) the difference in protein levels can be explained. The explanation why *attB_Tau[AP]* shows increased protein levels could be an altered ratio of soluble and microtubule-bound Tau protein [255]. An increase in microtubule-bound protein fraction could lead to a decreased Tau degradation (as Tau is “trapped” at microtubules). Still, differences observed in transcript levels cannot be explained.

In flies with GMR-mediated expression of *attB_Tau[E14]* decreased transcription levels were measured compared to *attB_Tau[WT]*, while protein levels did not differ. Tau[E14], mimicking hyperphosphorylation, is known to have a reduced microtubule binding ability. Thus, Tau[E14] is predisposed to form oligomers and reduced transcription might be a preventive effect. However, the reduction of *attB_Tau[E14]*

¹ To differentiate between hTau protein expressed by random and by site directed integration transgenes, the latter are referred to as *attB_Tau*.

transcription does not seem to have an impact on Tau protein levels, which might be rescued via increased aggregate formation preventing Tau degradation.

Nevertheless, expression of attB_Tau[WT], attB_Tau[R406W], attB_Tau[AP] and attB_Tau[E14] in post-mitotic cells of the compound eye induced comparable REPs in this study (Figure 16). For this reason comparison of candidate effects on the induced REPs is done using these four site-directed integration transgenes, although transcript and protein levels differ.

4.2 Modifiers of Tau-induced REP in the compound eye of *Drosophila*

In the primary screen 73 candidates were identified modifying Tau[R406W]-induced REP. Knockdown of 15 candidate genes were found to suppress and 58 candidate shRNAs enhanced the Tau-induced phenotype. The 73 candidate genes were grouped into four classes according to processes, in which the encoded proteins are involved in: 20 candidates in the protein anabolism and catabolism group, eight in a group of transport processes, six in the group of kinases and phosphatases. The remaining 39 were listed as miscellaneous. There are two published screens on modifiers of Tau-induced neurodegeneration. Shulman and Feany conducted a misexpression-based screen on modifiers in *Drosophila* [232], whereas Kraemer *et al.* used *Caenorhabditis elegans* (*C. elegans*) as a model organism for a genome-wide screen on modifiers of Tau pathology [256]. In the former *Drosophila* screen 24 candidates were identified and categorised according to their putative function into 5 main groups: protein kinases/phosphatases (7), apoptosis (2), cytoskeleton (3), miscellaneous and novel (7 and 5) [232]. Of these 24, none could be identified as a primary candidate using the RNAi approach in this work. However, two showed subtle changes of the phenotype, congruent with the results of Shulman and colleagues (TAOK1 and FEM1B). Using a genome-wide RNAi-mediated knockdown approach in *C. elegans*, Kraemer *et al.* identified 50 modifiers of Tau-induced phenotype (additional candidate genes were found without human homologues). The 50 candidate genes were categorised into 8 functional groups: phosphorylation (8), protein folding and stress response (7), nucleic acid function (8), proteolysis (4), transport and secretion (3), neurotransmission and signalling (8), enzymes (7), structural and extracellular matrix proteins (3) and unknown function (2) [256]. Again, no direct overlap in candidates was found between the published results and this work, although this study identified two candidates, each belonging to the same protein family as candidates of the *C. elegans* screen: While Kraemer *et al.* found DDX4 (Dead box

polypeptide 4) and SLC24A6 (solute carrier family 24 member 6) as genetic modifiers, the present work identified DDX42 (Dead box polypeptide 42) and SLC35E1 (solute carrier family 35 member 1) as modifiers of the Tau-induced phenotype. Notably, although the screen in *C. elegans* could only identify enhancers (due to systemic limitation), both DDX42 and SLC35E1 knockdown resulted in suppression of the Tau-induced REP in the present screen. In addition, knockdown of three candidate genes published by Kraemer *et al.* were found to be subtle modifiers in the present work (TAOK1, HSPA8 and AMD1). To complete comparison of the three screens, the overlap between candidate genes found by Shulman and Kraemer is restricted to two candidate genes each coding for a kinase: MARK3 (PAR-1, microtubule-affinity regulating kinase 3) and TAOK1 (MARKK, microtubule-affinity regulating kinase kinase) [232, 256]. The overlaps between the three screens are demonstrated in Figure 31.

Although the overlaps of the three screens on modifiers of Tauopathy are not extensive, the similarities of functional groups identified are obvious. In all three screens, kinases and phosphatases could be identified, as well as proteins involved in protein

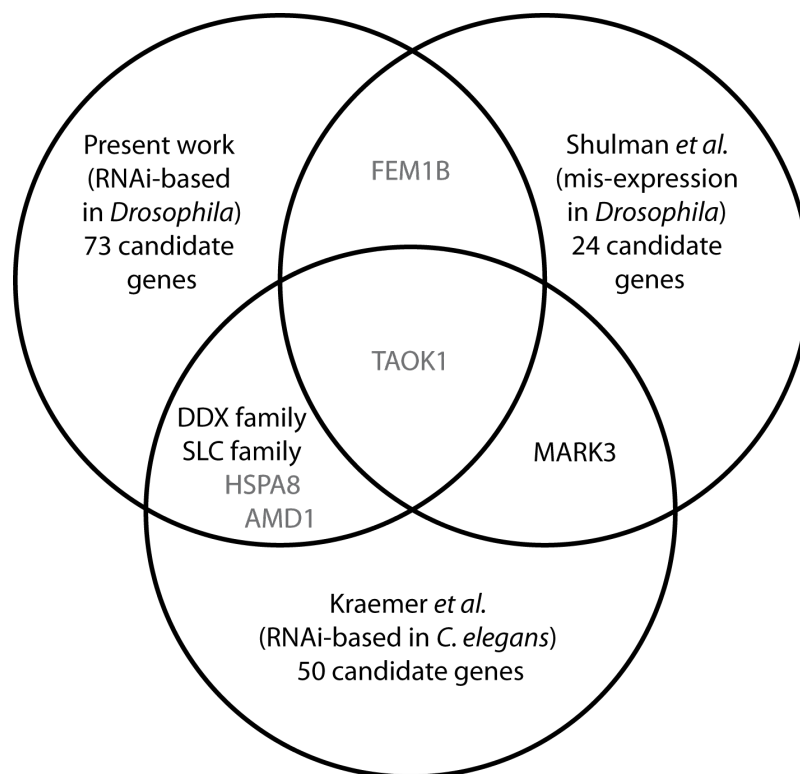


Figure 31: Overlaps between the three screens for modifiers of Tau-induced pathology.

A schematic overview of overlaps between the present work, a misexpression-based screen in *Drosophila* [232] and a RNAi-based screen in *Caenorhabditis elegans* [256]. Knockdown of genes inducing only subtle changes in the present study are depicted in **grey**. DDX family and SLC family delineate the overlap by two different genes coding for proteins of the same protein family, respectively.

anabolism and catabolism. In addition, gene products involved in intracellular transport processes and regulation of cytoskeleton and cell structure are common in all three screens. It is notable that, although there are no direct overlaps, the results of the present screen are functionally more similar to the *C. elegans* screen (both RNAi-based screening approaches), than to the misexpression-based screen in *Drosophila*. The type of screening approach seems to contribute to this similarity. Of the candidates identified in the misexpression-based approach of Shulman *et. al.*, 80 percent of candidates were found in overexpression of the target genes. This resembles an opposite gene regulation compared to the RNAi approach of this study. Therefore divergent results are not surprising.

4.3 Specificity of selected candidates for the R406W mutation of Tau

In humans the Tau[R406W] is associated with FTDP-17, in contrast to physiological Tau[WT]. The R406W mutation leads to a decreased affinity of Tau to bind microtubules, which alters the ratio between microtubule-bound and soluble Tau fractions [104, 105]. Overexpression of both Tau[WT] and Tau[R406W] induce neurodegenerative phenotypes in *Drosophila* [125]. This might be due to the overall increased Tau protein levels in both Tau[WT] and Tau[R406W] overexpression. Nevertheless, candidates might be specific to the pathological R406W mutation. To evaluate this specificity a secondary screen was conducted comparing shRNA effects on GMR-mediated expression of site directed integration transgenes *attB_Tau[WT]* and *attB_Tau[R406W]*. In general, the same effects were observed. Only a small number of candidate shRNAs showed differential effects on *attB_Tau[WT]*- and *attB_Tau[R406W]*-induced REPs (Figure 19). One enhancer was found to be stronger in Tau[WT]-induced REP (MED14) and two enhancers showed a stronger impact on the Tau[R406W] variant (PSMB7 and CWC25). Interestingly, all three candidates are grouped into the protein anabolism and catabolism group (PSMB7, MED14 and CWC25). The R406W mutation does not interfere with the microtubule-stabilising function of Tau, which is regulated by phosphorylation [257]. Thus, a lack of specific candidates in the kinase/phosphatase group is plausible. However, the reason that the three candidates (MED14, PSMB7 and CWC25) show differences in modification of Tau[WT]- and Tau[R406W]-induced REP remains unclear, but the results suggests a differential role of the R406W mutation in Tau protein turnover.

4.4 Alteration of intracellular Tau protein levels as a mechanism for modulation of toxicity

As described in chapter 1.4, there are different mechanistic models for Tau pathology. Instead of one pathomechanism, it is likely that loss of function, direct toxicity and toxicity aggregation of Tau rather work in concert [100]. One mechanism to modify the Tau-induced toxicity would be to interfere with Tau protein levels. It has been shown recently, that deletion of Tau significantly decreases neurodegeneration induced by A β -peptides in a mouse model [32]. Therefore Tau protein levels were evaluated to identify candidate shRNAs modifying Tau protein load. Evaluation was carried out for ten candidates from the protein anabolism and catabolism group (PSMB7, STIP1, ERI2, SMG5, C4orf31, RPS10, CDC20, LAMTOR1, TMEM135 and PTRH2) and three candidates from the transport group (IGF2R, DCTN1 and DNAH17). Although analysis could only be repeated twice allowing no conclusions of significance, changes in Tau protein levels, induced by candidate knockdown could be observed in three cases (STIP1, CDC20 and LAMTOR1). Interestingly, the changes in Tau protein levels did only correlate with the direction of GMR-mediated Tau[R406W]-induced REP modification in two cases (suppressor STIP1 and enhancer CDC20). The found reduction of hTau levels (5A6 band intensity) in flies pan-neurally co-expressing Tau[R406W] and shRNA directed against LAMTOR1 was contrary to the identification of LAMTOR1 knockdown suppressing Tau[R406W]-induced pathology in the compound eye. However, it could be shown that effects of STIP1 and CDC20 on Tau pathology are most likely mediated by affecting cellular protein load of Tau.

STIP1 codes for the stress induced phospho-protein 1, which is an adaptor protein coordinating HSP70 and HSP90 function in protein folding [258-260]. STIP1 knockdown was identified as a suppressor of Tau-induced REP in the primary screen and this suppression was still obvious in GMR-mediated attB_Tau[WT] and attB_Tau[AP] expression, but not present in attB_Tau[E14]-induced phenotype. Several HSP70 factors have been found by genetic screens to have an impact on Tau pathology [256] and the carboxyl terminus of HSP70 is known to be involved in degradation of Tau [261]. Thus, STIP1 as a regulator of HSP70 and HSP90 function might influence Tau degradation. The effect of STIP1 knockdown is not only restricted to Tau pathology, as it also suppresses Q₇₈-induced REP (Table 13). Hence, STIP1 knockdown seems to increase degradation of aggregates in general. This makes STIP1 a very interesting target for future research.

4.5 SP and TP phosphorylation sites in Tau-induced toxicity

Phosphorylation of Tau seems to be a critical process contributing to the mechanism of Tau pathology, as abnormally phosphorylated Tau is found in the brains of AD patients [62, 262]. Attention has especially been paid to the proline guided serine (SP) and threonine (TP) phosphorylation sites, as antibodies specific for phosphorylated SP or TP epitopes have been reported to preferentially detect Tau from brains of AD patients [263]. In addition, proteins contributing or inhibiting Tau pathology identified in genetic screens (e.g. MARK3 [232] and PP2A [232, 256]) evidently alter phosphorylation states significantly [69, 264]. Modifiers of Tau-induced toxicity identified in the present screen might also change phosphorylation of Tau. This possibility was analysed by a phenotypic screen, comparing the effects of candidate knockdown on attB_Tau[R406W]-induced REP with the effects on attB_Tau[AP]- and attB_Tau[E14]-induced REPs. GMR-mediated expression of attB_Tau[R406W], attB_Tau[AP] and attB_Tau[E14] induced comparable REPs allowing to compare shRNA effects (Figure 16). If the mechanistic interaction of Tau and a protein, coded by a candidate gene, depends on Tau phosphorylation state, differences in modification of attB_Tau[AP]- and attB_Tau[E14]-induced REP will occur.

Of the 73 candidate shRNAs modifying Tau[R406W]-induced REP, eight modified the REP induced by expression of attB_Tau[R406W], attB_Tau[AP] and attB_Tau[E14] differentially (Figure 20). Knockdown of the candidate genes TUBA1A, TUBA1C, ERI2, SMG5, ODF3 and SNRPC showed a more pronounced enhancement of the phenotype induced by expression of non-phosphorylatable attB_Tau[AP] compared to attB_Tau[R406W]. Toxicity of Tau[AP] is most probably induced by a shift in soluble and microtubule-bound Tau ratio towards the bound fraction, which is reported for comparable non-phosphorylatable Tau models in *Drosophila* [255]. This increase of the microtubule-bound fraction reduces microtubule-based transport processes. Thus, knockdown of TUBA1A and TUBA1C coding for Tubulin alpha 1a and c will contribute to the toxic Tau[AP] effects, as reduction of present microtubules worsens diminution of microtubule-based transport.

Improvement of the REP was found in attB_Tau[AP] after knockdown of the candidate gene PSMB7. PSMB7 codes for the proteasome subunit beta type 7, which is a catalytical subunit of the proteasome complex. Although the direct function of this subunit is not known, degradation of Tau via the proteasome is suggested to be one pathway of Tau degradation [96]. Why effects of PSMB7 knockdown are rather restricted to

Tau[R406W] and phospho-mimic Tau[E14], is unclear and should be addressed by future research.

Only shRNA directed against STIP1 led to an attB_Tau[E14] phenotype different from the R406W variant. As mentioned in chapter 4.4, STIP1 is regulating HSP70 function, which is known to be involved in degradation of Tau [261]. Thus, suppression of Tau-induced pathology by knockdown of STIP1 seems to be mediated by an increased HSP70 function, leading to an increased Tau degradation. Accordingly, STIP1 was identified in this study to reduce protein levels of Tau notably (see chapter 4.4). The link might not be due to direct interaction, but the data implies, that for suppression of Tau-induced toxicity via knockdown of STIP1, de-phosphorylation of one or more SP or TP phosphorylation sites is crucial.

A selection of four candidate shRNAs, shown to act differentially on REPs induced by GMR-mediated expression of attB_Tau[R406W], attB_Tau[AP] or attB_Tau[E14], were evaluated for their impact on Tau phosphorylation (at sites Thr¹⁸¹, Thr²³¹ and Ser²⁰²/Thr²⁰⁵) using phospho-specific antibodies (see chapter 3.6). No obvious modifications of Tau phosphorylation could be observed after knockdown of candidate genes in flies with pan-neural expression of Tau[R406W]. Observed differences rather reflect differences by altered Tau[R406W] levels (Figure 21). The selection was restricted to candidates that were found to depend on distinct Tau phosphorylation state (3.5.2). Though, candidates that depend on the phosphorylation state of Tau, might not alter Tau phosphorylation. Evaluation of the ability to change phosphorylation states of Tau should rather be performed for all candidate shRNAs. However, due to time limitations I was not able to finish this evaluation. This will be done in future work. However preliminary data suggests that there are several candidates that alter phosphorylation of Tau (see appendix).

4.6 The Dynein/Dynactin complex in Tau-induced neurodegeneration

A connection of Tau pathology and microtubule-based transport processes such as Dynein/Dynactin guided retrograde transport (as well as Kinesin guided anterograde transport) is known for several years [182]. However, research was always restricted to the effects of Tau on transport processes. In this study the opposite direction came in focus for the first time. As knockdown of several components of the Dynein/Dynactin

complex were found to enhance Tau pathology in the primary screen, several experiments were done to elucidate the impact of impaired retrograde transport on Tau pathology.

4.6.1 The axon as the putative site of Dynein/Dynactin and Tau interconnection

Tau is predominantly found in the axonal compartment and gets redistributed to the somatodendritic compartment in disease [197, 198]. It is not known if this re-localisation is the cause of, or an outcome of, Tau pathology. If clearance of Tau from the axon is a mechanism to rescue the axon from Tau toxicity, reduction of retrograde transport towards the somatodendritic compartment would contribute to Tau toxicity. Depletion of Dynein/Dynactin motor complexes by shRNAs reduces retrograde traffic from the axon (see chapters 3.7.4). Clearance of toxic Tau species from the axon as a mechanism to delay Tau-induced neurodegeneration was the first hypothesis raised for the involvement of the Dynein/Dynactin complex in Tau pathology in this study (Figure 32).

To facilitate experiments concerning axonal transport, expression of Tau[R406W] in *Drosophila* larval motorneurons was utilised. Before testing the hypothesis, microtubule networks in segmental nerves were evaluated and found not to be significantly altered by neither Tau[R406W] overexpression nor knockdown of Dynein/Dynactin complex

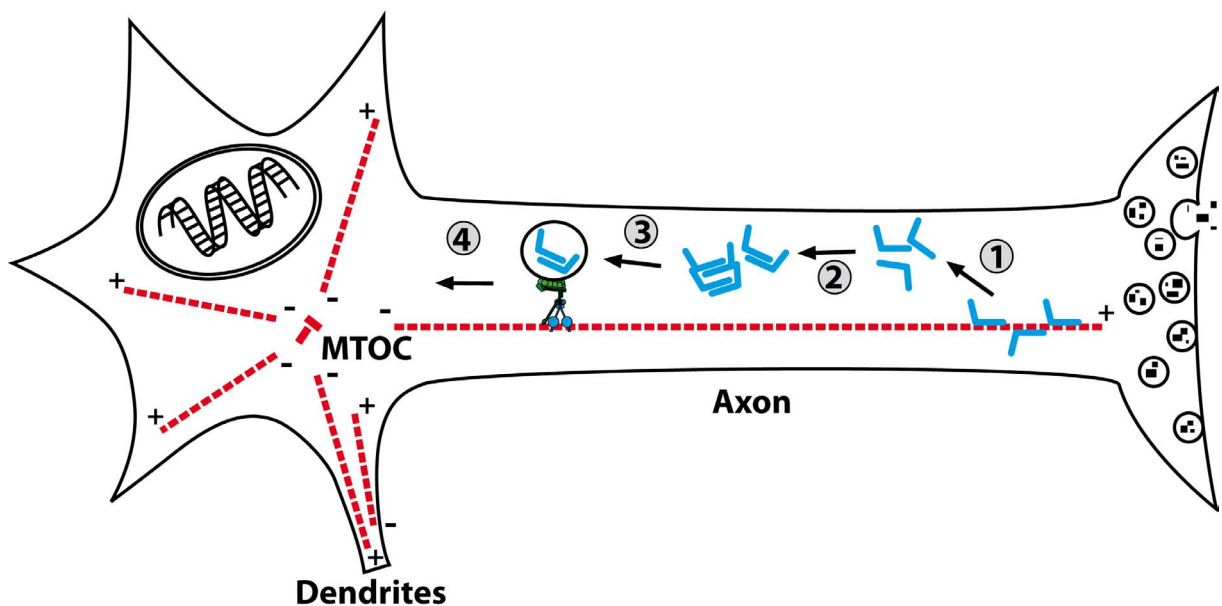


Figure 32: Model of Tau clearance from the axon by retrograde axonal transport.

A schematic view of the working hypothesis based on the finding that knockdown of Dynein/Dynactin complex increases Tau-induced toxicity. The microtubule-associated protein Tau is physiologically stabilising microtubules. Toxic triggers leading to toxicity eventually lead to a detachment (e.g. hyperphosphorylation) (1). A toxic species of Tau is accumulating in the axonal compartment (2). To evade toxic effects from the Tau species within the axon, Tau is cleared by retrograde transport (3) and brought to the somatodendritic compartment (4).

members (Figure 23). Disturbances of transport paths could be induced by expression of shRNAs directed against members of the Dynein/Dynactin complex as CSP accumulations (Figure 26 A) and staining intensity of neuronal membranes in the NMJs were increased (Figure 25). In addition, the velocity of retrograde transport was found to be reduced *in vivo* (Figure 27 B). Nevertheless when Tau[R406W] was co-expressed with shRNAs directed against members of the Dynein/Dynactin complex, neither hTau accumulations nor increased hTau staining intensity could be found in axons (or NMJs). The data even suggests that knockdown of members from the Dynein/Dynactin complex lead to decreased axonal Tau levels (Figure 24). This might be due to effects upstream of the proposed model of clearance. In fact the axonal localisation of Tau is partially maintained by a Dynein/Dynactin-mediated process (see chapter 1.5.6). However, the results of quantified CSP accumulations in segmental nerves (Figure 26 B) do not allow conclusions on the impact of Dynein/Dynactin knockdown on Tau pathology. The same holds true for the *in vivo* measurements of transport rates and velocities (Figure 27) in larvae expressing Tau[R406W] and shRNAs directed against the complex. The effects found in the primary screen were present in post-mitotic cells in the compound eye of adult *Drosophila*. Ambiguous results such as reduced hTau levels in the axon and restored transport rates and speeds due to knockdown of Dynein/Dynactin complex members were produced in axons of motoneurons in L3 larvae. However, effects seen in the axons of larval motoneurons might not be comparable to the Tau[R406W]-induced toxicity enhanced by Dynein/Dynactin silencing in the adult compound eye.

Finally, the hypothesis of retrograde Tau clearance from the axon as a mechanism to evade axonal Tau toxicity could not be endorsed. However, another possible connection between the Dynein/Dynactin complex and Tau-induced pathology was drawn, based on a lysosomal function of the retrograde transport complex.

4.6.2 Lysosomal involvement in Tau-induced pathology

Recent publications have shown that members of the Dynein/Dynactin complex are crucial for a lysosomal function [266, 267]. In addition to proteasomal degradation Tau is thought to be processed and eliminated by lysosomal pathways [265]. The general importance of the lysosome in Tau pathomechanism is underlined by several candidate genes identified in the primary screen of this study, which are involved in lysosomal processes. Knockdown of IGF2R (lysosomal transport), LAMTOR1 (lysosome organisation) and two proton transporting ATPases (ATP6V0C and ATP6V1D), which are

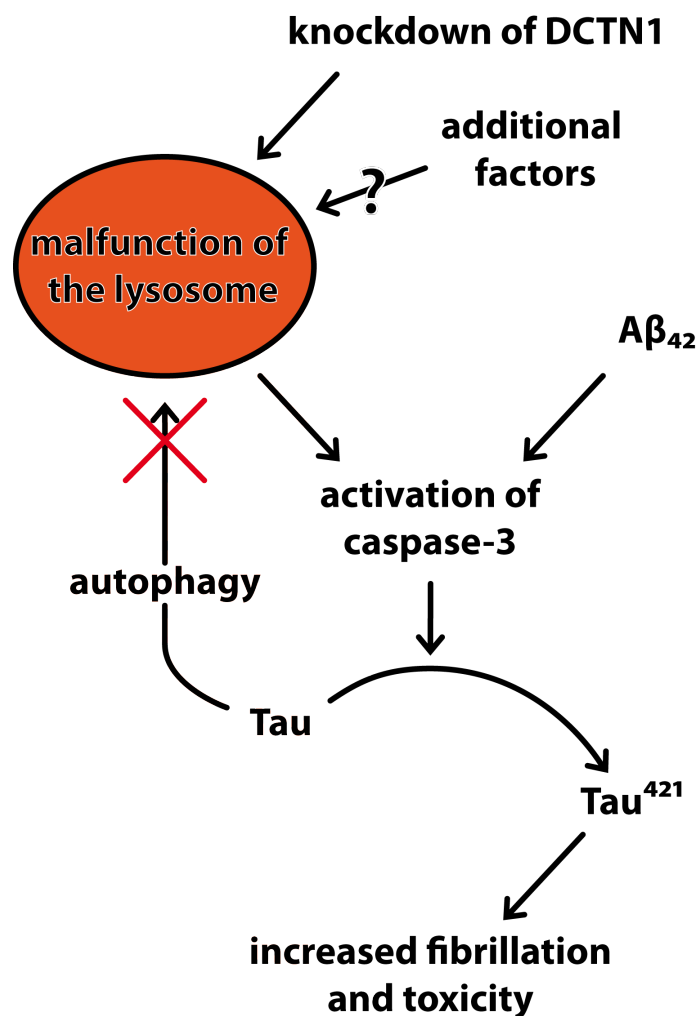


Figure 33: Increased Tau toxicity by lysosomal malfunction and caspase-3 activation.

The Tau⁴²¹ fragment is known to be more amyloidogenic and seeds Tau aggregates [38]. This truncation is created by activated caspase-3 cleavage. Caspase-3 is activated via A β ₄₂ [33] and by lysosomal dysfunction [211]. That this mechanism might be induced by depletion of Dynein/Dynactin motorcomplex is suggested by the present work. In addition, dysfunction of the lysosome increases Tau toxicity by impaired macroautophagy [265].

involved in organelle acidification, enhance Tau-induced REP. Thus, the effects by depletion of the Dynein/Dynactin retrograde transport on Tau pathology might be due to their lysosomal involvement. The lysosomal role in Tau pathology was evaluated in flies with pan-neural expression of Tau[R406W], the shRNA directed against DCTN1 (a key member of the Dynein/Dynactin complex) and the combination of both.

In the adult *Drosophila* brain, pan-neurally expressing Tau[R406W] and the shRNA directed against DCTN1 induced an increase of lysosomal size and/or number (increased lysosomal staining, Figure 30 H). A slight increase of lysosomal Lamp1 staining was already visible in brains with Tau[R406W] expression. Alteration in number and morphology of lysosomes is known to be induced by Tau expression and is also found in AD brains [199-201]. Co-expression of Tau[R406W] and the shRNA increased Lamp1 positive staining substantially and induced accumulation of C-terminal truncated Tau⁴²¹ in fibrillar structures (Figure 30 I). Most probably, these fibrillar structures resemble the projections of R7 and R8 photoreceptors into the medulla, as they show the same distinct morphology [268]. Why appearance of Tau⁴²¹ is restricted to photoreceptors in fly brains expressing Tau[R406W] in a pan-neural pattern remains unclear. However, lysosomal dysfunction, which may be accompanied by increased lysosome size and/or number is reported to activate caspases eventually leading to Tau truncation [211]. The present work suggests that Dynein/Dynactin knockdown increases Tau-induced toxicity via malfunction of the lysosome, inducing Tau truncation via caspase-3 activation (Figure 33). If caspase-3 actually is activated in DCTN1 depletion will be analysed in future work.

4.7 Summary and conclusions

Although decades of scientific research have attempted to illuminate the pathomechanisms of Tauopathies, still very little seems to be known about the complex disease processes. I conducted a screen identifying genetic modifiers of Tau[R406W]-induced neurodegeneration in *Drosophila* using a genome-wide RNAi-based approach.

This study opens a variety of directions for future research, as it provides a list of novel genetic modifiers interfering with Tau pathology. Secondary analyses also provide information about specificity of the candidates for modification of Tau[R406W]-, Tau[AP]- and Tau[E14]-induced neurodegeneration. In addition knockdown, of selected candidates was shown to alter Tau protein turnover and Tau phosphorylation.

As several candidate genes code for members of the Dynein/Dynactin complex, I focused on the evaluation of the impact of this complex on Tau pathology. This led me to

two different models for modification of Tau pathology by the Dynein/Dynactin complex. Clearance of a Tau toxic species from the axon by the retrograde transport complex could be a mechanism to evade axonal clogging or a starvation of the synapse. I was not able to confirm (or disprove) this model (see chapter 4.6.1). An explanation of enhanced toxicity in Dynein/Dynactin knockdown might rather be an impaired lysosomal function. I could show that knockdown of the Dynein/Dynactin complex key member DCTN1 led to alterations in lysosome morphology, which was accompanied by C-terminal truncation of Tau at amino acid 421. As Tau⁴²¹ is already known to have an increased toxicity compared to Tau[WT], results endorse the second model of increased Tau toxicity mediated by depletion of Dynein/Dynactin motor complexes resulting in lysosomal dysfunction. The direct role of the lysosomal pathway in Tau-induced toxicity still remains unclear and future research should uncover the several gaps in understanding lysosomal involvement. Although it is known that Tau⁴²¹ is a product of truncation by caspase-3, which is activated by lysosomal dysfunction, the mechanisms leading to caspase-3 activation as well as the lysosomal dysfunction itself remain elusive.

In conclusion, I conducted a screen producing a list of yet unknown modifiers of Tau-induced pathology and several results elucidating putative modes of modification. This work not only stands for itself, but also creates a variety of approaches, to investigate Tau pathology. This can be used for future research, which eventually might lead to the development of novel therapeutic strategies.

5 References

- [1] Pick, A. *Über die Beziehungen der senilen Hirnatrophie zur Aphasie*. Prager Medicinische Wochenschrift **17**, 165-167 (1892).
- [2] Foster, N. L. *et al. Frontotemporal dementia and parkinsonism linked to chromosome 17: a consensus conference. Conference Participants*. Ann Neurol **41**, 706-715 (1997).
- [3] Ingram, E. M. & Spillantini, M. G. *Tau gene mutations: dissecting the pathogenesis of FTDP-17*. Trends Mol Med **8**, 555-562 (2002).
- [4] Iqbal, K. *et al. Mechanisms of neurofibrillary degeneration and the formation of neurofibrillary tangles*. J Neural Transm Suppl **53**, 169-180 (1998).
- [5] Iqbal, K. *et al. Identification and localization of a tau peptide to paired helical filaments of Alzheimer disease*. Proc Natl Acad Sci U S A **86**, 5646-5650 (1989).
- [6] Ferri, C. P. *et al. Global prevalence of dementia: a Delphi consensus study*. Lancet **366**, 2112-2117 (2005).
- [7] Wimo, A., Winblad, B., Aguero-Torres, H. & von Strauss, E. *The magnitude of dementia occurrence in the world*. Alzheimer Dis Assoc Disord **17**, 63-67 (2003).
- [8] Thomas, P. & Fenech, M. *A review of genome mutation and Alzheimer's disease*. Mutagenesis **22**, 15-33 (2007).
- [9] Kawas, C. H. *Clinical practice. Early Alzheimer's disease*. N Engl J Med **349**, 1056-1063 (2003).
- [10] Janssen, J. C. *et al. Early onset familial Alzheimer's disease: Mutation frequency in 31 families*. Neurology **60**, 235-239 (2003).
- [11] Roses, A. D. *A model for susceptibility polymorphisms for complex diseases: apolipoprotein E and Alzheimer disease*. Neurogenetics **1**, 3-11 (1997).
- [12] Schellenberg, G. D. *Genetic dissection of Alzheimer disease, a heterogeneous disorder*. Proc Natl Acad Sci U S A **92**, 8552-8559 (1995).
- [13] Koo, E. H. *The beta-amyloid precursor protein (APP) and Alzheimer's disease: does the tail wag the dog?* Traffic **3**, 763-770 (2002).
- [14] Bennett, B. D. *et al. A furin-like convertase mediates propeptide cleavage of BACE, the Alzheimer's beta -secretase*. J Biol Chem **275**, 37712-37717 (2000).

-
- [15] Howlett, D. R., Simmons, D. L., Dingwall, C. & Christie, G. *In search of an enzyme: the beta-secretase of Alzheimer's disease is an aspartic proteinase*. Trends Neurosci **23**, 565-570 (2000).
- [16] Selkoe, D. J. *Alzheimer's disease: genes, proteins, and therapy*. Physiol Rev **81**, 741-766 (2001).
- [17] Selkoe, D. J. *Alzheimer disease: mechanistic understanding predicts novel therapies*. Ann Intern Med **140**, 627-638 (2004).
- [18] Gotz, J., Chen, F., Barmettler, R. & Nitsch, R. M. *Tau filament formation in transgenic mice expressing P301L tau*. J Biol Chem **276**, 529-534 (2001).
- [19] Lewis, J. *et al.* *Enhanced neurofibrillary degeneration in transgenic mice expressing mutant tau and APP*. Science **293**, 1487-1491 (2001).
- [20] Roberson, E. D. *et al.* *Reducing endogenous tau ameliorates amyloid beta-induced deficits in an Alzheimer's disease mouse model*. Science **316**, 750-754 (2007).
- [21] Hardy, J. A. & Higgins, G. A. *Alzheimer's disease: the amyloid cascade hypothesis*. Science **256**, 184-185 (1992).
- [22] Busciglio, J., Lorenzo, A., Yeh, J. & Yankner, B. A. *beta-amyloid fibrils induce tau phosphorylation and loss of microtubule binding*. Neuron **14**, 879-888 (1995).
- [23] Armstrong, R. A., Myers, D. & Smith, C. U. *The spatial patterns of plaques and tangles in Alzheimer's disease do not support the 'cascade hypothesis'*. Dementia **4**, 16-20 (1993).
- [24] Hyman, B. T. & Tanzi, R. E. *Amyloid, dementia and Alzheimer's disease*. Curr Opin Neurol Neurosurg **5**, 88-93 (1992).
- [25] Maccioni, R. B., Munoz, J. P. & Barbeito, L. *The molecular bases of Alzheimer's disease and other neurodegenerative disorders*. Arch Med Res **32**, 367-381 (2001).
- [26] Ghoshal, N. *et al.* *Tau conformational changes correspond to impairments of episodic memory in mild cognitive impairment and Alzheimer's disease*. Exp Neurol **177**, 475-493 (2002).
- [27] Maccioni, R. B., Farias, G., Morales, I. & Navarrete, L. *The revitalized tau hypothesis on Alzheimer's disease*. Arch Med Res **41**, 226-231 (2010).
- [28] Fernandez, J. A., Rojo, L., Kuljis, R. O. & Maccioni, R. B. *The damage signals hypothesis of Alzheimer's disease pathogenesis*. J Alzheimers Dis **14**, 329-333 (2008).
- [29] Morales, I., Farias, G. & Maccioni, R. B. *Neuroimmunomodulation in the pathogenesis of Alzheimer's disease*. Neuroimmunomodulation **17**, 202-204 (2010).

-
- [30] Eisele, Y. S. *et al.* *Peripherally applied Abeta-containing inoculates induce cerebral beta-amyloidosis.* *Science* **330**, 980-982 (2010).
- [31] Clavaguera, F. *et al.* *Transmission and spreading of tauopathy in transgenic mouse brain.* *Nat Cell Biol* **11**, 909-913 (2009).
- [32] Ittner, L. M. *et al.* *Dendritic function of tau mediates amyloid-beta toxicity in Alzheimer's disease mouse models.* *Cell* **142**, 387-397 (2010).
- [33] Troy, C. M. *et al.* *Caspase-2 mediates neuronal cell death induced by beta-amyloid.* *J Neurosci* **20**, 1386-1392 (2000).
- [34] Canu, N. *et al.* *Tau cleavage and dephosphorylation in cerebellar granule neurons undergoing apoptosis.* *J Neurosci* **18**, 7061-7074 (1998).
- [35] Fasulo, L. *et al.* *The neuronal microtubule-associated protein tau is a substrate for caspase-3 and an effector of apoptosis.* *J Neurochem* **75**, 624-633 (2000).
- [36] Chung, C. W. *et al.* *Proapoptotic effects of tau cleavage product generated by caspase-3.* *Neurobiol Dis* **8**, 162-172 (2001).
- [37] Gamblin, T. C. *et al.* *Caspase cleavage of tau: linking amyloid and neurofibrillary tangles in Alzheimer's disease.* *Proc Natl Acad Sci U S A* **100**, 10032-10037 (2003).
- [38] Guillozet-Bongaarts, A. L. *et al.* *Tau truncation during neurofibrillary tangle evolution in Alzheimer's disease.* *Neurobiol Aging* **26**, 1015-1022 (2005).
- [39] Rissman, R. A. *et al.* *Caspase-cleavage of tau is an early event in Alzheimer disease tangle pathology.* *J Clin Invest* **114**, 121-130 (2004).
- [40] Abraha, A. *et al.* *C-terminal inhibition of tau assembly in vitro and in Alzheimer's disease.* *J Cell Sci* **113 Pt 21**, 3737-3745 (2000).
- [41] Neve, R. L., Harris, P., Kosik, K. S., Kurnit, D. M. & Donlon, T. A. *Identification of cDNA clones for the human microtubule-associated protein tau and chromosomal localization of the genes for tau and microtubule-associated protein 2.* *Brain Res* **387**, 271-280 (1986).
- [42] Goedert, M., Wischik, C. M., Crowther, R. A., Walker, J. E. & Klug, A. *Cloning and sequencing of the cDNA encoding a core protein of the paired helical filament of Alzheimer disease: identification as the microtubule-associated protein tau.* *Proc Natl Acad Sci U S A* **85**, 4051-4055 (1988).
- [43] Gustke, N., Trinczek, B., Biernat, J., Mandelkow, E. M. & Mandelkow, E. *Domains of tau protein and interactions with microtubules.* *Biochemistry* **33**, 9511-9522 (1994).

-
- [44] Trinczek, B., Biernat, J., Baumann, K., Mandelkow, E. M. & Mandelkow, E. *Domains of tau protein, differential phosphorylation, and dynamic instability of microtubules.* Mol Biol Cell **6**, 1887-1902 (1995).
- [45] Goedert, M. & Jakes, R. *Expression of separate isoforms of human tau protein: correlation with the tau pattern in brain and effects on tubulin polymerization.* EMBO J **9**, 4225-4230 (1990).
- [46] Weingarten, M. D., Lockwood, A. H., Hwo, S. Y. & Kirschner, M. W. *A protein factor essential for microtubule assembly.* Proc Natl Acad Sci U S A **72**, 1858-1862 (1975).
- [47] Binder, L. I., Frankfurter, A. & Rebhun, L. I. *The distribution of tau in the mammalian central nervous system.* J Cell Biol **101**, 1371-1378 (1985).
- [48] Brandt, R. & Lee, G. *Functional organization of microtubule-associated protein tau. Identification of regions which affect microtubule growth, nucleation, and bundle formation in vitro.* J Biol Chem **268**, 3414-3419 (1993).
- [49] Drechsel, D. N., Hyman, A. A., Cobb, M. H. & Kirschner, M. W. *Modulation of the dynamic instability of tubulin assembly by the microtubule-associated protein tau.* Mol Biol Cell **3**, 1141-1154 (1992).
- [50] Knops, J. *et al.* *Overexpression of tau in a nonneuronal cell induces long cellular processes.* J Cell Biol **114**, 725-733 (1991).
- [51] Harada, A. *et al.* *Altered microtubule organization in small-calibre axons of mice lacking tau protein.* Nature **369**, 488-491 (1994).
- [52] Dawson, H. N. *et al.* *Inhibition of neuronal maturation in primary hippocampal neurons from tau deficient mice.* J Cell Sci **114**, 1179-1187 (2001).
- [53] Kempf, M., Clement, A., Faissner, A., Lee, G. & Brandt, R. *Tau binds to the distal axon early in development of polarity in a microtubule- and microfilament-dependent manner.* J Neurosci **16**, 5583-5592 (1996).
- [54] Carlier, M. F., Simon, C., Cassoly, R. & Pradel, L. A. *Interaction between microtubule-associated protein tau and spectrin.* Biochimie **66**, 305-311 (1984).
- [55] Lee, G., Newman, S. T., Gard, D. L., Band, H. & Panchamoorthy, G. *Tau interacts with src-family non-receptor tyrosine kinases.* J Cell Sci **111 (Pt 21)**, 3167-3177 (1998).
- [56] Jenkins, S. M. & Johnson, G. V. *Tau complexes with phospholipase C-gamma in situ.* Neuroreport **9**, 67-71 (1998).
- [57] Martin, L., Latypova, X. & Terro, F. *Post-translational modifications of tau protein: Implications for Alzheimer's disease.* Neurochem Int (2011).

-
- [58] Kondo, J. *et al.* *The carboxyl third of tau is tightly bound to paired helical filaments.* *Neuron* **1**, 827-834 (1988).
- [59] Kosik, K. S. *et al.* *Epitopes that span the tau molecule are shared with paired helical filaments.* *Neuron* **1**, 817-825 (1988).
- [60] Wischik, C. M. *et al.* *Isolation of a fragment of tau derived from the core of the paired helical filament of Alzheimer disease.* *Proc Natl Acad Sci U S A* **85**, 4506-4510 (1988).
- [61] Lee, V. M., Balin, B. J., Otvos, L., Jr. & Trojanowski, J. Q. *A68: a major subunit of paired helical filaments and derivatized forms of normal Tau.* *Science* **251**, 675-678 (1991).
- [62] Spillantini, M. G. & Goedert, M. *Tau protein pathology in neurodegenerative diseases.* *Trends Neurosci* **21**, 428-433 (1998).
- [63] Spillantini, M. G. *et al.* *Mutation in the tau gene in familial multiple system tauopathy with presenile dementia.* *Proc Natl Acad Sci U S A* **95**, 7737-7741 (1998).
- [64] Kenessey, A. & Yen, S. H. *The extent of phosphorylation of fetal tau is comparable to that of PHF-tau from Alzheimer paired helical filaments.* *Brain Res* **629**, 40-46 (1993).
- [65] Crowther, R. A. & Goedert, M. *Abnormal tau-containing filaments in neurodegenerative diseases.* *J Struct Biol* **130**, 271-279 (2000).
- [66] Buee, L., Bussiere, T., Buee-Scherrer, V., Delacourte, A. & Hof, P. R. *Tau protein isoforms, phosphorylation and role in neurodegenerative disorders.* *Brain Res Brain Res Rev* **33**, 95-130 (2000).
- [67] Hagestedt, T., Lichtenberg, B., Wille, H., Mandelkow, E. M. & Mandelkow, E. *Tau protein becomes long and stiff upon phosphorylation: correlation between paracrystalline structure and degree of phosphorylation.* *J Cell Biol* **109**, 1643-1651 (1989).
- [68] Drewes, G. *et al.* *Microtubule-associated protein/microtubule affinity-regulating kinase (p110mark). A novel protein kinase that regulates tau-microtubule interactions and dynamic instability by phosphorylation at the Alzheimer-specific site serine 262.* *J Biol Chem* **270**, 7679-7688 (1995).
- [69] Biernat, J., Gustke, N., Drewes, G., Mandelkow, E. M. & Mandelkow, E. *Phosphorylation of Ser262 strongly reduces binding of tau to microtubules: distinction between PHF-like immunoreactivity and microtubule binding.* *Neuron* **11**, 153-163 (1993).

-
- [70] Lindwall, G. & Cole, R. D. *Phosphorylation affects the ability of tau protein to promote microtubule assembly*. J Biol Chem **259**, 5301-5305 (1984).
- [71] Mondragon-Rodriguez, S. *et al.* *Cleavage and conformational changes of tau protein follow phosphorylation during Alzheimer's disease*. Int J Exp Pathol **89**, 81-90 (2008).
- [72] Saito, M., Chakraborty, G., Mao, R. F., Paik, S. M. & Vadasz, C. *Tau phosphorylation and cleavage in ethanol-induced neurodegeneration in the developing mouse brain*. Neurochem Res **35**, 651-659 (2010).
- [73] Rohn, T. T. *et al.* *Caspase-9 activation and caspase cleavage of tau in the Alzheimer's disease brain*. Neurobiol Dis **11**, 341-354 (2002).
- [74] Novak, M. *Truncated tau protein as a new marker for Alzheimer's disease*. Acta Virol **38**, 173-189 (1994).
- [75] Mena, R., Edwards, P. C., Harrington, C. R., Mukaetova-Ladinska, E. B. & Wischik, C. M. *Staging the pathological assembly of truncated tau protein into paired helical filaments in Alzheimer's disease*. Acta Neuropathol **91**, 633-641 (1996).
- [76] Ugolini, G., Cattaneo, A. & Novak, M. *Co-localization of truncated tau and DNA fragmentation in Alzheimer's disease neurones*. Neuroreport **8**, 3709-3712 (1997).
- [77] Garcia-Sierra, F., Ghoshal, N., Quinn, B., Berry, R. W. & Binder, L. I. *Conformational changes and truncation of tau protein during tangle evolution in Alzheimer's disease*. J Alzheimers Dis **5**, 65-77 (2003).
- [78] Takahashi, M. *et al.* *Glycosylation of microtubule-associated protein tau in Alzheimer's disease brain*. Acta Neuropathol **97**, 635-641 (1999).
- [79] Wang, J. Z., Grundke-Iqbal, I. & Iqbal, K. *Glycosylation of microtubule-associated protein tau: an abnormal posttranslational modification in Alzheimer's disease*. Nat Med **2**, 871-875 (1996).
- [80] Smith, M. A. *et al.* *Advanced Maillard reaction end products are associated with Alzheimer disease pathology*. Proc Natl Acad Sci U S A **91**, 5710-5714 (1994).
- [81] Lu, P. J., Wulf, G., Zhou, X. Z., Davies, P. & Lu, K. P. *The prolyl isomerase Pin1 restores the function of Alzheimer-associated phosphorylated tau protein*. Nature **399**, 784-788 (1999).
- [82] Reynolds, M. R., Berry, R. W. & Binder, L. I. *Site-specific nitration and oxidative dityrosine bridging of the tau protein by peroxynitrite: implications for Alzheimer's disease*. Biochemistry **44**, 1690-1700 (2005).

- [83] Singer, S. M., Zainelli, G. M., Norlund, M. A., Lee, J. M. & Muma, N. A. *Transglutaminase bonds in neurofibrillary tangles and paired helical filament tau early in Alzheimer's disease*. *Neurochem Int* **40**, 17-30 (2002).
- [84] Takahashi, K., Ishida, M., Komano, H. & Takahashi, H. *SUMO-1 immunoreactivity co-localizes with phospho-Tau in APP transgenic mice but not in mutant Tau transgenic mice*. *Neurosci Lett* **441**, 90-93 (2008).
- [85] Landino, L. M., Skreslet, T. E. & Alston, J. A. *Cysteine oxidation of tau and microtubule-associated protein-2 by peroxynitrite: modulation of microtubule assembly kinetics by the thioredoxin reductase system*. *J Biol Chem* **279**, 35101-35105 (2004).
- [86] Necula, M. & Kuret, J. *Pseudophosphorylation and glycation of tau protein enhance but do not trigger fibrillization in vitro*. *J Biol Chem* **279**, 49694-49703 (2004).
- [87] Horiguchi, T. *et al*. *Nitration of tau protein is linked to neurodegeneration in tauopathies*. *Am J Pathol* **163**, 1021-1031 (2003).
- [88] Halverson, R. A., Lewis, J., Frausto, S., Hutton, M. & Muma, N. A. *Tau protein is cross-linked by transglutaminase in P301L tau transgenic mice*. *J Neurosci* **25**, 1226-1233 (2005).
- [89] Lefebvre, T. *et al*. *Evidence of a balance between phosphorylation and O-GlcNAc glycosylation of Tau proteins--a role in nuclear localization*. *Biochim Biophys Acta* **1619**, 167-176 (2003).
- [90] Mori, H., Kondo, J. & Ihara, Y. *Ubiquitin is a component of paired helical filaments in Alzheimer's disease*. *Science* **235**, 1641-1644 (1987).
- [91] Manetto, V. *et al*. *Ubiquitin is associated with abnormal cytoplasmic filaments characteristic of neurodegenerative diseases*. *Proc Natl Acad Sci U S A* **85**, 4501-4505 (1988).
- [92] Bancher, C. *et al*. *Abnormal phosphorylation of tau precedes ubiquitination in neurofibrillary pathology of Alzheimer disease*. *Brain Res* **539**, 11-18 (1991).
- [93] Morishima-Kawashima, M. *et al*. *Ubiquitin is conjugated with amino-terminally processed tau in paired helical filaments*. *Neuron* **10**, 1151-1160 (1993).
- [94] Chau, V. *et al*. *A multiubiquitin chain is confined to specific lysine in a targeted short-lived protein*. *Science* **243**, 1576-1583 (1989).
- [95] Gregori, L., Poosch, M. S., Cousins, G. & Chau, V. *A uniform isopeptide-linked multiubiquitin chain is sufficient to target substrate for degradation in ubiquitin-mediated proteolysis*. *J Biol Chem* **265**, 8354-8357 (1990).

- [96] Liu, Y. H. *et al.* *Proteasome inhibition increases tau accumulation independent of phosphorylation.* *Neurobiol Aging* **30**, 1949-1961 (2009).
- [97] Futerman, A. H. & van Meer, G. *The cell biology of lysosomal storage disorders.* *Nat Rev Mol Cell Biol* **5**, 554-565 (2004).
- [98] Hutton, M. *et al.* *Association of missense and 5'-splice-site mutations in tau with the inherited dementia FTDP-17.* *Nature* **393**, 702-705 (1998).
- [99] Poorkaj, P. *et al.* *Tau is a candidate gene for chromosome 17 frontotemporal dementia.* *Ann Neurol* **43**, 815-825 (1998).
- [100] Brandt, R., Hundelt, M. & Shahani, N. *Tau alteration and neuronal degeneration in tauopathies: mechanisms and models.* *Biochim Biophys Acta* **1739**, 331-354 (2005).
- [101] Delisle, M. B. *et al.* *A mutation at codon 279 (N279K) in exon 10 of the Tau gene causes a tauopathy with dementia and supranuclear palsy.* *Acta Neuropathol* **98**, 62-77 (1999).
- [102] Reed, L. A. *et al.* *The neuropathology of a chromosome 17-linked autosomal dominant parkinsonism and dementia ("pallido-ponto-nigral degeneration").* *J Neuropathol Exp Neurol* **57**, 588-601 (1998).
- [103] Spillantini, M. G., Crowther, R. A. & Goedert, M. *Comparison of the neurofibrillary pathology in Alzheimer's disease and familial presenile dementia with tangles.* *Acta Neuropathol* **92**, 42-48 (1996).
- [104] Hong, M. *et al.* *Mutation-specific functional impairments in distinct tau isoforms of hereditary FTDP-17.* *Science* **282**, 1914-1917 (1998).
- [105] van Swieten, J. C. *et al.* *Phenotypic variation in hereditary frontotemporal dementia with tau mutations.* *Ann Neurol* **46**, 617-626 (1999).
- [106] Brion, J. P., Couck, A. M., Passareiro, E. & Flament-Durand, J. *Neurofibrillary tangles of Alzheimer's disease: an immunohistochemical study.* *J Submicrosc Cytol* **17**, 89-96 (1985).
- [107] Grundke-Iqbal, I. *et al.* *Microtubule-associated protein tau. A component of Alzheimer paired helical filaments.* *J Biol Chem* **261**, 6084-6089 (1986).
- [108] Cleveland, D. W., Hwo, S. Y. & Kirschner, M. W. *Physical and chemical properties of purified tau factor and the role of tau in microtubule assembly.* *J Mol Biol* **116**, 227-247 (1977).
- [109] Eidenmuller, J. *et al.* *Structural and functional implications of tau hyperphosphorylation: information from phosphorylation-mimicking mutated tau proteins.* *Biochemistry* **39**, 13166-13175 (2000).

-
- [110] Schweers, O., Schonbrunn-Hanebeck, E., Marx, A. & Mandelkow, E. *Structural studies of tau protein and Alzheimer paired helical filaments show no evidence for beta-structure.* J Biol Chem **269**, 24290-24297 (1994).
- [111] Kirschner, D. A., Abraham, C. & Selkoe, D. J. *X-ray diffraction from intraneuronal paired helical filaments and extraneuronal amyloid fibers in Alzheimer disease indicates cross-beta conformation.* Proc Natl Acad Sci U S A **83**, 503-507 (1986).
- [112] Berriman, J. *et al.* *Tau filaments from human brain and from in vitro assembly of recombinant protein show cross-beta structure.* Proc Natl Acad Sci U S A **100**, 9034-9038 (2003).
- [113] Sadqi, M. *et al.* *Alpha-helix structure in Alzheimer's disease aggregates of tau-protein.* Biochemistry **41**, 7150-7155 (2002).
- [114] Litersky, J. M. & Johnson, G. V. *Phosphorylation by cAMP-dependent protein kinase inhibits the degradation of tau by calpain.* J Biol Chem **267**, 1563-1568 (1992).
- [115] Grundke-Iqbal, I. *et al.* *Abnormal phosphorylation of the microtubule-associated protein tau (tau) in Alzheimer cytoskeletal pathology.* Proc Natl Acad Sci U S A **83**, 4913-4917 (1986).
- [116] Brandt, R. & Lee, G. *Orientation, assembly, and stability of microtubule bundles induced by a fragment of tau protein.* Cell Motil Cytoskeleton **28**, 143-154 (1994).
- [117] Braak, H. & Braak, E. *Neuropathological staging of Alzheimer-related changes.* Acta Neuropathol **82**, 239-259 (1991).
- [118] Allen, B. *et al.* *Abundant tau filaments and nonapoptotic neurodegeneration in transgenic mice expressing human P301S tau protein.* J Neurosci **22**, 9340-9351 (2002).
- [119] Lewis, J. *et al.* *Neurofibrillary tangles, amyotrophy and progressive motor disturbance in mice expressing mutant (P301L) tau protein.* Nat Genet **25**, 402-405 (2000).
- [120] Tanemura, K. *et al.* *Neurodegeneration with tau accumulation in a transgenic mouse expressing V337M human tau.* J Neurosci **22**, 133-141 (2002).
- [121] Ross, C. A. & Poirier, M. A. *Opinion: What is the role of protein aggregation in neurodegeneration?* Nat Rev Mol Cell Biol **6**, 891-898 (2005).
- [122] Fath, T., Eidenmuller, J. & Brandt, R. *Tau-mediated cytotoxicity in a pseudohyperphosphorylation model of Alzheimer's disease.* J Neurosci **22**, 9733-9741 (2002).

-
- [123] Shimura, H., Miura-Shimura, Y. & Kosik, K. S. *Binding of tau to heat shock protein 27 leads to decreased concentration of hyperphosphorylated tau and enhanced cell survival.* J Biol Chem **279**, 17957-17962 (2004).
- [124] Kraemer, B. C. *et al.* *Neurodegeneration and defective neurotransmission in a Caenorhabditis elegans model of tauopathy.* Proc Natl Acad Sci U S A **100**, 9980-9985 (2003).
- [125] Wittmann, C. W. *et al.* *Tauopathy in Drosophila: neurodegeneration without neurofibrillary tangles.* Science **293**, 711-714 (2001).
- [126] Baas, P. W. & Buster, D. W. *Slow axonal transport and the genesis of neuronal morphology.* J Neurobiol **58**, 3-17 (2004).
- [127] Hirokawa, N. & Takemura, R. *Molecular motors and mechanisms of directional transport in neurons.* Nat Rev Neurosci **6**, 201-214 (2005).
- [128] Hollenbeck, P. J. & Saxton, W. M. *The axonal transport of mitochondria.* J Cell Sci **118**, 5411-5419 (2005).
- [129] Miller, K. E. & Sheetz, M. P. *Direct evidence for coherent low velocity axonal transport of mitochondria.* J Cell Biol **173**, 373-381 (2006).
- [130] Baas, P. W., Deitch, J. S., Black, M. M. & Banker, G. A. *Polarity orientation of microtubules in hippocampal neurons: uniformity in the axon and nonuniformity in the dendrite.* Proc Natl Acad Sci U S A **85**, 8335-8339 (1988).
- [131] Kardon, J. R. & Vale, R. D. *Regulators of the cytoplasmic dynein motor.* Nat Rev Mol Cell Biol **10**, 854-865 (2009).
- [132] Zhao, C. *et al.* *Charcot-Marie-Tooth disease type 2A caused by mutation in a microtubule motor KIF1Bbeta.* Cell **105**, 587-597 (2001).
- [133] Gee, M. A., Heuser, J. E. & Vallee, R. B. *An extended microtubule-binding structure within the dynein motor domain.* Nature **390**, 636-639 (1997).
- [134] Karki, S. & Holzbaur, E. L. *Cytoplasmic dynein and dynactin in cell division and intracellular transport.* Curr Opin Cell Biol **11**, 45-53 (1999).
- [135] Traer, C. J. *et al.* *SNX4 coordinates endosomal sorting of TfnR with dynein-mediated transport into the endocytic recycling compartment.* Nat Cell Biol **9**, 1370-1380 (2007).
- [136] Liu, J. J. *et al.* *Retrolinkin, a membrane protein, plays an important role in retrograde axonal transport.* Proc Natl Acad Sci U S A **104**, 2223-2228 (2007).
- [137] Lee, K. H. *et al.* *Dazl can bind to dynein motor complex and may play a role in transport of specific mRNAs.* EMBO J **25**, 4263-4270 (2006).

-
- [138] Jaffrey, S. R. & Snyder, S. H. *PIN: an associated protein inhibitor of neuronal nitric oxide synthase*. *Science* **274**, 774-777 (1996).
- [139] Puthalakath, H., Huang, D. C., O'Reilly, L. A., King, S. M. & Strasser, A. *The proapoptotic activity of the Bcl-2 family member Bim is regulated by interaction with the dynein motor complex*. *Mol Cell* **3**, 287-296 (1999).
- [140] Naisbitt, S. *et al.* *Interaction of the postsynaptic density-95/guanylate kinase domain-associated protein complex with a light chain of myosin-V and dynein*. *J Neurosci* **20**, 4524-4534 (2000).
- [141] Ensembl Genome Browser. '*Dynein heavy chain*' in species *Homo sapiens*. <http://www.ensembl.org> (23.01.2011)
- [142] HomoloGene - Discover Homologues. <http://www.ncbi.nlm.nih.gov/homologene> (23.01.2011)
- [143] Blast (Basic Local Alignment Search Tool). *blastp* - protein blast. <http://blast.ncbi.nlm.nih.gov> (23.01.2011)
- [144] Schafer, D. A., Gill, S. R., Cooper, J. A., Heuser, J. E. & Schroer, T. A. *Ultrastructural analysis of the dynactin complex: an actin-related protein is a component of a filament that resembles F-actin*. *J Cell Biol* **126**, 403-412 (1994).
- [145] Schroer, T. A. *Dynactin*. *Annu Rev Cell Dev Biol* **20**, 759-779 (2004).
- [146] Holleran, E. A. *et al.* *beta III spectrin binds to the Arp1 subunit of dynactin*. *J Biol Chem* **276**, 36598-36605 (2001).
- [147] Schafer, D. A., Korshunova, Y. O., Schroer, T. A. & Cooper, J. A. *Differential localization and sequence analysis of capping protein beta-subunit isoforms of vertebrates*. *J Cell Biol* **127**, 453-465 (1994).
- [148] Eckley, D. M. *et al.* *Analysis of dynactin subcomplexes reveals a novel actin-related protein associated with the arp1 minifilament pointed end*. *J Cell Biol* **147**, 307-320 (1999).
- [149] Garces, J. A., Clark, I. B., Meyer, D. I. & Vallee, R. B. *Interaction of the p62 subunit of dynactin with Arp1 and the cortical actin cytoskeleton*. *Curr Biol* **9**, 1497-1500 (1999).
- [150] Karki, S., Tokito, M. K. & Holzbaur, E. L. *A dynactin subunit with a highly conserved cysteine-rich motif interacts directly with Arp1*. *J Biol Chem* **275**, 4834-4839 (2000).
- [151] Lee, I. H., Kumar, S. & Plamann, M. *Null mutants of the neurospora actin-related protein 1 pointed-end complex show distinct phenotypes*. *Mol Biol Cell* **12**, 2195-2206 (2001).

- [152] Bradley, P., Cowen, L., Menke, M., King, J. & Berger, B. *BETAWRAP: successful prediction of parallel beta -helices from primary sequence reveals an association with many microbial pathogens*. Proc Natl Acad Sci U S A **98**, 14819-14824 (2001).
- [153] Vaughan, P. S., Miura, P., Henderson, M., Byrne, B. & Vaughan, K. T. *A role for regulated binding of p150(Glued) to microtubule plus ends in organelle transport*. J Cell Biol **158**, 305-319 (2002).
- [154] Waterman-Storer, C. M., Karki, S. & Holzbaur, E. L. *The p150Glued component of the dynactin complex binds to both microtubules and the actin-related protein centractin (Arp-1)*. Proc Natl Acad Sci U S A **92**, 1634-1638 (1995).
- [155] King, S. J. & Schroer, T. A. *Dynactin increases the processivity of the cytoplasmic dynein motor*. Nat Cell Biol **2**, 20-24 (2000).
- [156] Puls, I. *et al. Mutant dynactin in motor neuron disease*. Nat Genet **33**, 455-456 (2003).
- [157] Karki, S. & Holzbaur, E. L. *Affinity chromatography demonstrates a direct binding between cytoplasmic dynein and the dynactin complex*. J Biol Chem **270**, 28806-28811 (1995).
- [158] Vaughan, K. T. & Vallee, R. B. *Cytoplasmic dynein binds dynactin through a direct interaction between the intermediate chains and p150Glued*. J Cell Biol **131**, 1507-1516 (1995).
- [159] King, S. J., Brown, C. L., Maier, K. C., Quintyne, N. J. & Schroer, T. A. *Analysis of the dynein-dynactin interaction in vitro and in vivo*. Mol Biol Cell **14**, 5089-5097 (2003).
- [160] Park, J.-H. *Roles for the dynactin complex in the glucocorticoid receptor signalling pathway*. PhD thesis, The Johns Hopkins University (2003).
- [161] Echeverri, C. J., Paschal, B. M., Vaughan, K. T. & Vallee, R. B. *Molecular characterization of the 50-kD subunit of dynactin reveals function for the complex in chromosome alignment and spindle organization during mitosis*. J Cell Biol **132**, 617-633 (1996).
- [162] Quintyne, N. J. *et al. Dynactin is required for microtubule anchoring at centrosomes*. J Cell Biol **147**, 321-334 (1999).
- [163] Valetti, C. *et al. Role of dynactin in endocytic traffic: effects of dynamitin overexpression and colocalization with CLIP-170*. Mol Biol Cell **10**, 4107-4120 (1999).

- [164] Karki, S., LaMonte, B. & Holzbaur, E. L. *Characterization of the p22 subunit of dynactin reveals the localization of cytoplasmic dynein and dynactin to the midbody of dividing cells.* J Cell Biol **142**, 1023-1034 (1998).
- [165] Williamson, T. L. & Cleveland, D. W. *Slowing of axonal transport is a very early event in the toxicity of ALS-linked SOD1 mutants to motor neurons.* Nat Neurosci **2**, 50-56 (1999).
- [166] Rossoll, W. *et al.* *Smn, the spinal muscular atrophy-determining gene product, modulates axon growth and localization of beta-actin mRNA in growth cones of motoneurons.* J Cell Biol **163**, 801-812 (2003).
- [167] Reid, E. *Science in motion: common molecular pathological themes emerge in the hereditary spastic paraplegias.* J Med Genet **40**, 81-86 (2003).
- [168] Ishihara, T. *et al.* *Age-dependent emergence and progression of a tauopathy in transgenic mice overexpressing the shortest human tau isoform.* Neuron **24**, 751-762 (1999).
- [169] Zhang, B. *et al.* *Retarded axonal transport of R406W mutant tau in transgenic mice with a neurodegenerative tauopathy.* J Neurosci **24**, 4657-4667 (2004).
- [170] Stokin, G. B. *et al.* *Axonopathy and transport deficits early in the pathogenesis of Alzheimer's disease.* Science **307**, 1282-1288 (2005).
- [171] Lee, W. C., Yoshihara, M. & Littleton, J. T. *Cytoplasmic aggregates trap polyglutamine-containing proteins and block axonal transport in a Drosophila model of Huntington's disease.* Proc Natl Acad Sci U S A **101**, 3224-3229 (2004).
- [172] Gunawardena, S. *et al.* *Disruption of axonal transport by loss of huntingtin or expression of pathogenic polyQ proteins in Drosophila.* Neuron **40**, 25-40 (2003).
- [173] Chang, D. T., Rintoul, G. L., Pandipati, S. & Reynolds, I. J. *Mutant huntingtin aggregates impair mitochondrial movement and trafficking in cortical neurons.* Neurobiol Dis **22**, 388-400 (2006).
- [174] Saha, A. R. *et al.* *Parkinson's disease alpha-synuclein mutations exhibit defective axonal transport in cultured neurons.* J Cell Sci **117**, 1017-1024 (2004).
- [175] Baloh, R. H., Schmidt, R. E., Pestronk, A. & Milbrandt, J. *Altered axonal mitochondrial transport in the pathogenesis of Charcot-Marie-Tooth disease from mitofusin 2 mutations.* J Neurosci **27**, 422-430 (2007).
- [176] de Waegh, S. & Brady, S. T. *Altered slow axonal transport and regeneration in a myelin-deficient mutant mouse: the trembler as an in vivo model for Schwann cell-axon interactions.* J Neurosci **10**, 1855-1865 (1990).

- [177] De Vos, K. J. *et al.* *Familial amyotrophic lateral sclerosis-linked SOD1 mutants perturb fast axonal transport to reduce axonal mitochondria content.* Hum Mol Genet **16**, 2720-2728 (2007).
- [178] Cowan, C. M., Bossing, T., Page, A., Shepherd, D. & Mudher, A. *Soluble hyperphosphorylated tau causes microtubule breakdown and functionally compromises normal tau in vivo.* Acta Neuropathol **120**, 593-604 (2010).
- [179] Mudher, A. *et al.* *GSK-3beta inhibition reverses axonal transport defects and behavioural phenotypes in Drosophila.* Mol Psychiatry **9**, 522-530 (2004).
- [180] Mandelkow, E. M., Thies, E., Trinczek, B., Biernat, J. & Mandelkow, E. *MARK/PAR1 kinase is a regulator of microtubule-dependent transport in axons.* J Cell Biol **167**, 99-110 (2004).
- [181] Shemesh, O. A., Erez, H., Ginzburg, I. & Spira, M. E. *Tau-induced traffic jams reflect organelles accumulation at points of microtubule polar mismatching.* Traffic **9**, 458-471 (2008).
- [182] Mandelkow, E. M., Stamer, K., Vogel, R., Thies, E. & Mandelkow, E. *Clogging of axons by tau, inhibition of axonal traffic and starvation of synapses.* Neurobiol Aging **24**, 1079-1085 (2003).
- [183] Magnani, E. *et al.* *Interaction of tau protein with the dynactin complex.* EMBO J **26**, 4546-4554 (2007).
- [184] Dixit, R., Ross, J. L., Goldman, Y. E. & Holzbaur, E. L. *Differential regulation of dynein and kinesin motor proteins by tau.* Science **319**, 1086-1089 (2008).
- [185] Falzone, T. L. *et al.* *Axonal stress kinase activation and tau misbehavior induced by kinesin-1 transport defects.* J Neurosci **29**, 5758-5767 (2009).
- [186] Falzone, T. L., Gunawardena, S., McCleary, D., Reis, G. F. & Goldstein, L. S. *Kinesin-1 transport reductions enhance human tau hyperphosphorylation, aggregation and neurodegeneration in animal models of tauopathies.* Hum Mol Genet **19**, 4399-4408 (2010).
- [187] Drubin, D. G. & Kirschner, M. W. *Tau protein function in living cells.* J Cell Biol **103**, 2739-2746 (1986).
- [188] Kosik, K. S. & Finch, E. A. *MAP2 and tau segregate into dendritic and axonal domains after the elaboration of morphologically distinct neurites: an immunocytochemical study of cultured rat cerebrum.* J Neurosci **7**, 3142-3153 (1987).

-
- [189] Black, M. M., Slaughter, T., Moshiach, S., Obrocka, M. & Fischer, I. *Tau is enriched on dynamic microtubules in the distal region of growing axons.* J Neurosci **16**, 3601-3619 (1996).
- [190] Mercken, M., Fischer, I., Kosik, K. S. & Nixon, R. A. *Three distinct axonal transport rates for tau, tubulin, and other microtubule-associated proteins: evidence for dynamic interactions of tau with microtubules in vivo.* J Neurosci **15**, 8259-8267 (1995).
- [191] Utton, M. A., Noble, W. J., Hill, J. E., Anderton, B. H. & Hanger, D. P. *Molecular motors implicated in the axonal transport of tau and alpha-synuclein.* J Cell Sci **118**, 4645-4654 (2005).
- [192] Weissmann, C. *et al.* *Microtubule binding and trapping at the tip of neurites regulate tau motion in living neurons.* Traffic **10**, 1655-1668 (2009).
- [193] Konzack, S., Thies, E., Marx, A., Mandelkow, E. M. & Mandelkow, E. *Swimming against the tide: mobility of the microtubule-associated protein tau in neurons.* J Neurosci **27**, 9916-9927 (2007).
- [194] Wang, L. & Brown, A. *Rapid movement of microtubules in axons.* Curr Biol **12**, 1496-1501 (2002).
- [195] Baas, P. W., Vidya Nadar, C. & Myers, K. A. *Axonal transport of microtubules: the long and short of it.* Traffic **7**, 490-498 (2006).
- [196] Cuchillo-Ibanez, I. *et al.* *Phosphorylation of tau regulates its axonal transport by controlling its binding to kinesin.* FASEB J **22**, 3186-3195 (2008).
- [197] Braak, E., Braak, H. & Mandelkow, E. M. *A sequence of cytoskeleton changes related to the formation of neurofibrillary tangles and neuropil threads.* Acta Neuropathol **87**, 554-567 (1994).
- [198] Khatoon, S., Grundke-Iqbal, I. & Iqbal, K. *Brain levels of microtubule-associated protein tau are elevated in Alzheimer's disease: a radioimmuno-slot-blot assay for nanograms of the protein.* J Neurochem **59**, 750-753 (1992).
- [199] Lim, F. *et al.* *FTDP-17 mutations in tau transgenic mice provoke lysosomal abnormalities and Tau filaments in forebrain.* Mol Cell Neurosci **18**, 702-714 (2001).
- [200] Cataldo, A. M. *et al.* *Gene expression and cellular content of cathepsin D in Alzheimer's disease brain: evidence for early up-regulation of the endosomal-lysosomal system.* Neuron **14**, 671-680 (1995).

-
- [201] Nixon, R. A. & Cataldo, A. M. *Lysosomal system pathways: genes to neurodegeneration in Alzheimer's disease.* J Alzheimers Dis **9**, 277-289 (2006).
- [202] Boya, P. & Kroemer, G. *Lysosomal membrane permeabilization in cell death.* Oncogene **27**, 6434-6451 (2008).
- [203] Bendiske, J. & Bahr, B. A. *Lysosomal activation is a compensatory response against protein accumulation and associated synaptopathogenesis--an approach for slowing Alzheimer disease?* J Neuropathol Exp Neurol **62**, 451-463 (2003).
- [204] Wang, Y. *et al.* *Tau fragmentation, aggregation and clearance: the dual role of lysosomal processing.* Hum Mol Genet **18**, 4153-4170 (2009).
- [205] Zhang, L., Sheng, R. & Qin, Z. *The lysosome and neurodegenerative diseases.* Acta Biochim Biophys Sin (Shanghai) **41**, 437-445 (2009).
- [206] Callahan, L. M., Vaules, W. A. & Coleman, P. D. *Quantitative decrease in synaptophysin message expression and increase in cathepsin D message expression in Alzheimer disease neurons containing neurofibrillary tangles.* J Neuropathol Exp Neurol **58**, 275-287 (1999).
- [207] Cataldo, A. M., Hamilton, D. J., Barnett, J. L., Paskevich, P. A. & Nixon, R. A. *Properties of the endosomal-lysosomal system in the human central nervous system: disturbances mark most neurons in populations at risk to degenerate in Alzheimer's disease.* J Neurosci **16**, 186-199 (1996).
- [208] Beyer, K., Lao, J. I., Latorre, P. & Ariza, A. *Age at onset: an essential variable for the definition of genetic risk factors for sporadic Alzheimer's disease.* Ann N Y Acad Sci **1057**, 260-278 (2005).
- [209] Papassotiropoulos, A. *et al.* *A genetic variation of cathepsin D is a major risk factor for Alzheimer's disease.* Ann Neurol **47**, 399-403 (2000).
- [210] Yamashima, T. & Oikawa, S. *The role of lysosomal rupture in neuronal death.* Prog Neurobiol **89**, 343-358 (2009).
- [211] Khurana, V. *et al.* *Lysosomal dysfunction promotes cleavage and neurotoxicity of tau in vivo.* PLoS Genet **6**, e1001026 (2010).
- [212] Brand, A. H., Manoukian, A. S. & Perrimon, N. *Ectopic expression in Drosophila.* Methods Cell Biol **44**, 635-654 (1994).
- [213] Brand, A. H. & Perrimon, N. *Targeted gene expression as a means of altering cell fates and generating dominant phenotypes.* Development **118**, 401-415 (1993).
- [214] Phelps, C. B. & Brand, A. H. *Ectopic gene expression in Drosophila using GAL4 system.* Methods **14**, 367-379 (1998).

- [215] Rorth, P. *A modular misexpression screen in Drosophila detecting tissue-specific phenotypes*. Proc Natl Acad Sci U S A **93**, 12418-12422 (1996).
- [216] Lee, R. C., Feinbaum, R. L. & Ambros, V. *The C. elegans heterochronic gene lin-4 encodes small RNAs with antisense complementarity to lin-14*. Cell **75**, 843-854 (1993).
- [217] Dietzl, G. *et al.* *A genome-wide transgenic RNAi library for conditional gene inactivation in Drosophila*. Nature **448**, 151-156 (2007).
- [218] Fire, A. *et al.* *Potent and specific genetic interference by double-stranded RNA in Caenorhabditis elegans*. Nature **391**, 806-811 (1998).
- [219] Hammond, S. M., Bernstein, E., Beach, D. & Hannon, G. J. *An RNA-directed nuclease mediates post-transcriptional gene silencing in Drosophila cells*. Nature **404**, 293-296 (2000).
- [220] Hamilton, A. J. & Baulcombe, D. C. *A species of small antisense RNA in posttranscriptional gene silencing in plants*. Science **286**, 950-952 (1999).
- [221] Zamore, P. D., Tuschl, T., Sharp, P. A. & Bartel, D. P. *RNAi: double-stranded RNA directs the ATP-dependent cleavage of mRNA at 21 to 23 nucleotide intervals*. Cell **101**, 25-33 (2000).
- [222] Elbashir, S. M., Lendeckel, W. & Tuschl, T. *RNA interference is mediated by 21- and 22-nucleotide RNAs*. Genes Dev **15**, 188-200 (2001).
- [223] Elbashir, S. M., Martinez, J., Patkaniowska, A., Lendeckel, W. & Tuschl, T. *Functional anatomy of siRNAs for mediating efficient RNAi in Drosophila melanogaster embryo lysate*. EMBO J **20**, 6877-6888 (2001).
- [224] Lee, Y. S. *et al.* *Distinct roles for Drosophila Dicer-1 and Dicer-2 in the siRNA/miRNA silencing pathways*. Cell **117**, 69-81 (2004).
- [225] Liu, Q. *et al.* *R2D2, a bridge between the initiation and effector steps of the Drosophila RNAi pathway*. Science **301**, 1921-1925 (2003).
- [226] Tomari, Y., Matranga, C., Haley, B., Martinez, N. & Zamore, P. D. *A protein sensor for siRNA asymmetry*. Science **306**, 1377-1380 (2004).
- [227] Rand, T. A., Petersen, S., Du, F. & Wang, X. *Argonaute2 cleaves the anti-guide strand of siRNA during RISC activation*. Cell **123**, 621-629 (2005).
- [228] Marsh, J. L. & Thompson, L. M. *Drosophila in the study of neurodegenerative disease*. Neuron **52**, 169-178 (2006).
- [229] Wolff, T. & Ready, D. F. *Cell death in normal and rough eye mutants of Drosophila*. Development **113**, 825-839 (1991).

- [230] Cao, W. *et al.* Identification of novel genes that modify phenotypes induced by Alzheimer's beta-amyloid overexpression in *Drosophila*. *Genetics* **178**, 1457-1471 (2008).
- [231] Blard, O. *et al.* Cytoskeleton proteins are modulators of mutant tau-induced neurodegeneration in *Drosophila*. *Hum Mol Genet* **16**, 555-566 (2007).
- [232] Shulman, J. M. & Feany, M. B. Genetic modifiers of tauopathy in *Drosophila*. *Genetics* **165**, 1233-1242 (2003).
- [233] Ellis, M. C., O'Neill, E. M. & Rubin, G. M. Expression of *Drosophila* glass protein and evidence for negative regulation of its activity in non-neuronal cells by another DNA-binding protein. *Development* **119**, 855-865 (1993).
- [234] Lin, D. M. & Goodman, C. S. Ectopic and increased expression of Fasciclin II alters motoneuron growth cone guidance. *Neuron* **13**, 507-523 (1994).
- [235] Steinhilb, M. L., Dias-Santagata, D., Fulga, T. A., Felch, D. L. & Feany, M. B. Tau phosphorylation sites work in concert to promote neurotoxicity in vivo. *Mol Biol Cell* **18**, 5060-5068 (2007).
- [236] Steinhilb, M. L. *et al.* S/P and T/P phosphorylation is critical for tau neurotoxicity in *Drosophila*. *J Neurosci Res* **85**, 1271-1278 (2007).
- [237] Fulga, T. A. *et al.* Abnormal bundling and accumulation of F-actin mediates tau-induced neuronal degeneration in vivo. *Nat Cell Biol* **9**, 139-148 (2007).
- [238] Kretzschmar, D. *et al.* Glial and neuronal expression of polyglutamine proteins induce behavioral changes and aggregate formation in *Drosophila*. *Glia* **49**, 59-72 (2005).
- [239] <http://www.ncbi.nlm.nih.gov/gene> (13.03.2011)
- [240] Nomenclature, F. Genetic nomenclature for *Drosophila melanogaster*, <http://flybase.org/static_pages/docs/nomenclature/nomenclature3.html> (2011).
- [241] Finelli, A., Kelkar, A., Song, H. J., Yang, H. & Konsolaki, M. A model for studying Alzheimer's Abeta42-induced toxicity in *Drosophila melanogaster*. *Mol Cell Neurosci* **26**, 365-375 (2004).
- [242] Bischof, J., Maeda, R. K., Hediger, M., Karch, F. & Basler, K. An optimized transgenesis system for *Drosophila* using germ-line-specific *phiC31* integrases. *Proc Natl Acad Sci U S A* **104**, 3312-3317 (2007).
- [243] Sullivan, W., Ashburner, M. & Hawley, R. S. *Drosophila Protocols*. (Cold Spring Harbor Press, 2000).

-
- [244] Vandesompele, J. *et al.* *Accurate normalization of real-time quantitative RT-PCR data by geometric averaging of multiple internal control genes.* *Genome Biol* **3**, RESEARCH0034 (2002).
- [245] Fuger, P., Behrends, L. B., Mertel, S., Sigrist, S. J. & Rasse, T. M. *Live imaging of synapse development and measuring protein dynamics using two-color fluorescence recovery after photo-bleaching at Drosophila synapses.* *Nat Protoc* **2**, 3285-3298 (2007).
- [246] Pilling, A. D., Horiuchi, D., Lively, C. M. & Saxton, W. M. *Kinesin-1 and Dynein are the primary motors for fast transport of mitochondria in Drosophila motor axons.* *Mol Biol Cell* **17**, 2057-2068 (2006).
- [247] Gustafson, K. & Boulianne, G. L. *Distinct expression patterns detected within individual tissues by the GAL4 enhancer trap technique.* *Genome* **39**, 174-182 (1996).
- [248] Warrick, J. M. *et al.* *Expanded polyglutamine protein forms nuclear inclusions and causes neural degeneration in Drosophila.* *Cell* **93**, 939-949 (1998).
- [249] Hsiung, F. & Moses, K. *Retinal development in Drosophila: specifying the first neuron.* *Hum Mol Genet* **11**, 1207-1214 (2002).
- [250] Weismann, A. *Die nachembryonale Entwicklung der Musciden nach Beobachtungen an Musca vomitoria und Sarcophaga carnaria.* *Z. wiss. Zool.* **14**, 187-336 (1864).
- [251] Thomas, B. J. & Wassarman, D. A. *A fly's eye view of biology.* *Trends Genet* **15**, 184-190 (1999).
- [252] Spreij, T. E. *Cell death during the development of the imaginal discs of Calliphora erythrocephala.* *Neth. J. Zool.* **21**, 221-264 (1971).
- [253] Gene Ontology Annotation database. <http://www.ebi.ac.uk/GOA/> (13.03.2011)
- [254] Jan, L. Y. & Jan, Y. N. *Antibodies to horseradish peroxidase as specific neuronal markers in Drosophila and in grasshopper embryos.* *Proc Natl Acad Sci U S A* **79**, 2700-2704 (1982).
- [255] Chatterjee, S., Sang, T. K., Lawless, G. M. & Jackson, G. R. *Dissociation of tau toxicity and phosphorylation: role of GSK-3beta, MARK and Cdk5 in a Drosophila model.* *Hum Mol Genet* **18**, 164-177 (2009).
- [256] Kraemer, B. C., Burgess, J. K., Chen, J. H., Thomas, J. H. & Schellenberg, G. D. *Molecular pathways that influence human tau-induced pathology in Caenorhabditis elegans.* *Hum Mol Genet* **15**, 1483-1496 (2006).

- [257] Bunker, J. M., Kamath, K., Wilson, L., Jordan, M. A. & Feinstein, S. C. *FTDP-17 mutations compromise the ability of tau to regulate microtubule dynamics in cells.* J Biol Chem **281**, 11856-11863 (2006).
- [258] Chen, S. & Smith, D. F. *Hop as an adaptor in the heat shock protein 70 (Hsp70) and hsp90 chaperone machinery.* J Biol Chem **273**, 35194-35200 (1998).
- [259] Nicolet, C. M. & Craig, E. A. *Isolation and characterization of STI1, a stress-inducible gene from Saccharomyces cerevisiae.* Mol Cell Biol **9**, 3638-3646 (1989).
- [260] Song, Y. & Masison, D. C. *Independent regulation of Hsp70 and Hsp90 chaperones by Hsp70/Hsp90-organizing protein Sti1 (Hop1).* J Biol Chem **280**, 34178-34185 (2005).
- [261] Zhang, Y. J. *et al.* *Carboxyl terminus of heat-shock cognate 70-interacting protein degrades tau regardless its phosphorylation status without affecting the spatial memory of the rats.* J Neural Transm **115**, 483-491 (2008).
- [262] Spillantini, M. G., Crowther, R. A., Kamphorst, W., Heutink, P. & van Swieten, J. C. *Tau pathology in two Dutch families with mutations in the microtubule-binding region of tau.* Am J Pathol **153**, 1359-1363 (1998).
- [263] Goedert, M. *et al.* *Epitope mapping of monoclonal antibodies to the paired helical filaments of Alzheimer's disease: identification of phosphorylation sites in tau protein.* Biochem J **301 (Pt 3)**, 871-877 (1994).
- [264] Sontag, E., Nunbhakdi-Craig, V., Lee, G., Bloom, G. S. & Mumby, M. C. *Regulation of the phosphorylation state and microtubule-binding activity of Tau by protein phosphatase 2A.* Neuron **17**, 1201-1207 (1996).
- [265] Wang, D. *et al.* *Antioxidants protect PINK1-dependent dopaminergic neurons in Drosophila.* Proc Natl Acad Sci U S A **103**, 13520-13525 (2006).
- [266] Ravikumar, B. *et al.* *Dynein mutations impair autophagic clearance of aggregate-prone proteins.* Nat Genet **37**, 771-776 (2005).
- [267] Batlevi, Y. *et al.* *Dynein light chain 1 is required for autophagy, protein clearance, and cell death in Drosophila.* Proc Natl Acad Sci U S A **107**, 742-747 (2010).
- [268] Strausfeld, N. J. *The organization of the insect visual system (Light microscopy).* Cell and Tissue Research **121**, 377-441 (1971).

Curriculum Vitae

Name	Malte Butzlaff
Residence	Passtraße 4 52070 Aachen Germany
Date of birth	29.12.1983
Place of birth	Celle, Lower Saxony, Germany
Nationality	German
Parents	Joachim Butzlaff, Department Manager Sales Sabine Butzlaff, Teacher

School education

1988 - 1989	Buea Mountain School, Buea, Cameroun
1989 - 1993	Ameisenschule Meinersen, Germany (elementary school)
1993 - 1995	Orientierungsstufe Meinersen, Germany (5 th and 6 th gr.)
1995 - 2002	Gymnasium Uetze, Germany (secondary school)
10.06.2002	Allgemeine Hochschulreife (A-levels)

Civilian service

2002/2003	2002/2003 Civilian service in nursing at the account-ward (Urology, phlebology und surgery) of the county-hospital Emmendingen (Baden-Württemberg, Germany)
------------------	---

Studies

WS 2003/2004	First semester in major of the Diploma-program Molecular Medicine at the Friedrich-Schiller-University Jena, Germany
SS 2004 – SS 2006	Second till sixth semester in major of the bachelor-program Molecular Medicine at the Georg-August-University Göttingen, Germany Absolved lab-rotations: 3-week practical course in the dept. for transfusion medicine, Dr. Legeler (1,7) 3-week practical course in the dept. human genetics, Dr. Adham (1,0) 6-week practical course in the Max-Planck-Institute for experimental Medicine, dept. clinical neuro-sciences, Prof. Dr. Ehrenreich (1,0) 6-week practical course in the dept. neurodegeneration and

- neurorestoration research, Dr. Gerhardt (1,0)
- 13.08.2006** Degree Bachelor of Science (B.Sc.) in the program Molecular Medicine (1,7)
Thesis in the dept. neurodegeneration and neuro-restoration research, Prof. Dr. J. Schulz, „*Entwicklung eines lentiviralen Vektors zur spezifischen Expression von Zielgenen in dopaminergen Neuronen für „in vitro“ und „in vivo“ Anwendungen*“ (1,0)
- WS 2006/2007 – SS 2008** Master-program Molecular Medicine at the Georg-August-University of Göttingen, Germany
Absolved lab-rotations:
8-week practical course, dept. Haematology and Oncology, JProf. Dr. G. Wulff (1,0)
8-week practical course at the German Primate Centre, dept. Immunology und Virology, Dr. S. Froede (1,0)
8-week practical course in the dept. neurodegeneration and neurorestoration research, Dr. Voigt (1,0)
- 05.07.2008** Degree Master of Science (M.Sc.) in the international program Molecular Medicine (1,7)
Thesis in the dept. neurodegeneration and neurorestoration research, Prof. Dr. J. Schulz, „*Characterisation of Drosophila models for Alzheimer's and Machado-Joseph's disease - requirements for a genome-wide modifier-screen using RNAi mediated gene silencing*“ (1,0)
- Since WS 2007/2008** PhD program Molecular Medicine at the Georg-August-University of Göttingen, Germany
- 24.09.2007 – 31.10.2009** Doctoral candidate in the dept. neurodegeneration and neurorestoration research, university medicine Göttingen with the working title „*Genome-wide screen for modifiers of A β 42, Tau and ATXN3 induced neurodegeneration using RNAi-mediated gene silencing in Drosophila*“
- Since 01.11.2009** Doctoral candidate in the clinic for neurology at the University hospital of the RWTH Aachen (same working title)

Additional activities

- 2007** Tutor of the lecture series Biochemistry
- 2007/2008** Voting member of the subcommittee “web presence” of the study program Molecular Medicine
- 2007/2008** Fee-based freelance translator for instructions in scientific school education

Private Danksagungen

Ich möchte mich hiermit bei allen bedanken, die mich während meiner Schulzeit, meines Studiums und meiner Promotion unterstützt und mir beigestanden haben. Insbesondere meinen Eltern Sabine und Joachim und meinem Bruder Felix bin ich für die jahrelange Unterstützung und Motivation unendlich dankbar. Die Kraft, die ich in letzter Zeit für diese Arbeit benötigt habe, verdanke ich jedoch vor allem dir Annette und unserer gemeinsamen Zukunft. Ich liebe dich. Zudem danke ich meinem langjährigen Begleiter Hannes für seinen Beistand und die lukullische Versorgung in der harten Zeit. Ich werde deine Gegenwart missen.

Das waren natürlich nicht alle, die mich in meinem bisherigen Werdegang gestützt haben oder die mich zu dem gemacht haben, der ich jetzt bin. Ich danke meinen Großeltern Kurt und Christa, Iris und Lisa, meinen Paten Eckhard und Brigitte sowie meiner (Paten)-Tante Hanna, Gisela, meinem Onkel Martin, meinen Cousins und Cousinen Moritz, Janosch, Paul, Titus und Rosa, und der gesamten Großfamilie, die mir sehr viel bedeutet. Desweiteren danke ich Anna Lena und Anna für eure großartige Freundschaft, ebenso wie Alexandra, Julia, Nadine, Nils, Karen und dem ganzen Jahrgang des Studiengangs Molekulare Medizin in Göttingen. Desweiteren danke ich noch Wiebke, Anne, Stefan, Maik, Dennis und Benjamin.

Außerdem möchte ich mich noch explizit bei Erik Meskauskas und Werner Albig bedanken, die mich mein gesamtes Studium hindurch begleitet und geleitet haben.

Appendix

I List of screened RNAi lines provided by the VDRC as the human homologue sublibrary	104
II Fly lines used for verification of RNAi effects.....	128
III Phenotypes induced by candidate shRNA lines	130
IV Preliminary western blot for altered phosphorylation of Tau induced by candidate shRNAs.....	140

I List of screened RNAi lines provided by the VDRC as the human homologue sublibrary

Gene-ID	TID								
		CG10105	18002	CG10221	1163	CG10320	8837	CG10426	16048
CG10001	1326	CG10106	7934	CG10222	18038	CG10324	31226	CG10435	38384
CG10002	37063	CG10107	18004	CG10223	30625	CG10325	51900	CG10438	23296
CG10002	49961	CG10110	18009	CG10225	38363	CG10326	5894	CG10443	36270
CG10006	44539	CG10117	4871	CG10226	5055	CG10326	47194	CG10444	4722
CG10009	17954	CG10118	3308	CG10228	38365	CG10327	38377	CG10446	3066
CG10011	45096	CG10122	12688	CG10229	38368	CG10333	18132	CG10446	27049
CG10018	37591	CG10123	10635	CG10230	31206	CG10335	40612	CG10447	45660
CG10021	3774	CG10126	44104	CG10231	18041	CG10336	16019	CG10449	7183
CG10023	17957	CG10128	8868	CG10233	28702	CG10338	3215	CG10459	41451
CG10029	16583	CG10130	8785	CG10234	37124	CG10340	16020	CG10463	31248
CG10030	44480	CG10133	18014	CG10236	18873	CG10341	52092	CG10466	23367
CG10032	51688	CG10137	38342	CG10238	15990	CG10343	38380	CG10467	27263
CG10033	38319	CG10142	15246	CG10240	33238	CG10344	48026	CG10470	3897
CG10034	30525	CG10143	51564	CG10242	4880	CG10346	31228	CG10473	16052
CG10036	15425	CG10144	18019	CG10242	50169	CG10347	16025	CG10474	41455
CG10037	10756	CG10145	15194	CG10243	7398	CG10348	39663	CG10479	45098
CG10037	47182	CG10149	18022	CG10243	49532	CG10353	5550	CG10480	38388
CG1004	51953	CG10153	31186	CG10245	3313	CG10354	27254	CG10483	33276
CG10043	17966	CG10155	18024	CG10246	29980	CG10355	9308	CG10484	49423
CG10047	33317	CG10157	14004	CG10246	50262	CG10361	16034	CG10489	13625
CG10050	30020	CG10158	47388	CG10247	3317	CG10362	8317	CG1049	18628
CG10052	44717	CG10160	31192	CG10249	15009	CG10363	13466	CG10491	50358
CG10053	17972	CG10162	23362	CG10250	51311	CG10365	16036	CG10492	12357
CG10053	50811	CG10165	3909	CG10251	9534	CG10369	3886	CG10493	45364
CG10055	17973	CG10166	13731	CG10253	3321	CG10371	47623	CG10495	18631
CG10060	28150	CG10166	46385	CG10254	15992	CG10372	31238	CG10497	13322
CG10061	17975	CG10168	1151	CG10255	18600	CG10373	6375	CG10505	6593
CG10062	4697	CG1017	15610	CG10257	8710	CG10374	30884	CG10510	18635
CG10064	38322	CG10170	1141	CG10260	15993	CG10374	48109	CG10517	44107
CG10066	23303	CG10171	43837	CG10261	2907	CG10375	16039	CG10523	47636
CG10067	17979	CG10174	31195	CG10262	37672	CG10376	35473	CG10524	22755
CG10068	15948	CG10175	1140	CG10272	16001	CG10377	16040	CG10524	33837
CG10069	6591	CG10178	8064	CG10272	47199	CG10379	16044	CG10528	16067
CG10072	29434	CG10181	9019	CG10275	36246	CG10383	33911	CG10531	16071
CG10073	11133	CG10184	3311	CG10275	37283	CG10384	16045	CG10532	16073
CG10075	15399	CG10185	18135	CG10277	7518	CG10385	9239	CG10535	45366
CG10075	50067	CG10186	30768	CG10278	10418	CG10387	31240	CG10536	16078
CG10076	44092	CG10188	18029	CG10279	46908	CG10390	37563	CG10537	41101
CG10078	17981	CG10189	51692	CG10280	5733	CG10392	18611	CG10539	18126
CG10078	48823	CG1019	18593	CG10281	51209	CG10393	11796	CG10541	31253
CG10079	43268	CG10191	38353	CG10286	16002	CG10395	31244	CG10542	15620
CG10080	46133	CG10192	18031	CG10289	16006	CG10396	1482	CG10545	31257
CG10081	10066	CG10193	45109	CG10293	13756	CG10399	18617	CG10546	31258
CG10082	38326	CG10198	31198	CG10295	12553	CG10406	23363	CG10546	49655
CG10083	38330	CG10202	9427	CG10298	28706	CG10406	50865	CG10549	40789
CG10084	38336	CG10203	31202	CG1030	3033	CG10413	3882	CG10555	16961
CG10089	17991	CG10206	31204	CG1030	46499	CG10414	47391	CG10555	50115
CG1009	35354	CG1021	37336	CG10302	22837	CG10415	12591	CG10564	51979
CG10090	37346	CG10210	38356	CG10305	16012	CG10417	27259	CG10565	38393
CG10096	50765	CG10211	12352	CG10308	31216	CG10418	50245	CG10566	27281
CG10097	6090	CG10212	10711	CG1031	31220	CG10419	47373	CG1057	27284
CG10098	50126	CG10214	18033	CG10315	27152	CG10420	1753	CG10571	49078
CG10103	31174	CG10215	12622	CG10315	48708	CG10423	12795	CG10572	45370
CG10104	13969	CG10220	45999	CG10318	15451	CG10425	6734	CG10573	31266

CG10574	39053	CG10674	11366	CG10806	33149	CG10950	41462	CG11077	42671
CG10575	31270	CG10679	28445	CG10808	8784	CG10951	16120	CG11079	23374
CG10576	28761	CG10681	27305	CG10809	38408	CG10952	9127	CG1108	16184
CG10578	31271	CG10682	27306	CG10811	17002	CG10954	45013	CG11081	4740
CG10579	47859	CG10685	17847	CG10814	27319	CG10955	27341	CG11081	27238
CG1058	8549	CG10686	31319	CG1082	45102	CG10958	26763	CG11082	45349
CG10580	51977	CG10687	31320	CG10822	17005	CG10960	8359	CG11084	11099
CG10581	18650	CG10688	39715	CG10823	1783	CG10961	16125	CG11085	10493
CG10581	48315	CG10689	31324	CG10824	16588	CG10962	30850	CG11086	18690
CG10582	52094	CG10691	12358	CG10825	31360	CG10966	3024	CG11089	31420
CG10583	45092	CG10692	37816	CG10827	30823	CG10967	16133	CG1109	16186
CG10584	28681	CG10693	6723	CG10830	31362	CG10971	16138	CG11092	16188
CG10585	31273	CG10694	13649	CG10833	7870	CG10973	41463	CG11093	15478
CG10588	18655	CG10695	27307	CG10837	31364	CG10975	942	CG11094	11096
CG1059	39711	CG10697	3329	CG10838	28289	CG10975	4789	CG11095	37910
CG10590	5035	CG10698	44309	CG10839	17013	CG10975	27090	CG11096	38444
CG10590	5036	CG10699	45231	CG1084	40613	CG10977	37238	CG11098	7625
CG10592	38171	CG10701	37917	CG10840	31365	CG10979	16144	CG11099	9272
CG10593	3324	CG10702	3691	CG10846	8057	CG1098	27346	CG11102	13478
CG10594	51081	CG10703	35486	CG10847	15291	CG10981	16149	CG11103	5562
CG10597	6157	CG10706	28155	CG10849	7480	CG10984	15627	CG11105	51705
CG10600	31276	CG1071	45743	CG10850	18847	CG10986	31390	CG11107	44119
CG10601	22841	CG10711	16846	CG10859	27322	CG10988	2983	CG11109	17528
CG10601	50133	CG10716	38399	CG1086	13326	CG1099	16158	CG11110	3801
CG10602	31280	CG10718	31329	CG10861	29790	CG10990	16162	CG11111	6226
CG10603	31285	CG10719	31333	CG10862	31373	CG10992	45345	CG11115	49942
CG10604	15716	CG1072	9830	CG10863	48619	CG10993	16165	CG1112	42942
CG10605	2931	CG1072	46755	CG10866	3234	CG10996	16168	CG11121	8950
CG10610	31286	CG10721	33098	CG10868	45009	CG10997	28303	CG11123	18142
CG10616	36605	CG10722	44128	CG10869	27326	CG10999	16171	CG11124	13911
CG10617	3303	CG10723	30304	CG10872	30717	CG1100	18676	CG11125	18143
CG10619	45859	CG10724	22850	CG10873	38235	CG11001	45015	CG11128	45587
CG10620	5236	CG10726	26759	CG10877	45750	CG11006	31394	CG1113	31426
CG10621	31291	CG10728	50141	CG1088	45374	CG11007	40833	CG11130	18145
CG10622	30889	CG10732	18664	CG10881	35495	CG11009	16173	CG11133	18150
CG10623	31294	CG10739	31337	CG10882	37543	CG1101	12031	CG11136	4758
CG10624	44928	CG1074	35488	CG10887	16082	CG11010	47537	CG11136	44991
CG10626	22845	CG10742	10140	CG10889	27329	CG11015	30892	CG11137	8464
CG10627	31298	CG10743	16850	CG1089	27332	CG1102	18970	CG11137	48241
CG10628	47392	CG10747	38403	CG10890	50554	CG11024	46489	CG11138	18154
CG1063	6484	CG10748	14072	CG10895	44981	CG11025	45497	CG11139	17530
CG10632	39714	CG10749	27311	CG10897	38413	CG11027	12931	CG11140	37726
CG10635	35481	CG10750	27313	CG10898	13643	CG11029	44228	CG11141	18157
CG10635	46220	CG10751	22761	CG10899	16084	CG11030	43530	CG11143	5616
CG10637	35482	CG10753	31343	CG1090	26783	CG11033	31402	CG11144	1793
CG10638	31306	CG10754	31347	CG10903	27334	CG11034	37941	CG11146	50598
CG10639	30737	CG10756	44466	CG10907	16085	CG11035	8478	CG11148	18159
CG1064	12645	CG10757	45494	CG10908	44211	CG1104	31406	CG11149	7882
CG10640	30890	CG1076	40807	CG10909	17522	CG11041	45061	CG11151	18129
CG10641	31307	CG10760	13996	CG1091	16088	CG11043	23370	CG11153	19022
CG10642	45372	CG10761	5474	CG10910	46896	CG11044	16178	CG11154	37812
CG10645	31311	CG10772	22853	CG10913	3245	CG11048	31407	CG11156	31432
CG10646	38396	CG10776	865	CG10914	38419	CG1105	28305	CG1116	18161
CG10648	51699	CG10776	42244	CG10915	31377	CG11050	12371	CG11162	8326
CG1065	27298	CG10777	46933	CG10918	23190	CG11052	23373	CG11163	13311
CG10653	35483	CG10778	3166	CG10920	16091	CG11055	18686	CG11164	3180
CG10655	2985	CG1078	27317	CG10922	2989	CG11058	31409	CG11165	18166
CG10657	3326	CG10791	18140	CG10923	52105	CG11059	36348	CG11166	31435
CG1066	46889	CG10792	15444	CG10924	13929	CG11059	37291	CG11168	18170
CG10662	31318	CG10793	31351	CG10927	16094	CG1106	37867	CG11170	41302
CG10663	27299	CG10795	8833	CG1093	27335	CG11061	38441	CG11172	30566
CG10664	3923	CG10797	26299	CG10931	52107	CG11062	12174	CG11173	18172
CG10667	46522	CG10798	2947	CG10932	16099	CG11063	38442	CG11176	18175
CG10670	47601	CG10802	31354	CG10938	16104	CG11064	6878	CG11177	45975
CG10671	44435	CG10803	27318	CG10939	16958	CG11069	51367	CG11178	18178
CG10672	18661	CG10804	30225	CG10947	16117	CG1107	16182	CG11180	31438
CG10673	27301	CG10805	17000	CG10948	31388	CG11070	31413	CG11181	18179

CG11182	15318	CG11315	38273	CG11450	41069	CG11611	39157	CG11807	38564
CG11183	31442	CG11315	46906	CG11454	45116	CG11614	3004	CG11811	30917
CG11184	31444	CG11318	3395	CG11455	12838	CG11617	30533	CG11814	38567
CG11186	15919	CG11319	7621	CG11459	16573	CG11621	16240	CG11819	31571
CG11188	18182	CG1132	30553	CG11459	48053	CG11622	16244	CG11820	39724
CG1119	10942	CG11320	18054	CG11465	28457	CG11639	23285	CG11821	26796
CG11190	14821	CG11321	18055	CG11466	38045	CG11641	30537	CG11821	46858
CG11194	30561	CG11323	18057	CG1147	9605	CG11642	50359	CG11823	12044
CG11196	36497	CG11324	18061	CG11474	31507	CG11648	12024	CG11824	23381
CG11197	41368	CG11325	9546	CG11475	22864	CG1165	13886	CG11825	33917
CG11198	8105	CG11326	7535	CG11482	12685	CG11652	38549	CG11825	49834
CG11199	51707	CG11329	18065	CG11486	51713	CG11654	16251	CG11833	4417
CG1120	18184	CG1133	51292	CG11488	31508	CG11655	9131	CG11836	38570
CG11200	4725	CG11333	44110	CG11489	47544	CG11658	16255	CG11837	38574
CG11201	31456	CG11334	38485	CG11490	20040	CG11659	16260	CG11838	31575
CG11202	37656	CG11335	17259	CG11495	6459	CG11660	18526	CG11839	31576
CG11206	42943	CG11337	16420	CG11502	37087	CG11661	12778	CG11840	7247
CG11207	7833	CG11339	45390	CG11505	15286	CG11661	50393	CG11844	17245
CG11208	4720	CG1134	7481	CG11508	38519	CG11665	7314	CG11847	38578
CG11210	7363	CG11342	38488	CG11511	38526	CG11669	15794	CG11848	18717
CG11217	28762	CG11348	33824	CG11513	16206	CG1167	6225	CG11849	37753
CG11221	42947	CG11348	39421	CG11514	13705	CG11671	41146	CG11851	3419
CG11228	7823	CG1135	15613	CG11518	19692	CG11678	17242	CG11856	38581
CG11233	45386	CG11356	33812	CG1152	38041	CG11679	14834	CG11857	23203
CG11236	38460	CG11357	5027	CG11522	51715	CG1168	30816	CG11858	31579
CG11237	38462	CG11360	38491	CG11523	16210	CG11680	19691	CG11858	49586
CG11242	38463	CG11367	40900	CG11523	46794	CG11685	16267	CG11859	47401
CG11246	11203	CG11367	40900	CG11525	13654	CG11687	46097	CG11861	16331
CG11250	35501	CG11374	15561	CG11526	16211	CG11699	15861	CG11866	31582
CG11251	38467	CG11376	40673	CG11529	37098	CG11709	5594	CG11870	16334
CG11253	31473	CG11386	38493	CG11533	45120	CG11716	16283	CG11873	16337
CG11254	18198	CG11386	38493	CG11534	16216	CG1172	44113	CG11874	4418
CG11255	17534	CG11386	49657	CG11537	4118	CG11722	44114	CG11875	16342
CG11257	31475	CG11386	49657	CG11539	31518	CG11726	17545	CG11877	49372
CG11258	23376	CG11387	5687	CG11539	49580	CG11727	17549	CG11880	22867
CG11259	17537	CG11388	3604	CG11546	31522	CG11734	45302	CG11881	16352
CG1126	18200	CG1139	8907	CG11547	31525	CG11737	5807	CG11883	38590
CG11262	16912	CG11392	42959	CG11551	48368	CG11738	16289	CG11886	42970
CG11263	31112	CG11393	33839	CG11556	52439	CG11739	44562	CG11887	17560
CG11265	41097	CG11393	47725	CG11561	9542	CG11750	45978	CG11888	44134
CG11266	12945	CG11395	16696	CG11567	44232	CG11753	33829	CG11895	51379
CG11267	47087	CG11396	18073	CG11568	30060	CG11755	17555	CG11896	38596
CG11268	5240	CG11397	10937	CG11569	8706	CG11757	16296	CG11897	28259
CG11270	8322	CG11399	31489	CG11573	52126	CG11759	16298	CG11898	4430
CG11274	6439	CG1140	22859	CG11576	7577	CG11760	11925	CG11899	43549
CG11276	35718	CG11401	16768	CG11577	14334	CG11760	39217	CG11900	6430
CG11276	50021	CG11408	45394	CG11579	7767	CG11761	9963	CG11901	31589
CG11278	8361	CG1141	18081	CG1158	9455	CG11763	45981	CG11907	49328
CG1128	6420	CG11412	49370	CG11582	35379	CG11765	18708	CG11909	14735
CG11280	5242	CG11414	31494	CG11586	31531	CG11770	16801	CG11913	16366
CG11281	5247	CG11416	40674	CG11588	8348	CG11771	18946	CG11921	13719
CG11282	3046	CG11417	18087	CG11589	30353	CG11778	7374	CG11922	13721
CG11282	27097	CG11418	31497	CG11590	19867	CG11779	16309	CG11926	38600
CG11284	31482	CG11419	20027	CG11591	22770	CG11780	42092	CG1193	31598
CG1129	38471	CG11423	38500	CG11592	2495	CG11781	24483	CG11935	15472
CG11290	37527	CG11426	42600	CG11593	16227	CG11781	49584	CG11936	37927
CG11294	10497	CG11427	38504	CG11594	28311	CG11783	10958	CG11940	16369
CG11295	31484	CG11428	38508	CG11596	35505	CG11788	47245	CG11943	38608
CG11299	38481	CG11430	12221	CG11597	38541	CG1179	14123	CG11949	9787
CG1130	41070	CG11440	42592	CG11598	49831	CG1179	49832	CG11951	16532
CG11301	15344	CG11444	31501	CG11600	42964	CG11793	31551	CG11951	48791
CG11305	18043	CG11444	50278	CG11601	42737	CG11796	31563	CG11956	3335
CG11306	8448	CG11446	26839	CG11601	50814	CG11799	45697	CG11958	1335
CG11308	31487	CG11446	43370	CG11606	44093	CG1180	13842	CG11963	20097
CG11309	7513	CG11447	16199	CG11607	15876	CG11801	30042	CG11963	50300
CG1131	18048	CG11448	16202	CG11608	19932	CG11802	31570	CG11964	35511
CG11312	31488	CG11449	31503	CG1161	44964	CG11804	16313	CG11968	20130

CG11975	26799	CG12101	18739	CG12210	30605	CG12333	23091	CG1252	4566
CG11980	38616	CG12104	16398	CG12211	38634	CG12334	17079	CG12524	28745
CG11981	31608	CG12106	16400	CG12211	38634	CG12338	35521	CG12529	3337
CG11982	38623	CG12107	8731	CG12212	3788	CG12339	17081	CG12531	6203
CG11984	31615	CG12108	5499	CG12214	31689	CG1234	17084	CG12532	7720
CG11985	22773	CG12109	20151	CG12215	8754	CG12340	22878	CG12533	11670
CG11986	20136	CG12110	38626	CG12217	31690	CG12341	7391	CG12533	11670
CG11987	10735	CG12111	16513	CG12218	31693	CG12342	31736	CG12539	38689
CG11988	10662	CG12113	18742	CG12220	23040	CG12343	31737	CG12542	51748
CG11989	31619	CG12116	6498	CG12223	41029	CG12345	20183	CG12544	31961
CG11990	28318	CG12117	17018	CG12225	31701	CG12345	20183	CG12548	31964
CG11992	49413	CG12118	13340	CG12230	4548	CG12345x	40918	CG12560	29725
CG11994	18719	CG1212	41479	CG12231	31705	CG12346	20185	CG1257	31974
CG11999	16423	CG12125	5492	CG12233	41191	CG12346	48112	CG1258	46137
CG1200	50007	CG12127	3295	CG12233	50829	CG12352	31741	CG12582	15028
CG12000	16381	CG12128	42979	CG12234	31706	CG12355	47109	CG12598	7763
CG12001	16383	CG12129	17065	CG12235	31711	CG12357	50433	CG12600	31993
CG12002	15277	CG1213	6487	CG12238	38637	CG12358	46299	CG12602	6121
CG12004	10287	CG12130	7388	CG12240	6655	CG12359	31744	CG12605	20250
CG12005	11205	CG12131	45744	CG12244	20166	CG1236	17789	CG12605	49556
CG12006	39481	CG12132	31651	CG12245	2961	CG12360	41487	CG12608	24629
CG12007	20137	CG12134	31654	CG12245	2961	CG12361	10513	CG12608	49840
CG12008	37075	CG12135	17032	CG1225	31716	CG12362	31747	CG1263	17262
CG12010	6463	CG12136	5520	CG12252	38640	CG12363	31749	CG12630	18762
CG12012	33097	CG12139	1110	CG12253	31719	CG12366	44045	CG12630	48656
CG12014	13990	CG12139	5094	CG12254	47922	CG12367	31920	CG1264	2990
CG12016	22871	CG12139	27242	CG12259	38646	CG12369	35524	CG12646	17267
CG12018	13621	CG1214	4080	CG12261	17060	CG12370	43314	CG12647	22781
CG12019	47776	CG12140	15508	CG12262	15053	CG12373	24521	CG12648	23518
CG12020	18727	CG12149	17035	CG12263	10060	CG12374	13919	CG1265	44951
CG12021	31620	CG12151	31661	CG12265	43112	CG12375	45309	CG12653	12668
CG12024	20143	CG12152	17037	CG12267	43528	CG12376	22879	CG12657	29843
CG12025	4098	CG12153	13690	CG12268	1166	CG12384	36388	CG12659	31757
CG12026	42480	CG12154	51480	CG1227	38648	CG1239	17100	CG12661	47422
CG12026	43385	CG12156	31666	CG12272	18749	CG12390	38682	CG1268	9174
CG12029	26980	CG12157	13177	CG12273	42919	CG12395	17101	CG12690	15743
CG12030	16385	CG1216	17043	CG12275	44589	CG12396	31927	CG12698	18256
CG12031	15877	CG12161	31669	CG12276	18528	CG12397	47517	CG12701	38706
CG12038	51178	CG12162	20156	CG12276	47257	CG12398	11540	CG12702	24588
CG12042	31623	CG12163	12787	CG12278	29484	CG12399	12635	CG1271	13044
CG12048	1346	CG12163	15366	CG12279	44123	CG1240	45758	CG12713	17296
CG12050	42976	CG12163	46406	CG1228	38652	CG12400	37462	CG12723	41389
CG12051	12456	CG12165	17044	CG12283	4761	CG12403	17102	CG12727	17302
CG12052	12574	CG12169	38630	CG12283	36252	CG12403	46397	CG12728	24592
CG12054	45986	CG12170	31672	CG12283	43521	CG12404	1463	CG12728	52287
CG12055	31631	CG12171	47411	CG12286	37348	CG12405	24522	CG12733	24601
CG12058	31635	CG12173	31674	CG12287	30708	CG12405	50772	CG12734	32008
CG12068	16388	CG12175	32503	CG12287	52272	CG12410	9727	CG12737	24604
CG12068	50111	CG12175	48909	CG12289	31724	CG1242	7716	CG1274	43254
CG12070	51129	CG12176	12627	CG12297	7926	CG12424	25222	CG12740	18090
CG12071	49512	CG12178	7245	CG12298	45402	CG1245	13697	CG12740	49123
CG12072	9928	CG1218	31685	CG12301	51733	CG12455	3849	CG12743	47431
CG12076	31639	CG1218	46777	CG12304	38654	CG12467	41377	CG12746	33313
CG12077	4125	CG12186	17068	CG12306	20177	CG12467	46883	CG12749	51759
CG12078	15288	CG12189	13617	CG1231	17076	CG12477	31942	CG1275	4103
CG12079	13856	CG12190	52138	CG12311	5583	CG12478	35526	CG12750	17304
CG12081	31642	CG12192	41484	CG12313	4075	CG12489	20239	CG12752	44146
CG12082	17568	CG12194	7846	CG12314	48764	CG1249	31947	CG12752	52631
CG12083	7434	CG12194	46796	CG12317	45191	CG12497	24549	CG12753	1617
CG12084	31646	CG12200	31688	CG12318	12375	CG12498	17793	CG12756	31761
CG12085	20144	CG12200	50229	CG12320	17781	CG12499	24550	CG12759	17306
CG12090	16390	CG12201	42648	CG12321	17077	CG1250	24552	CG1276	17917
CG12091	13985	CG12202	17571	CG12323	38658	CG12505	31122	CG12765	17307
CG12092	35514	CG12203	42983	CG12324	17785	CG12505	48131	CG12766	50403
CG12093	41293	CG12207	18747	CG12324	49105	CG12506	19879	CG12770	31894
CG12099	18734	CG12208	20157	CG12325	31726	CG12506	50327	CG12772	46140
CG1210	18736	CG1221	15396	CG12327	8372	CG12511	12451	CG12773	9899

CG12775	32016	CG1303	41494	CG13309	14133	CG13521	4329	CG13773	43011
CG12782	31857	CG1303	50742	CG13310	43960	CG13521	42241	CG13775	44814
CG12785	31830	CG13030	17117	CG13311	51574	CG13521	42578	CG13777	41507
CG12787	7854	CG13032	29454	CG13312	14060	CG13526	32206	CG13778	17701
CG12788	23044	CG13035	14247	CG1332	32175	CG13531	17230	CG13779	31789
CG12788	49610	CG13037	32138	CG13320	23866	CG13533	6633	CG13779	49153
CG12789	33153	CG13072	18099	CG13322	32178	CG1354	17235	CG1378	6236
CG12792	41489	CG13072	49484	CG13326	18784	CG13551	31786	CG13780	7629
CG12795	32019	CG13076	45906	CG1333	51169	CG13559	6644	CG13784	8042
CG12797	32021	CG13077	51496	CG13334	15005	CG13567	43344	CG1379	41030
CG12799	20260	CG13078	3917	CG13343	17137	CG13570	23895	CG1380	44934
CG12812	32025	CG1308	44503	CG13344	17141	CG1358	13313	CG13801	45925
CG12813	31094	CG13089	2810	CG13345	17145	CG13585	13323	CG13807	47439
CG12816	17314	CG1309	37227	CG13348	36555	CG13585	50392	CG13809	24793
CG12817	40655	CG13090	43558	CG13349	23873	CG13588	45755	CG1381	24797
CG12818	31898	CG13091	11729	CG13350	44474	CG13597	32225	CG13822	38068
CG12818	46248	CG13095	15541	CG13364	28464	CG13598	32230	CG13827	24481
CG12822	32031	CG13096	41499	CG13364	48265	CG13601	19953	CG13829	28321
CG12833	32038	CG13097	38675	CG13366	29606	CG13602	32235	CG13830	44583
CG12836	24614	CG13098	38015	CG13367	17157	CG13603	6778	CG13832	24802
CG12846	52561	CG13108	43559	CG13369	17161	CG13604	32239	CG13833	6845
CG12848	31900	CG13109	15709	CG13375	2944	CG13605	1170	CG13842	17714
CG12855	5639	CG1311	39695	CG13379	17167	CG13608	22713	CG13844	29689
CG12858	1688	CG13124	29648	CG13383	23886	CG13609	17326	CG13849	52165
CG12859	8787	CG13125	17123	CG13383	50566	CG13610	1176	CG13850	15233
CG1287	12127	CG13137	41500	CG13384	44246	CG13610	48870	CG13852	17716
CG12876	32047	CG13139	32146	CG13387	3347	CG13611	45793	CG13855	17717
CG12877	20265	CG13142	24511	CG13388	5647	CG13617	32247	CG13859	17718
CG12878	38722	CG1315	47096	CG13389	17168	CG1362	32249	CG13859	48179
CG12879	4407	CG13151	39782	CG13390	17169	CG13623	17334	CG1386	13188
CG12891	4047	CG1316	23851	CG13391	17171	CG13624	32250	CG13867	24806
CG12892	20270	CG13160	4629	CG13393	33164	CG13626	1209	CG13875	44819
CG12895	18093	CG13162	32148	CG13396	30760	CG13628	29253	CG13876	39817
CG12895	49607	CG13163	39785	CG13398	38669	CG13633	14398	CG13880	24809
CG12896	32111	CG13167	18770	CG13399	31781	CG13645	32255	CG13886	17730
CG12904	10268	CG13168	18776	CG13399	50778	CG13646	1421	CG13887	23207
CG12909	32114	CG1317	4106	CG1340	32192	CG13651	11515	CG13889	17732
CG1291	32116	CG13175	50775	CG13400	29954	CG13654	13550	CG1389	1016
CG12913	44296	CG13176	24643	CG13401	43572	CG13661	14730	CG1389	4298
CG12915	38737	CG13178	44816	CG13402	30051	CG13663	6731	CG1389	36280
CG12918	38082	CG13185	18782	CG13404	30255	CG13667	36578	CG13890	24813
CG12919	45252	CG1319	39792	CG13409	47577	CG13671	52026	CG13892	44823
CG12921	20271	CG13190	43001	CG1341	17176	CG13686	31867	CG13893	32077
CG12924	20280	CG13192	32157	CG13410	13443	CG13688	43824	CG13898	23905
CG12929	4180	CG13197	36422	CG13415	17178	CG13690	24648	CG13900	18955
CG12935	47569	CG1320	18101	CG13415	49138	CG13691	32058	CG13906	12584
CG12936	38750	CG1320	52257	CG13418	39049	CG13693	46527	CG1391	17740
CG12938	38754	CG13201	2976	CG13423	45404	CG13702	50000	CG13916	51569
CG12938	50331	CG13202	28290	CG13424	10514	CG1371	13276	CG13917	32082
CG12948	41492	CG13213	43004	CG13425	2912	CG1372	4309	CG13919	4086
CG12951	16569	CG1322	42856	CG13426	8821	CG1372	36346	CG13920	46993
CG12951	46921	CG13221	32164	CG1343	12606	CG13722	30939	CG13922	41516
CG12954	18765	CG13223	1684	CG13430	49662	CG13722	46470	CG13926	15261
CG12956	13014	CG13232	28772	CG13431	40834	CG1374	16892	CG13927	4084
CG12959	17946	CG13251	17127	CG13442	4736	CG13743	40974	CG13929	17752
CG12975	18098	CG13252	33301	CG1345	17187	CG13744	44796	CG13930	17753
CG12990	6160	CG13263	17129	CG13458	17193	CG13745	24655	CG13937	3375
CG12993	20304	CG1327	31086	CG13466	3152	CG13746	41403	CG13941	3464
CG12994	11864	CG13277	23862	CG13467	17196	CG13748	43985	CG13946	17858
CG12995	13346	CG13281	12648	CG1347	24515	CG1375	39808	CG1395	17760
CG12997	33914	CG13287	36601	CG13470	17198	CG13752	877	CG13956	17766
CG13001	42347	CG13293	39797	CG13472	32193	CG13752	3070	CG13957	31840
CG13016	37428	CG13295	32171	CG13473	32195	CG13756	29592	CG13969	8070
CG13018	33859	CG13296	17133	CG13475	12608	CG13758	42724	CG13972	47444
CG13019	31769	CG13298	31777	CG1349	17214	CG13760	17698	CG13977	1294
CG13020	17116	CG13306	44960	CG13502	32203	CG13771	31868	CG13978	47488
CG13029	8502	CG13308	13862	CG13510	28433	CG13772	44236	CG13985	51447

CG1399	24826	CG14174	17416	CG14407	43020	CG14621	8661	CG14813	41549
CG13993	18210	CG1418	37728	CG1441	4034	CG14622	24885	CG14814	41553
CG13994	31791	CG14181	42548	CG14411	17579	CG1463	31877	CG14815	43473
CG13994	48622	CG14182	5370	CG14413	22740	CG14630	24894	CG14816	51655
CG13996	46532	CG14183	17423	CG14414	18217	CG1464	42845	CG14817	26894
CG13999	7889	CG14184	35613	CG14414	48176	CG14641	38790	CG14818	40700
CG14001	45028	CG14185	32097	CG1442	17580	CG14647	18297	CG14820	15456
CG1401	52176	CG14192	35684	CG14428	9730	CG14648	23918	CG14824	45594
CG14013	17343	CG14194	6181	CG14428	39362	CG14650	45458	CG14825	41554
CG14015	45891	CG14198	51785	CG14429	11683	CG1467	8644	CG1484	39528
CG14016	28329	CG14199	40884	CG1443	1333	CG14670	32301	CG14853	39734
CG14016	49613	CG1420	32100	CG14435	17600	CG14671	51803	CG14861	47458
CG1402	39251	CG14201	37047	CG14437	17602	CG14680	32304	CG14865	28532
CG14020	44221	CG14206	49844	CG1444	40949	CG14683	52664	CG14866	18419
CG14022	31796	CG14208	37420	CG14440	23916	CG14685	24905	CG14868	51810
CG14022	48332	CG14208	50572	CG14440	48156	CG14688	39840	CG14869	33347
CG14023	36480	CG14209	49642	CG14444	17621	CG14689	24907	CG1487	41559
CG14024	13402	CG14210	31803	CG14446	10274	CG14690	5985	CG14870	46307
CG14025	13998	CG14210	49168	CG14463	44552	CG14693	18332	CG14881	31821
CG14026	862	CG14211	3146	CG1447	19831	CG14694	5994	CG14882	38838
CG14026	3059	CG14212	17429	CG14472	17648	CG14701	28517	CG14883	8028
CG14028	13403	CG14213	32104	CG14476	48375	CG14704	13159	CG14885	46916
CG14028	33841	CG14214	11989	CG14477	28731	CG14709	6053	CG14887	48256
CG14029	5650	CG14214	46474	CG14480	32270	CG1471	30189	CG1489	24936
CG1403	17344	CG14216	18212	CG14480	46974	CG14712	18347	CG1489	46803
CG14030	24833	CG14217	17432	CG14482	33849	CG14715	12829	CG14893	43598
CG14031	48920	CG1422	44510	CG1449	13305	CG14717	38813	CG14895	39843
CG14033	23052	CG14221	32106	CG14490	17660	CG14718	32311	CG14898	18229
CG14034	32085	CG14222	18213	CG14505	17683	CG1472	44460	CG14898	49177
CG14036	28475	CG14224	47449	CG14507	35712	CG14721	18354	CG1490	18231
CG1404	24835	CG14228	7161	CG1451	51468	CG14721	50259	CG14902	43028
CG14040	13399	CG14230	46903	CG14511	4426	CG14722	23919	CG14903	40658
CG14041	39821	CG14232	47897	CG14512	41527	CG14724	44490	CG14903	49107
CG14043	17351	CG14234	30309	CG14512	47661	CG14739	18358	CG14905	39848
CG14048	39648	CG14235	26848	CG14513	26806	CG1474	42996	CG14906	31851
CG1405	31908	CG14238	2673	CG14514	41530	CG14740	32318	CG14909	9082
CG14057	22718	CG14255	39397	CG14514	49989	CG14743	4142	CG1492	8320
CG14057	48963	CG14256	35615	CG14515	51637	CG14744	40829	CG14921	32331
CG1406	17358	CG14267	24615	CG14517	42693	CG14745	6444	CG14933	7683
CG14066	24841	CG14268	14535	CG14522	32275	CG14745	52289	CG14933	33920
CG1407	50031	CG1427	17457	CG1453	41534	CG14746	43201	CG14934	15833
CG14073	39823	CG14270	17459	CG14536	11725	CG14746	50792	CG14936	6123
CG14077	7563	CG14271	31807	CG14542	24869	CG14749	24917	CG14938	7779
CG14079	14337	CG14283	37802	CG14543	4563	CG1475	24921	CG14939	32334
CG14080	45415	CG14283	50292	CG14544	32279	CG14750	38821	CG14940	31038
CG14084	8420	CG14286	17463	CG14547	14767	CG14757	38293	CG14941	5690
CG14085	45757	CG1429	15549	CG14549	43588	CG14763	8737	CG14945	13459
CG1409	30988	CG14290	15858	CG1455	32283	CG14767	50355	CG14946	38306
CG1410	24845	CG14291	16897	CG1455	49987	CG14771	45498	CG14956	3254
CG1410	50568	CG14296	24617	CG14550	4369	CG14777	9737	CG14962	39855
CG14100	46739	CG14299	17469	CG14550	50317	CG14778	44970	CG14965	31848
CG14105	17388	CG1430	17473	CG14551	24625	CG14783	18226	CG14966	43612
CG1411	15320	CG14303	17474	CG14562	32286	CG14786	42899	CG14966	47189
CG1412	43955	CG14305	17477	CG14575	13384	CG14788	18379	CG14967	44431
CG14122	51782	CG14322	30026	CG14575	43325	CG14789	41361	CG14969	8913
CG14127	32914	CG14325	17485	CG14577	9117	CG14792	38823	CG14971	39479
CG14130	31911	CG1433	17490	CG1458	4439	CG14792	50129	CG14977	18233
CG14133	23322	CG14339	17493	CG1458	33925	CG14793	3195	CG14980	18479
CG1414	12630	CG1434	30996	CG14591	9945	CG14801	38826	CG14983	32341
CG14142	17410	CG14353	24860	CG14593	1658	CG14802	28264	CG14985	32342
CG14149	24851	CG14366	17505	CG14611	31811	CG14802	48491	CG14991	18484
CG1416	41548	CG1438	8631	CG14615	24872	CG14803	18395	CG14991	46494
CG14163	5201	CG14394	39307	CG14617	24874	CG14804	18396	CG14992	39857
CG14164	17863	CG14396	842	CG14618	50597	CG14805	32325	CG14993	43032
CG14164	48825	CG14396	12292	CG14619	37930	CG14806	45107	CG14994	32344
CG14168	17414	CG14396	29907	CG1462	6862	CG14808	8305	CG14995	12725
CG1417	18561	CG1440	24622	CG14620	24881	CG14812	31815	CG14996	5654

CG14997	47016	CG15150	19332	CG15388	32599	CG15619	40007	CG15819	32385
CG14998	18491	CG15154	51821	CG15388	32599	CG15624	7858	CG1582	19617
CG14999	37756	CG1516	41576	CG15389	52199	CG15625	29368	CG15820	43874
CG1500	39575	CG15160	44601	CG15389	52199	CG15626	7844	CG1583	8928
CG15000	6273	CG15161	25198	CG1539	32601	CG15629	7839	CG1583	50353
CG15000	6273	CG15168	12248	CG15390	25112	CG15629	49077	CG15835	32652
CG15001	24943	CG15168	48614	CG15395	39929	CG15635	46490	CG1584	10677
CG15011	51517	CG1517	3306	CG15398	8873	CG15636	13072	CG15862	39437
CG15012	9176	CG1518	12250	CG15399	19450	CG15637	44029	CG15865	19157
CG15014	43615	CG1518	48653	CG15400	7261	CG15644	41587	CG1587	19061
CG15015	18492	CG15187	30628	CG15403	29945	CG15645	20206	CG15871	43691
CG15016	38842	CG1519	46544	CG15405	52652	CG15645	52291	CG15877	40031
CG15019	28438	CG15191	16751	CG1542	39976	CG15651	37206	CG15879	38899
CG1502	14894	CG15191	48720	CG15427	3064	CG15653	8827	CG15879	46754
CG15021	52038	CG1520	13757	CG15427	27046	CG15655	6586	CG15881	32390
CG15027	24627	CG15208	19368	CG15429	19462	CG15661	16904	CG15890	11538
CG1503	32349	CG15211	35704	CG1543	51667	CG15663	15445	CG15897	41618
CG15035	32352	CG15216	32541	CG15432	19466	CG15666	40013	CG15898	33897
CG15037	37789	CG15218	36216	CG15432	49216	CG15667	19150	CG15898	41114
CG1506	33217	CG1522	5551	CG15433	19470	CG15669	19536	CG15902	8577
CG15069	44611	CG15220	15380	CG15434	29236	CG15671	2938	CG15907	40762
CG1507	12765	CG15224	32378	CG15438	7303	CG15676	20121	CG15908	19623
CG1507	48249	CG1523	25199	CG15439	19490	CG1569	19152	CG1591	38908
CG15072	39866	CG15237	47255	CG15440	19494	CG15693	32383	CG15910	38910
CG15077	18524	CG1524	39870	CG15441	29123	CG15694	40018	CG15912	32654
CG15078	10061	CG15253	30729	CG15442	49184	CG15696	16979	CG15914	41571
CG15081	32361	CG15254	15604	CG15442	49184	CG15697	32511	CG15916	19627
CG15087	32527	CG15255	12412	CG15444	8880	CG15701	19541	CG15923	37373
CG15093	5655	CG15257	3837	CG15445	29158	CG15706	4907	CG15925	8982
CG15094	5002	CG15261	24964	CG15448	30894	CG1571	51846	CG15929	26830
CG15096	39463	CG15262	25100	CG15450	8645	CG15715	28563	CG1594	40037
CG15097	25188	CG15266	51827	CG15455	30539	CG15723	28566	CG1597	37383
CG15099	20126	CG15270	3829	CG15456	23106	CG1573	22915	CG1598	32391
CG15100	25193	CG1528	25101	CG15467	41584	CG15730	19582	CG1599	13317
CG15101	13749	CG15283	28550	CG15468	25116	CG15735	33813	CG1607	13793
CG15102	30909	CG15287	19379	CG15471	19504	CG15736	23926	CG1609	32664
CG15104	10642	CG15288	3141	CG1548	31012	CG15737	19584	CG1615	40953
CG15105	19290	CG15297	29623	CG15481	32612	CG15738	47929	CG1616	44484
CG15106	5008	CG15298	38884	CG15483	30763	CG15739	14890	CG1617	23822
CG1511	4771	CG15299	43501	CG15498	19508	CG15743	42685	CG1618	46483
CG1511	6545	CG1530	45166	CG15507	19512	CG15744	1095	CG1620	12682
CG1511	27236	CG15300	25140	CG15509	6212	CG15744	4801	CG1622	38915
CG15110	37185	CG15304	11317	CG15523	47481	CG15749	16744	CG1624	41623
CG15111	37189	CG15304	47846	CG15524	25072	CG1575	19153	CG1625	32668
CG15112	43056	CG15305	29622	CG15525	39993	CG15751	19594	CG1627	14900
CG15113	9558	CG15309	19388	CG15525	48660	CG15752	43686	CG1628	47475
CG15113	46485	CG1531	22901	CG15526	19518	CG15759	41597	CG1630	19159
CG15116	30877	CG15318	32382	CG15527	39323	CG15762	29871	CG1634	6688
CG15117	47527	CG15319	3787	CG15528	14865	CG1577	23356	CG1634	27202
CG15118	16854	CG1532	19398	CG15529	14867	CG15771	43689	CG1635	32672
CG1512	19298	CG15329	32564	CG15529	50227	CG15772	46284	CG1637	12932
CG15120	32374	CG15331	39285	CG1553	52179	CG15775	28570	CG1638	32676
CG15120	46222	CG1534	43097	CG15532	39877	CG15775	39358	CG1638	46275
CG1513	39148	CG15340	39973	CG15533	42520	CG15776	19611	CG1639	23825
CG1513	48600	CG15341	43660	CG15534	30186	CG15776	47248	CG1640	32680
CG15130	43491	CG15342	19428	CG15535	26825	CG1578	41599	CG1646	32682
CG15133	8059	CG15343	29569	CG15547	32621	CG15792	7819	CG1650	12568
CG15134	19305	CG15358	13372	CG1555	11322	CG15793	40025	CG1652	38104
CG1514	5467	CG1536	32579	CG15551	10263	CG15797	41603	CG1656	35555
CG15141	19307	CG15362	38282	CG15552	45961	CG15803	43635	CG1657	19649
CG15142	19309	CG15365	47648	CG15556	1791	CG15804	48153	CG1658	19066
CG15143	25195	CG15368	32583	CG15561	41582	CG15804	48544	CG1658	19066
CG15144	19315	CG15372	13184	CG1560	29619	CG15811	19696	CG1658	19066
CG15145	19316	CG15373	19439	CG15602	40001	CG15814	30429	CG1659	19653
CG15147	19320	CG15378	22908	CG15609	43406	CG15816	19616	CG1660	28801
CG15148	19323	CG15385	51859	CG15610	25074	CG15817	41605	CG1662	12197
CG1515	19329	CG15387	35759	CG15618	40006	CG15818	15537	CG1662	50409

CG1664	32690	CG1688	30269	CG17035	44443	CG17221	25229	CG1743	32929
CG1665	9958	CG16882	52426	CG17036	2869	CG17223	2608	CG17437	38925
CG1666	32693	CG16884	51363	CG1704	32451	CG17224	41177	CG17440	20445
CG1666	50144	CG16885	48049	CG17043	8777	CG17227	13330	CG17441	13444
CG1667	4031	CG16886	38026	CG17048	8780	CG17230	20409	CG17446	20453
CG1669	52246	CG16889	32766	CG17051	25209	CG17233	25231	CG17446	47221
CG16700	6145	CG16890	40044	CG17054	40047	CG1724	30315	CG17450	50795
CG16705	30972	CG16892	23844	CG17059	23535	CG17245	8383	CG17461	43639
CG16708	43413	CG16894	10067	CG17060	28758	CG17245	27220	CG17462	19801
CG1671	32697	CG16896	20316	CG17060	46791	CG17245	46687	CG1747	32932
CG16716	40042	CG16899	15732	CG17064	32841	CG17248	44011	CG1748	32933
CG16717	29199	CG16901	32395	CG17065	32845	CG17248	49202	CG1749	32937
CG16718	37472	CG16902	37067	CG17068	32850	CG17249	19170	CG17492	40078
CG16719	39934	CG16903	37572	CG1707	26832	CG1725	41136	CG17494	8199
CG16721	25201	CG16905	12130	CG17075	2487	CG17251	48024	CG17498	25264
CG16725	45447	CG16905	48663	CG17077	7170	CG17252	20410	CG17498	47918
CG1673	25204	CG16908	32767	CG17081	14194	CG17255	48633	CG17508	1487
CG16732	1148	CG1691	20321	CG17083	39937	CG17256	40052	CG17509	36527
CG16733	47020	CG16910	7723	CG1709	22925	CG17257	2611	CG1751	51149
CG16738	15749	CG16912	20327	CG17090	32855	CG17258	44372	CG17514	47269
CG16740	7210	CG1692	20329	CG17097	41244	CG17262	2614	CG17521	19084
CG16742	23832	CG16928	30476	CG17098	46309	CG17265	36479	CG17523	32945
CG16749	7555	CG1693	43841	CG1710	46998	CG17266	25243	CG17525	20472
CG16749	46390	CG16932	19165	CG17100	42821	CG17268	40056	CG1753	32946
CG1675	32712	CG16933	35558	CG17109	32858	CG17268	46876	CG1754	8651
CG16751	19069	CG16938	20334	CG17109	50820	CG17272	32874	CG17540	32948
CG16756	45655	CG16940	51853	CG17117	12764	CG1728	28805	CG17544	47934
CG16757	19658	CG16941	20338	CG17118	37624	CG17280	12965	CG17556	20483
CG16758	32714	CG16944	11968	CG17119	51127	CG17284	2558	CG17556	49518
CG1676	32719	CG16944	48582	CG17121	49341	CG17286	36623	CG17559	6547
CG16764	26976	CG1695	20340	CG17122	25212	CG17287	49415	CG17559	8002
CG16766	51387	CG1695	48062	CG17124	19078	CG17291	49672	CG17559	27057
CG1677	50195	CG16952	19166	CG17134	18110	CG17293	25246	CG1756	37517
CG16771	6386	CG16954	19167	CG17136	21083	CG17294	39105	CG17560	52002
CG16779	40824	CG1696	12939	CG17137	39107	CG17301	25252	CG17562	37365
CG16781	7018	CG16965	32782	CG17141	50241	CG17302	32875	CG17564	47273
CG16783	32724	CG1697	44414	CG17143	46676	CG17309	32877	CG17565	32951
CG16784	48045	CG16975	52247	CG17146	25214	CG1732	13359	CG17566	25271
CG16785	30214	CG16979	51594	CG17149	25218	CG17320	49013	CG17569	41657
CG16787	19661	CG16982	32399	CG1715	52253	CG17324	6379	CG17574	45729
CG16787	48685	CG16983	32790	CG17150	35624	CG17326	32878	CG17577	4664
CG16788	51851	CG16983	46605	CG17158	45668	CG17327	41654	CG1759	3361
CG16789	32729	CG16985	32401	CG1716	30707	CG17329	19171	CG1759	49563
CG16790	19160	CG16986	39129	CG17161	12680	CG17331	19079	CG17592	30452
CG16799	35709	CG16987	13418	CG17166	20388	CG17332	19173	CG17593	13029
CG16801	37617	CG16988	32798	CG17168	41625	CG17335	46117	CG17595	29228
CG16804	16806	CG16989	32802	CG17170	32868	CG17336	37408	CG17596	5702
CG16807	23843	CG16995	23078	CG17173	8370	CG17342	32885	CG17597	25276
CG1681	43041	CG17002	39883	CG1718	44449	CG17348	3047	CG17597	49204
CG16812	14972	CG17003	32804	CG17180	29141	CG17348	27053	CG17598	32956
CG16817	15309	CG17004	11471	CG17181	20396	CG17349	32887	CG17599	14682
CG16827	37172	CG17018	32810	CG17183	32459	CG17358	12654	CG1760	32961
CG1683	45174	CG17019	48749	CG17184	20401	CG1736	32889	CG17603	41099
CG16833	32741	CG1702	48635	CG17187	40051	CG17360	40070	CG17604	32962
CG16837	32749	CG17024	50187	CG17195	1435	CG17367	32892	CG17608	51162
CG16838	32754	CG17026	32813	CG17196	6743	CG17369	46553	CG17610	3121
CG16840	20305	CG17026	49199	CG17197	1433	CG17370	1438	CG17610	4331
CG16857	4806	CG17027	32817	CG17198	1432	CG17378	47367	CG17610	36251
CG16857	24479	CG17027	50076	CG17200	6024	CG1738	32464	CG17617	32965
CG16857	36224	CG17028	32819	CG17202	41628	CG17386	5701	CG17618	32403
CG16858	16986	CG17029	32822	CG17203	45360	CG17387	32902	CG1762	893
CG16863	20312	CG17029	49565	CG17204	32872	CG1739	32904	CG1762	40895
CG16865	19162	CG1703	32826	CG17204	32872	CG17396	10833	CG1762	42234
CG16868	8209	CG17030	32827	CG17207	46640	CG1740	24968	CG17633	47634
CG16873	15758	CG17031	32829	CG17209	30512	CG1740	49848	CG17636	8675
CG16874	13247	CG17033	32830	CG1721	52336	CG17419	40076	CG1764	20507
CG16879	32759	CG17034	8136	CG17219	41635	CG1742	44445	CG17642	30719

CG17642	51611	CG17919	38204	CG18174	19272	CG18437	1310	CG1868	25379
CG17645	41658	CG17919	46473	CG18176	20604	CG1844	23268	CG1869	42877
CG1765	37059	CG17921	12773	CG18177	40844	CG18445	4039	CG1871	39287
CG17657	40088	CG17922	6599	CG18182	40134	CG1845	30436	CG1873	40156
CG17660	2684	CG17923	3976	CG18208	10215	CG1846	41672	CG1873	52343
CG17664	49979	CG17927	7164	CG1821	24977	CG18466	5705	CG18730	30745
CG17665	46744	CG1793	51476	CG18214	40138	CG18467	47282	CG18730	50098
CG17669	36538	CG17934	19093	CG18217	41665	CG1847	43701	CG18732	35641
CG1768	20518	CG17935	23556	CG1824	5554	CG18472	40148	CG18734	1020
CG17680	45211	CG17941	4312	CG18241	47967	CG18473	25341	CG18735	30914
CG17681	40972	CG17941	36219	CG18247	25304	CG1848	25343	CG1874	41680
CG17683	19180	CG17945	23558	CG18251	40143	CG18480	1072	CG18740	6969
CG17691	40686	CG17945	42407	CG18258	20621	CG18480	3821	CG18741	3391
CG17697	43077	CG17946	23560	CG18259	50094	CG1849	3025	CG18745	20686
CG1770	20522	CG17947	19182	CG1826	33049	CG18493	18930	CG18746	33399
CG1771	5671	CG17949	33025	CG1827	46039	CG18495	43705	CG18747	41252
CG17712	32987	CG17949	50797	CG18278	22936	CG18495	49680	CG18766	20694
CG17716	6561	CG1795	37738	CG18278	50084	CG18497	20637	CG18767	38251
CG17716	42237	CG17950	19026	CG1828	10916	CG18497	48846	CG18769	9501
CG17723	7461	CG17952	39468	CG18281	8438	CG18497	49543	CG1877	42445
CG17725	20529	CG1796	44862	CG18281	50086	CG18505	28285	CG18780	52484
CG17725	50252	CG17960	33029	CG18284	31030	CG18508	52071	CG18787	20697
CG17726	32991	CG17964	3014	CG18284	49221	CG1851	33133	CG18787	49686
CG17734	13791	CG17970	16988	CG18287	36660	CG18516	46403	CG18789	20699
CG17734	49497	CG17973	20571	CG18296	18866	CG1852	8309	CG18789	49689
CG17735	50189	CG17985	7355	CG1830	33054	CG18528	40149	CG18799	5528
CG17737	29215	CG1799	40116	CG18301	31023	CG18530	6109	CG18801	37110
CG17739	36542	CG17991	1277	CG18313	44735	CG18530	47205	CG18802	5838
CG1774	16622	CG17998	1835	CG18313	49211	CG18549	6098	CG18803	43082
CG17743	39529	CG1800	40118	CG18315	19101	CG1855	40150	CG18809	20702
CG17746	40102	CG18000	48333	CG18315	48613	CG18558	33366	CG18810	40825
CG1775	19689	CG18005	25290	CG18317	44203	CG1856	10855	CG18811	14011
CG17753	20536	CG18009	10443	CG18319	9413	CG18572	33375	CG18812	39224
CG17754	47274	CG18012	20580	CG18324	33234	CG18578	8573	CG18814	5283
CG17757	35772	CG18013	33041	CG18331	48500	CG18582	46044	CG18815	33414
CG17759	19088	CG18024	41080	CG18332	12821	CG18585	19917	CG18818	20705
CG17759	51116	CG18026	25291	CG18335	52470	CG18591	23569	CG1882	41406
CG17765	32405	CG1803	39945	CG18339	25317	CG18594	20650	CG18820	20706
CG17766	14531	CG18039	40929	CG18340	33128	CG18596	41675	CG18826	13336
CG17768	49674	CG18041	46031	CG18341	52475	CG18599	25363	CG18827	9894
CG17769	20544	CG18048	19184	CG18345	35571	CG18600	32470	CG18828	23572
CG17779	45670	CG18065	15361	CG18347	6076	CG18605	33377	CG18829	33415
CG17785	1181	CG18065	49677	CG1836	30498	CG18609	4994	CG1883	20711
CG17800	3115	CG18069	47280	CG18362	52606	CG1861	14872	CG18831	13007
CG17800	36233	CG18085	49924	CG1837	15660	CG18619	19110	CG18833	39189
CG17809	39572	CG1809	43231	CG18371	19193	CG18620	40811	CG18833	39352
CG17818	19089	CG18096	30873	CG18374	52478	CG18624	29883	CG18834	14590
CG17821	4997	CG18102	3798	CG18375	25332	CG18624	33893	CG18838	12187
CG17828	39887	CG18104	14933	CG18378	25333	CG18627	33386	CG1884	12571
CG17829	41659	CG18104	47186	CG1838	33132	CG18630	25366	CG18842	6932
CG1783	33007	CG18110	1349	CG18380	20634	CG18631	47215	CG18843	24340
CG17835	49950	CG18112	43415	CG18381	25335	CG18635	8993	CG18844	28816
CG17838	33012	CG1812	15491	CG18389	13075	CG1864	2971	CG18844	39335
CG17840	45037	CG18128	40127	CG1839	15476	CG18642	7266	CG18845	14934
CG17841	5530	CG18130	20599	CG18398	43647	CG18647	9409	CG18846	29892
CG1785	52467	CG18136	13128	CG18402	991	CG18654	38239	CG18848	45684
CG17856	33016	CG1814	19096	CG18405	4743	CG18656	14038	CG18849	42391
CG1787	5503	CG18144	23306	CG18405	36147	CG1866	20670	CG18851	20721
CG17870	48724	CG18146	3120	CG18408	19054	CG18660	51459	CG18853	50099
CG17888	37769	CG18146	3705	CG18412	50024	CG18662	26833	CG18858	50800
CG1789	20567	CG18146	36261	CG18412	50027	CG18667	25371	CG1886	8315
CG17894	37673	CG1815	40132	CG18414	10679	CG18668	20673	CG1890	39894
CG17896	5580	CG18155	42446	CG18418	9008	CG18671	33394	CG1891	42456
CG17903	33019	CG1817	1101	CG18419	42776	CG18675	33397	CG1891	46350
CG17904	41660	CG1817	8010	CG18428	35638	CG18678	23225	CG1893	20729
CG17907	3968	CG18171	25299	CG18432	25336	CG18679	3128	CG1894	41574
CG17912	40107	CG18173	4092	CG18436	16523	CG18679	36153	CG1897	7791

CG1898	33420	CG2019	10004	CG2158	20824	CG2380	14918	CG2781	48139
CG1900	29259	CG2022	9049	CG2160	33490	CG2381	24989	CG2789	2507
CG1903	28341	CG2025	25392	CG2161	20826	CG2397	4019	CG2790	20903
CG1905	48768	CG2028	13664	CG2162	33493	CG2412	1494	CG2791	42622
CG1906	32476	CG2031	20783	CG2163	33499	CG2453	20872	CG2803	25160
CG1907	1341	CG2033	19198	CG2165	30203	CG2471	39140	CG2807	25161
CG1909	20745	CG2033	50635	CG2168	43627	CG2478	12482	CG2812	52485
CG1911	33423	CG2034	20786	CG2168	50311	CG2488	10461	CG2816	29700
CG1912	43711	CG2038	40690	CG2173	36516	CG2493	3929	CG2818	25441
CG1913	33427	CG2048	9241	CG2174	37530	CG2503	20876	CG2826	46588
CG1913	52346	CG2051	33459	CG2177	51084	CG2505	20879	CG2827	25444
CG1915	47301	CG2052	20790	CG2179	20829	CG2508	52280	CG2829	20905
CG1916	38079	CG2053	13546	CG2182	20834	CG2520	12732	CG2830	29339
CG1919	15265	CG2060	9953	CG2183	13762	CG2522	14877	CG2835	24959
CG1921	6948	CG2060	49044	CG2184	51201	CG2525	15880	CG2839	17952
CG1922	10663	CG2061	44186	CG2185	29477	CG2528	33532	CG2843	38933
CG1924	42397	CG2062	4018	CG2187	7575	CG2534	7769	CG2843	52326
CG1924	52348	CG2063	33462	CG2189	7782	CG2540	33536	CG2845	20909
CG1925	24472	CG2064	8728	CG2189	50110	CG2543	25417	CG2848	33571
CG1935	52670	CG2065	19119	CG2194	19279	CG2551	29635	CG2849	43623
CG1937	6870	CG2069	43382	CG2198	22944	CG2574	40173	CG2852	15069
CG1938	41686	CG2070	20793	CG2201	33502	CG2578	32482	CG2854	41703
CG1939	44765	CG2072	43714	CG2204	19124	CG2595	43717	CG2855	16820
CG1941	3998	CG2075	13673	CG2205	43630	CG2608	20886	CG2856	10970
CG1942	7942	CG2076	5537	CG2210	33198	CG2614	32407	CG2857	7417
CG1942	48583	CG2076	50221	CG2212	5469	CG2615	49365	CG2859	15334
CG1945	2955	CG2078	25402	CG2216	12925	CG2616	11052	CG2861	20918
CG1945	30679	CG2079	20796	CG2216	49537	CG2617	3931	CG2863	33573
CG1946	33428	CG2083	20798	CG2218	32517	CG2621	7005	CG2864	23962
CG1946	48259	CG2086	4830	CG2219	41690	CG2637	22348	CG2867	20926
CG1951	33430	CG2086	27084	CG2221	1054	CG2641	25422	CG2872	3399
CG1954	33434	CG2087	16427	CG2221	27247	CG2647	5709	CG2872	39221
CG1956	33437	CG2091	20799	CG2221	39505	CG2655	30564	CG2872	48496
CG1957	29575	CG2092	33465	CG2222	20849	CG2656	25423	CG2875	33575
CG1960	28342	CG2093	29971	CG2224	20852	CG2662	33544	CG2881	33577
CG1961	40161	CG2095	45032	CG2239	43044	CG2666	42611	CG2883	14646
CG1962	33444	CG2096	2964	CG2241	25412	CG2669	47309	CG2887	33581
CG1963	19117	CG2097	33469	CG2241	49245	CG2670	11499	CG2890	25446
CG1963	48872	CG2098	20804	CG2244	20855	CG2671	51249	CG2892	14868
CG1964	28347	CG2099	39895	CG2245	25415	CG2674	7167	CG2899	45041
CG1965	43944	CG2100	38037	CG2246	24987	CG2675	10149	CG2901	12209
CG1966	33446	CG2101	33473	CG2246	48877	CG2677	25427	CG2902	37333
CG1967	12196	CG2102	2929	CG2248	49247	CG2679	37435	CG2903	20933
CG1968	20767	CG2103	33264	CG2249	40977	CG2681	33549	CG2905	52486
CG1970	38224	CG2104	30016	CG2252	51305	CG2682	44783	CG2906	25449
CG1972	33450	CG2105	39535	CG2253	33507	CG2684	13308	CG2910	20942
CG1973	19275	CG2108	13145	CG2254	5470	CG2685	20887	CG2911	25452
CG1975	20771	CG2109	45000	CG2256	40170	CG2694	33551	CG2913	7028
CG1977	25387	CG2112	25405	CG2257	33510	CG2699	33556	CG2914	51225
CG1981	13657	CG2118	25406	CG2259	33512	CG2701	25433	CG2916	25456
CG1982	3761	CG2121	3386	CG2260	25154	CG2702	33557	CG2917	13613
CG1982	47191	CG2124	14869	CG2262	14609	CG2708	33561	CG2918	18440
CG1983	24980	CG2125	51479	CG2263	33514	CG2713	5587	CG2919	25457
CG1986	51669	CG2126	47598	CG2272	33516	CG2714	6308	CG2921	33585
CG1989	39898	CG2128	20814	CG2275	10835	CG2715	32413	CG2922	25166
CG1989	46977	CG2128	50213	CG2277	20869	CG2716	8307	CG2925	20943
CG1994	13479	CG2135	16625	CG2286	52049	CG2718	40174	CG2926	33589
CG1998	37395	CG2136	33486	CG2292	51933	CG2720	41696	CG2929	25458
CG2005	6705	CG2137	41235	CG2304	4448	CG2727	12232	CG2930	7031
CG2005	8009	CG2140	43065	CG2309	33522	CG2747	33566	CG2931	20946
CG2005	27208	CG2143	20819	CG2316	12170	CG2759	30033	CG2934	20950
CG2009	48037	CG2144	3996	CG2321	33523	CG2762	5712	CG2937	30087
CG2013	23229	CG2145	14874	CG2328	9285	CG2765	43721	CG2938	7035
CG2013	46927	CG2146	44292	CG2330	46555	CG2766	28819	CG2939	37658
CG2014	40165	CG2151	47307	CG2331	24354	CG2766	33888	CG2943	8477
CG2014	50731	CG2152	19121	CG2358	9055	CG2772	15577	CG2944	8688
CG2017	20780	CG2155	3349	CG2371	15483	CG2779	24992	CG2945	19280

CG2947	43725	CG30084	36564	CG30338	29188	CG3061	5868	CG31126	23395
CG2948	33593	CG30085	33672	CG30342	21136	CG3064	6972	CG31126	49277
CG2956	37091	CG3009	12216	CG30345	42868	CG3069	15872	CG31132	40209
CG2957	25462	CG30093	17893	CG30346	45429	CG3071	29589	CG31133	33774
CG2958	45294	CG30097	8977	CG30349	39959	CG3073	25627	CG31136	33112
CG2960	25466	CG30100	43236	CG3035	21139	CG3074	6617	CG31137	13365
CG2962	5526	CG30100	48945	CG30354	23575	CG3075	41034	CG31138	29541
CG2962	50422	CG30101	15514	CG30359	43151	CG3077	25631	CG3114	4559
CG2964	42293	CG30102	33677	CG3036	42755	CG3078	51390	CG31140	38936
CG2969	42751	CG30103	4949	CG30360	47951	CG3083	25020	CG31141	29537
CG2970	43497	CG30104	10050	CG30368	13913	CG3085	43421	CG31145	25036
CG2970	48124	CG30105	19204	CG30372	19287	CG3086	3170	CG31146	42616
CG2971	14637	CG30106	1678	CG30373	4013	CG3090	10856	CG31148	14698
CG2972	48771	CG30109	50925	CG30378	21153	CG3093	33733	CG31151	51341
CG2974	32484	CG3011	19208	CG30382	21156	CG3095	14524	CG31152	14480
CG2975	2601	CG30112	42444	CG30387	3468	CG3099	25636	CG31155	39134
CG2976	20962	CG30113	41562	CG30387	48313	CG3100	14526	CG31156	44478
CG2980	25470	CG30115	39952	CG30388	41735	CG31000	33735	CG31158	42321
CG2984	33599	CG30123	25571	CG30389	19002	CG31002	22960	CG31159	46144
CG2986	28822	CG30124	4998	CG30390	41740	CG31002	48225	CG31163	25701
CG2987	7182	CG30131	52556	CG30392	12862	CG31004	40940	CG31168	43222
CG2988	9419	CG30144	39920	CG30394	3470	CG31007	33739	CG31169	25706
CG2988	48649	CG30147	25580	CG30398	21166	CG31008	19227	CG31170	25707
CG2989	46286	CG30149	21109	CG3040	19219	CG31009	3733	CG31175	19230
CG2990	30507	CG30152	38848	CG30401	2725	CG31009	3739	CG31183	861
CG2991	2604	CG3016	7090	CG30404	29385	CG31009	27211	CG31183	4773
CG2993	33605	CG30163	39687	CG3041	47602	CG31009	27216	CG31183	36323
CG2994	8176	CG30164	3633	CG30410	40176	CG3101	21275	CG31187	43739
CG2995	25473	CG30165	19709	CG30418	38152	CG31012	38854	CG31188	15364
CG2996	14613	CG3017	21110	CG3042	25620	CG31014	30975	CG31189	22962
CG2998	35783	CG30170	25590	CG30420	7414	CG31015	41351	CG31192	42318
CG2998	42419	CG30171	29412	CG30421	33726	CG3102	33744	CG31194	45433
CG2999	33609	CG30173	35794	CG30423	10600	CG31022	2464	CG31196	15884
CG3000	25553	CG30174	45060	CG30426	21173	CG31027	25644	CG31201	49547
CG30000	41965	CG30175	24378	CG30427	7423	CG31033	25651	CG31202	43522
CG30005	25555	CG30176	25593	CG30429	21175	CG31038	25655	CG3121	25712
CG3001	21054	CG30178	21111	CG30438	37106	CG3104	21289	CG31211	33787
CG30010	33660	CG30179	26836	CG30440	21178	CG31040	39926	CG31212	40214
CG30010	48606	CG3018	33684	CG30441	50583	CG31042	9704	CG31223	43426
CG30011	43070	CG30183	25594	CG3045	25621	CG31046	9701	CG31229	9660
CG30012	21057	CG3019	25597	CG30460	40624	CG31048	21293	CG31232	13090
CG30013	41415	CG30193	39474	CG30462	10046	CG31049	21294	CG31234	30389
CG30014	25557	CG30194	3527	CG30463	4923	CG3105	25662	CG31237	23308
CG30016	40488	CG30194	50234	CG30467	21203	CG31050	23934	CG31240	10424
CG30019	32429	CG30197	9586	CG3047	21206	CG31050	48824	CG31241	29503
CG3002	3269	CG30203	33913	CG30476	23495	CG31053	33750	CG31243	14385
CG30021	29965	CG3021	25603	CG3048	21214	CG31057	25023	CG31249	43740
CG30022	30880	CG3022	50176	CG30481	13320	CG31063	45246	CG31251	25739
CG30035	8126	CG3024	30985	CG30483	21216	CG31064	33756	CG31256	40218
CG30035	52360	CG30259	19211	CG30489	21235	CG31069	25026	CG31259	46362
CG30038	21068	CG3026	33688	CG30489	49271	CG3107	40196	CG3126	21306
CG3004	46557	CG30268	42703	CG30491	12817	CG31072	1251	CG3127	33797
CG30043	11708	CG3027	25610	CG30493	43131	CG31075	25676	CG31274	40222
CG30046	13947	CG30271	32436	CG30495	21241	CG31076	28776	CG31278	38938
CG30047	4623	CG30271	50158	CG30496	21244	CG3108	25680	CG31285	33799
CG30048	4634	CG30275	25612	CG30497	41745	CG31089	12449	CG31289	39091
CG30051	43066	CG3028	25615	CG30498	13457	CG3109	14529	CG3129	40228
CG30051	49256	CG30280	34743	CG30499	25016	CG31091	33085	CG31290	38860
CG30059	13010	CG30284	21118	CG30502	21253	CG31092	25684	CG31291	21308
CG30059	50732	CG3029	25014	CG30503	9036	CG31095	14756	CG31293	21312
CG3006	38148	CG30290	41564	CG3051	1827	CG31106	3415	CG31299	45442
CG30062	15433	CG30290	49962	CG3052	13724	CG31110	25030	CG3130	40229
CG30063	48780	CG30291	21120	CG3054	13555	CG31111	40198	CG31301	40232
CG30075	25563	CG30295	47790	CG3057	47965	CG31115	25693	CG31302	40235
CG30077	25568	CG30327	33705	CG3058	21258	CG31120	3402	CG31304	45035
CG30078	30610	CG3033	7086	CG3059	7265	CG31122	40207	CG31306	40236
CG3008	43731	CG30336	21134	CG3060	2993	CG31123	25034	CG3131	2593

CG31311	23079	CG31548	13144	CG31703	32493	CG31851	3754	CG32031	34036
CG31314	44406	CG31550	25779	CG31704	8900	CG31852	25179	CG32039	38867
CG31317	21317	CG31551	40278	CG31704	39450	CG31855	34295	CG3204	45230
CG31318	21985	CG3156	12182	CG31708	38261	CG31858	3367	CG32041	43632
CG31319	40238	CG3157	19130	CG3171	7219	CG3186	25129	CG32045	40308
CG3132	16779	CG3157	47163	CG31711	25814	CG31860	7688	CG32048	19251
CG31320	25742	CG3158	21374	CG31712	21402	CG31864	28079	CG32048	50237
CG31321	44942	CG3160	7070	CG31713	39150	CG31864	50051	CG32049	40312
CG31325	45139	CG31601	21378	CG31715	21505	CG31865	25897	CG32051	21435
CG31332	16813	CG31605	2789	CG31716	10850	CG31865	50589	CG32052	21437
CG31332	49701	CG31605	43306	CG31717	7662	CG31866	25899	CG32062	34046
CG31342	51330	CG3161	44487	CG31719	41758	CG3187	40295	CG32063	15207
CG31345	24656	CG3161	44487	CG3172	25817	CG31871	51241	CG32064	34051
CG31346	45943	CG3161	49291	CG31721	21405	CG31872	31028	CG32066	44825
CG31349	38863	CG3161	49291	CG31725	7836	CG31873	36375	CG32067	13066
CG3135	14803	CG31613	33972	CG31726	25823	CG31874	41766	CG32068	23412
CG31352	25750	CG31617	33975	CG31729	7697	CG31884	36297	CG32069	9202
CG31352	49112	CG31618	25782	CG3173	25825	CG3189	34017	CG32072	9206
CG31357	40248	CG31619	33102	CG31730	21407	CG31908	51924	CG32075	19255
CG3136	36504	CG3162	21380	CG31731	11082	CG31911	7618	CG32076	52402
CG31363	25044	CG31623	21383	CG31738	998	CG31913	3376	CG3208	41779
CG31367	37625	CG31624	33976	CG31738	29906	CG31915	37944	CG32082	21438
CG31373	21726	CG31624	50803	CG31739	21410	CG31916	25906	CG32082	50019
CG31381	14720	CG31628	46295	CG3174	42829	CG31917	25909	CG32085	34053
CG31385	3704	CG31629	37935	CG31740	33850	CG31919	52494	CG32086	19261
CG31385	8394	CG31632	21386	CG31741	7930	CG3192	30413	CG32087	8345
CG31385	27178	CG31634	2650	CG31743	7538	CG31922	36386	CG32087	47238
CG3139	8875	CG31634	2650	CG31746	35727	CG31924	36469	CG32089	8340
CG31390	11504	CG31635	33980	CG31751	21414	CG31928	12276	CG3209	10281
CG31391	33801	CG31637	7614	CG31756	25833	CG3193	25919	CG32090	7495
CG31391	49286	CG31638	33981	CG31758	23522	CG31935	25922	CG32092	41785
CG3140	25046	CG31639	32443	CG31759	47321	CG31937	3449	CG32094	21442
CG31408	41420	CG31639	48790	CG31760	7686	CG31938	40306	CG32095	13833
CG3141	7074	CG31640	3498	CG31761	46014	CG3194	7333	CG32099	43650
CG31414	21336	CG31641	32370	CG31762	41568	CG3195	32450	CG3210	44156
CG31421	25760	CG31648	44225	CG31762	48237	CG31950	34751	CG32101	41786
CG31426	21340	CG31649	50192	CG3178	19819	CG31953	49301	CG32103	29439
CG3143	30556	CG3165	25785	CG31783	3875	CG31954	13028	CG32104	41790
CG31445	51642	CG31650	30690	CG31784	39192	CG31956	7284	CG32105	51269
CG31447	25761	CG31651	2629	CG31787	6372	CG31956	46910	CG32108	21454
CG31447	50997	CG31652	33993	CG31790	46057	CG31957	25926	CG32110	34062
CG31450	26319	CG31653	25786	CG31792	50152	CG31960	50102	CG32113	41792
CG31452	3744	CG31654	15565	CG31793	8069	CG31961	29359	CG32120	11690
CG31452	27194	CG31655	45883	CG31794	25853	CG31964	25929	CG32130	34408
CG31453	21350	CG31657	25787	CG31795	7560	CG31965	44154	CG32131	23279
CG31454	5811	CG31659	23310	CG3180	45959	CG31967	25933	CG32133	13061
CG31460	33323	CG31660	7852	CG31800	28162	CG31968	25934	CG32134	949
CG31467	40268	CG31663	2533	CG31802	18562	CG31988	25939	CG32134	27108
CG31467	52637	CG31665	8021	CG31803	45277	CG31988	50935	CG32135	21665
CG31469	23396	CG3167	11149	CG31807	25863	CG31989	9402	CG32137	37872
CG31473	14059	CG31671	25793	CG31809	32521	CG31990	34752	CG32138	34412
CG31477	42108	CG31673	25797	CG31809	50643	CG31990	34752	CG32139	41098
CG31478	21358	CG31678	1473	CG3181	29354	CG31991	6367	CG3214	34079
CG31482	45931	CG31679	21392	CG31810	6757	CG31992	45773	CG32145	5263
CG3149	47560	CG3168	48010	CG31810	49296	CG31999	29155	CG32146	10299
CG31501	25773	CG31682	7257	CG31811	37521	CG3200	14125	CG32147	34419
CG3151	33939	CG31683	6400	CG31812	23403	CG32000	29174	CG32149	41861
CG31522	37329	CG31684	29130	CG31812	50487	CG32008	25945	CG3215	12723
CG31523	9807	CG31687	21393	CG3182	3606	CG3201	31160	CG32155	5279
CG31527	43255	CG31688	50139	CG31821	15496	CG32016	34755	CG32158	45641
CG31528	30811	CG31689	2584	CG31823	43145	CG32018	21610	CG3216	6115
CG3153	16652	CG3169	10818	CG31832	47633	CG32019	46253	CG3216	29915
CG31531	40276	CG31690	43813	CG31837	23407	CG32022	10105	CG32163	14259
CG31534	21366	CG31692	21396	CG3184	25880	CG32024	52031	CG32164	34423
CG31536	25049	CG31693	37131	CG31842	21429	CG32026	34032	CG32164	49304
CG31546	13140	CG31694	21398	CG31843	43198	CG3203	41778	CG32165	26112
CG31547	8551	CG31702	25807	CG31849	2876	CG32030	34034	CG32165	49307

CG32168	34429	CG32387	1003	CG3269	34766	CG33242	49760	CG3388	9277
CG32169	29799	CG32387	36287	CG32698	50316	CG33246	49762	CG3389	8408
CG32171	34081	CG32392	34537	CG3270	41196	CG3325	30490	CG3389	36164
CG32174	21468	CG32394	24736	CG32708	49325	CG33250	46450	CG33931	50510
CG32176	30015	CG3240	12677	CG3271	3983	CG3326	24746	CG33932	50690
CG32178	8413	CG32407	26131	CG32727	48271	CG33260	47820	CG33933	50694
CG32179	1038	CG32409	34543	CG3274	34581	CG3327	2620	CG3394	3621
CG32179	6119	CG3241	29356	CG32750	52403	CG33276	48363	CG3397	34604
CG32179	27110	CG32412	38277	CG32754	46509	CG33277	47828	CG3399	34278
CG32180	45900	CG32413	5043	CG32754	50591	CG33288	51189	CG3400	25959
CG32183	38208	CG32417	34547	CG32756	49853	CG33289	48289	CG3401	34607
CG3219	48576	CG32418	34549	CG32775	46421	CG3329	24749	CG3402	21483
CG32190	5319	CG32423	37863	CG32778	48869	CG33300	46768	CG3403	40442
CG32191	14294	CG32425	41142	CG32782	46425	CG3331	45689	CG3408	36306
CG3220	23511	CG32427	27252	CG32789	49744	CG3332	3451	CG3409	37141
CG32202	26325	CG32434	36625	CG3279	45726	CG3333	34597	CG3410	37836
CG32210	41865	CG32435	26051	CG32791	48926	CG3333	46279	CG3412	34273
CG32211	34452	CG32438	38969	CG32792	47047	CG33331	50209	CG3412	34274
CG32217	34458	CG32441	13134	CG3280	42556	CG3337	29169	CG3415	34613
CG3222	34459	CG32442	6481	CG3282	47599	CG3337	29170	CG3416	26183
CG32220	23280	CG32444	41899	CG32823	50763	CG3338	21678	CG3419	3626
CG32225	5383	CG32446	23058	CG32832	47810	CG3339	41917	CG3420	39052
CG32226	34464	CG32447	5417	CG3284	11219	CG3340	40873	CG3421	41934
CG32227	43928	CG32448	9120	CG32847	48422	CG3342	40324	CG3422	26187
CG3223	30003	CG32451	22975	CG32854	50338	CG3344	15212	CG3422	48735
CG32230	9804	CG32454	26141	CG3289	41913	CG33466	46260	CG3424	44536
CG32238	29424	CG32463	7254	CG3290	6622	CG33466	46260	CG3425	26190
CG3224	29561	CG32464	12781	CG3290	52378	CG33474	51188	CG3425	48882
CG32245	14017	CG32465	5783	CG3291	21677	CG33479	48461	CG3427	43445
CG3225	24725	CG32473	8281	CG3292	19989	CG33489	48465	CG3427	50372
CG32250	7491	CG32478	24740	CG3294	26110	CG3350	11259	CG3428	41938
CG32251	34477	CG32479	37859	CG3295	24709	CG33503	50506	CG3430	40444
CG32253	34479	CG3248	26055	CG3297	42485	CG33505	49525	CG3431	34618
CG3226	47034	CG32483	22977	CG32971	49456	CG3351	21480	CG3433	19045
CG32262	44923	CG32484	41905	CG3298	43751	CG3352	9396	CG3434	45130
CG32263	33272	CG32485	34565	CG3299	34585	CG3353	41920	CG3437	34221
CG32276	15911	CG32486	41908	CG33002	46440	CG3353	41921	CG3443	10133
CG32276	49568	CG32487	26154	CG3301	43225	CG33533	51100	CG3445	26196
CG3228	37079	CG32488	46571	CG33012	48408	CG33544	48807	CG3446	42696
CG32280	15908	CG3249	48005	CG3303	9916	CG3355	13037	CG3450	26871
CG32281	41873	CG32490	21477	CG3304	7280	CG33558	46456	CG3454	34620
CG3229	34498	CG32495	49719	CG3305	7308	CG3356	34601	CG3455	34624
CG32296	34502	CG32500	49724	CG33051	48793	CG3358	41819	CG3455	49574
CG32297	34506	CG3251	34574	CG33052	48410	CG3359	37889	CG3458	30627
CG32300	7442	CG32516	48377	CG33054	48413	CG3360	8287	CG3460	46165
CG3231	34515	CG3253	26159	CG33057	49458	CG3362	26171	CG3461	6975
CG32315	45459	CG32531	47915	CG3306	34588	CG3363	26176	CG3466	30218
CG32316	34087	CG3254	26162	CG3307	34589	CG33635	48813	CG3469	24759
CG32319	24728	CG32579	48384	CG3308	43756	CG33649	49765	CG3473	26201
CG32333	26118	CG3258	29041	CG3309	15415	CG3365	43763	CG3474	43956
CG32335	44172	CG32581	49727	CG33104	49750	CG33650	49769	CG3476	2734
CG3234	2886	CG32584	48387	CG3312	24742	CG33665	51606	CG3479	3010
CG32343	15741	CG3259	46163	CG3313	43758	CG33670	51016	CG3480	26205
CG32344	21675	CG3260	11521	CG3314	43760	CG33671	49772	CG3483	41939
CG32346	46645	CG32602	50435	CG3315	42858	CG33672	49774	CG3488	7534
CG32350	24732	CG32616	49729	CG33172	49462	CG33694	49776	CG3491	34631
CG32351	41881	CG3263	26328	CG33178	49464	CG33695	49777	CG3493	40450
CG32351	46784	CG3264	43250	CG33182	46444	CG33713	49611	CG3494	24760
CG32369	45129	CG3265	24451	CG3319	10442	CG33714	51020	CG3495	26208
CG32371	24735	CG32656	46776	CG33193	46445	CG33718	49781	CG3496	43768
CG32374	14107	CG32668	46666	CG33198	46214	CG33722	49646	CG3497	9925
CG32376	41885	CG32669	47916	CG3321	46764	CG3373	1278	CG3499	33256
CG3238	34533	CG3267	13259	CG33217	47818	CG3376	12226	CG3500	19703
CG32380	39482	CG32675	46667	CG3322	42559	CG33785	50678	CG3501	26025
CG32381	41835	CG32679	47158	CG33230	48803	CG33786	50682	CG3504	26211
CG32384	42302	CG3268	3988	CG33237	49758	CG3380	39469	CG3506	9271
CG32386	26126	CG32688	47804	CG3324	34595	CG3385	3618	CG3508	34632

CG3510	43771	CG3658	41084	CG3770	4064	CG3909	12758	CG4019	46880
CG3511	21733	CG3661	23416	CG3772	7238	CG3911	21738	CG4020	3290
CG3515	34636	CG3663	12879	CG3773	26281	CG3915	40484	CG4023	43781
CG3520	40455	CG3664	34096	CG3774	30238	CG3917	34731	CG4025	6924
CG3522	4053	CG3665	8392	CG3776	38269	CG3918	34734	CG4027	7139
CG3523	29349	CG3665	36351	CG3780	40471	CG3918	47144	CG4029	12610
CG3524	4290	CG3668	37637	CG3781	7113	CG3921	52608	CG4030	26368
CG3525	34286	CG3671	44000	CG3782	41949	CG3922	25964	CG4032	2897
CG3526	26214	CG3675	26057	CG3788	21715	CG3923	34737	CG4033	37581
CG3527	24762	CG3678	26267	CG3790	4667	CG3924	30454	CG4035	7800
CG3530	26216	CG3678	49792	CG3791	41954	CG3925	40486	CG4036	26370
CG3532	26221	CG3680	34675	CG3792	7862	CG3926	34738	CG4038	21775
CG3534	41276	CG3682	47027	CG3792	48233	CG3929	7795	CG4039	13661
CG3536	11816	CG3683	25961	CG3793	40475	CG3931	26309	CG4040	26372
CG3539	26223	CG3683	46799	CG3794	20117	CG3935	4542	CG4040	48694
CG3542	26227	CG3688	26269	CG3796	7756	CG3936	1112	CG4041	34780
CG3544	21684	CG3689	45280	CG3798	28365	CG3936	27228	CG4042	26377
CG3552	30952	CG3692	45939	CG3799	41960	CG3938	47941	CG4043	21776
CG3560	34090	CG3694	26872	CG3803	3596	CG3939	21513	CG4045	34784
CG3561	43773	CG3695	28361	CG3806	34711	CG3940	13806	CG4046	21516
CG3564	7039	CG3696	10762	CG3808	34713	CG3943	21745	CG4049	6981
CG3570	48219	CG3696	46685	CG3809	43780	CG3944	21749	CG4050	33248
CG3571	43778	CG3697	12670	CG3810	6922	CG3947	40886	CG4051	21779
CG3572	21686	CG3699	5667	CG3811	22984	CG3948	34768	CG4057	21780
CG3573	34649	CG3702	7296	CG3812	44418	CG3949	21755	CG4058	16668
CG3587	37902	CG3703	34679	CG3814	4671	CG3953	16416	CG4059	2959
CG3589	38154	CG3704	34684	CG3817	21716	CG3954	21756	CG4061	40498
CG3590	6343	CG3705	23179	CG3820	41964	CG3956	6232	CG4062	21782
CG3593	21688	CG3707	34686	CG3821	7750	CG3956	50003	CG4063	40862
CG3595	7916	CG3708	26272	CG3822	40985	CG3959	34770	CG4064	26382
CG3597	21693	CG3709	34687	CG3825	15238	CG3960	34098	CG4065	3614
CG3599	16665	CG3710	22979	CG3830	16896	CG3961	37305	CG4067	26385
CG3603	51663	CG3711	11166	CG3832	52052	CG3964	38981	CG4068	34786
CG3604	9394	CG3712	36406	CG3835	30979	CG3967	26338	CG4069	21783
CG3604	48507	CG3712	42412	CG3837	44576	CG3969	26065	CG4070	12259
CG3605	26252	CG3714	26275	CG3839	12704	CG3971	47519	CG4071	26388
CG3609	52600	CG3715	40464	CG3839	47122	CG3973	34772	CG4071	47653
CG3612	34663	CG3717	45284	CG3842	7117	CG3977	46757	CG4074	26070
CG3613	26332	CG3719	21495	CG3843	40477	CG3978	6224	CG4076	21784
CG3615	10045	CG3723	41947	CG3845	34719	CG3979	9981	CG4078	37607
CG3618	6977	CG3725	4474	CG3848	10749	CG3980	34773	CG4079	30442
CG3619	3720	CG3727	37525	CG3849	21500	CG3981	40495	CG4080	9026
CG3619	27187	CG3730	34291	CG3849	47126	CG3983	26066	CG4082	13639
CG3619	37288	CG3731	40467	CG3850	21719	CG3985	35813	CG4083	34789
CG3620	21490	CG3733	26277	CG3857	44734	CG3985	46482	CG4086	14268
CG3625	40855	CG3734	12899	CG3858	51221	CG3986	13875	CG4087	12944
CG3626	34667	CG3735	26278	CG3861	26301	CG3988	26346	CG4088	33197
CG3629	11529	CG3736	30470	CG3862	34721	CG3989	2901	CG4090	34792
CG3630	21697	CG3737	45133	CG3869	40478	CG3991	26348	CG4091	34102
CG3631	13770	CG3739	29508	CG3871	30456	CG3994	3836	CG4094	34797
CG3632	26254	CG3740	13525	CG3871	48598	CG3996	34778	CG4095	26074
CG3633	34670	CG3743	30455	CG3874	47543	CG3997	23578	CG4095	47685
CG3634	16720	CG3744	34695	CG3876	44201	CG3999	26354	CG4097	34801
CG3638	6914	CG3751	34699	CG3878	34179	CG4001	3016	CG4098	14265
CG3639	34671	CG3752	21707	CG3879	42514	CG4005	40497	CG4101	9089
CG3640	15241	CG3753	34701	CG3880	34725	CG4006	2902	CG4103	26390
CG3641	40314	CG3756	15675	CG3881	42779	CG4007	841	CG4105	47499
CG3642	26261	CG3758	9794	CG3885	35806	CG4007	9653	CG4107	21786
CG3644	15453	CG3759	15602	CG3886	30586	CG4007	36282	CG4108	21788
CG3647	47973	CG3760	43437	CG3889	34727	CG4008	21772	CG4109	42561
CG3648	10156	CG3760	46862	CG3891	11270	CG4009	19942	CG4111	38950
CG3652	35574	CG3761	40468	CG3893	40479	CG4012	28367	CG4114	22994
CG3653	3111	CG3762	34389	CG3894	21721	CG4013	14915	CG4119	26395
CG3653	6695	CG3763	33173	CG3896	4913	CG4015	26356	CG4120	34806
CG3653	27227	CG3764	34707	CG3903	37115	CG4016	10020	CG4123	8493
CG3654	21700	CG3766	34709	CG3905	43869	CG4017	13282	CG4124	35580
CG3656	12190	CG3769	40469	CG3905	50368	CG4019	6650	CG4125	951

CG4125	27225	CG4247	25967	CG4396	48891	CG4553	14743	CG4670	7984
CG4128	8890	CG4252	11251	CG4400	21618	CG4554	21620	CG4672	8380
CG4129	21789	CG4257	43867	CG4402	33252	CG4555	41990	CG4673	21917
CG4132	21792	CG4258	34821	CG4405	48531	CG4556	40540	CG4675	3664
CG4140	26396	CG4260	4267	CG4407	34228	CG4557	51263	CG4676	4689
CG4141	38986	CG4261	30495	CG4410	26536	CG4560	26548	CG4677	28376
CG4143	12751	CG4262	37915	CG4412	35385	CG4561	40541	CG4678	28379
CG4145	28369	CG4264	26465	CG4415	34839	CG4562	6770	CG4679	38111
CG4147	14882	CG4264	50222	CG4420	40512	CG4565	5665	CG4681	40552
CG4152	21793	CG4265	26469	CG4422	26537	CG4567	34874	CG4683	22173
CG4153	9416	CG4266	26475	CG4426	7143	CG4568	1405	CG4684	44282
CG4153	48911	CG4268	45127	CG4427	15555	CG4569	21871	CG4685	14751
CG4154	21797	CG4270	34105	CG4428	34843	CG4572	16428	CG4686	46370
CG4157	21799	CG4272	26479	CG4429	34301	CG4573	21874	CG4690	45740
CG4158	6248	CG4274	44834	CG4429	48119	CG4574	26557	CG4692	13324
CG4159	26397	CG4276	26482	CG4433	29468	CG4579	21878	CG4696	40554
CG4161	26400	CG4278	26487	CG4434	21521	CG4583	39562	CG4696	46854
CG4162	21805	CG4279	28793	CG4435	40519	CG4584	21883	CG4697	34308
CG4163	51493	CG4279	50653	CG4438	34845	CG4586	21886	CG4698	38011
CG4164	22996	CG4288	8620	CG4438	50033	CG4587	3840	CG4700	15810
CG4165	41977	CG4289	42591	CG4439	41232	CG4589	6662	CG4701	9763
CG4166	45775	CG4290	26496	CG4443	34109	CG4591	42643	CG4703	26601
CG4167	21806	CG4291	21819	CG4445	42864	CG4592	6255	CG4704	21921
CG4169	26404	CG4293	6885	CG4447	38195	CG4593	21888	CG4706	34888
CG4170	26408	CG4299	21827	CG4448	34847	CG4594	13284	CG4709	21923
CG4173	26412	CG4300	26500	CG4450	42770	CG4596	35590	CG4713	21928
CG4179	7054	CG4301	6125	CG4451	42658	CG4598	34879	CG4719	21932
CG4180	41980	CG4302	37207	CG4452	40525	CG4599	26075	CG4720	34892
CG4183	6983	CG4303	12673	CG4453	47155	CG4600	26562	CG4722	8892
CG4184	21809	CG4307	12794	CG4466	40530	CG4602	51088	CG4722	46675
CG4185	3161	CG4311	26504	CG4481	42891	CG4603	21893	CG4729	5284
CG4186	35814	CG4314	40875	CG4482	33186	CG4604	15389	CG4729	48592
CG4187	7226	CG4316	1613	CG4483	5176	CG4606	42652	CG4733	34893
CG4192	6354	CG4317	14163	CG4484	5174	CG4608	5732	CG4735	26615
CG4193	21811	CG4320	13112	CG4485	12498	CG4609	21895	CG4738	21937
CG4195	43120	CG4321	21615	CG4488	26543	CG4610	34881	CG4739	6019
CG4196	11926	CG4322	1800	CG4494	34113	CG4611	21898	CG4742	21534
CG4199	26424	CG4324	37211	CG4495	49350	CG4613	14089	CG4743	9487
CG4200	7173	CG4328	30516	CG4497	21859	CG4617	26568	CG4746	21629
CG4201	26427	CG4330	11078	CG4498	10330	CG4618	41993	CG4749	21941
CG4202	26432	CG4332	37392	CG4498	39411	CG4619	2755	CG4750	41998
CG4202	49946	CG4334	49330	CG4500	34852	CG4621	21903	CG4751	45530
CG4204	12952	CG4335	26514	CG4501	34853	CG4622	21904	CG4752	40557
CG4205	24497	CG4337	23299	CG4502	34858	CG4623	21624	CG4753	1730
CG4206	51217	CG4341	29341	CG4510	26544	CG4624	34303	CG4753	46850
CG4207	26439	CG4342	21519	CG4511	34861	CG4625	1429	CG4755	34895
CG4207	46688	CG4346	37389	CG4520	34862	CG4627	4681	CG4756	13683
CG4208	30505	CG4347	21832	CG4521	33135	CG4629	26573	CG4757	38052
CG4209	21611	CG4349	40505	CG4523	21860	CG4630	4687	CG4758	8895
CG4210	49494	CG4350	38988	CG4525	34864	CG4633	21905	CG4759	21943
CG4211	26441	CG4351	26517	CG4527	43784	CG4634	3200	CG4760	21536
CG4212	45774	CG4353	47507	CG4532	21861	CG4636	21908	CG4764	26625
CG4214	3857	CG4354	10709	CG4533	40531	CG4637	1402	CG4766	21944
CG4215	10374	CG4356	33123	CG4535	21862	CG4638	34885	CG4767	21946
CG4217	37819	CG4357	30000	CG4536	7128	CG4643	26578	CG4768	21541
CG4220	42813	CG4364	27607	CG4537	28832	CG4645	10164	CG4769	9180
CG4221	34810	CG4365	6261	CG4537	48669	CG4646	21461	CG4770	6783
CG4222	48009	CG4370	4341	CG4538	16432	CG4648	21914	CG4774	6742
CG4225	37356	CG4372	36431	CG4539	21865	CG4649	26585	CG4775	42499
CG4226	51438	CG4376	7760	CG4542	7132	CG4649	46701	CG4779	21544
CG4233	26452	CG4379	6993	CG4545	11346	CG4654	12722	CG4780	44535
CG4236	26455	CG4380	16893	CG4546	34868	CG4656	21916	CG4785	21948
CG4237	26459	CG4386	41291	CG4547	21870	CG4659	42852	CG4787	21949
CG4238	41982	CG4389	21845	CG4548	10618	CG4660	50362	CG4789	26626
CG4239	11857	CG4393	21616	CG4550	44179	CG4662	41260	CG4792	24667
CG4241	50706	CG4394	34835	CG4551	40534	CG4663	39544	CG4795	13086
CG4244	21813	CG4395	7223	CG4552	40537	CG4666	36293	CG4798	26627

CG4799	34265	CG4920	37001	CG5030	31092	CG5165	34953	CG5282	5387
CG4800	26632	CG4921	24672	CG5032	46172	CG5166	34955	CG5284	6465
CG4802	42001	CG4924	43786	CG5033	30551	CG5167	6092	CG5285	10376
CG4803	34898	CG4924	50123	CG5037	42786	CG5168	22021	CG5287	51882
CG4805	44412	CG4925	45142	CG5038	52421	CG5169	22024	CG5288	24440
CG4806	26633	CG4926	935	CG5041	12559	CG5170	37583	CG5289	22052
CG4807	41005	CG4926	29930	CG5044	40570	CG5174	29752	CG5290	22057
CG4810	26637	CG4928	6143	CG5045	26687	CG5178	9780	CG5295	37880
CG4813	21950	CG4931	34907	CG5047	26692	CG5179	30448	CG5300	34983
CG4816	21951	CG4933	24674	CG5048	34120	CG5183	9235	CG5310	39402
CG4817	44343	CG4934	45457	CG5053	42019	CG5184	23249	CG5313	37762
CG4821	45232	CG4935	12563	CG5055	2914	CG5186	15185	CG5315	40936
CG4822	42730	CG4937	24679	CG5057	12755	CG5187	37634	CG5316	25953
CG4824	42004	CG4938	23004	CG5059	9847	CG5188	34320	CG5317	46572
CG4825	5391	CG4942	42888	CG5063	49383	CG5189	40318	CG5319	34986
CG4827	49359	CG4943	24680	CG5064	27351	CG5190	28282	CG5320	22059
CG4832	44526	CG4944	21549	CG5065	4921	CG5192	1836	CG5321	22061
CG4836	41431	CG4945	24683	CG5067	40867	CG5195	31044	CG5322	34989
CG4840	21959	CG4946	21550	CG5068	27352	CG5196	6096	CG5323	21563
CG4841	26645	CG4947	41644	CG5069	43858	CG5197	22028	CG5325	22064
CG4842	37490	CG4952	2942	CG5070	6150	CG5198	27370	CG5327	25972
CG4842	50516	CG4953	41214	CG5072	40576	CG5201	42840	CG5330	27392
CG4843	42010	CG4954	26664	CG5073	46549	CG5202	27373	CG5333	22066
CG4845	21960	CG4956	24487	CG5075	34927	CG5202	49982	CG5335	22068
CG4847	3230	CG4957	40565	CG5076	45198	CG5203	34125	CG5336	10455
CG4848	40559	CG4960	2732	CG5077	6766	CG5205	34128	CG5337	22069
CG4849	21962	CG4960	52392	CG5078	8085	CG5206	44284	CG5338	22074
CG4851	1459	CG4963	12342	CG5081	5413	CG5208	27378	CG5339	22075
CG4852	9014	CG4965	46064	CG5085	21999	CG5214	34966	CG5341	22077
CG4853	19877	CG4966	24687	CG5091	2782	CG5215	34969	CG5342	44404
CG4858	26649	CG4968	21978	CG5093	30550	CG5216	23201	CG5342	50058
CG4860	34899	CG4969	27610	CG5094	22002	CG5219	45542	CG5343	10468
CG4863	23420	CG4972	2777	CG5098	27356	CG5220	34972	CG5344	22082
CG4863	46265	CG4973	42015	CG5099	11784	CG5222	27380	CG5347	22088
CG4866	34116	CG4974	14136	CG5102	51300	CG5226	37181	CG5348	1698
CG4867	30360	CG4975	26673	CG5103	34931	CG5227	9437	CG5352	40587
CG4871	47955	CG4976	10836	CG5103	46604	CG5229	5684	CG5353	7752
CG4875	1830	CG4980	26676	CG5104	13787	CG5231	22039	CG5354	22095
CG4875	47226	CG4984	10055	CG5105	22003	CG5232	22040	CG5355	40588
CG4877	21966	CG4991	30264	CG5108	34934	CG5235	16705	CG5358	15645
CG4878	26651	CG4993	45863	CG5109	22004	CG5237	45780	CG5359	21565
CG4879	13363	CG4994	8366	CG5110	34935	CG5241	34976	CG5362	27399
CG4881	28386	CG4996	34913	CG5111	28642	CG5242	17830	CG5363	41838
CG4882	15718	CG4998	16453	CG5112	14747	CG5242	48166	CG5364	2781
CG4884	23421	CG4999	37252	CG5114	36618	CG5245	27381	CG5365	18988
CG4887	21970	CG5000	21982	CG5116	16476	CG5247	16758	CG5366	12067
CG4887	49022	CG5002	10058	CG5119	22007	CG5248	9248	CG5367	12392
CG4889	13351	CG5003	26680	CG5121	34316	CG5249	34978	CG5370	34328
CG4893	22358	CG5004	26683	CG5122	27358	CG5249	50171	CG5370	46616
CG4894	52644	CG5005	13725	CG5124	22010	CG5252	27383	CG5371	15683
CG4896	26652	CG5009	21991	CG5125	27359	CG5254	6887	CG5372	6646
CG4896	48197	CG5012	26684	CG5127	47030	CG5258	35729	CG5374	34070
CG4897	21973	CG5012	50149	CG5131	42025	CG5261	48939	CG5375	22099
CG4898	34119	CG5013	38992	CG5133	16747	CG5263	22044	CG5377	34392
CG4899	6470	CG5013	48108	CG5140	22013	CG5264	30465	CG5378	22104
CG4899	46766	CG5014	30404	CG5142	22015	CG5264	50658	CG5379	14461
CG4901	34905	CG5017	21582	CG5144	30946	CG5265	34323	CG5380	11228
CG4904	26653	CG5018	42018	CG5147	37114	CG5266	29686	CG5383	22108
CG4907	6832	CG5021	36440	CG5149	34944	CG5268	13796	CG5384	27405
CG4908	44845	CG5022	8262	CG5150	15298	CG5270	27390	CG5387	34990
CG4909	26657	CG5023	34914	CG5155	27364	CG5271	34325	CG5389	22112
CG4911	45141	CG5025	26685	CG5157	34947	CG5274	22046	CG5392	52427
CG4912	26658	CG5026	34915	CG5160	22019	CG5275	47621	CG5394	34995
CG4913	15671	CG5027	12106	CG5161	34951	CG5276	47995	CG5395	34999
CG4916	49379	CG5029	29733	CG5162	14661	CG5277	34979	CG5403	51314
CG4917	42665	CG5029	33803	CG5163	12746	CG5280	22050	CG5404	40907
CG4918	31005	CG5029	39418	CG5164	40582	CG5281	6049	CG5405	43790

CG5406	27406	CG5510	49025	CG5634	27199	CG5748	37699	CG5864	12913
CG5407	27411	CG5514	27445	CG5637	22693	CG5748	48692	CG5869	34145
CG5408	22113	CG5515	27447	CG5638	1748	CG5751	37250	CG5870	42053
CG5411	25976	CG5516	51402	CG5639	1305	CG5753	27503	CG5871	41822
CG5412	27413	CG5517	15957	CG5640	37663	CG5755	3879	CG5874	43211
CG5412	50266	CG5519	22146	CG5641	42043	CG5757	28654	CG5876	3855
CG5413	14356	CG5521	22150	CG5641	48200	CG5760	44002	CG5877	39004
CG5414	35001	CG5522	40595	CG5642	46592	CG5771	22198	CG5880	1264
CG5417	23422	CG5523	5038	CG5643	27470	CG5772	6750	CG5882	27532
CG5422	28649	CG5524	13650	CG5645	9289	CG5776	27507	CG5884	19730
CG5423	44702	CG5525	22155	CG5648	35023	CG5783	23429	CG5884	19731
CG5424	33200	CG5526	27450	CG5650	35025	CG5784	49386	CG5886	22216
CG5428	43796	CG5528	924	CG5651	44325	CG5786	39001	CG5887	33338
CG5429	22123	CG5528	36308	CG5653	14064	CG5788	27515	CG5887	47142
CG5430	44712	CG5529	19834	CG5654	27472	CG5788	48146	CG5889	27535
CG5432	27417	CG5532	30346	CG5656	18119	CG5789	1204	CG5890	23431
CG5433	22125	CG5535	42584	CG5657	51526	CG5790	45044	CG5892	6807
CG5434	21641	CG5537	22157	CG5658	40605	CG5792	34143	CG5893	2940
CG5435	35005	CG5543	27454	CG5659	35029	CG5793	35044	CG5893	49549
CG5439	27418	CG5545	13056	CG5660	29445	CG5793	47883	CG5894	27538
CG5440	49030	CG5546	27457	CG5661	1052	CG5794	27517	CG5898	23432
CG5442	40590	CG5547	27459	CG5661	9428	CG5796	40607	CG5899	15679
CG5443	46573	CG5548	24714	CG5662	35030	CG5798	8931	CG5902	6274
CG5443x	47331	CG5549	8222	CG5663	27475	CG5798	8931	CG5903	31098
CG5444	12600	CG5550	31000	CG5669	45300	CG5799	3780	CG5904	35048
CG5446	41797	CG5553	30623	CG5670	12330	CG5800	27519	CG5905	7108
CG5447	21566	CG5554	20101	CG5671	35731	CG5802	6801	CG5906	5227
CG5450	42114	CG5555	35013	CG5675	27479	CG5803	941	CG5907	23433
CG5451	42035	CG5558	39560	CG5675	28652	CG5803	3091	CG5907	49870
CG5452	39137	CG5558	46814	CG5676	47731	CG5803	42229	CG5911	42716
CG5454	22132	CG5560	14814	CG5677	1414	CG5804	23587	CG5912	4819
CG5455	35011	CG5561	27461	CG5680	34139	CG5805	35592	CG5912	6707
CG5458	27420	CG5561	47055	CG5682	7696	CG5807	6726	CG5912	36286
CG5461	19679	CG5565	27463	CG5684	28396	CG5808	22199	CG5913	40336
CG5462	27424	CG5567	44319	CG5685	42660	CG5809	43148	CG5915	40338
CG5462	27424	CG5569	21568	CG5686	7777	CG5810	44988	CG5917	8347
CG5462	27424	CG5571	22160	CG5687	33262	CG5811	1258	CG5919	28402
CG5463	22135	CG5577	22163	CG5688	27482	CG5813	28401	CG5920	20963
CG5465	14916	CG5580	41845	CG5690	28651	CG5814	22201	CG5921	37875
CG5467	45556	CG5582	5322	CG5692	27486	CG5815	22203	CG5926	24996
CG5469	39000	CG5583	10932	CG5695	37535	CG5818	40608	CG5927	17853
CG5473	21567	CG5585	22166	CG5703	22194	CG5821	37850	CG5930	41011
CG5474	12101	CG5586	22169	CG5704	42044	CG5823	8301	CG5931	43962
CG5475	34238	CG5589	44322	CG5705	19854	CG5826	27521	CG5933	20968
CG5475	52277	CG5590	42039	CG5706	42046	CG5827	23590	CG5934	20970
CG5479	22138	CG5591	22170	CG5707	22195	CG5828	27522	CG5935	25477
CG5481	11823	CG5594	10278	CG5708	23425	CG5830	40611	CG5937	33613
CG5482	4991	CG5595	27465	CG5714	28398	CG5832	16755	CG5938	32418
CG5483	22139	CG5596	34331	CG5715	14710	CG5836	13426	CG5939	33615
CG5484	2679	CG5599	16506	CG5718	34239	CG5837	22207	CG5940	32421
CG5485	5341	CG5602	51315	CG5720	27487	CG5838	22210	CG5941	48773
CG5486	26027	CG5603	15340	CG5721	27488	CG5840	22214	CG5942	37721
CG5488	11570	CG5604	27467	CG5722	42782	CG5841	27526	CG5946	5226
CG5489	45558	CG5605	45027	CG5723	51173	CG5842	5261	CG5949	41028
CG5491	27433	CG5608	45569	CG5725	44157	CG5844	27528	CG5950	5150
CG5492	11901	CG5610	1189	CG5728	24696	CG5846	21645	CG5952	17849
CG5493	26082	CG5610	48159	CG5729	27490	CG5847	3162	CG5954	13994
CG5493	50637	CG5611	46344	CG5730	27493	CG5850	1456	CG5955	15836
CG5495	27436	CG5613	24694	CG5731	15543	CG5851	42051	CG5958	20982
CG5497	41800	CG5621	47549	CG5733	27495	CG5854	15649	CG5960	20983
CG5498	27440	CG5625	45570	CG5734	43798	CG5855	37722	CG5961	20988
CG5499	12768	CG5626	27469	CG5735	27498	CG5857	3408	CG5962	20989
CG5500	15376	CG5627	35019	CG5737	41048	CG5859	45677	CG5964	33617
CG5502	49443	CG5629	40601	CG5741	5158	CG5861	6360	CG5965	20994
CG5505	11152	CG5632	39087	CG5742	36428	CG5861	47665	CG5966	13164
CG5508	1316	CG5634	1106	CG5744	23428	CG5862	45155	CG5969	47116
CG5510	28393	CG5634	8016	CG5745	35034	CG5863	14366	CG5970	20998

CG5973	24998	CG6092	44165	CG6198	22300	CG6332	43799	CG6463	34171
CG5974	2889	CG6094	27564	CG6199	45484	CG6335	43998	CG6464	3029
CG5977	33110	CG6094	48721	CG6201	13245	CG6338	12632	CG6464	3029
CG5978	21000	CG6095	30111	CG6202	5883	CG6339	15879	CG6465	27632
CG5980	21003	CG6096	37691	CG6203	8933	CG6340	34160	CG6472	22495
CG5986	25479	CG6096	47124	CG6204	30135	CG6341	22488	CG6475	40932
CG5987	21005	CG6098	27566	CG6205	9149	CG6342	30153	CG6476	33834
CG5989	5149	CG6106	30120	CG6205	47864	CG6343	14444	CG6476	39377
CG5991	25483	CG6110	22221	CG6206	49352	CG6345	27588	CG6477	27639
CG5992	16456	CG6113	31021	CG6208	40348	CG6347	16837	CG6479	45648
CG5992	50426	CG6114	22225	CG6210	5215	CG6349	11227	CG6480	23449
CG5994	21010	CG6115	29711	CG6213	25986	CG6350	50009	CG6484	4954
CG5996	9337	CG6120	3422	CG6218	35069	CG6352	51289	CG6485	14281
CG5998	25484	CG6121	22233	CG6220	40350	CG6353	40363	CG6486	43804
CG6000	23436	CG6122	22235	CG6222	10854	CG6355	27592	CG6492	6162
CG6004	25489	CG6125	12141	CG6223	15419	CG6358	40368	CG6493	25090
CG6005	25492	CG6126	7326	CG6224	22476	CG6359	34165	CG6495	42796
CG6007	21012	CG6127	27172	CG6225	8276	CG6363	43802	CG6498	35100
CG6008	5717	CG6128	50641	CG6226	22480	CG6364	11693	CG6500	2916
CG6009	33623	CG6129	22237	CG6227	40351	CG6369	27598	CG6502	27645
CG6009	46891	CG6133	37601	CG6230	8897	CG6372	52508	CG6504	6940
CG6011	13760	CG6136	22239	CG6232	31020	CG6375	27600	CG6506	34349
CG6013	33625	CG6137	30125	CG6233	24700	CG6376	15887	CG6508	28413
CG6014	31067	CG6139	4856	CG6235	34340	CG6378	16677	CG6509	22496
CG6015	41708	CG6140	50305	CG6238	30136	CG6379	29611	CG6509	46234
CG6016	7988	CG6141	22244	CG6246	6217	CG6380	29950	CG6512	8515
CG6017	8487	CG6142	19930	CG6249	30140	CG6383	39177	CG6513	34173
CG6018	33629	CG6143	22245	CG6251	44808	CG6385	27601	CG6514	27649
CG6019	47606	CG6144	41847	CG6253	44629	CG6386	48980	CG6515	13392
CG6020	13130	CG6145	48698	CG6255	40355	CG6390	4385	CG6516	27654
CG6022	45020	CG6146	10639	CG6258	12618	CG6391	25995	CG6517	39622
CG6025	17826	CG6147	22252	CG6259	25990	CG6392	35081	CG6518	2894
CG6027	43633	CG6148	22253	CG6262	25993	CG6393	40376	CG6519	13860
CG6028	52314	CG6149	40847	CG6264	5963	CG6395	34168	CG6521	22497
CG6030	21018	CG6151	39596	CG6267	30079	CG6395	47208	CG6522	22500
CG6034	33631	CG6152	41825	CG6267	42260	CG6396	35082	CG6523	34174
CG6036	21023	CG6153	22257	CG6269	10825	CG6396	35082	CG6524	33286
CG6042	25168	CG6154	23008	CG6271	50744	CG6396	35082	CG6533	19870
CG6042	49491	CG6155	34151	CG6272	34156	CG6401	39552	CG6534	30462
CG6045	21032	CG6156	22258	CG6275	845	CG6405	35087	CG6535	22502
CG6045	48191	CG6167	22268	CG6275	3053	CG6407	32257	CG6538	12602
CG6046	15710	CG6168	28405	CG6278	23598	CG6410	24701	CG6539	7154
CG6049	25497	CG6169	22272	CG6279	37267	CG6412	44327	CG6539	49505
CG6050	48982	CG6171	30128	CG6281	15372	CG6413	35090	CG6543	27658
CG6051	25500	CG6171	49472	CG6284	22483	CG6414	44328	CG6544	34066
CG6052	5311	CG6172	13062	CG6287	40358	CG6415	51541	CG6545	12662
CG6053	35052	CG6173	14703	CG6292	37562	CG6418	40379	CG6546	24703
CG6054	35055	CG6176	30131	CG6293	33220	CG6420	42060	CG6547	46065
CG6056	34148	CG6177	22280	CG6299	46105	CG6422	27614	CG6549	27661
CG6057	6532	CG6178	1172	CG6302	28794	CG6424	27619	CG6550	4947
CG6058	27542	CG6179	40341	CG6303	48309	CG6428	27622	CG6551	27662
CG6058	47667	CG6180	47677	CG6304	48212	CG6432	43451	CG6554	40388
CG6059	35056	CG6181	37945	CG6308	30273	CG6434	36424	CG6562	46070
CG6061	35061	CG6182	14705	CG6311	30149	CG6437	45275	CG6565	39006
CG6064	27545	CG6184	40920	CG6312	10416	CG6438	37023	CG6567	27667
CG6066	35065	CG6186	14666	CG6315	27577	CG6439	14443	CG6570	30461
CG6070	1262	CG6187	34152	CG6318	10759	CG6443	15736	CG6570	52323
CG6072	27546	CG6188	25983	CG6320	27581	CG6444	27626	CG6571	35105
CG6073	17256	CG6189	22287	CG6321	27584	CG6445	36320	CG6574	40902
CG6074	31148	CG6190	45876	CG6321	47682	CG6449	5208	CG6576	26695
CG6081	7868	CG6191	27133	CG6322	34242	CG6450	40382	CG6577	12588
CG6083	27549	CG6192	24719	CG6323	4391	CG6451	27630	CG6578	6170
CG6084	27551	CG6193	22290	CG6325	35072	CG6453	37991	CG6582	51472
CG6087	9699	CG6194	22294	CG6327	43988	CG6454	36655	CG6584	25999
CG6089	27554	CG6196	22297	CG6330	44326	CG6455	11938	CG6589	46072
CG6090	22218	CG6196	47140	CG6331	6782	CG6459	15520	CG6593	27673
CG6091	27558	CG6197	46312	CG6331	47132	CG6461	18545	CG6597	28237

CG6603	27680	CG6717	18961	CG6840	23290	CG6949	40405	CG7051	22340
CG6604	28416	CG6719	27727	CG6841	34253	CG6950	22321	CG7052	35611
CG6604	50849	CG6721	23016	CG6842	35126	CG6951	27756	CG7053	27815
CG6605	27683	CG6723	13769	CG6844	1194	CG6953	1530	CG7054	40416
CG6607	27688	CG6724	27730	CG6846	40402	CG6954	27759	CG7055	37684
CG6608	6005	CG6725	37361	CG6847	22451	CG6961	35150	CG7056	15719
CG6612	42064	CG6726	34247	CG6850	16467	CG6963	26003	CG7057	27820
CG6613	42065	CG6733	50172	CG6851	44306	CG6964	13687	CG7059	21651
CG6614	26700	CG6736	12890	CG6852	26001	CG6966	22326	CG7060	42883
CG6615	27691	CG6737	46197	CG6854	12762	CG6967	27769	CG7061	27823
CG6618	8052	CG6738	27736	CG6856	34354	CG6971	35153	CG7062	34190
CG6619	15622	CG6738	48918	CG6857	7231	CG6971	48986	CG7066	36572
CG6620	35107	CG6741	16826	CG6859	12426	CG6972	27772	CG7067	27831
CG6621	27695	CG6742	27738	CG6860	7306	CG6975	6314	CG7068	44241
CG6622	27699	CG6743	22407	CG6863	2656	CG6976	37532	CG7069	27834
CG6623	40390	CG6744	48329	CG6866	22453	CG6978	7041	CG7070	35165
CG6625	22379	CG6745	46746	CG6867	37416	CG6980	29148	CG7070	49533
CG6627	42798	CG6746	46513	CG6868	1216	CG6983	35158	CG7071	46823
CG6630	26701	CG6747	28431	CG6869	5271	CG6984	21649	CG7073	34191
CG6632	52510	CG6750	9408	CG6870	52570	CG6987	27775	CG7074	12721
CG6633	6016	CG6751	12577	CG6871	6283	CG6988	23358	CG7075	3666
CG6634	30519	CG6752	43605	CG6873	22454	CG6990	27782	CG7076	28740
CG6637	21658	CG6753	16600	CG6875	2910	CG6990	50520	CG7077	33835
CG6643	28418	CG6754	28215	CG6876	35131	CG6993	10715	CG7077	42713
CG6649	7320	CG6755	6282	CG6877	22455	CG6998	43116	CG7081	5136
CG6650	8363	CG6756	18112	CG6878	9224	CG6999	41829	CG7082	2554
CG6652	26706	CG6757	22412	CG6881	1815	CG7000	42496	CG7083	22342
CG6653	8574	CG6758	43606	CG6883	22703	CG7002	37005	CG7085	46150
CG6656	1630	CG6759	52667	CG6884	27750	CG7004	27785	CG7090	14610
CG6657	8144	CG6760	27743	CG6888	26094	CG7005	9797	CG7092	27837
CG6658	8569	CG6762	35734	CG6890	9430	CG7006	29512	CG7097	35166
CG6659	8038	CG6763	18940	CG6890	13549	CG7007	33342	CG7098	46320
CG6660	6835	CG6766	38035	CG6890	27099	CG7007	47187	CG7099	27848
CG6662	26713	CG6767	35112	CG6891	50055	CG7008	19013	CG7100	1092
CG6664	12780	CG6768	13645	CG6892	30552	CG7009	27789	CG7103	6175
CG6665	8202	CG6770	35825	CG6894	9154	CG7009	27790	CG7103	46875
CG6666	6031	CG6772	30673	CG6897	35134	CG7010	40410	CG7106	45634
CG6667	45998	CG6775	26090	CG6898	37358	CG7011	46860	CG7107	27853
CG6668	6719	CG6778	44603	CG6899	1012	CG7013	12834	CG7108	43870
CG6672	12132	CG6779	37742	CG6899	4297	CG7014	27792	CG7109	41924
CG6673	41806	CG6781	34227	CG6899	27232	CG7014	49879	CG7111	27858
CG6674	26716	CG6782	50714	CG6900	23602	CG7015	41858	CG7112	35174
CG6677	7141	CG6784	39312	CG6900	49629	CG7015	49498	CG7113	37083
CG6678	26719	CG6788	42912	CG6903	3285	CG7018	15355	CG7115	9404
CG6682	26721	CG6788	48054	CG6904	35136	CG7020	27796	CG7121	839
CG6684	52603	CG6789	27747	CG6905	13492	CG7023	27799	CG7121	17903
CG6686	21573	CG6790	12134	CG6906	8357	CG7024	27803	CG7121	44705
CG6690	14439	CG6792	35118	CG6907	22460	CG7025	43187	CG7123	23121
CG6691	3951	CG6794	30578	CG6910	22464	CG7026	8254	CG7125	22344
CG6692	13959	CG6796	6494	CG6913	46690	CG7026	48830	CG7127	27867
CG6693	27717	CG6798	1199	CG6914	35139	CG7028	27808	CG7128	27870
CG6695	36656	CG6800	40397	CG6915	35141	CG7033	41190	CG7129	52571
CG6696	28426	CG6811	34250	CG6919	47896	CG7034	35162	CG7131	52520
CG6696	49114	CG6812	8534	CG6920	13310	CG7035	22331	CG7134	27881
CG6697	27720	CG6814	22442	CG6921	30179	CG7036	13070	CG7137	27884
CG6699	42071	CG6815	39675	CG6923	26096	CG7037	22335	CG7139	35177
CG6700	39007	CG6816	5601	CG6928	5231	CG7038	40413	CG7140	27888
CG6701	36557	CG6817	10102	CG6930	35147	CG7038	47159	CG7143	44721
CG6702	41812	CG6818	26723	CG6931	22468	CG7039	26007	CG7144	51346
CG6703	34185	CG6818	49479	CG6931	49058	CG7041	26097	CG7145	40422
CG6704	46856	CG6819	47693	CG6932	22307	CG7042	23452	CG7146	40427
CG6706	1784	CG6822	5142	CG6937	22315	CG7044	27811	CG7149	43821
CG6707	44557	CG6824	12663	CG6938	37271	CG7047	15203	CG7152	27893
CG6711	37548	CG6827	9039	CG6939	22317	CG7048	29811	CG7154	37669
CG6712	39012	CG6831	40399	CG6944	45635	CG7049	15846	CG7156	26036
CG6713	27722	CG6835	49800	CG6946	27752	CG7050	4306	CG7158	35179
CG6716	6221	CG6838	35123	CG6948	22318	CG7050	36328	CG7161	35186

CG7162	13054	CG7269	22556	CG7394	9210	CG7508	2924	CG7637	23669
CG7163	38247	CG7272	8374	CG7395	9379	CG7508	48674	CG7637	42402
CG7168	27894	CG7274	40440	CG7397	13429	CG7509	51585	CG7638	8235
CG7169	44999	CG7275	22561	CG7398	4769	CG7510	8532	CG7639	33641
CG7172	27898	CG7277	30691	CG7398	6543	CG7511	52654	CG7640	23671
CG7176	42915	CG7279	18107	CG7398	30066	CG7512	13829	CG7642	25172
CG7177	35194	CG7280	18550	CG7399	35240	CG7513	35250	CG7646	35742
CG7178	34196	CG7281	27937	CG7400	9406	CG7514	37233	CG7650	41714
CG7180	34368	CG7281	48835	CG7400	48719	CG7515	35251	CG7654	47988
CG7183	40429	CG7282	27941	CG7402	37302	CG7516	28058	CG7655	12429
CG7184	34373	CG7282	50406	CG7405	10398	CG7518	26745	CG7656	26881
CG7186	27904	CG7283	23458	CG7408	8415	CG7519	21653	CG7659	12639
CG7187	28610	CG7283	52411	CG7413	10696	CG7520	15927	CG7659	46805
CG7188	37108	CG7285	13560	CG7414	18804	CG7524	35252	CG7662	43094
CG7190	31070	CG7288	47663	CG7415	35242	CG7530	5872	CG7662	46962
CG7192	52526	CG7289	34281	CG7417	37555	CG7532	12405	CG7664	26885
CG7193	40434	CG7291	30725	CG7420	46316	CG7536	11576	CG7665	13566
CG7194	24723	CG7292	35200	CG7421	27995	CG7538	10967	CG7669	29200
CG7195	28160	CG7293	27943	CG7423	28003	CG7542	47336	CG7670	44595
CG7195	39303	CG7301	39384	CG7424	44630	CG7546	35253	CG7671	33645
CG7197	19736	CG7305	48072	CG7425	26011	CG7550	35254	CG7678	11649
CG7199	37072	CG7307	18553	CG7427	28006	CG7555	13121	CG7685	5919
CG7199	48979	CG7311	41813	CG7429	28008	CG7556	28621	CG7686	33650
CG7200	27913	CG7317	28694	CG7430	28011	CG7558	35258	CG7693	41719
CG7206	22530	CG7319	27949	CG7431	2857	CG7560	28063	CG7694	25520
CG7207	27914	CG7322	9258	CG7432	31091	CG7562	30441	CG7697	21045
CG7211	35386	CG7323	15631	CG7433	28014	CG7563	35261	CG7698	39557
CG7212	40436	CG7324	31064	CG7435	48430	CG7564	29462	CG7700	12152
CG7215	27916	CG7328	27951	CG7436	28019	CG7565	3707	CG7704	45957
CG7215	49802	CG7329	48340	CG7437	28023	CG7565	8396	CG7706	25524
CG7217	35196	CG7331	27955	CG7438	12558	CG7565	36291	CG7708	30301
CG7217	49806	CG7332	27959	CG7439	49473	CG7568	45783	CG7709	9865
CG7218	5908	CG7334	13375	CG7441	28027	CG7571	37295	CG7712	50214
CG7220	34198	CG7335	27962	CG7446	5329	CG7573	8337	CG7716	25526
CG7221	22536	CG7337	35204	CG7447	30934	CG7577	36659	CG7717	25528
CG7222	34377	CG7338	27963	CG7449	9471	CG7578	33634	CG7718	25532
CG7223	6692	CG7339	13629	CG7449	27065	CG7580	28839	CG7719	21046
CG7223	40627	CG7340	3174	CG7449	40898	CG7581	21037	CG7722	25534
CG7224	36437	CG7343	35206	CG7452	36595	CG7582	1353	CG7724	43927
CG7225	13863	CG7343	35206	CG7457	26740	CG7583	37609	CG7725	33654
CG7228	33155	CG7343	35206	CG7457	46671	CG7590	25506	CG7726	45427
CG7230	15900	CG7345	10813	CG7459	5805	CG7595	9265	CG7727	42673
CG7231	2783	CG7347	46011	CG7460	13115	CG7597	25510	CG7728	21048
CG7233	27919	CG7349	51481	CG7461	28028	CG7598	14861	CG7729	37010
CG7234	7878	CG7351	27966	CG7462	40638	CG7600	47473	CG7734	3226
CG7235	22539	CG7352	40636	CG7464	10558	CG7601	4456	CG7735	43508
CG7238	34382	CG7354	14305	CG7466	42462	CG7602	37594	CG7736	1501
CG7241	5851	CG7356	26100	CG7467	7810	CG7605	43730	CG7737	49437
CG7245	22541	CG7359	9888	CG7469	28033	CG7609	21041	CG7739	51521
CG7245	22541	CG7360	40773	CG7470	38955	CG7610	16539	CG7740	51956
CG7246	34256	CG7362	7556	CG7471	30599	CG7611	25511	CG7741	33655
CG7250	927	CG7364	7706	CG7471	46930	CG7614	12575	CG7742	25535
CG7250	7995	CG7365	14318	CG7473	39151	CG7615	47312	CG7744	33247
CG7250	27103	CG7367	43822	CG7478	9776	CG7616	41408	CG7747	44854
CG7254	27928	CG7368	27978	CG7479	45048	CG7620	30391	CG7749	3749
CG7255	8373	CG7371	27984	CG7480	44263	CG7621	48032	CG7749	5098
CG7257	22548	CG7371	48711	CG7484	13358	CG7622	39914	CG7749	27113
CG7259	5273	CG7375	35220	CG7485	26876	CG7623	12149	CG7757	25547
CG7260	43909	CG7376	35222	CG7486	28041	CG7625	30382	CG7758	12823
CG7261	27931	CG7378	35226	CG7487	10614	CG7626	19793	CG7759	21052
CG7262	22552	CG7378	47855	CG7490	28618	CG7627	2807	CG7760	37611
CG7263	2544	CG7379	27988	CG7494	28042	CG7628	19713	CG7761	8692
CG7264	22554	CG7382	47494	CG7494	48961	CG7628	49973	CG7762	25549
CG7265	27932	CG7387	27993	CG7497	9374	CG7632	45675	CG7764	12596
CG7266	26009	CG7390	35229	CG7499	9179	CG7633	6178	CG7765	44337
CG7266	48992	CG7391	42834	CG7504	28050	CG7635	9160	CG7766	52573
CG7268	24453	CG7392	35232	CG7507	28053	CG7636	13828	CG7768	35266

CG7769	44976	CG7887	1374	CG7993	35314	CG8114	35349	CG8243	26952
CG7770	34203	CG7887	43329	CG7995	22652	CG8116	45735	CG8244	30642
CG7771	26888	CG7888	37264	CG7997	16840	CG8117	23254	CG8244	33842
CG7772	30431	CG7891	26085	CG7998	22654	CG8117	47174	CG8245	28878
CG7773	35267	CG7892	3002	CG7999	15878	CG8127	44851	CG8250	11446
CG7776	35268	CG7893	6241	CG8001	35317	CG8128	47740	CG8251	24257
CG7777	8124	CG7894	869	CG8003	22659	CG8129	24201	CG8253	35411
CG7779	29046	CG7894	3060	CG8005	22664	CG8129	46959	CG8254	13716
CG7785	36650	CG7894	42251	CG8007	11462	CG8132	17254	CG8256	19565
CG7787	45715	CG7895	12656	CG8008	4158	CG8134	24204	CG8257	35865
CG7788	28065	CG7896	907	CG8009	41105	CG8135	42635	CG8257	50371
CG7791	35272	CG7896	3813	CG8009	48955	CG8138	24208	CG8258	45789
CG7793	42848	CG7896	36340	CG8013	42423	CG8142	10881	CG8261	28844
CG7804	28067	CG7899	3579	CG8014	22671	CG8144	24214	CG8266	35867
CG7804	49886	CG7900	43157	CG8019	41022	CG8146	23126	CG8267	35870
CG7806	2804	CG7904	848	CG8020	44076	CG8146	48210	CG8268	23678
CG7807	41130	CG7904	37279	CG8021	23675	CG8147	2892	CG8269	23728
CG7808	35278	CG7908	2733	CG8023	34210	CG8149	24215	CG8270	23755
CG7809	22564	CG7910	51546	CG8025	26039	CG8151	12581	CG8271	4607
CG7810	22565	CG7911	23075	CG8026	4163	CG8152	13978	CG8272	24262
CG7811	2890	CG7912	1377	CG8029	48016	CG8153	15695	CG8273	28887
CG7813	22566	CG7913	22614	CG8031	35326	CG8155	24218	CG8274	24265
CG7814	35279	CG7914	22619	CG8032	28175	CG8156	24224	CG8276	28888
CG7815	22567	CG7915	22620	CG8036	35330	CG8161	35843	CG8277	24267
CG7816	1362	CG7917	22623	CG8038	28179	CG8166	8137	CG8280	24270
CG7818	13541	CG7919	5117	CG8039	29473	CG8167	44761	CG8280	49890
CG7818	48559	CG7921	1381	CG8042	35331	CG8169	39193	CG8282	24275
CG7820	26015	CG7923	7492	CG8043	28181	CG8171	23131	CG8284	35872
CG7821	40641	CG7925	52533	CG8046	7380	CG8173	35845	CG8285	4365
CG7823	46154	CG7926	7748	CG8048	46563	CG8174	26933	CG8286	14154
CG7825	44723	CG7927	22627	CG8049	22675	CG8177	39492	CG8287	28092
CG7826	28628	CG7929	12920	CG8053	26022	CG8184	26935	CG8288	24278
CG7828	7728	CG7931	21578	CG8058	13314	CG8186	49888	CG8289	24279
CG7830	4253	CG7931	50524	CG8060	22684	CG8187	24230	CG8290	12739
CG7831	22570	CG7935	38963	CG8060	46991	CG8189	14210	CG8293	2972
CG7832	49339	CG7940	22633	CG8064	28182	CG8190	43917	CG8297	8972
CG7833	44030	CG7943	28632	CG8064	49076	CG8194	13018	CG8297	46760
CG7834	36661	CG7945	35296	CG8067	22687	CG8197	42125	CG8298	43541
CG7837	22573	CG7946	35298	CG8067	47871	CG8199	24231	CG8300	24291
CG7838	26109	CG7948	14021	CG8068	30709	CG8200	42130	CG8302	51943
CG7839	12691	CG7949	21657	CG8069	28189	CG8202	35410	CG8303	4917
CG7840	47495	CG7950	22635	CG8070	35333	CG8203	35855	CG8306	23134
CG7842	14279	CG7951	46696	CG8073	23020	CG8207	24236	CG8308	24297
CG7842	46334	CG7954	52538	CG8075	7376	CG8208	9261	CG8311	8985
CG7843	22574	CG7955	40838	CG8079	23023	CG8209	35858	CG8314	1691
CG7845	22578	CG7956	22638	CG8083	37162	CG8211	24237	CG8315	28892
CG7847	9921	CG7957	44027	CG8085	28192	CG8211	24239	CG8318	35877
CG7849	22588	CG7958	28070	CG8086	23028	CG8212	44731	CG8320	8797
CG7850	3018	CG7960	13679	CG8090	30341	CG8213	7372	CG8321	8765
CG7851	33157	CG7961	35306	CG8091	23033	CG8214	24240	CG8322	30280
CG7852	7178	CG7962	5121	CG8092	28196	CG8219	24244	CG8323	4861
CG7855	22590	CG7964	50645	CG8093	19561	CG8222	976	CG8325	35881
CG7860	34395	CG7966	22639	CG8094	35337	CG8222	13503	CG8326	23760
CG7861	34388	CG7970	8857	CG8095	4891	CG8222	43459	CG8327	35883
CG7864	46613	CG7971	34262	CG8097	28199	CG8223	35861	CG8330	23763
CG7865	15782	CG7972	28072	CG8098	6455	CG8224	853	CG8331	35377
CG7867	28069	CG7974	28074	CG8102	16898	CG8224	3825	CG8332	35415
CG7870	2802	CG7975	40645	CG8103	10766	CG8226	8747	CG8333	10950
CG7872	9134	CG7978	51974	CG8104	29788	CG8230	37160	CG8334	18982
CG7873	26019	CG7979	5126	CG8105	8037	CG8231	23751	CG8335	15506
CG7875	1365	CG7980	28169	CG8107	23037	CG8233	24248	CG8336	23729
CG7878	35288	CG7985	8257	CG8107	46241	CG8234	40980	CG8338	28240
CG7879	15260	CG7986	22646	CG8108	35343	CG8234	49889	CG8339	5070
CG7882	8103	CG7988	22651	CG8109	11329	CG8237	9324	CG8340	35890
CG7883	40321	CG7988	46277	CG8110	35345	CG8239	24253	CG8343	7735
CG7885	14000	CG7989	28172	CG8111	29391	CG8240	28877	CG8344	15692
CG7886	22610	CG7990	46157	CG8112	37345	CG8241	47782	CG8349	48682

CG8351	28895	CG8453	4615	CG8584	26988	CG8693	7947	CG8808	37966
CG8353	35896	CG8454	23769	CG8587	26989	CG8694	28292	CG8809	39076
CG8354	28848	CG8455	47953	CG8589	24180	CG8695	15791	CG8811	29774
CG8355	20210	CG8461	24103	CG8590	35975	CG8696	15789	CG8814	2606
CG8356	7317	CG8464	24104	CG8591	30713	CG8705	11791	CG8815	10808
CG8357	30485	CG8465	24107	CG8593	47001	CG8706	3710	CG8816	36045
CG8360	41643	CG8468	6452	CG8594	4642	CG8706	8397	CG8816	50135
CG8361	16753	CG8470	40712	CG8595	6541	CG8706	39215	CG8817	13081
CG8362	35901	CG8472	28243	CG8595	39176	CG8707	36003	CG8819	49637
CG8363	35904	CG8474	51285	CG8596	5089	CG8708	45194	CG8821	37660
CG8364	52541	CG8475	2800	CG8598	35982	CG8709	36007	CG8821	49640
CG8365	37685	CG8481	28906	CG8601	28932	CG8711	44829	CG8823	30821
CG8368	45259	CG8481	49470	CG8603	26992	CG8714	9951	CG8824	4637
CG8370	42509	CG8483	41263	CG8603	47148	CG8717	8739	CG8825	28958
CG8372	8043	CG8485	35940	CG8604	9264	CG8719	39121	CG8825	46268
CG8376	37791	CG8486	2796	CG8605	29435	CG8719	50531	CG8827	41219
CG8378	40705	CG8487	42140	CG8606	48214	CG8721	30038	CG8830	28960
CG8379	35911	CG8491	23142	CG8609	14032	CG8722	40717	CG8831	42153
CG8380	12082	CG8492	14929	CG8610	35986	CG8725	28942	CG8833	36408
CG8383	35915	CG8493	24109	CG8611	28936	CG8726	40719	CG8839	4620
CG8384	6315	CG8494	42609	CG8612	15199	CG8727	11765	CG8841	23625
CG8385	23082	CG8495	28849	CG8614	42146	CG8728	23617	CG8841	48253
CG8386	35919	CG8497	24111	CG8615	42152	CG8728	48677	CG8843	28873
CG8390	46229	CG8498	35388	CG8616	38249	CG8729	15533	CG8844	35437
CG8392	35923	CG8500	28795	CG8624	26995	CG8730	23772	CG8846	35439
CG8394	45917	CG8506	24114	CG8625	6208	CG8732	3222	CG8849	36050
CG8395	24305	CG8507	42640	CG8627	23680	CG8733	51921	CG8853	51322
CG8396	47383	CG8509	28915	CG8628	35392	CG8734	7949	CG8855	19050
CG8400	35419	CG8517	28093	CG8629	39155	CG8735	4025	CG8857	23475
CG8401	45237	CG8520	36546	CG8630	33340	CG8739	47750	CG8858	23634
CG8402	24308	CG8522	37640	CG8630	50290	CG8743	45989	CG8860	8768
CG8403	42478	CG8523	51165	CG8631	2998	CG8749	23150	CG8862	38085
CG8404	45482	CG8524	30460	CG8632	4654	CG8757	13110	CG8863	23637
CG8405	11127	CG8525	28916	CG8635	24131	CG8759	36017	CG8865	23639
CG8407	23504	CG8527	39580	CG8636	28937	CG8760	28945	CG8873	45618
CG8408	12432	CG8529	44360	CG8637	35988	CG8764	35829	CG8874	36053
CG8409	31995	CG8531	24122	CG8639	29968	CG8766	4658	CG8877	18567
CG8411	28897	CG8532	35949	CG8641	35993	CG8767	36533	CG8881	28975
CG8412	5934	CG8534	49893	CG8641	52260	CG8768	36022	CG8882	28976
CG8415	35421	CG8536	4867	CG8642	35997	CG8771	36023	CG8884	35445
CG8415	50956	CG8538	35952	CG8645	35431	CG8772	7192	CG8885	7860
CG8416	12734	CG8542	24125	CG8646	38092	CG8773	10203	CG8886	46702
CG8417	49508	CG8544	37792	CG8647	38189	CG8774	5862	CG8887	28982
CG8418	35929	CG8545	35954	CG8648	15698	CG8776	7909	CG8888	30336
CG8419	24097	CG8546	5110	CG8649	6276	CG8776	40803	CG8890	24148
CG8421	52589	CG8548	28920	CG8649	47514	CG8778	23621	CG8891	36055
CG8425	44049	CG8549	28924	CG8651	37715	CG8779	979	CG8892	28985
CG8426	37545	CG8552	35957	CG8652	46514	CG8779	30073	CG8893	23645
CG8427	35934	CG8553	35959	CG8654	4715	CG8779	37282	CG8893	50351
CG8428	3229	CG8556	28926	CG8655	40715	CG8781	36025	CG8895	7866
CG8431	26959	CG8556	50349	CG8656	24184	CG8782	28950	CG8895	33919
CG8432	28866	CG8557	28927	CG8657	4659	CG8783	40721	CG8896	965
CG8433	4902	CG8561	44361	CG8660	35432	CG8784	15989	CG8896	36305
CG8433	49808	CG8566	23464	CG8663	44486	CG8785	4650	CG8896	44386
CG8434	4319	CG8566	47171	CG8664	47568	CG8786	36028	CG8900	23083
CG8434	42570	CG8567	39592	CG8665	35999	CG8789	26910	CG8902	23650
CG8434	43898	CG8568	18534	CG8667	44470	CG8790	5863	CG8905	42162
CG8435	28900	CG8569	35962	CG8668	33156	CG8793	36033	CG8907	28987
CG8439	47742	CG8571	35967	CG8669	2935	CG8795	1768	CG8909	29900
CG8440	6216	CG8577	51237	CG8675	26997	CG8798	36035	CG8912	28989
CG8442	44439	CG8578	35969	CG8676	37694	CG8799	39539	CG8914	26915
CG8443	42136	CG8580	24130	CG8677	23608	CG8800	42117	CG8915	28857
CG8444	5830	CG8581	16923	CG8678	36002	CG8803	4174	CG8916	9138
CG8445	47743	CG8581	24475	CG8679	30778	CG8804	6446	CG8918	28994
CG8446	23141	CG8581	29909	CG8680	23467	CG8804	51091	CG8919	28996
CG8448	39126	CG8582	35970	CG8681	1479	CG8805	4176	CG8920	28998
CG8449	24102	CG8583	33282	CG8690	15798	CG8806	40723	CG8922	36060

CG8923	36063	CG9031	42189	CG9143	46330	CG9257	6406	CG9386	47755
CG8928	23480	CG9032	23685	CG9144	27006	CG9258	46542	CG9388	24017
CG8930	905	CG9032	50958	CG9144	48207	CG9261	2660	CG9389	44663
CG8930	4753	CG9033	44287	CG9147	29050	CG9265	46577	CG9391	23723
CG8930	29931	CG9035	8759	CG9148	45224	CG9267	2879	CG9393	44400
CG8933	7802	CG9038	29012	CG9150	16877	CG9270	29961	CG9394	13879
CG8936	47207	CG9041	28163	CG9151	9827	CG9271	15547	CG9398	29110
CG8937	45596	CG9042	29013	CG9151	47881	CG9272	41018	CG9399	13788
CG8938	23084	CG9044	42193	CG9153	37221	CG9273	30572	CG9400	43296
CG8938	50140	CG9045	37711	CG9154	29054	CG9277	24138	CG9401	28132
CG8939	40726	CG9046	13230	CG9154	49534	CG9279	45052	CG9406	29765
CG8942	1031	CG9047	23153	CG9155	49345	CG9283	15223	CG9406	48893
CG8942	9976	CG9049	36085	CG9156	29057	CG9286	23735	CG9410	44669
CG8942	40747	CG9053	10168	CG9159	7893	CG9288	46191	CG9412	29113
CG8946	37974	CG9054	29019	CG9160	39232	CG9290	14349	CG9413	45180
CG8947	14218	CG9056	29021	CG9160	43503	CG9291	15302	CG9414	30479
CG8948	42165	CG9057	40734	CG9163	1025	CG9294	29092	CG9415	15347
CG8949	48307	CG9060	12665	CG9163	30075	CG9296	29096	CG9416	10064
CG8950	36069	CG9062	3810	CG9163	45927	CG9300	24139	CG9418	37665
CG8954	23659	CG9063	40738	CG9166	28109	CG9302	15544	CG9422	30171
CG8956	3343	CG9064	2647	CG9169	27008	CG9304	11142	CG9423	36103
CG8958	42169	CG9065	29838	CG9170	29066	CG9305	30523	CG9426	10843
CG8959	14837	CG9065	33879	CG9171	13451	CG9306	23088	CG9427	15375
CG8962	29003	CG9066	45185	CG9171	50541	CG9307	23163	CG9428	3986
CG8963	42110	CG9067	35744	CG9172	23255	CG9308	6606	CG9429	51272
CG8967	878	CG9071	4062	CG9176	40964	CG9310	12692	CG9430	7339
CG8967	30834	CG9075	42201	CG9177	29070	CG9311	14173	CG9433	41021
CG8967	42565	CG9081	38218	CG9181	37437	CG9313	29099	CG9436	24026
CG8968	26923	CG9084	45609	CG9184	10283	CG9314	44647	CG9438	37148
CG8968	48894	CG9086	28961	CG9187	44366	CG9320	24141	CG9441	33923
CG8969	30483	CG9088	42203	CG9191	52549	CG9322	29100	CG9443	5843
CG8972	45845	CG9089	40966	CG9195	9130	CG9323	44984	CG9444	43275
CG8974	5572	CG9090	44297	CG9198	29072	CG9325	29101	CG9446	44671
CG8975	7965	CG9092	51445	CG9200	36092	CG9326	24157	CG9448	24030
CG8976	7394	CG9093	9696	CG9201	29073	CG9328	28125	CG9450	24031
CG8977	36071	CG9095	23159	CG9203	29075	CG9330	44651	CG9451	14344
CG8978	42171	CG9096	29023	CG9204	28111	CG9331	44653	CG9452	51202
CG8979	28860	CG9098	27001	CG9206	3785	CG9333	52551	CG9453	47262
CG8980	42175	CG9099	28106	CG9207	12616	CG9334	30774	CG9454	24032
CG8981	28098	CG9099	49895	CG9209	44638	CG9334	49899	CG9455	13263
CG8983	51675	CG9100	27002	CG9210	11547	CG9339	44655	CG9456	37955
CG8987	3133	CG9102	8943	CG9211	1001	CG9342	15775	CG9458	48700
CG8988	4601	CG9102	49042	CG9211	29898	CG9343	41095	CG9459	5948
CG8989	12771	CG9104	10472	CG9211	42577	CG9344	23689	CG9459	48905
CG8993	41126	CG9108	30030	CG9212	28116	CG9345	16643	CG9460	24036
CG8995	23665	CG9109	16982	CG9214	42209	CG9346	27013	CG9461	24039
CG8996	44378	CG9111	39183	CG9218	28119	CG9347	29108	CG9463	15587
CG8998	28102	CG9113	3275	CG9219	35750	CG9350	30619	CG9463	48063
CG9000	37179	CG9115	29032	CG9220	29085	CG9351	24143	CG9465	52269
CG9001	4931	CG9116	38139	CG9222	27010	CG9353	35447	CG9466	13040
CG9002	49812	CG9116	50537	CG9224	37407	CG9354	49902	CG9466	46288
CG9003	23481	CG9117	52545	CG9227	40858	CG9357	44656	CG9467	45806
CG9004	40727	CG9118	14931	CG9231	9101	CG9359	24144	CG9468	15590
CG9005	36079	CG9118	49813	CG9232	29087	CG9360	13189	CG9469	15469
CG9009	12016	CG9119	46326	CG9236	39161	CG9361	8564	CG9471	24042
CG9010	40728	CG9120	49896	CG9238	24149	CG9362	24012	CG9472	8424
CG9012	23666	CG9124	36086	CG9240	14833	CG9363	37012	CG9473	15339
CG9013	4964	CG9126	47073	CG9242	24152	CG9364	30730	CG9474	48033
CG9014	36084	CG9126	47074	CG9243	37422	CG9373	44658	CG9480	35452
CG9015	35697	CG9127	47972	CG9244	12455	CG9375	28129	CG9484	44676
CG9018	40732	CG9128	37216	CG9245	11852	CG9376	9457	CG9485	45809
CG9019	33909	CG9131	44362	CG9246	24136	CG9377	42837	CG9488	29720
CG9020	42185	CG9134	48756	CG9247	52612	CG9378	28130	CG9490	23316
CG9022	45173	CG9135	36091	CG9248	41226	CG9379	22824	CG9491	27015
CG9023	51936	CG9138	1047	CG9249	47643	CG9381	44662	CG9493	40743
CG9025	44428	CG9139	46329	CG9250	36095	CG9383	23737	CG9494	44877
CG9027	37794	CG9140	43184	CG9250	48548	CG9384	14169	CG9495	3795

CG9496	2824	CG9630	31081	CG9779	29275	CG9941	29596
CG9499	7900	CG9633	11210	CG9783	29276	CG9941	29902
CG9501	7903	CG9636	28133	CG9784	30098	CG9943	5081
CG9508	24052	CG9637	9073	CG9786	11775	CG9943	48887
CG9510	44683	CG9638	24076	CG9790	23702	CG9945	23742
CG9512	14809	CG9643	24081	CG9796	36452	CG9946	7799
CG9514	37403	CG9646	14982	CG9799	29280	CG9949	50178
CG9517	24162	CG9648	15351	CG9802	39207	CG9951	29457
CG9518	8328	CG9650	23170	CG9804	46579	CG9951	36172
CG9519	16501	CG9655	37309	CG9805	28140	CG9952	29903
CG9519	47195	CG9657	43922	CG9811	30103	CG9953	9024
CG9520	2826	CG9660	24083	CG9818	29285	CG9954	12712
CG9521	16497	CG9662	7278	CG9819	30105	CG9958	28145
CG9521	47136	CG9662	7278	CG9828	29289	CG9958	49822
CG9522	19861	CG9666	45658	CG9834	29290	CG9961	36175
CG9523	1451	CG9667	36127	CG9836	29295	CG9968	29693
CG9526	51451	CG9668	46919	CG9839	36455	CG9968	36185
CG9527	24054	CG9670	24086	CG9842	46873	CG9973	36187
CG9528	44687	CG9674	24089	CG9847	12863	CG9973	36584
CG9533	5569	CG9677	27032	CG9849	12850	CG9976	38002
CG9536	7907	CG9678	23342	CG9852	48717	CG9977	36193
CG9537	29374	CG9680	36131	CG9854	42283	CG9977	49573
CG9539	42763	CG9682	16549	CG9855	33309	CG9981	11566
CG9540	14807	CG9683	22830	CG9862	29302	CG9983	29523
CG9542	45620	CG9688	43887	CG9865	40701	CG9984	42217
CG9543	24059	CG9695	13005	CG9867	44570	CG9985	6229
CG9548	35453	CG9696	7787	CG9868	45506	CG9986	46113
CG9550	43996	CG9699	7742	CG9870	44215	CG9987	36198
CG9554	43911	CG9701	3358	CG9873	29760	CG9987	36494
CG9556	48044	CG9702	6859	CG9876	10481	CG9994	36201
CG9564	45717	CG9703	6137	CG9878	23705	CG9994	43486
CG9565	37803	CG9705	40665	CG9878	50446	CG9995	29531
CG9569	1820	CG9706	49347	CG9879	29311	CG9995	36205
CG9569	1820	CG9709	29119	CG9881	28141	CG9996	36207
CG9571	10480	CG9712	23944	CG9882	29312	CG9998	24177
CG9573	49820	CG9715	36138	CG9884	38258	CG9999	30568
CG9576	47261	CG9717	42669	CG9886	29320		
CG9577	24064	CG9722	6679	CG9886	48079		
CG9578	45082	CG9723	37412	CG9887	2574		
CG9580	50546	CG9725	23945	CG9890	23062		
CG9581	39208	CG9726	41347	CG9895	41035		
CG9581	48220	CG9727	30575	CG9899	46584		
CG9582	2845	CG9728	42895	CG9900	24171		
CG9586	28250	CG9730	36139	CG9901	29944		
CG9588	47763	CG9732	27035	CG9903	42690		
CG9590	29482	CG9734	23483	CG9904	45478		
CG9591	44696	CG9735	23951	CG9906	5597		
CG9593	24165	CG9738	26928	CG9907	6131		
CG9594	13636	CG9739	44390	CG9908	7001		
CG9595	24068	CG9741	51061	CG9910	24175		
CG9596	27025	CG9742	39256	CG9910	24175		
CG9597	36117	CG9747	1394	CG9911	46585		
CG9598	15975	CG9748	6299	CG9913	36459		
CG9601	24070	CG9749	36142	CG9914	29322		
CG9602	29498	CG9750	19021	CG9916	41015		
CG9603	37496	CG9752	28138	CG9920	29326		
CG9606	44699	CG9752	50282	CG9921	14921		
CG9609	30469	CG9753	1385	CG9922	35465		
CG9610	48121	CG9755	45815	CG9924	28798		
CG9611	36120	CG9761	23171	CG9925	29328		
CG9613	5801	CG9762	11381	CG9927	29332		
CG9615	24072	CG9764	28674	CG9930	47793		
CG9619	36121	CG9770	43462	CG9931	7743		
CG9620	42623	CG9772	15636	CG9934	36464		
CG9621	16641	CG9774	3793	CG9936	13777		
CG9623	5600	CG9776	29266	CG9938	29337		
CG9629	44700	CG9778	11037	CG9940	40756		







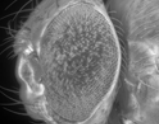
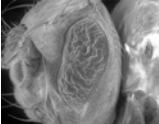
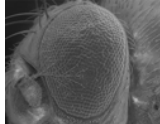
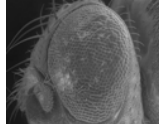
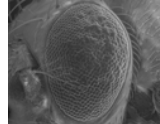
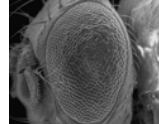








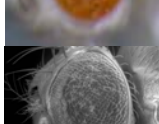
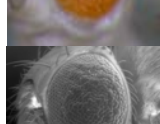



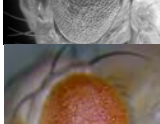
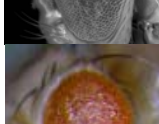


II Fly lines used for verification of RNAi effects



















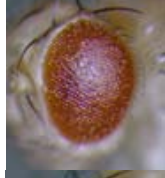


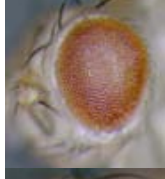
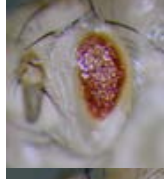















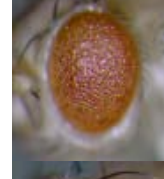


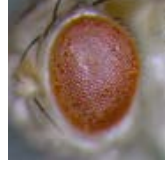


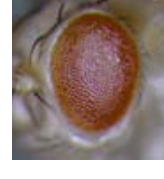
Lines, which produced analogue results compared to candidate shRNA are selectively listed in results.

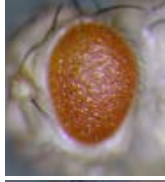












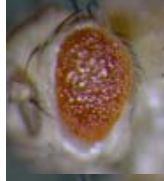







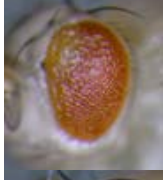


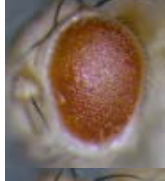


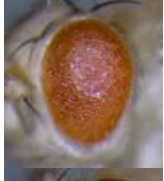

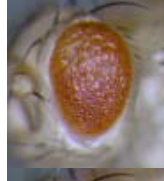
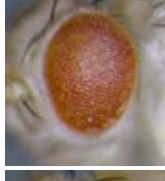

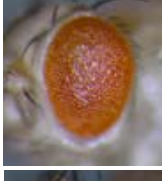






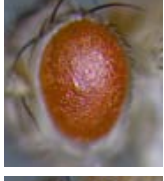
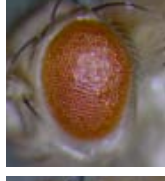







shRNA directed against	Bloomington	NIG-Fly
HARS		
TUBA1A		1913R-2
C4orf31	22671	
PSMBZ		
ADHFE1		3425R-3
CNTNAP2		
RPS10	17155	12275R-2
MAP2K7		4353R-2
ZBTB20	17254	
TRAPPC9		
CDC20		
DCTN2	8784, 11159	8269R-3
STIP1	17166	2720R-1
IGF2R	24748	
LAMTOR1		
TMEM135		
PARD6G		
MED14		
NEDD8		
C1orf55		5986R-1
HIPK2	22484, 20824, 20760	
DSTN		
PRPF8	25905	
ARV1		
UCK2		6364R-2
DCTN1	24760, 24761	
DDX42		
ERI2	15513, 17462	
NAA10	22609	
RDBP		
DAB1	16974	9695R-2
FLOT2		
BMI1	5549, 5573	
HM13	24475	
C18orf32		
TEX261	14861	3500R-2
PCLO		8664R-3
MORF4L1	10290	
SCAMP1		
MAD1L1		2072R-3
FRMPD4		31304R-2
BTF3L4	20236	
RAB30		
LAP3		32351R-1
IGFALS		
PTRH2		17327R-1
SMG5		
LM07		
TRMT2A	17847	
C17orf90		
CWC25		
CIZ1		8108R-4
TUBA1C		
SHROOM3	20251	
TCEB2	15707	



















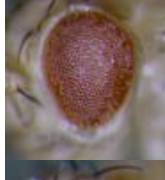

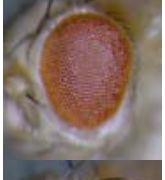



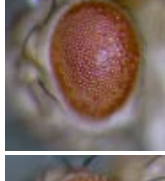


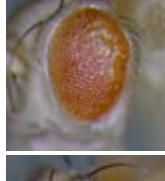
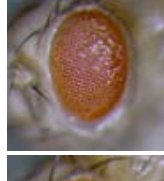


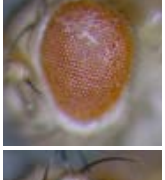



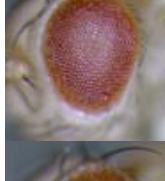





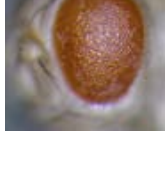
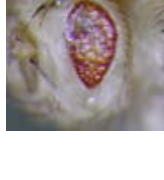



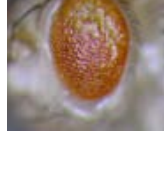
shRNA directed against	Bloomington	NIG-Fly
GDI1		
ZNF800		
UPP2		
ODF3		8086R-2
PSMA3		
AP3D1	3958	
ATP6V0C	19893	
SLC35E1		
PSMD13	15642	
SF3B5	21381	
CCNJ	20525	10308R-3
PTF1A		
STK17A		
DNAH17		
ARRB1		
NUDT2		
SNRPC		5454R-2
ATP6V1D		










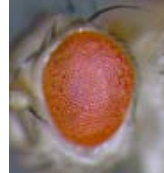


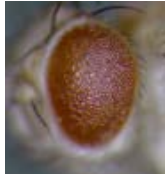






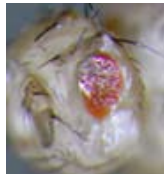






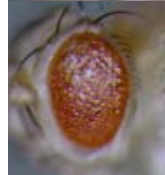
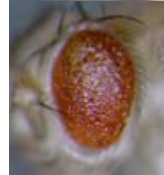








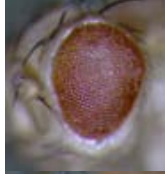





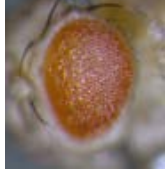


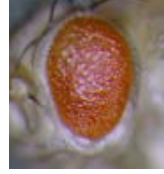

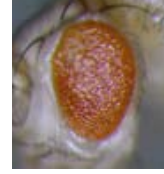
III Phenotypes induced by candidate shRNA lines











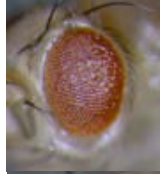




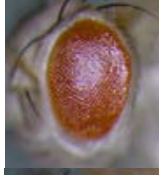

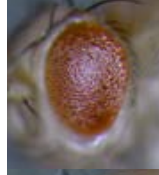





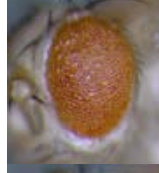
























shRNA directed against	Phenotype in Control	Phenotype in GMR_Tau[R406W]	Phenotype in GMR_attB_Tau[WT]	Phenotype in GMR_attB_Tau[R406W]	Phenotype in GMR_attB_Tau[AP]	Phenotype in GMR_attB_Tau[E14]
ABCG4 Control						
ZIC4 Control						
LRP2 Control						
HARS		N.A.				
TUBA1A						














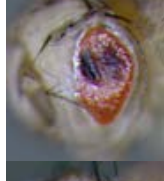
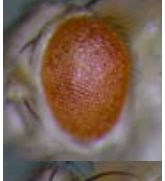

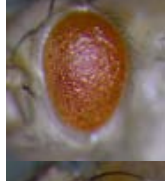







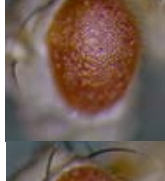
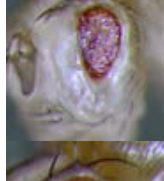


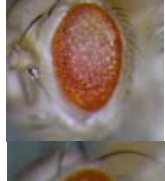

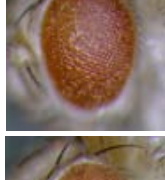
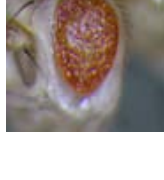
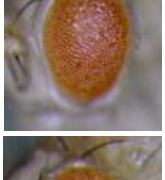
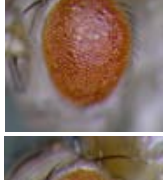


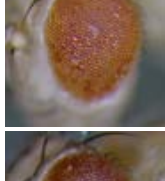

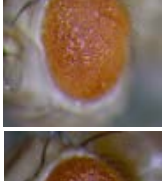

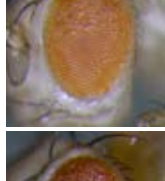
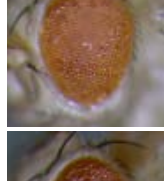






shRNA directed against	Phenotype in Control	Phenotype in GMR_Tau[R406W]	Phenotype in GMR_attB_Tau[WT]	Phenotype in GMR_attB_Tau[R406W]	Phenotype in GMR_attB_Tau[AP]	Phenotype in GMR_attB_Tau[E14]
C4orf31						
PSMBZ						
ADHFE1						
CNTNAP2			N.A.		N.A.	N.A.
RPS10						
MAP2K7						
ZBTB20						
TRAPPC9						














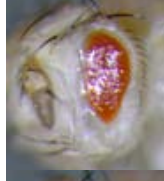




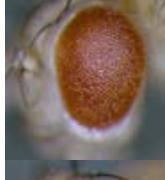




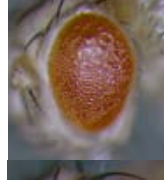
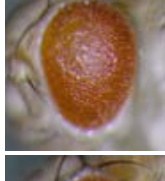


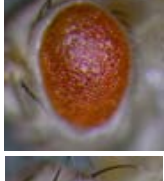











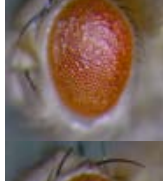



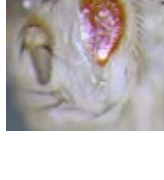




shRNA directed against	Phenotype in Control	Phenotype in GMR_Tau[R406W]	Phenotype in GMR_attB_Tau[WT]	Phenotype in GMR_attB_Tau[R406W]	Phenotype in GMR_attB_Tau[AP]	Phenotype in GMR_attB_Tau[E14]
CDC20						
DCTN2						
STIP1						
IGF2R						
LAMTOR1						
TMEM135						
PARD6G						
MED14						





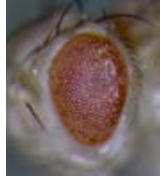







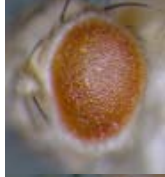

















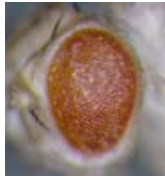






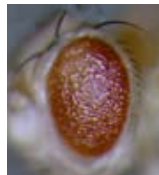
shRNA directed against	Phenotype in Control	Phenotype in GMR_Tau[R406W]	Phenotype in GMR_attB_Tau[WT]	Phenotype in GMR_attB_Tau[R406W]	Phenotype in GMR_attB_Tau[AP]	Phenotype in GMR_attB_Tau[E14]
NEDD8						
C1orf55						
HIPK2						
DSTN						
PRPF8				N.A.		
ARV1						
UCK2						
DCTN1						







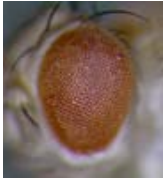


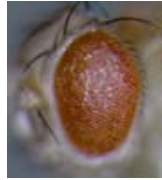







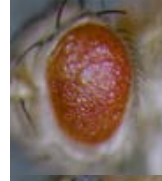
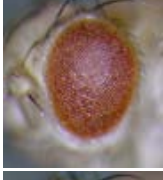





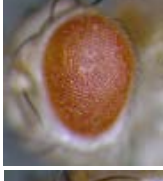
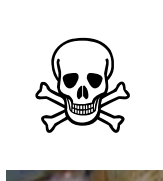


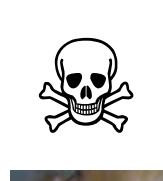




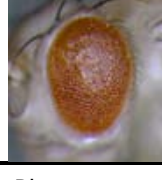


shRNA directed against	Phenotype in Control	Phenotype in GMR_Tau[R406W]	Phenotype in GMR_attB_Tau[WT]	Phenotype in GMR_attB_Tau[R406W]	Phenotype in GMR_attB_Tau[AP]	Phenotype in GMR_attB_Tau[E14]
DDX42						
ERI2						
NAA10						
RDBP						
DAB1						
FLOT2						
BMI1						
HM13						

shRNA directed against	Phenotype in Control	Phenotype in GMR_Tau[R406W]	Phenotype in GMR_attB_Tau[WT]	Phenotype in GMR_attB_Tau[R406W]	Phenotype in GMR_attB_Tau[AP]	Phenotype in GMR_attB_Tau[E14]
C18orf32						
TEX261						
PCLO						
MORF4L1						
SCAMP1						
MAD1L1						
FRMPD4						
BTF3L4						

shRNA directed against	Phenotype in Control	Phenotype in GMR_Tau[R406W]	Phenotype in GMR_attB_Tau[WT]	Phenotype in GMR_attB_Tau[R406W]	Phenotype in GMR_attB_Tau[AP]	Phenotype in GMR_attB_Tau[E14]
RAB30						
LAP3						
IGFALS						
PTRH2						
SMG5						
LMO7						
TRMT2A						
C17orf90						

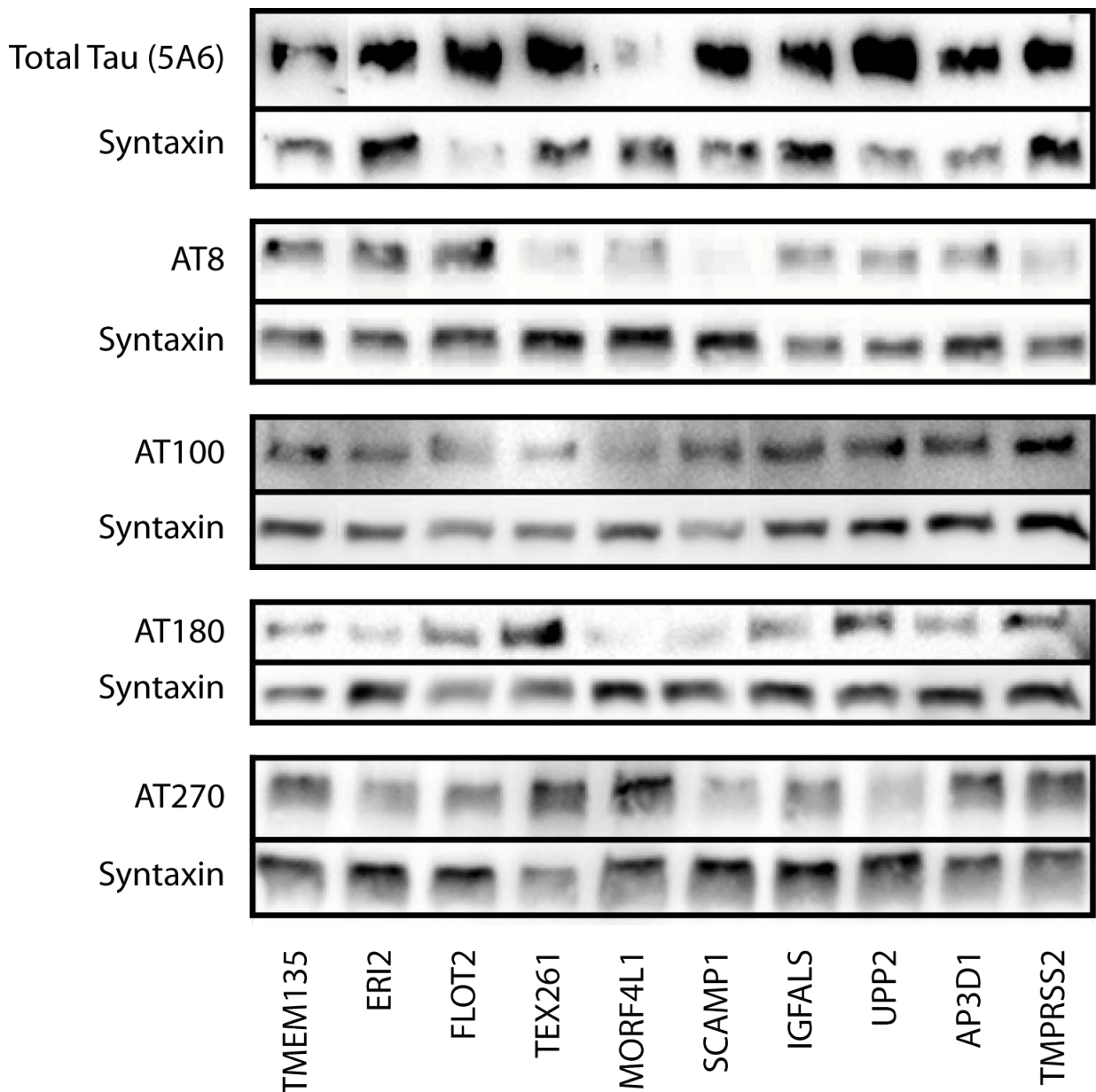
shRNA directed against	Phenotype in Control	Phenotype in GMR_Tau[R406W]	Phenotype in GMR_attB_Tau[WT]	Phenotype in GMR_attB_Tau[R406W]	Phenotype in GMR_attB_Tau[AP]	Phenotype in GMR_attB_Tau[E14]
CWC25						
CIZ1						
TUBA1C						
SHROOM3						
TCEB2						
GDI1						
ZNF800						
UPP2						

shRNA directed against	Phenotype in Control	Phenotype in GMR_Tau[R406W]	Phenotype in GMR_attB_Tau[WT]	Phenotype in GMR_attB_Tau[R406W]	Phenotype in GMR_attB_Tau[AP]	Phenotype in GMR_attB_Tau[E14]
ODF3						
PSMA3						
AP3D1						
ATP6V0C						
SLC35E1	N.A.	N.A.	N.A.	N.A.	N.A.	N.A.
PSMD13						
SF3B5			N.A.	N.A.	N.A.	N.A.
CCNJ						

shRNA directed against	Phenotype in Control	Phenotype in GMR_Tau[R406W]	Phenotype in GMR_attB_Tau[WT]	Phenotype in GMR_attB_Tau[R406W]	Phenotype in GMR_attB_Tau[AP]	Phenotype in GMR_attB_Tau[E14]
PTF1A	N.A.	N.A.	N.A.	N.A.	N.A.	N.A.
STK17A						
DNAH17						
ARRB1						
NUDT2						
SNRPC						
ATP6V1D						

N.A.: For phenotypes in GMR-Gal4 and GMR_Tau[R406W]: Phenotype was analysed three times, but could not be documented. For phenotypes in GMR_attB_Tau[*]: Phenotype could not be analysed and documented.

IV Preliminary western blot for altered phosphorylation of Tau induced by candidate shRNAs



Appendix Figure 1: Alterations in Tau phosphorylation induced by candidate shRNAs.

Immunoblotting analysis of Tau phosphorylation after knockdown of candidate genes. This is preliminary data suggesting, that selected candidates do have impact on the state of phospho-epitopes recognised by AT8, AT100, AT180 and AT270. As these are preliminary blots, normalisation antibody does not show identical band intensities. However differences are obvious for AT8, AT180 and AT270 (and 5A6). AT100 produces high background signal and does not show any obvious differences in phosphorylation state.